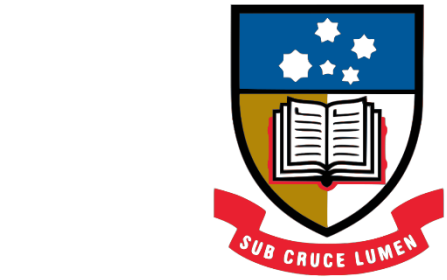

THE UNIVERSITY of ADELAIDE

Pharmacological Modulation of Cancer Migration and Invasion Through Targeting AQP1 Ion and Water Channel Activity

A thesis submitted in fulfilment for degree of

DOCTOR OF PHILOSOPHY

In

The Discipline of Physiology
Adelaide Medical School
The University of Adelaide

By

Michael Lucio De Ieso

27.2.2019

Table of Contents

Thesis Abstract

Cancer invasion and metastasis are the leading causes of cancer-related deaths. Aquaporin-1 is a dual water and ion channel that is upregulated in many aggressive cancers including colon, breast, and brain cancer; aquaporin-1 enhances cell migration, invasion and metastasis in these cancer types. Other aquaporins with water channel function are not able to substitute for aquaporin-1 in facilitating cell migration. There is a gap in knowledge regarding the properties of aquaporin-1 that permit its migration-enhancing effect, but both the ion and water channel activities appear to be involved. Thus, it was hypothesised that aquaporin-1 water and ion channels exhibit a coordinated role in aquaporin-1-facilitated cancer cell motility. The aims of this thesis were to test whether pharmacological block of the aquaporin-1 water and ion channel would impede cell migration and invasion in aquaporin-1-expressing cancer cell lines, and to see if the efficacy of aquaporin-1 inhibitors depended on membrane localisation of the channel. Proposed aquaporin-1 blocker AqB050, AQP1 water channel blocker bacopaside II, and an aquaporin-1 ion channel blocker AqB011 were used. The circular wound closure assay is an innovative alternative approach for measuring cell migration and was introduced and utilised in this thesis. Cell viability and proliferation was quantified using an alamarBlue assay. Cell invasion was measured with the transwell assay. Glioblastoma, colorectal adenocarcinoma, and mammary gland tumour cell lines were used. Results showed that combined pharmacological inhibition of aquaporin-1 water and ion conductance amplified the block of cancer cell migration as compared to block by each inhibitor alone, suggesting a cooperative role of aquaporin-1 water and ion channels in cell migration. Cancer cells that express aquaporin-1 on the membrane were more sensitive to block by aquaporin-1 inhibitors; this could be an important screening tool for identifying cancer subtypes likely to respond to AQP1 inhibitors. AqB011 and AqB050 inhibited glioblastoma, breast and colon cancer invasiveness. A newly generated mixture of compounds (AqB051) containing the proposed AQP1 blocker AqB050 and related derivatives was found to strongly block cancer transwell invasion. The potent biologically active agent (not AqB050) was then narrowed to one fraction (fraction E) from AqB051. AqB051 and fraction E significantly inhibited invasiveness in all glioblastoma cell lines. Work in this thesis paves the way for improving methods

utilized for measuring cell migration, investigating the role of AQP1 ion conductance and subcellular localisation in cancer migration and growth, investigating a novel and potent inhibitor for glioblastoma invasion, and testing the effects of AQP1 modulators in treating other non-neoplastic diseases.

Declaration

I certify that this work contains no material which has been accepted for the award of any other degree or diploma in my name in any university or other tertiary institution and, to the best of my knowledge and belief, contains no material previously published or written by another person, except where due reference has been made in the text. In addition, I certify that no part of this work will, in the future, be used in a submission in my name for any other degree or diploma in any university or other tertiary institution without the prior approval of the University of Adelaide and where applicable, any partner institution responsible for the joint award of this degree.

I acknowledge that copyright of published works contained within this thesis resides with the copyright holder(s) of those works.

I also give permission for the digital version of my thesis to be made available on the web, via the University's digital research repository, the Library Search and also through web search engines, unless permission has been granted by the University to restrict access for a period of time.

I acknowledge the support I have received for my research through the provision of an Australian Government Research Training Program Scholarship.

Michael Lucio De Ieso

Acknowledgements

I would like to begin by sincerely thanking my primary supervisor and mentor, Professor Andrea J Yool. Andrea, I honestly could not have imagined this journey without you. You have supported me, taught me, encouraged me, and motivated me every step of the way. When I needed direction, you were always available. When times were tough, you were always there. The positive impact you have had on my life has been profound, and I am truly grateful.

Thank you to my secondary supervisor, Dr Jenny Hardingham. Jenny, I truly appreciate your support and guidance throughout my candidature. Our regular meetings, discussions, and email correspondence was of considerable value to me. I would also like to thank the amazing team at the Basil Hetzel Institute for always making me feel welcome when I visited. Specifically, thank you to Dr Eric Smith, Dr Helen Palethorpe, and Dr Yoko Tomita for the many hours they donated to helping me with my experiments. You are all brilliant scientists, and I was very fortunate to learn from you.

I would like to thank my awesome lab buddies; Jinxin Pei, Mohamad Kourghi, Pak Hin Chow, and Saeed Nourmohammadi. I am so grateful for all the time you each contributed to helping me with experiments, writing, data analysis, conference presentations, and so much more. Although more importantly, you made the journey fun. Thank you, my friends.

I would also like to thank my best mates, who have supported me from the very beginning. Chris Panousakis, you always believed in me and it meant the world. Dennis Liu, we lived together through the worst of it, and we are still best mates! Peter Pazios, I couldn't hope for a more loyal, wise, and supportive mate. Yani Giannakodakis, our gym/dins/beer nights kept me going every week. I am very grateful to have each of you in my life.

I would especially like to thank my family. To my brother Nick De Ieso, I would not be here if it were not for your encouragement to aim high. To my mum Jacqui Yates, you gave me strength I never would have had on my own. To my papa Tony

De Ieso, I would not be the man I am today without your unconditional dedication and support. To my gorgeous, supportive, and loving girlfriend, Chloé Chenoweth. Thank you for never giving up on me. I can’t wait for the next exciting chapter in our lives together.

Finally, I would like to dedicate the glioblastoma work in this thesis to Chris Simon Adams and his family. Chris, for the short time we were friends at the end of your life, you had a long-lasting impact on me. You inspired me to redirect my PhD research towards glioblastoma. Your courage was inspirational, your positivity was contagious, and your character was admirable. You are a legend mate. S.E.T.L.

Publications Arising From This Thesis

First author:

De Ieso ML & Yool AJ (2018) Mechanisms of aquaporin-facilitated cancer invasion and metastasis. *Frontiers in Chemistry,* vol. 6, pp. 135.

De Ieso ML & Pei JV (2018) An Accurate and Cost-Effective Alternative Method for Measuring Cell Migration with the Circular Wound Closure Assay. *Bioscience Reports,* vol. 38, pp. 5.

Co-author:

Kourghi M, Pei JV, **De Ieso ML**, Nourmohammadi S, Chow PH & Yool AJ (2017) Fundamental structural and functional properties of Aquaporin ion channels found across the kingdoms of life. *Clinical and Experimental Pharmacology and Physiology*, vol. 45, no.4, pp. 401-409.

Pei JV, Kourghi M, **De Ieso ML**, Campbell EM & Yool AJ (2016) Differential inhibition of water and ion channel activities of mammalian Aquaporin-1 by two structurally related bacopaside compounds derived from the medicinal plant *Bacopa monnieri*. *Molecular Pharmacology,* vol. 90, no. 3.

Kourghi M, Pei JV, **De Ieso ML**, Flynn G, Yool AJ (2015) Bumetanide Derivatives AqB007 and AqB011 Selectively Block the Aquaporin-1 ion Channel Conductance and Slow Cancer Cell Migration. *Molecular Pharmacology,* vol. 89, no. 1, pp. 133-140.

PDFs of above publications can be found in Appendix I and II.

Chapter 1: Mechanisms of Aquaporin-Facilitated Cancer Invasion and Metastasis

Michael L De Ieso[1] and Andrea J Yool[1]

[1]Department of Physiology, Adelaide Medical School, University of Adelaide, Adelaide, SA, Australia

Chapter 1 is an introductory chapter, setting the premise of this thesis. It incorporates a published review paper: Mechanisms of Aquaporin-Facilitated Cancer Invasion and Metastasis. **M. De Ieso** and A.J. Yool. Frontiers in Chemistry 2018;6:135.

1.1 Abstract

Cancer is a leading cause of death worldwide, and its incidence is rising with numbers expected to increase 70% in the next two decades. The fact that current mainline treatments for cancer patients are accompanied by debilitating side effects prompts a growing demand for new therapies that not only inhibit growth and proliferation of cancer cells, but also control invasion and metastasis. One class of targets gaining international attention is the aquaporins, a family of membrane-spanning water channels with diverse physiological functions and extensive tissue-specific distributions in humans. Aquaporins -1, -2, -3, -4, -5, -8, and -9 have been linked to roles in cancer proliferation, invasion and metastasis, but their mechanisms of action remain to be fully defined. Aquaporins are implicated in the metastatic cascade in processes of angiogenesis, cellular dissociation, migration and invasion. Cancer invasion and metastasis are proposed to be potentiated by aquaporins in boosting tumour angiogenesis, enhancing cell volume regulation, regulating cell-cell and cell-matrix adhesions, interacting with actin cytoskeleton, regulating proteases and extracellular-matrix degrading molecules, contributing to the regulation of epithelial-mesenchymal transitions, and interacting with signalling pathways enabling motility and invasion. Pharmacological modulators of aquaporin channels are being identified and tested for therapeutic potential, including compounds derived from loop diuretics, metal-containing organic compounds,

plant natural products, and other small molecules. Further studies on aquaporin-dependent functions in cancer metastasis are needed to define the differential contributions of different classes of aquaporin channels to regulation of fluid balance, cell volume, small solute transport, signal transduction, their possible relevance as rate limiting steps, and potential values as therapeutic targets for proliferation and invasion.

1.2 Statement of Authorship

Statement of Authorship

Title of Paper	Mechanisms of Aquaporin-Facilitated Cancer Invasion and Metastasis
Publication Status	☑ Published ☐ Accepted for Publication ☐ Submitted for Publication ☐ Unpublished and Unsubmitted work written in manuscript style
Publication Details	Frontiers in Chemistry 2018; 6:135

Principal Author

Name of Principal Author (Candidate)	Michael L. De Ieso
Contribution to the Paper	First author and main contributor. Concept and methodological design, investigation, figure and table generation, project administration, formulation of primary draft in addition to reviewing and incorporating editor and coauthor comments and suggestions.
Overall percentage (%)	90%
Certification:	This paper reports on original research I conducted during the period of my Higher Degree by Research candidature and is not subject to any obligations or contractual agreements with a third party that would constrain its inclusion in this thesis. I am the primary author of this paper.
Signature	Date: 7th August 2018

Co-Author Contributions

By signing the Statement of Authorship, each author certifies that:

i. the candidate's stated contribution to the publication is accurate (as detailed above);
ii. permission is granted for the candidate in include the publication in the thesis; and
iii. the sum of all co-author contributions is equal to 100% less the candidate's stated contribution.

Name of Co-Author	Andrea J. Yool
Contribution to the Paper	Reviewed and edited the manuscript.
Signature	Date: 7th August 2018

1.3 Introduction

1.3.1 Aquaporins

Aquaporins (AQPs) are a family of water channels that also include a subset of classes shown to mediate transport of glycerol, ions and other molecules [1]. The first aquaporin to be cloned, aquaporin-1 (AQP1), was identified in red blood cells and renal proximal tubules [2, 3]. In the *Xenopus laevis* expression system, introduced AQP1 channels enabled high osmotic water flux across the plasma membrane as compared to non-AQP control oocytes [4], explaining the mechanism enabling rapid transmembrane passage of water in certain types of cells. To date, fifteen classes of aquaporin genes have been identified in mammals (AQP0-AQP14), with AQPs 13 and 14 found in older lineages of mammals (Metatheria and Prototheria) [5-7]. The first thirteen aquaporins (AQP0-AQP12) have been divided into categories based on functional properties [1]. One comprises the classical aquaporins (AQP0, -1, -2, -4, -5, -6, -8), which were thought initially to transport only water, though some also transport gases, urea, hydrogen peroxide, ammonia, and charged particles [4, 8-22]. A second category consists of the aquaglyceroporins (AQP3, -7, -9 and -10), which are permeable to water and glycerol, with some also exhibiting urea, arsenite, and hydrogen peroxide permeability [23-31]. A possible third category consists of AQP11 and AQP12, distantly related paralogs with only 20% homology with other mammalian AQPs [32], which appear to carry both water and glycerol [33, 34]. The permeability of AQP11 to glycerol could be important for its function in human adipocytes, in which it is natively expressed [35]. Aquaporins assemble as homo-tetramers, with monomers ranging 26 to 34kDa [36]. In most AQPs, each monomer is composed of six transmembrane domains and intracellular amino and carboxyl termini, with highly conserved asparagine-proline-alanine (NPA) motifs in cytoplasmic loop B and in extracellular loop E [37]. The NPA motifs in loops B and E contribute to a monomeric pore structure that mediates selective, bidirectional, single-file transport of water in the classical aquaporins [38], and water and glycerol in aquaglyceroporins [39].

Intracellular signalling processes regulate AQP channels by altering functional activity, intracellular localization, and levels of expression in different cells and

tissues. For example, the peptide hormone vasopressin regulates excretion of water in the kidney by augmenting water permeability of collecting duct cells. Vasopressin induces phosphorylation of AQP2 [40], stimulating the reversible translocation of AQP2 from intracellular vesicles to the apical plasma membrane [41]. Guanosine triphosphate (GTP) stimulates AQP1-induced swelling of secretory vesicles in the exocrine pancreas [42], with functional implications in pancreatic exocrine secretions. Additionally, AQP1 ion channel activity is activated by intracellular cGMP [8], and phosphorylation of Y253 in the carboxyl terminal domain regulates responsiveness of AQP1 ion channels to cGMP (Campbell et al., 2012). Given the diverse array of functional properties, mechanisms of regulation, and tissue-specific distributions being discovered for aquaporins, it is not surprising that different classes of aquaporins (AQP-1, -2, -3, -4, -5, -8, and -9) have been implicated specifically in the complex steps associated with cancer invasion and metastasis (Tab 1.1), suggesting specialized roles for these channels have been arrogated into the pathological processes.

1.3.2 Cancer Invasion and Metastasis

Cancer is a leading cause of death worldwide, accounting for 8.2 million deaths in 2012 [43]. The incidence of cancer is rising steadily in an aging population, with numbers expected to increase 70% in the next two decades [43]. Current treatments involve chemotherapy, radiation therapy, and surgery [44], associated with an array of side effects including nausea [45], impaired fertility and premature menopause [46, 47], painful neuropathy [48, 49], increased risk of cardiovascular disease [50, 51], and loss of bone density [52]. Inhibiting proliferation remains the primary focus of cancer treatments, although the predominant cause of death is cancer metastasis [53, 54]. Less devastating cancer therapies might be achievable via a combination of strategies that not only inhibit proliferation, but also control metastasis of tumour cells from their primary site to distant organs (Friedl & Wolf, 2003). Cancer cell migration through the body exploits pathways including blood stream, lymphatic system, and transcoelomic movement across body cavities [55-57]. The hierarchical nature of the metastatic cascade suggests it should be vulnerable to intervention at multiple levels including angiogenesis, detachment of cells from the primary tumour, and infiltration of dissociated tumour cells into and

out of circulatory pathways via intravasation and extravasation, respectively (Fig 1.1). AQPs that serve as rate-limiting steps in the metastatic cascade should have substantial value as prognostic markers and pharmacological targets for treatments.

Table 1.1: Key roles of AQPs involved in cancer invasion and metastasis

AQP	Permeable to:	Key physiological role(s)	Cancer(s) up-regulated	Key role(s) in cancer invasion and metastasis
AQP1	Water [4], monovalent cations [8], CO_2 [58], H_2O_2 [20], NO [59] & NH_3 [19]	• Water reabsorption in proximal tubule of the kidney for concentrating urine [60, 61] • Secretion of aqueous fluid from ciliary epithelium in the eye, and cerebrospinal fluid from the choroid plexus [62, 63] • Perception of thermal inflammatory pain and cold-induced pain [64]	Glioma [65, 66], mammary carcinoma [67], lung adenocarcinoma [68], colorectal carcinoma [69], laryngeal cancer [70], hemangioblastoma [71], & multiple myeloma (microvessels) [72]	• Upregulated in response to tumour tissue hypoxia. Enables recruitment of new tumour vasculature by enhancing endothelial cell migration. • Polarizes to leading and trailing edge of migrating cell, and enhances tumour cell migration and invasion by enabling rapid membrane protrusion formation via cell volume regulation and interaction with cytoskeletal dynamics • Enhances mesenchymal stem cell migration via FAK and β-catenin pathways • Might contribute to EMT • Possible interaction with ECM-degrading proteases
AQP2	Water [11]	• Water reabsorption in collecting duct of the kidney to concentrate urine [73]	Endometrial carcinoma [74]	• Enables “traction” for migrating cell by contributing to the regulation and recycling of focal adhesion proteins (e.g. integrin) • Necessary in estradiol-induced invasion and adhesion of endometrial carcinoma cells, through reorganization of F-actin

Table 1.1 (continued): Key roles of AQPs involved in cancer invasion and metastasis

AQP	Permeable to:	Key physiological role(s)	Cancer(s) up-regulated	Key role(s) in cancer invasion and metastasis
AQP3	Water [75], glycerol, urea [76], H_2O_2 [28], arsenite [31] & NH_3 [77]	• Water reabsorption in collecting duct of the kidney to concentrate urine [78] • Skin hydration [79] • Skin wound healing [80]	Lung cancer [81], hepatocellular carcinoma [82], gastric cancer [83], prostate cancer [84], oesophageal and oral squamous cell carcinoma [85], colorectal carcinoma [69], skin squamous cell carcinoma [86], ovarian cancer [87], pancreatic cancer [88], and breast cancer [89]	• Upregulated by EGF, and contributes to EGF-induced EMT and cancer migration • Contributes to chemokine-dependent cancer migration via enabling H_2O_2 influx and its downstream cell signalling. • Interacts with ECM-degrading proteases • Might enhance tumour cell migration and invasion via regulation of cell protrusion formation.
AQP4	Water [12]	• Water reabsorption in collecting duct of the kidney to concentrate urine [90] • Transport of water into and out of the brain and spinal cord via blood-brain barrier [91] • Neuroexcitation [92] • Enables astrocyte cell migration following injury [93]	Glioma [94] & meningioma [95]	• Co-localizes with ion channels at leading and trailing edges of migrating cancer cells • Enhances tumour cell migration and invasion by enabling rapid membrane protrusion formation via cell volume regulation and interaction with cytoskeletal dynamics • Might interact with ECM-degrading proteases

Table 1.1 (continued): Key roles of AQPs involved in cancer invasion and metastasis

AQP	Permeable to:	Key physiological role(s)	Cancer(s) up-regulated	Key role(s) in cancer invasion and metastasis
AQP5	Water [13] & H_2O_2 [22]	• Secretion of saliva [96] and airway mucus [97]	Prostate cancer [98], chronic myelogenous leukemia [99], colorectal carcinoma [100], hepatocellular carcinoma [82], lung cancer [101], cervical cancer [102], pancreatic cancer [88], & breast cancer [103]	• Promotes EMT • Co-localizes with ion channels at leading and trailing edges of migrating cancer cells • Enhances tumour cell migration and invasion by enabling rapid membrane protrusion formation via cell volume regulation • Might interact with EGFR/ERK1/2 signalling pathway
AQP8	Water, urea [17], H_2O_2 [21] & NH_3 [77, 104]	• Canalicular bile water secretion [105] • Colonic water reabsorption [106]	Cervical cancer [107, 108]	• Not yet known
AQP9	Water, urea [26], glycerol [109], arsenite [30] & H_2O_2 [29]	• Hepatic glycerol uptake and metabolism for glucose production [110-112] • Route for excretion of arsenic by the liver [113] and modulates arsenic sensitivity in leukemia [114, 115]	Glioblastoma [116], astrocytoma [117], prostate cancer [118]	• Overexpression might correspond with reduced EMT and growth in hepatocellular carcinoma • Might interact with ERK1/2 and MMP9 to enhance prostate cancer invasion and migration

1.4 Angiogenesis

Both cancer invasion and metastasis are enhanced by angiogenesis. Angiogenesis, activated in response to inadequate oxygen perfusion, triggers extracellular matrix breakdown; endothelial cell proliferation, differentiation and migration; and recruitment of periendothelial cells (Clapp & de la Escalera, 2006) which form discontinuous layers around vessels and exert developmental and homeostatic control (Njauw et al., 2008). Under physiological conditions, angiogenesis is seen in the proliferative phase of the menstrual cycle (Demir et al., 2010), development of fetal and placental vasculature (Demir et al., 2007), and skeletal muscle following physical activity (Egginton, 2009). In pathological scenarios such as tumourigenesis, tissue hypoxia stimulates the formation of new vasculature, enabling tumours to better obtain nutrients, exchange gases, and excrete waste (Nishida et al., 2006). Folkman and colleagues (1966) showed that tumours up to 2mm in diameter could survive via passive diffusion from surrounding tissue; but angiogenesis was essential for support of larger tumours.

AQP1, expressed in peripheral vascular endothelial cells, is involved in tumour angiogenesis (Nielsen et al., 1993; Endo et al., 1999; Saadoun et al., 2002a; El Hindy et al., 2013; Verkman et al., 2014). AQP1 knock-down in chick embryo chorioallantoic membrane resulted in a dramatic inhibition of angiogenesis (Camerino et al., 2006). Saadoun and colleagues (2005) found AQP1-deficient mice exhibited reduced tumour growth and angiogenesis as compared to wild type, following subcutaneous or intracranial B16F10 melanoma cell implantation. Their work showed AQP1-null endothelial cells from mouse aorta had reduced motility as compared to wild-type, suggesting AQP1 was needed to facilitate cell migration for angiogenesis. Monzani and colleagues (2009) confirmed a reduced migration capacity in human microvascular endothelial cells (HMEC-1) after AQP1 knockdown by siRNA. AQP1 mRNA and protein levels are increased in response to tissue hypoxia (Kaneko et al., 2008; Abreu-Rodríguez et al., 2011). AQP1 facilitates hypoxia-induced angiogenesis by enhancing endothelial cell migration.

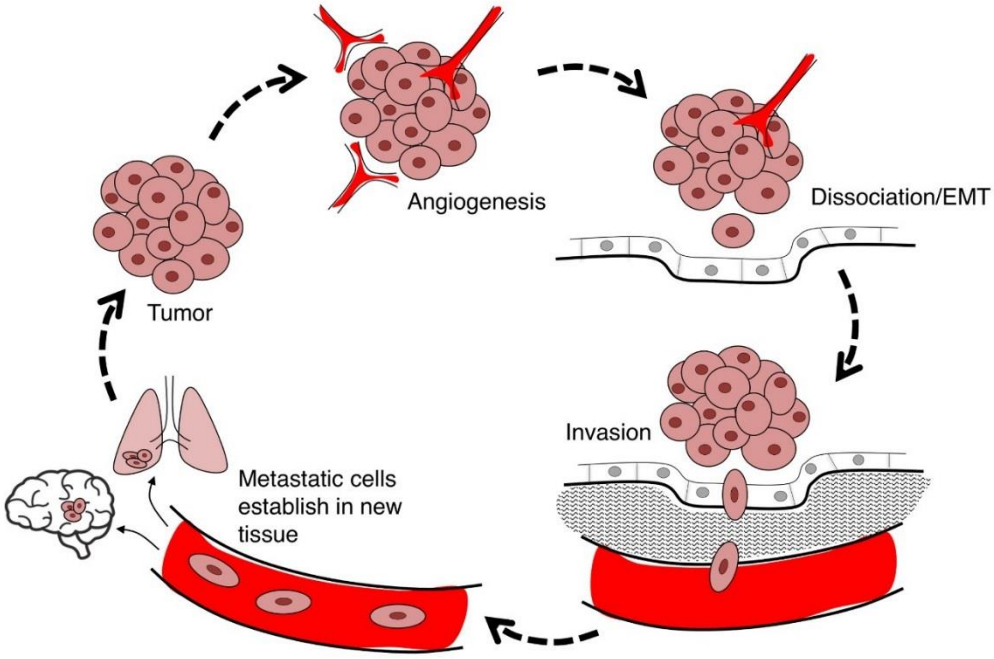

Figure 1.1: Flow diagram summarizing the steps in cancer metastasis. Metastasis involves the migration of cells from the primary tumour to distant organs. Large tumours with tissue hypoxia rely on angiogenesis for vascular exchange of nutrients and waste. Primary tumour cells undergo phenotypic changes including loss of cell-cell adhesions which enables cells to dissociate from primary tumour, invade the adjacent extracellular matrix (ECM), and intravasate into the blood or lymph systems. Circulating tumour cells extravasate to seed secondary sites at which the process can reoccur.

Angiogenesis is regulated by growth factors such as vascular endothelial growth factor (VEGF), which stimulates endothelial cell proliferation and angiogenesis in response to hypoxia (Suzuki et al., 2006), through processes that could augment AQP1 activity indirectly. Pan and colleagues (2008) found a positive correlation between levels of AQP1 expression, intratumoural microvascular density, and VEGF in endometrial adenocarcinoma. Similarly, AQP1 gene deletion correlated with reduced VEGF receptor expression in mouse primary breast tumour cells (Esteva-Font et al., 2014), and knockdown of AQP1 in human retinal vascular endothelial cells with concurrent inhibition of VEGF caused an additive inhibition of hypoxia-induced angiogenesis (Kaneko et al. 2008). However, application of VEGF-neutralizing antibodies did not alter AQP1 expression (Kaneko et al., 2008), and levels of VEGF in primary breast tumours were not different between AQP1-null and wild-type mice (Esteva-Font et al., 2014), supporting the idea that VEGF is regulated independently of AQP1 expression or activity.

Other angiogenic factors, such as hypoxia-inducible factor 1-alpha (HIF-1α), induce AQP1 expression in low oxygen conditions (Abreu-Rodríguez et al., 2011). The AQP1 gene promoter carries a HIF-1α binding site which drives AQP1 expression in response to hypoxia in cultured human retinal vascular endothelial cells (HRVECs) (Tanaka et al. 2011), and involves phosphorylation of p38 mitogen-activated protein kinase (MAPK) (Tie et al. (2012)). Estrogen signalling also targets the promoter region of the AQP1 gene to increase transcription, inducing enhanced tubulogenesis of vascular endothelial cells as a model for angiogenesis (Zou et al., 2013). In summary, AQP1 is upregulated by angiogenic factors in response to hypoxia, and necessary for endothelial cell migration and angiogenesis. Therapies aimed at blocking transcriptional activation of AQP1 could impede cancer angiogenesis, if the treatment could be spatially limited to the tumour site without impacting normal cell functions.

1.5 Cellular Dissociation and Epithelial-Mesenchymal Transition

Epithelial-mesenchymal transition (EMT) occurs in normal physiological conditions such as implantation, embryogenesis and organ development, as well as pathological processes such as cancer invasion and metastasis [119, 120]. During

EMT, polarized epithelial cells undergo biochemical changes to adopt a mesenchymal phenotype, characterized by a loss of cell polarity, reduced cell-cell adhesiveness, and enhanced invasive capacity [120-124]. Epithelial cadherin (E-cadherin), a transmembrane glycoprotein, enables calcium-dependent tight adhesions between epithelial cells and links to cytoskeletal elements [125, 126]. Downregulation of E-cadherin is a hallmark feature of EMT [127-129]. EMT in cancer is induced by signals from the tumour-associated stroma, including epidermal growth factor (EGF), platelet-derived growth factor (PDGF), hepatocyte-derived growth factor (HGF), and transforming growth factor beta (TGF-β) [130-134]. These signals stimulate transcription factors such as SNAI1 (SNAIL), SNAI2 (SLUG), zinc finger E-box binding homeobox 1 (ZEB1), Mothers against decapentaplegic homolog 2 (SMAD-2) and Twist, which are all E-cadherin transcription repressors [135, 136].

Classes of aquaporins such as AQP3 have been implicated in the EMT process. AQP3 up-regulation in response to EGF in colorectal, gastric, and pancreatic cancers, is associated with augmented cell migration, invasion, and metastasis [137-139]. In gastric cancer, EGF-induced AQP3 upregulation enhances the mesenchymal transformation [140]. Chen et al. (2014) determined that mRNA and protein levels of vimentin and fibronectin (proteins associated with mesenchymal phenotype) were significantly increased in cells with high levels of AQP3 expression but decreased in AQP3-deficient cells. Conversely, E-cadherin expression was significantly lower in cells with high AQP3 and increased in AQP3-knockdown cells. The mechanisms for AQP3-facilitated pancreatic and colorectal cancer cell migration have not yet been determined. It will be interesting to investigate whether AQP3 promotes EMT in these cancers.

In addition to AQP3, AQPs 1, 4, 5 and 9 also have been linked to EMT in different types of cancer cells. In lung adenocarcinoma cells, AQP1 overexpression correlated with the down-regulation of E-cadherin, and up-regulation of vimentin [141]. AQP4 knockdown in human breast cancer was associated with increased levels of E-cadherin, and in glioma cells with increased β-catenin (involved in actin reorganization and cell-cell adhesion) and connexin-43 (a gap junction protein that

contributes to cell-cell signalling and adhesion) [142, 143], suggesting AQP4 might enhance cell detachment from primary tumours. However, opposing evidence showed knockdown of AQP4 in primary human astrocytes correlated with down-regulation of connexin-43 [144]; and transfection of wild type AQP4 into glioma cell lines caused enhanced adhesion [145]. In primary glial cells, AQP4 expression levels had no appreciable effect on cell-cell adhesion under the conditions tested [146]. In human non-small cell lung cancer cells (NSCLCs), AQP5 increased invasiveness; conversely, expression of AQP5 mutant channels lacking membrane targeting signals or the S156 phosphorylation site did not augment invasiveness (Chae et al. (2008)). Overexpression of AQP5 in NSCLCs was associated with a reduction in epithelial cell markers such as E-cadherin, α-catenin and γ-catenin, and an increase in mesenchymal cell markers such as fibronectin and vimentin, concomitant with a mesenchymal change in morphology. Similarly, AQP3 and AQP5 overexpression in pancreatic ductal adenocarcinoma is accompanied by downregulation of E-cadherin and upregulation of vimentin [88]. The invasion-promoting properties of AQP5 expression appear to depend on the c-Src signalling pathway, a potent trigger of EMT [101, 147]. High AQP5 expression correlated with an increase in phosphorylated SMAD2, promoting EMT in colorectal cancer, whereas AQP5 silencing was associated with a down-regulation of phosphorylated SMAD2, and a repressed EMT response [148]. AQP9 is downregulated in hepatocellular carcinoma; overexpression corresponds to reduced growth and EMT, thus reducing cancer invasion and metastasis [149, 150]. Evidence suggests that AQPs have different effects depending on the type of cancer. Moreover, the state of cancer progression, environmental factors, and the types of assays used will be complicating factors; nevertheless, AQPs have clear potential as diagnostic and prognostic biomarkers, and as therapeutic targets for modulation of EMT, cell-cell adhesion, and dissociation phases of cancer progression.

1.6 Invasion and Cell Migration

Cell migration involves the translocation of individual and collective groups of cells through fluid or tissues, relevant for survival in multicellular and single-celled organisms [151, 152]. Migration enables physiological morphogenesis, immunity, and tissue repair [152, 153]. In most mammalian cells, migration is highest during

development and morphogenesis and decreases after terminal differentiation. In pathological circumstances such as cancer, migration machinery can be reactivated. AQPs -1, -3, -4, and -5, -8, and -9 are known to contribute to cancer cell migration and invasion. Translocation of cancer cells can be initiated by chemokines released from host tissues, and growth factors such as EGF secreted by stromal cells [154, 155].

AQP3 has been suggested to increase EGF-induced cancer growth and migration by mediating H_2O_2 flux [28, 156]. H_2O_2 is known as an oxidative stressor, but is also a second messenger in cell proliferation, differentiation and migration [157, 158]. AQP3 knockdown in skin and lung cancer cell lines reduced EGF-induced H_2O_2 influx, and attenuated EGF signalling cascades [156], reducing migration and growth. H_2O_2 also influenced chemokine-dependent migration of T-cells and breast cancer cells [159, 160]. AQP1, -3, -5, -8, and -9 have all been suggested to transport H_2O_2 [20-22, 28, 29]. All of these classes also have been linked with cancer cell migration [98, 149, 161-163]; however, H_2O_2 transport has thus far been linked only to AQP3 as a control mechanism in cancer cell migration. Further work might show H_2O_2 transport in other classes of AQPs regulates cell motility and invasion.

1.6.1 Polarization

Key molecular and cellular events involved in cell migration can be classified into five inter-dependent stages, which are polarization, protrusion, cell-matrix adhesion, extracellular matrix (ECM) degradation and retraction (Figure 1.2). Cell polarization provides functionally specialized domains in the membrane and cytoplasm [164], typified by asymmetric distributions of organelles, signalling mechanisms, and membrane channels, transporters and receptors [165]. In movement, changes in cell polarization generate leading and trailing edges, predominantly regulated by small GTPases such as CDC42 [166, 167], which controls the recruitment of partitioning-defective (PAR) proteins, atypical protein kinase C (aPKC), and actin polymerization machinery [168, 169]. AQPs -1, -4, -5, and -9 have been shown to show polarized localization at the leading edges of migrating cells. Specific co-distributions with ion transporters such as the Na^+/H^+ exchanger, the Cl^-/HCO_3^- exchanger, and the $Na^+/\text{-}HCO_3$ co-transporter, suggest

sophisticated mechanisms for regulation of fluid influx and efflux [170-174], potentially driving membrane protrusions for cell locomotion [175].

1.6.2 Protrusion

A migrating cell extends its leading edge into the ECM by assembling a branched network of intracellular actin filaments, predicted to yield a physical force that dynamically pushes the membrane out, alternating with relaxation and actin depolymerization [176-178]. Membrane expansion requires the vesicle fusion to support the increase in surface area [179-181]. Three types of protrusions found in motile cells are lamellipodia, filopodia, and invadopodia. Lamellipodia are broad, flat, actin-rich protrusions that extend in the direction of locomotion and provide a foundation on which the cell moves forward [182]. Filopodia are long, thin protrusions of the membrane thought to be exploratory, "sensing" the local environment [183]. Lamellipodial and filopodial formations are modulated by small GTPases in the Rho family, such as Rac1 and CDC42 [184-187], which stimulate actin polymerization in response to growth factor [185] and integrin receptor activations [188]. Interestingly, AQP9-facilitated water flux appears to critical for filopodial protrusion formation in fibroblasts, via the CDC42 pathway [189]. The Arp2/3 (actin-related protein 2/3) complex regulates the formation of new actin filaments in migrating cancer cells, and is regulated by Scar/WAVE complex (otherwise known as WANP), which interacts with the small GTPase Rac1 for lamellipodial assembly [190]. Invadopodia are actin-rich, matrix-degrading protrusions that appear when ECM degradation and cell deadhesion are needed to create space for movement, involving proteases such as MMP2, MMP9, and MT1-MMP and src tyrosine kinase [191]. Changes in cell volume during protrusion are assumed to require rapid water flow [192], and could occur in part in response to osmotic gradients governed by ion transport and actin polymerization state [175, 193, 194].

AQPs at the leading edges of migrating cells are well positioned to facilitate cell volume changes and cytoskeletal modifications during protrusion formation [195-199]. AQP1 overexpression in B16F10 melanoma cells and 4T1 mammary gland tumour cells enhanced cell migration and lamellipodial width *in vitro*, and

augmented metastasis in a mouse model [161]. AQP1 is proposed to enhance lamellipodial formation by increasing membrane osmotic water permeability [161, 171, 200], allowing water entry at the leading edge to impose hydrostatic pressure, drive membrane extension, and create space for actin polymerization. In addition to water channel activity, AQP1 is also thought to be an ion channel, proposed to allow gated conduction of monovalent cations through the central tetrameric pore [8, 201]. The dual water and ion conductance of AQP1 is essential for colon cancer cell migration *in vitro* [202]. Conversely, in clinical cases of cholangiocarcinoma, high AQP1 expression has been correlated with low metastasis [203, 204], suggesting that AQP1 might play different roles in different types of cancers.

Other classes of AQP water channels are not necessarily interchangeable with AQP1 in facilitating cell migration [145], suggesting features of AQP1 other than simple osmotic water permeability are involved. AQP1-enhanced cell migration might also be due to interactions with cytoskeletal proteins. For example, Monzani et al. (2009) demonstrated that AQP1 knockdown dramatically impeded actin cytoskeletal organization in migrating human melanoma and endothelial cell lines via interaction with Lin-7/β-catenin. The Lin-7/β-catenin complex enables asymmetrical organization of filamentous actin (F-actin). AQP1 might act as a scaffolding protein at the leading edges. Jiang (2009) found that knocking down AQP1 was associated with re-localization of actin in migrating HT20 colon cancer cells, and a reduction in the activity of actin regulatory factors RhoA and Rac. A PDZ domain in Lin-7 could mediate interaction with rhotekin protein, which inhibits Rho GTPase signalling that is involved in cell migration, invasion, and cytoskeletal reorganization [205]. Rhotekin merits further evaluation in models of AQP1-dependent cytoskeletal organization.

A role for AQP4 in glioma cell migration has similarly been proposed to occur through regulation of cell volume and cytoskeletal interactions. Protein kinase C (PKC)-mediated phosphorylation of AQP4 at serine 180 correlated with a decreased glioma cell invasion [206]. AQP4-facilitated glioma invasion is dependent on co-expression of chloride channels (ClC2) and the potassium-chloride co-transporter 1 (KCC1) in invadopodia, which could provide the ionic

driving force for water efflux leading to cell shrinkage that could augment invasiveness through ECM [206, 207]. AQP4 effects on actin cytoskeleton suggest a role for α-syntrophin, interacting with the C-terminal domain of AQP4 at a PDZ-binding site [208]. In human glioma and primary astrocytes, reduced AQP4 expression correlated with dramatic morphological elongation, reduced invasiveness, and impaired F-actin polymerization [142, 144].

AQP5 facilitates protrusion formation, volume regulation, cell migration, and metastasis. AQP5 expression is correlated with cell invasiveness and metastasis of human prostate cancer [98], lymph node metastasis in patients with colon cancer [209] and metastatic potential of lung cancer cells [210]. Moreover, Jung et al. (2011) showed that a shRNA-induced reduction in AQP5 expression in MCF7 breast cancer cells was associated with significantly reduced cell proliferation and migration. The mechanism of AQP5-facilitated cancer cell invasion and metastasis might be due to its direct or indirect interaction with the epidermal growth factor receptor/extracellular signal-regulated kinase (ERK1/2) pathway [210, 211], known to be important in cancer metastasis and aggressiveness [212]. Additionally, AQP5 mediates lung cancer cell membrane osmotic water permeability, and has been suggested to contribute to cancer cell migration and invasion by enabling rapid cell volume regulation and subsequent protrusion formation [213]. The complementary role of ion transport for migration in AQP5-expressing cells was supported by Stroka et al. (2014), who found that cell migration through physically confined spaces occurred despite block of actin polymerization and myosin contraction, but relied on co-expression of the Na^+/H^+ exchanger with AQP5, supporting AQP5-induced cell volume regulation and its importance in cell motility.

AQP8 expression influences migration and invasion of cervical cancer cells, and AQP3 expression enhances pancreatic and colorectal cancer cell invasion and metastasis [137, 139, 163]. Further work is needed to investigate whether mechanisms of AQP3- and AQP8-facilitated cancer cell migration and invasion involve cell volume regulation, protrusion formation, cytoskeletal interaction, or other functional properties of the AQP channels that remain to be defined.

1.6.3 Cell Matrix Adhesion

Cell-matrix adhesions, first observed in cultured fibroblasts, connect the extracellular matrix to the actin cytoskeleton [214]. During migration, contacts with substratum must form to facilitate extension, and must detach to allow forward displacement of the cell. Insufficient anchoring causes protrusions to collapse, leading to a "membrane ruffling" phenomenon [215]. Protrusions adhere to ECM via integrin receptors, in turn linked to intracellular actin filaments [216]. The extracellular binding of integrin receptors to ECM ligands initiates integrin clustering, and activates protein tyrosine kinases and small GTPases. The organization of actin cytoskeleton and cell polarity controls the positions of focal adhesions for cell locomotion [217, 218]. Cell-matrix adhesions create the focal points for generation of traction to pull the cell forward over the substratum.

Classes of aquaporins (AQP1-4) have been shown to interact with adhesion molecules and to influence adhesive properties of migrating cells. Increased AQP1 in mesenchymal stem cells enhances migration by a mechanism involving β-catenin and the focal adhesion kinase (FAK) [219], which regulates integrin signalling at focal adhesion sites [220-222]. Whether AQP1 and FAK also interact in cancer cell migration remains to be tested. AQP2 appears to promote cell migration by modulating integrin β1 at focal adhesion sites, by a mechanism thought to involve an arginine-glycine-aspartate (RGD) motif in the second extracellular loop of AQP2 [223]. When AQP2 is absent, integrin β1 is retained at focal adhesion sites, delaying recycling of focal adhesions, thus reducing migration rate. AQP2 also enables estradiol-induced migration and adhesion of endometrial carcinoma cells by mechanisms involving annexin-2 and reorganization of F-actin [74]. Knockdown of AQP3 in human esophageal and oral squamous cell carcinoma with siRNA correlated with reduced phosphorylation of FAK, impaired cell adhesion and cell death [85]; these effects would be predicted to impair cancer cell migration. AQP4 expression has been suggested to enhance cell-matrix adhesion in cancer cells [145]. More research is needed to identify the intracellular signalling mechanisms and to determine whether other AQP classes alter cell migration via modulation of cell adhesion.

1.6.4 Extracellular Matrix Degradation

Extracellular matrix degradation widens pathways through which cells can penetrate tissues, and reduces the distortion of the rounded cell body needed for physical progress [224, 225]. Invadopodia sprout from leading edge filopodia, extending through tiny channels in the ECM, and adhere to ECM collagen fibers [191, 226]. To accommodate displacement of the cell body, constraining ECM fibers are cleared by local proteolysis, using surface proteases such as zinc-dependent matrix metalloproteinases (MMP) and serine proteases [227-229]. AQPs -1, -3, -4, and -9 have been shown to interact with specific MMPs to facilitate ECM degradation and invasion.

In lung cancer cells, migration was facilitated by AQP1 expression, linked to expression of MMP2 and MMP9 [198]. In gastric cancer cells (SGC7901), AQP3 levels were correlated with MMP2, MMP9, and MT1-MMP levels, and enhanced invasiveness via phosphoinositide 3-kinase signalling [230]. Positive correlations between AQP3, MMP2, and MMP9 and cancer invasiveness also occur in lung cancer [231, 232]. In prostate cancer, AQP3 expression is correlated with up-regulation of MMP3 via ERK1/2 signalling, with increased cell motility and invasion [162]. In glioma, AQP4 levels correlated with migration and invasiveness *in vitro* and *in vivo* through a mechanism involving MMP2 [142]. AQP9 upregulation in prostate cancer could enhance growth, migration, and invasion involving ERK1/2 signalling; reduced levels of phosphorylated ERK1/2 and MMP9 were observed in AQP9-deficient cell lines [118]. These studies suggest one of the key components of AQP-mediated facilitation of cancer cell invasion is the regulation of MMP proteases needed for degradation of ECM.

1.6.5 Retraction

Following integrin-ligand binding, cross-linking proteins such as myosin II contract the actin filament strands [233], developing tension against the intact adhesion points [234]. The final step in the cycle of cell movement is retraction of the trailing edge. A working model is that membrane tension opens stretch-activated Ca^{2+} channels, activating calpain and triggering disassembly of focal adhesion proteins

on the trailing edge, while concurrent K^+ efflux drives volume loss at the cell rear, resulting in detachment and net translocation along the substrate. In this model, the role of AQP channels is to facilitate osmotic water efflux in response to K^+ efflux [175, 235, 236] presumably in parallel with electroneutral efflux of chloride ions.

1.7 AQP Pharmacology and Therapeutic Implications in Cancer Invasion and Metastasis

Aquaporin pharmacological agents have attracted keen interest for their potential therapeutic uses in diseases involving impaired fluid homeostasis. Aquaporins in cancer metastasis are new translational targets for AQP modulators. Known and proposed inhibitors of AQPs include cysteine-reactive metals such as mercury (II) chloride ($HgCl_2$) [237], gold-based compounds [238], carbonic anhydrase inhibitor acetazolamide [239, 240], and small molecule inhibitors such as tetraethylammonium (TEA^+) [241], although the small molecule blockers vary in efficacy between preparations. The pharmacological panel for AQPs has been expanding steadily, with new compounds being discovered around the world, including for example the University of Niigata, Japan [242], Radboud University, Netherlands [243], the Faculty of Pharmacy, University of Lisbon, Portugal [244], the Institute of Food and Agricultural Research and Technology, Barcelona, Spain [245], the University of Adelaide, Australia [246, 247], the University of Groningen, Netherlands [238], the University of Kiel, Germany [248], and others. This review focuses specifically on selected AQP pharmacological agents that to date have been tested in models of cancer cell migration and metastasis (Table 2).

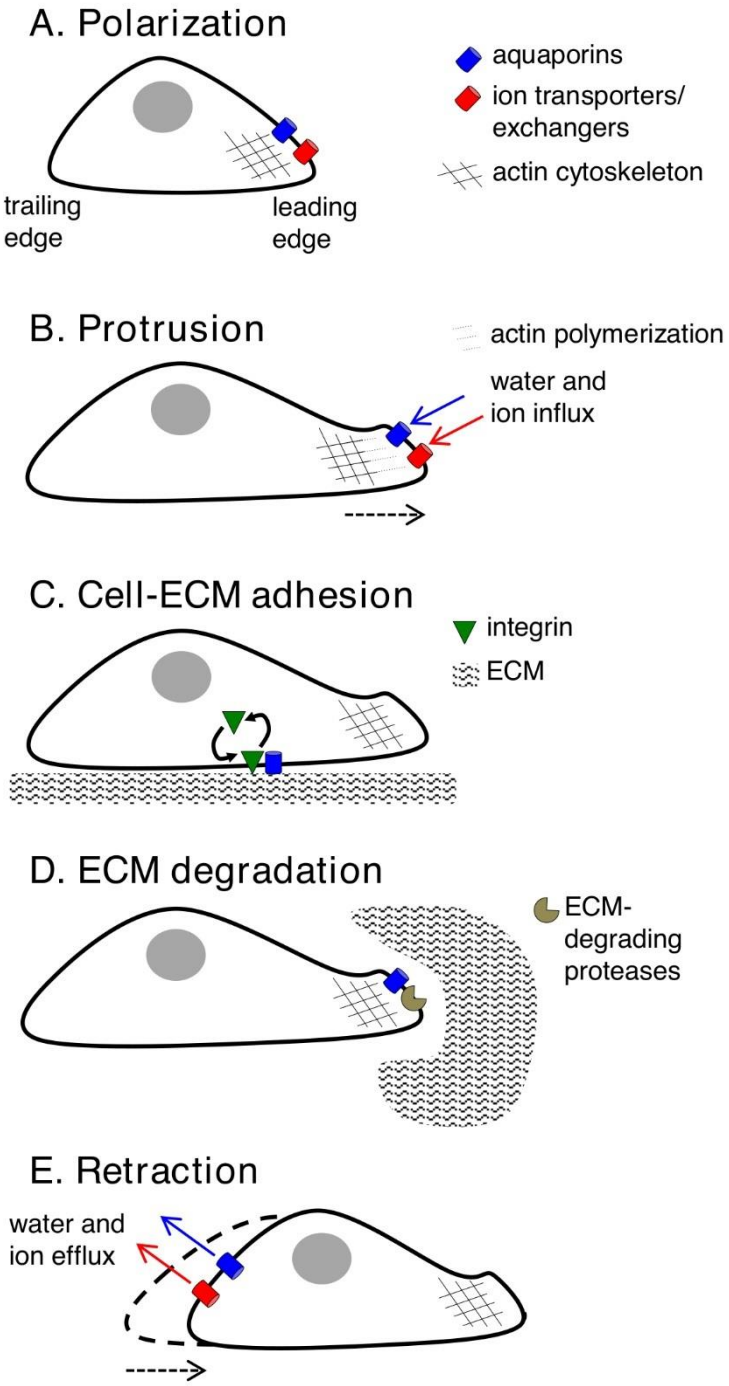

Figure 1.2: Key contributions of aquaporins in cell migration. (A) Forward movement is preceded by establishing specialized loci within the cell, with redistribution of aquaporins, ion transporters/exchangers, and actin polymerization machinery to the leading edge. AQP-1, -4, -5, or -9 can be found on leading edges of migrating cancer cells. (B) Protrusions of the membrane might use water influx (down an osmotic gradient established by ion transporters/exchangers) and actin polymerization beneath the plasma membrane to dynamically push the membrane

forward. AQP-1, -4, and -5 are implicated in water influx for protrusion extension in cancer cells; AQPs-1 and -4 also appear to interact with actin cytoskeleton. (C) Protrusions adhere to the ECM using integrin to generate “traction” for cellular movement. AQP2 might modulate turnover of integrin at adhesion sites, enabling forward cellular movement. (D) ECM degradation by enzymes can widen gaps through which the cell body can penetrate. AQP-1, -3, -4 and -9 are suggested to interact with ECM-degrading enzymes. (E) The final step is retraction of the cell trailing edge, thought to use aquaporins for water efflux following by K^+ export.

1.7.1 Acetazolamide and Topiramate

Acetazolamide and topiramate are FDA-approved drugs that inhibit carbonic anhydrase. Acetazolamide at 100μM was reported to inhibit water channel activity by 39% for AQP1 expressed in human embryonic kidney (HEK293) cells [240], and by 81% at 10μM in the *Xenopus* oocyte expression system [239]. AQP4 activity was inhibited by 47% at 1250 μM in proteoliposomes [249]. However, acetazolamide (at doses up to 10,000 μM) did not block water flux in erythrocytes with native AQP1 expression, or epithelial cells transfected with AQP1 [250, 251]. Acetazolamide inhibited angiogenesis in a chick chorioallantoic membrane assay, and tumour growth and metastasis in mice with Lewis lung carcinoma [252, 253], perhaps as a result of reduced AQP1 expression [254]. Topiramate reduces Lewis lung carcinoma growth and metastasis, with effects similarly attributed to suppression of AQP1 expression [255]. It will be of interest to compare the effects of acetazolamide and topiramate on angiogenesis, tumour growth, and metastasis with those of AQP1 channel inhibitors.

1.7.2 Tetraethylammonium

TEA^+ is an inhibitor of voltage-gated potassium channels, calcium-dependent potassium channels, the nicotinic acetylcholine receptor, and it has also been shown to block AQP-1, -2, and -4 water permeability in *Xenopus laevis* oocytes and kidney derived cell lines [241, 243, 256]. However, inhibition of AQP1 water permeability by TEA^+ is variable, having been confirmed by some groups [243], and challenged by others [251]. Yang et al. (2006) reported no block of water flux by TEA^+ in erythrocytes with native AQP1, or in epithelial cells transfected with AQP1, and suggested previous positive results might have been due to inhibition of K^+ channels and altered baseline cell volume; however, the observation that site-directed mutation of AQP1 altered TEA sensitivity [241] ruled out this alternative explanation. TEA^+ block of AQP1 water permeability reduced cell migration and invasion in *in vitro* models of osteosarcoma and hepatocellular carcinoma [196], with outcomes interpreted as consistent with action of TEA^+ as a possible AQP1 inhibitor. However, given the variability in efficacy and cross-talk with other channels, TEA^+ is not an ideal candidate for clinical development, although the

targets causing the observed block of cancer cell migration and invasion might merit further investigation.

1.7.3 Bumetanide Derivatives

Bumetanide is a sulfamoylanthranilic acid derivative used clinically to increase diuresis by blocking sodium cotransporter activity at the loop of Henle in the nephron. Molecular derivatives of bumetanide have been synthesized and found to exhibit inhibitory effects on classes of AQP channels. For example, the bumetanide derivative AqB013 blocks osmotic water fluxes mediated by mammalian AQP1 and AQP4 channels expressed in *Xenopus laevis* oocytes [257]. The water channel blocker AqB013 was shown to inhibit endothelial tube formation and colon cancer cell migration and invasion *in vitro* [258]. Other bumetanide derivatives, AqB011 and AqB007, block the AQP1 ion conductance, but not water flux [202]. In AQP1, the central tetrameric pore is thought to be permeable to monovalent cations, CO_2, and NO [58, 59, 201, 259], although some work questioned AQP1-mediated CO_2 and cation transport properties [260-262]. An ionic conductance in AQP1-expressing *Xenopus* oocytes stimulated with forskolin was first reported in 1996 (Yool et al., 1996); however, the forskolin response proved to be inconsistent when repeated by other groups [263]. Further work showed the forskolin effect was indirect; the direct regulation of the AQP1 cation conductance depended on cGMP binding [8]. The reason that AQP1 cation channels have low opening probability [264] or are not detectable [260] reflects the availability of AQP1 to be gated by cGMP, which depends on tyrosine phosphorylation status of the carboxyl terminal domain, suggesting the AQP1 ion channel function is highly regulated [265]. With the discovery of AQP1 ion blocking agents, AqB011 and AqB007, the physiological function of the ion channel activity could finally be addressed. When applied to AQP1-expressing HT29 colon cancer cells, these inhibitory compounds significantly reduced cancer cell motility [202], suggesting a physiological role of AQP1 ion conductance in cell migration. Mutation of the candidate binding site in the AQP1 intracellular loop D domain removed sensitivity to AqB011, showing that the inhibitory mechanism directly involved the AQP1 channel and could not readily be attributed to off-target actions on other channels or transporters [266]. Another bumetanide derivative AqB050 was shown to inhibit mesothelioma cell

motility and metastatic potential *in vitro*, but not *in vivo* [197]. The mechanism of action of AqB050 in blocking mesothelioma cell motility *in vitro* remains to be determined.

1.7.4 Plant-Based Derivatives

Plant-based derivatives that reduce cancer cell migration and invasion include agents that have also been found to inhibit AQPs. Bacopa monnieri is a perennial herb native to the wetlands of India that is used in alternative medicinal therapies. Chemical constituents bacopaside-I and bacopaside-II, were shown to block AQP1 but not AQP4 water channels [267]. Pei and colleagues also found that bacopaside-I and bacopaside-II attenuated migration of colon cancer cell lines expressing high levels of AQP1, but had no effect on lines with low AQP1, suggesting the inhibitory effects were AQP1-specific. Ginsenoside Rg3 from a traditional Asian medicinal plant Panax ginseng is an intriguing candidate for possible anti-metastatic therapies. Ginsenoside Rg3 inhibited prostate cancer cell migration and was associated with downregulation of AQP1 expression via the p38 MAPK pathway and transcription factors [268]. Effects of Ginsenoside Rg3 directly on water channel activity, or on expression levels of other aquaporins, remain unknown. Curcumin is a naturally occurring ingredient in turmeric, used as therapeutic tool for pathologies including cancer [269]. Curcumin was found to inhibit EGF-induced upregulation of AQP3 and migration in human ovarian cancer cells, via inhibition of AKT/ERK and PI3K pathways [87]; however, curcumin affects a number of biochemical pathways and might not be suited when AQP-specific modulation is required [270]. Research on the effects of curcumin in other cancers such as gastric cancer, in which EGF-induced AQP3 up-regulation occurs, might further understanding of the role of AQP3 in cell migration and invasion [138].

1.7.5 Metal-Based Inhibitors

Mercury has classically been used as an AQP1 inhibitor. In the human AQP1 monomer, the NPA motif in loop E is near cysteine 189, which is the site at which mercury inhibits osmotic water permeability [271]. Lack of a cysteine in the corresponding position is consistent with mercury insensitivity in mammalian AQP4 [237]. However, mercury is not a promising candidate for AQP-specific

modulation or therapeutic application due to its toxicity and non-specific side-effects. Metal-based inhibitors that have been tested in models of cancer include AQP3 inhibitors such as $NiCl_2$ [272] and $CuSO_4$ [273], which inhibited EGF-induced cell migration in human ovarian cancer cells. Auphen is a gold-based compound which, when administered at concentrations of 100μM, blocks AQP3 glycerol transport by 90%, and water transport by 20% in human red blood cells [244]. Auphen also blocks proliferation in various mammalian cell lines, including human epidermoid carcinoma, by inhibiting AQP3 glycerol transport [274]. This merits more research into the importance of AQP3-facilitated glycerol transport in cancer invasiveness, and whether gold-based compounds such as auphen can also be used to suppress cancer invasion and metastasis.

1.8 Conclusion

Aquaporin-dependent mechanisms serve as key steps throughout the process of metastasis, in angiogenesis, cellular dissociation, cell migration and invasion. AQPs-1, -2, -3, -4, -5, -8, and -9 contribute to one or more processes, generally potentiating cancer invasion and metastasis by boosting tumour angiogenesis, enhancing cell volume regulation, regulating cell-cell and cell-matrix adhesions, interacting with the actin cytoskeleton, regulating proteases and ECM degrading molecules, contributing to the regulation of epithelial-mesenchymal transition in cancer cells, and interacting with specific signalling pathways important in cancer cell motility and invasions. Pharmacological agents for aquaporin channels have therapeutic promise for improving cancer treatment, and include derivatives of bumetanide, organic metal compounds, plant medicinal agents, and other small molecule compounds. Although conflicting evidence has been raised for some compounds, there is nevertheless a compelling need to continue identifying novel candidates for AQP-specific modulators relevant not only for the treatment of cancer, but other pathological conditions. In conclusion, although much remains to be defined for molecular mechanisms in cancer invasion and metastasis, the roles of AQP channel function in cancer progression will inspire new therapeutic targets for improving treatment of malignant and invasive carcinomas.

Table 1.2: Summary of AQP pharmacology used in cancer invasion and metastasis

Molecule name	Molecular structure	AQP activity	Effect
TEA^+	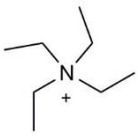	• Inhibits AQP1, AQP2, and AQP4 water flux [243, 256, 275]	• Inhibits osteosarcoma and hepatocellular carcinoma cell migration and invasion (*in vitro*) [196]
Acetazolamide	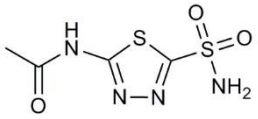	• Inhibits AQP1 and AQP4 water flux [239, 249] • Suppresses AQP1 expression [252]	• Inhibits angiogenesis and metastasis in Lewis lung carcinoma (*in vivo*) [252, 253] • Suppresses tumour growth in colon cancer (*in vivo*) [254]
Topiramate	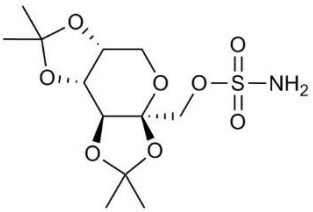	• Suppresses AQP1 expression [255]	• Suppresses Lewis lung carcinoma growth and metastasis (*in vivo*) [255]
AqB007	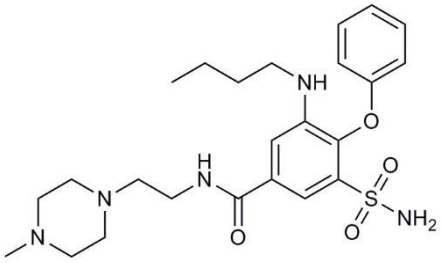	• Inhibits AQP1 ion flux [202]	• Inhibits colon cancer cell migration (*in vitro*) [202]
AqB011	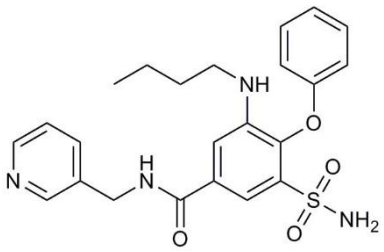	• Inhibits AQP1 ion flux [202]	• Inhibits colon cancer cell migration (*in vitro*) [202]

Table 1.2 (continued): Summary of AQP pharmacology used in cancer invasion and metastasis

Molecule name	Molecular structure	AQP activity	Effect
AqB013	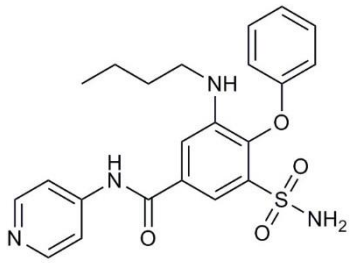	• Inhibits AQP1 and AQP4 water flux [257]	• Inhibits endothelial tube formation and colon cancer cell migration (*in vitro*) [258]
Bacopaside I	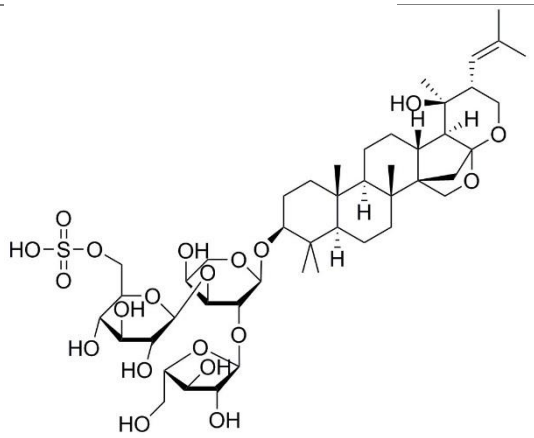	• Inhibits AQP1 water flux [267]	• Inhibits colon cancer cell migration (*in vitro*) [267]
Curcumin	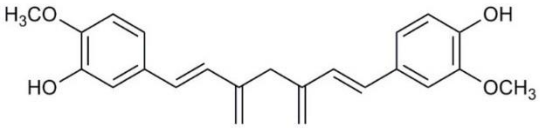	• Inhibits EGF-induced AQP3 upregulation [87]	• Inhibits ovarian cancer cell migration (*in vitro*) [87]
Bacopaside II	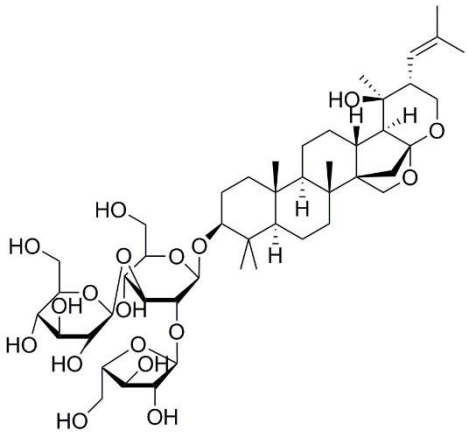	• Inhibits AQP1 water flux [267]	• Inhibits colon cancer cell migration (*in vitro*) [267]

Table 1.2 (continued): Summary of AQP pharmacology used in cancer invasion and metastasis

Ginsenoside Rg3	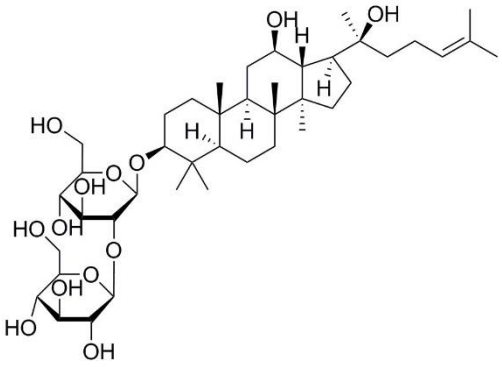	• Suppresses AQP1 expression [268]	• Inhibits prostate cancer cell migration (*in vitro*) [268]

1.9 Thesis Hypothesis and Aims

AQP1 enhances cell migration in some cancer cell lines. Knockdown of AQP1 expression in cancer impairs cell migration *in vitro* [172, 219, 276], and increasing AQP1 levels by transfection into deficient lines accelerates cell migration *in vitro* and increases the likelihood of lung metastases in mice *in vivo* [161]. AQP1 also possesses a dual function, mediating water and ion flow [38, 201, 277]. There is a gap in knowledge regarding the properties of AQP1 that permit its migration-enhancing effect, but both the ion and water channel activities appear to be involved [175]

Thus, three hypotheses were tested with human cancer cell lines *in vitro*.

1. AQP1 water and ion channels exhibit a coordinated role in AQP1-facilitated cancer cell motility.
2. Efficacy of AQP1 inhibitors depends on plasma membrane localisation of AQP1.
3. The biologically active component of the AqB051 mixture inhibits chemokine-dependent glioblastoma invasiveness, independently of interaction with local extracellular matrix.

These hypotheses led to the generation of 4 main aims:

1. To test whether pharmacological block of AQP1 ion channel will impede cell migration and invasion in AQP1-expressing cancer cell lines.
2. To see if combined pharmacological block of AQP1 water and ion channels will enhance the inhibitory effect on cancer cell motility.
3. To see if the efficacy of AQP1 inhibitors depends on membrane localisation of the channel, by testing inhibitors in cells that express intracellular AQP1 compared to cells that express membrane-bound AQP1.
4. To identify the compound in the AqB051 mixture that potently inhibits glioblastoma invasiveness.

1.10 References

1. Li, C. and W. Wang, *Molecular Biology of Aquaporins*, in *Aquaporins*. 2017, Springer. p. 1-34.
2. Denker, B.M., et al., *Identification, purification, and partial characterization of a novel Mr 28,000 integral membrane protein from erythrocytes and renal tubules.* Journal of Biological Chemistry, 1988. **263**(30): p. 15634-15642.
3. Preston, G.M. and P. Agre, *Isolation of the cDNA for erythrocyte integral membrane protein of 28 kilodaltons: member of an ancient channel family.* Proceedings of the National Academy of Sciences, 1991. **88**(24): p. 11110-11114.
4. Preston, G.M., et al., *Appearance of water channels in Xenopus oocytes expressing red cell CHIP28 protein.* Science, 1992. **256**(5055): p. 385-387.
5. Ishibashi, K., S. Hara, and S. Kondo, *Aquaporin water channels in mammals.* Clinical and experimental nephrology, 2009. **13**(2): p. 107-117.
6. Finn, R.N. and J. Cerda, *Evolution and functional diversity of aquaporins.* The Biological Bulletin, 2015. **229**(1): p. 6-23.
7. Finn, R.N., et al., *The lineage-specific evolution of aquaporin gene clusters facilitated tetrapod terrestrial adaptation.* PLoS One, 2014. **9**(11): p. e113686.
8. Anthony, T.L., et al., *Cloned human aquaporin-1 is a cyclic GMP-gated ion channel.* Mol Pharmacol, 2000. **57**(3): p. 576-88.
9. Chandy, G., et al., *Comparison of the water transporting properties of MIP and AQP1.* Journal of Membrane Biology, 1997. **159**(1): p. 29-39.
10. Ehring, G. and J. Hall. *Single channel properties of lens MIP 28 reconstituted into planar lipid bilayers*. in *Proceedings of the Western Pharmacology Society*. 1988.
11. Fushimi, K., et al., *Cloning and expression of apical membrane water channel of rat kidney collecting tubule.* Nature, 1993. **361**(6412): p. 549.
12. Hasegawa, H., et al., *Molecular cloning of a mercurial-insensitive water channel expressed in selected water-transporting tissues.* Journal of Biological Chemistry, 1994. **269**(8): p. 5497-5500.
13. Raina, S., et al., *Molecular cloning and characterization of an aquaporin cDNA from salivary, lacrimal, and respiratory tissues.* Journal of Biological Chemistry, 1995. **270**(4): p. 1908-1912.
14. Yasui, M., et al., *Rapid gating and anion permeability of an intracellular aquaporin.* Nature, 1999. **402**(6758): p. 184-187.
15. Ma, T., et al., *cDNA Cloning and Gene Structure of a Novel Water Channel Expressed Exclusively in Human Kidney: Evidence for a Gene Cluster of Aquaporins at Chromosome Locus 12q13.* Genomics, 1996. **35**(3): p. 543-550.
16. Herrera, M. and J.L. Garvin, *Aquaporins as gas channels.* Pflügers Archiv-European Journal of Physiology, 2011. **462**(4): p. 623.
17. Ma, T., B. Yang, and A. Verkman, *Cloning of a novel water and urea-permeable aquaporin from mouse expressed strongly in colon, placenta, liver, and heart.* Biochemical and biophysical research communications, 1997. **240**(2): p. 324-328.

18. Ishibashi, K., et al., *Cloning and functional expression of a second new aquaporin abundantly expressed in testis.* Biochemical and biophysical research communications, 1997. **237**(3): p. 714-718.
19. Nakhoul, N.L., et al., *Transport of NH3/NH 4+ in oocytes expressing aquaporin-1.* American Journal of Physiology-Renal Physiology, 2001. **281**(2): p. F255-F263.
20. Almasalmeh, A., et al., *Structural determinants of the hydrogen peroxide permeability of aquaporins.* The FEBS journal, 2014. **281**(3): p. 647-656.
21. Bienert, G.P., et al., *Specific aquaporins facilitate the diffusion of hydrogen peroxide across membranes.* Journal of Biological Chemistry, 2007. **282**(2): p. 1183-1192.
22. Rodrigues, C., et al., *Rat Aquaporin-5 is pH-Gated induced by phosphorylation and is implicated in oxidative stress.* International journal of molecular sciences, 2016. **17**(12): p. 2090.
23. Rojek, A., et al., *A current view of the mammalian aquaglyceroporins.* Annu. Rev. Physiol., 2008. **70**: p. 301-327.
24. Yang, B. and A. Verkman, *Water and glycerol permeabilities of aquaporins 1–5 and MIP determined quantitatively by expression of epitope-tagged constructs inXenopus oocytes.* Journal of Biological Chemistry, 1997. **272**(26): p. 16140-16146.
25. Ishibashi, K., et al., *Cloning and functional expression of a new water channel abundantly expressed in the testis permeable to water, glycerol, and urea.* Journal of Biological Chemistry, 1997. **272**(33): p. 20782-20786.
26. Ishibashi, K., et al., *Cloning and functional expression of a new aquaporin (AQP9) abundantly expressed in the peripheral leukocytes permeable to water and urea, but not to glycerol.* Biochemical and biophysical research communications, 1998. **244**(1): p. 268-274.
27. Ishibashi, K., et al., *Cloning and identification of a new member of water channel (AQP10) as an aquaglyceroporin.* Biochimica et Biophysica Acta (BBA)-Gene Structure and Expression, 2002. **1576**(3): p. 335-340.
28. Miller, E.W., B.C. Dickinson, and C.J. Chang, *Aquaporin-3 mediates hydrogen peroxide uptake to regulate downstream intracellular signaling.* Proceedings of the National Academy of Sciences, 2010. **107**(36): p. 15681-15686.
29. Watanabe, S., et al., *Aquaporin-9 facilitates membrane transport of hydrogen peroxide in mammalian cells.* Biochemical and biophysical research communications, 2016. **471**(1): p. 191-197.
30. Liu, Z., et al., *Arsenite transport by mammalian aquaglyceroporins AQP7 and AQP9.* Proceedings of the National Academy of Sciences, 2002. **99**(9): p. 6053-6058.
31. Lee, T.-C., et al., *Enhanced expression of multidrug resistance-associated protein 2 and reduced expression of aquaglyceroporin 3 in an arsenic-resistant human cell line.* Journal of Biological Chemistry, 2006. **281**(27): p. 18401-18407.
32. Ishibashi, K., *New members of mammalian aquaporins: AQP10–AQP12.* Aquaporins, 2009: p. 251-262.
33. Yakata, K., K. Tani, and Y. Fujiyoshi, *Water permeability and characterization of aquaporin-11.* Journal of structural biology, 2011. **174**(2): p. 315-320.

34. Bjørkskov, F.B., et al., *Purification and functional comparison of nine human Aquaporins produced in Saccharomyces cerevisiae for the purpose of biophysical characterization.* Scientific reports, 2017. **7**(1): p. 16899.
35. Madeira, A., et al., *Human aquaporin-11 is a water and glycerol channel and localizes in the vicinity of lipid droplets in human adipocytes.* Obesity, 2014. **22**(9): p. 2010-2017.
36. Verkman, A. and A.K. Mitra, *Structure and function of aquaporin water channels.* American Journal of Physiology-Renal Physiology, 2000. **278**(1): p. F13-F28.
37. Jung, J.S., et al., *Molecular structure of the water channel through aquaporin CHIP. The hourglass model.* Journal of Biological Chemistry, 1994. **269**(20): p. 14648-14654.
38. Sui, H., et al., *Structural basis of water-specific transport through the AQP1 water channel.* Nature, 2001. **414**(6866): p. 872-878.
39. Jensen, M.Ø., E. Tajkhorshid, and K. Schulten, *The mechanism of glycerol conduction in aquaglyceroporins.* Structure, 2001. **9**(11): p. 1083-1093.
40. Hoffert, J.D., et al., *Quantitative phosphoproteomics of vasopressin-sensitive renal cells: regulation of aquaporin-2 phosphorylation at two sites.* Proceedings of the National Academy of Sciences, 2006. **103**(18): p. 7159-7164.
41. Nielsen, S., et al., *Vasopressin increases water permeability of kidney collecting duct by inducing translocation of aquaporin-CD water channels to plasma membrane.* Proceedings of the National Academy of Sciences, 1995. **92**(4): p. 1013-1017.
42. Cho, S.-J., et al., *Aquaporin 1 regulates GTP-induced rapid gating of water in secretory vesicles.* Proceedings of the National Academy of Sciences, 2002. **99**(7): p. 4720-4724.
43. Ferlay, J., et al., *Cancer incidence and mortality worldwide: sources, methods and major patterns in GLOBOCAN 2012.* International Journal of Cancer, 2015. **136**(5): p. E359-E386.
44. Miller, K.D., et al., *Cancer treatment and survivorship statistics, 2016.* CA: a cancer journal for clinicians, 2016. **66**(4): p. 271-289.
45. Koeller, J.M., et al., *Antiemetic guidelines: creating a more practical treatment approach.* Supportive Care in Cancer, 2002. **10**(7): p. 519-522.
46. Howard-Anderson, J., et al., *Quality of life, fertility concerns, and behavioral health outcomes in younger breast cancer survivors: a systematic review.* Journal of the National Cancer Institute, 2012. **104**(5): p. 386-405.
47. Wasilewski-Masker, K., et al., *Male infertility in long-term survivors of pediatric cancer: a report from the childhood cancer survivor study.* Journal of Cancer Survivorship, 2014. **8**(3): p. 437-447.
48. Rivera, E. and M. Cianfrocca, *Overview of neuropathy associated with taxanes for the treatment of metastatic breast cancer.* Cancer chemotherapy and pharmacology, 2015. **75**(4): p. 659-670.
49. Gamelin, E., et al. *Clinical aspects and molecular basis of oxaliplatin neurotoxicity: current management and development of preventive measures*. in *Seminars in oncology*. 2002. Elsevier.
50. Willemse, P., et al., *Prevalence of the metabolic syndrome and cardiovascular disease risk in chemotherapy-treated testicular germ cell tumour survivors.* British journal of cancer, 2013. **109**(1): p. 60-67.

51. Monsuez, J.-J., et al., *Cardiac side-effects of cancer chemotherapy.* International journal of cardiology, 2010. **144**(1): p. 3-15.
52. Gralow, J.R., et al., *NCCN task force report: bone health in cancer care.* Journal of the National Comprehensive Cancer Network, 2013. **11**(suppl 3): p. S-1-S-50.
53. Spano, D., et al. *Molecular networks that regulate cancer metastasis*. in *Seminars in cancer biology*. 2012. Elsevier.
54. Yamaguchi, H., J. Wyckoff, and J. Condeelis, *Cell migration in tumors.* Curr Opin Cell Biol, 2005. **17**(5): p. 559-564.
55. Pepper, M.S., et al., *Lymphangiogenesis and tumor metastasis.* Cell and tissue research, 2003. **314**(1): p. 167-177.
56. Wyckoff, J.B., et al., *A critical step in metastasis: in vivo analysis of intravasation at the primary tumor.* Cancer research, 2000. **60**(9): p. 2504-2511.
57. Tan, D.S., R. Agarwal, and S.B. Kaye, *Mechanisms of transcoelomic metastasis in ovarian cancer.* The lancet oncology, 2006. **7**(11): p. 925-934.
58. Nakhoul, N.L., et al., *Effect of expressing the water channel aquaporin-1 on the CO2 permeability of Xenopus oocytes.* American Journal of Physiology-Cell Physiology, 1998. **274**(2): p. C543-C548.
59. Herrera, M., N.J. Hong, and J.L. Garvin, *Aquaporin-1 transports NO across cell membranes.* Hypertension, 2006. **48**(1): p. 157-164.
60. Ma, T., et al., *Severely impaired urinary concentrating ability in transgenic mice lacking aquaporin-1 water channels.* J Biol Chem, 1998. **273**(8): p. 4296-9.
61. Schnermann, J., et al., *Defective proximal tubular fluid reabsorption in transgenic aquaporin-1 null mice.* Proceedings of the National Academy of Sciences, 1998. **95**(16): p. 9660-9664.
62. Zhang, D., L. Vetrivel, and A. Verkman, *Aquaporin deletion in mice reduces intraocular pressure and aqueous fluid production.* The Journal of general physiology, 2002. **119**(6): p. 561-569.
63. Oshio, K., et al., *Reduced cerebrospinal fluid production and intracranial pressure in mice lacking choroid plexus water channel Aquaporin-1.* The FASEB journal, 2005. **19**(1): p. 76-78.
64. Zhang, H. and A.S. Verkman, *Aquaporin-1 tunes pain perception by interaction with Nav1. 8 Na+ channels in dorsal root ganglion neurons.* Journal of Biological Chemistry, 2010. **285**(8): p. 5896-5906.
65. Saadoun, S., et al., *Increased aquaporin 1 water channel expression inhuman brain tumours.* Brit J Cancer, 2002. **87**(6): p. 621-623.
66. El Hindy, N., et al., *Correlation of aquaporin-1 water channel protein expression with tumor angiogenesis in human astrocytoma.* Anticancer Res, 2013. **33**(2): p. 609-13.
67. Endo, M., et al., *Water channel (aquaporin 1) expression and distribution in mammary carcinomas and glioblastomas.* Microvascular research, 1999. **58**(2): p. 89-98.
68. Hoque, M.O., et al., *Aquaporin 1 is overexpressed in lung cancer and stimulates NIH-3T3 cell proliferation and anchorage-independent growth.* Am J Pathol, 2006. **168**(4): p. 1345-1353.
69. Moon, C., et al., *Involvement of aquaporins in colorectal carcinogenesis.* Oncogene, 2003. **22**(43): p. 6699-6703.

70. Guan, B., et al., *Expression and distribution of aquaporin 1 in laryngeal carcinoma.* Lin Chuang Er Bi Yan Hou Tou Jing Wai Ke Za Zhi, 2007. **21**(6): p. 269-272.
71. Chen, Y., et al., *Increased expression of aquaporin 1 in human hemangioblastomas and its correlation with cyst formation.* Journal of neuro-oncology, 2006. **80**(3): p. 219-225.
72. Vacca, A., et al., *Microvessel overexpression of aquaporin 1 parallels bone marrow angiogenesis in patients with active multiple myeloma.* British journal of haematology, 2001. **113**(2): p. 415-421.
73. Rojek, A., et al., *Severe urinary concentrating defect in renal collecting duct-selective AQP2 conditional-knockout mice.* Proceedings of the National Academy of Sciences, 2006. **103**(15): p. 6037-6042.
74. Zou, L.-B., et al., *Identification of estrogen response element in the aquaporin-2 gene that mediates estrogen-induced cell migration and invasion in human endometrial carcinoma.* The Journal of Clinical Endocrinology & Metabolism, 2011. **96**(9): p. E1399-E1408.
75. Echevarria, M., et al., *Cloning and expression of AQP3, a water channel from the medullary collecting duct of rat kidney.* Proceedings of the National Academy of Sciences, 1994. **91**(23): p. 10997-11001.
76. Ishibashi, K., et al., *Molecular cloning and expression of a member of the aquaporin family with permeability to glycerol and urea in addition to water expressed at the basolateral membrane of kidney collecting duct cells.* Proceedings of the National Academy of Sciences, 1994. **91**(14): p. 6269-6273.
77. Holm, L.M., et al., *NH3 and NH4+ permeability in aquaporin-expressing Xenopus oocytes.* Pflügers Archiv, 2005. **450**(6): p. 415-428.
78. Ma, T., et al., *Nephrogenic diabetes insipidus in mice lacking aquaporin-3 water channels.* Proceedings of the National Academy of Sciences, 2000. **97**(8): p. 4386-4391.
79. Ma, T., et al., *Impaired stratum corneum hydration in mice lacking epidermal water channel aquaporin-3.* Journal of Biological Chemistry, 2002. **277**(19): p. 17147-17153.
80. Hara-Chikuma, M. and A. Verkman, *Aquaporin-3 facilitates epidermal cell migration and proliferation during wound healing.* Journal of Molecular Medicine, 2008. **86**(2): p. 221-231.
81. Liu, Y.L., et al., *Expression of aquaporin 3 (AQP3) in normal and neoplastic lung tissues.* Human pathology, 2007. **38**(1): p. 171-178.
82. Guo, X., et al., *Prognostic value of combined aquaporin 3 and aquaporin 5 overexpression in hepatocellular carcinoma.* BioMed research international, 2013. **2013**.
83. Shen, L., et al., *Expression profile of multiple aquaporins in human gastric carcinoma and its clinical significance.* Biomed Pharmacother, 2010. **64**(5): p. 313-8.
84. Hwang, I., et al., *Expression and Localization of Aquaporins in Benign Prostate Hyperplasia and Prostate Cancer.* Chonnam Med J, 2012. **48**(3): p. 174-178.
85. Kusayama, M., et al., *Critical role of aquaporin 3 on growth of human esophageal and oral squamous cell carcinoma.* Cancer science, 2011. **102**(6): p. 1128-1136.

86. Hara-Chikuma, M. and A. Verkman, *Prevention of skin tumorigenesis and impairment of epidermal cell proliferation by targeted aquaporin-3 gene disruption.* Molecular and cellular biology, 2008. **28**(1): p. 326-332.
87. Ji, C., et al., *Curcumin attenuates EGF-induced AQP3 up-regulation and cell migration in human ovarian cancer cells.* Cancer chemotherapy and pharmacology, 2008. **62**(5): p. 857-865.
88. Direito, I., et al., *Differential expression of aquaporin-3 and aquaporin-5 in pancreatic ductal adenocarcinoma.* Journal of surgical oncology, 2017. **115**(8): p. 980-996.
89. Mobasheri, A. and R. Barrett-Jolley, *Aquaporin water channels in the mammary gland: from physiology to pathophysiology and neoplasia.* Journal of mammary gland biology and neoplasia, 2014. **19**(1): p. 91-102.
90. Ma, T., et al., *Generation and phenotype of a transgenic knockout mouse lacking the mercurial-insensitive water channel aquaporin-4.* Journal of Clinical Investigation, 1997. **100**(5): p. 957.
91. Manley, G.T., et al., *Aquaporin-4 deletion in mice reduces brain edema after acute water intoxication and ischemic stroke.* Nat Med, 2000. **6**(2): p. 159-63.
92. Binder, D.K., et al., *Increased seizure duration and slowed potassium kinetics in mice lacking aquaporin-4 water channels.* Glia, 2006. **53**(6): p. 631-636.
93. Saadoun, S., et al., *Involvement of aquaporin-4 in astroglial cell migration and glial scar formation.* Journal of cell science, 2005. **118**(24): p. 5691-5698.
94. Saadoun, S., et al., *Aquaporin-4 expression is increased in oedematous human brain tumours.* J Neurol Neurosurg Psychiatry, 2002. **72**(2): p. 262-265.
95. Ng, W.H., et al., *Aquaporin-4 expression is increased in edematous meningiomas.* Journal of Clinical Neuroscience, 2009. **16**(3): p. 441-443.
96. Ma, T., et al., *Defective secretion of saliva in transgenic mice lacking aquaporin-5 water channels.* Journal of Biological Chemistry, 1999. **274**(29): p. 20071-20074.
97. Song, Y. and A. Verkman, *Aquaporin-5 dependent fluid secretion in airway submucosal glands.* Journal of Biological Chemistry, 2001. **276**(44): p. 41288-41292.
98. Li, J., et al., *Over-expression of a poor prognostic marker in prostate cancer: AQP5 promotes cells growth and local invasion.* World journal of surgical oncology, 2014. **12**(1): p. 284.
99. Chae, Y.K., et al., *Human AQP5 plays a role in the progression of chronic myelogenous leukemia (CML).* PLoS One, 2008. **3**(7): p. e2594.
100. Wang, W., et al., *Expression of AQP5 and AQP8 in human colorectal carcinoma and their clinical significance.* World journal of surgical oncology, 2012. **10**(1): p. 242.
101. Chae, Y.K., et al., *Expression of aquaporin 5 (AQP5) promotes tumor invasion in human non small cell lung cancer.* PLoS One, 2008. **3**(5): p. e2162.
102. Zhang, T., et al., *Overexpression of AQP5 in cervical cancer: correlation with clinicopathological features and prognosis.* Medical oncology, 2012. **29**(3): p. 1998-2004.

103. Jung, H.J., et al., *Aquaporin-5: a marker protein for proliferation and migration of human breast cancer cells.* PloS one, 2011. **6**(12): p. e28492.
104. Saparov, S.M., et al., *Fast and selective ammonia transport by aquaporin-8.* Journal of Biological Chemistry, 2007. **282**(8): p. 5296-5301.
105. Calamita, G., et al., *Expression and subcellular localization of the AQP8 and AQP1 water channels in the mouse gall-bladder epithelium.* Biology of the Cell, 2005. **97**(6): p. 415-423.
106. Yamamoto, T., H. Kuramoto, and M. Kadowaki, *Downregulation in aquaporin 4 and aquaporin 8 expression of the colon associated with the induction of allergic diarrhea in a mouse model of food allergy.* Life sciences, 2007. **81**(2): p. 115-120.
107. Shi, Y.-H., et al., *Aquaporin 8 involvement in human cervical cancer SiHa migration via the EGFR-Erk1/2 pathway.* Asian Pacific journal of cancer prevention: APJCP, 2014. **15**(15): p. 6391-6395.
108. Shi, Y.-H., et al., *Significance and expression of aquaporin 1, 3, 8 in cervical carcinoma in Xinjiang Uygur women of China.* Asian Pacific Journal of Cancer Prevention, 2012. **13**(5): p. 1971-1975.
109. Tsukaguchi, H., et al., *Molecular characterization of a broad selectivity neutral solute channel.* Journal of Biological Chemistry, 1998. **273**(38): p. 24737-24743.
110. Kuriyama, H., et al., *Coordinated Regulation of Fat-Specific and Liver-Specific Glycerol Channels, Aquaporin Adipose and Aquaporin 9.* Diabetes, 2002. **51**(10): p. 2915-2921.
111. Maeda, N., T. Hibuse, and T. Funahashi, *Role of aquaporin-7 and aquaporin-9 in glycerol metabolism; involvement in obesity*, in *Aquaporins*. 2009, Springer. p. 233-249.
112. Rojek, A.M., et al., *Defective glycerol metabolism in aquaporin 9 (AQP9) knockout mice.* Proceedings of the National Academy of Sciences, 2007. **104**(9): p. 3609-3614.
113. Carbrey, J.M., et al., *Reduced arsenic clearance and increased toxicity in aquaglyceroporin-9-null mice.* Proceedings of the National Academy of Sciences, 2009. **106**(37): p. 15956-15960.
114. Leung, J., et al., *Relationship of expression of aquaglyceroporin 9 with arsenic uptake and sensitivity in leukemia cells.* Blood, 2007. **109**(2): p. 740-746.
115. Bhattacharjee, H., et al., *Drug uptake and pharmacological modulation of drug sensitivity in leukemia by AQP9.* Biochemical and Biophysical Research Communications, 2004. **322**(3): p. 836-841.
116. Fossdal, G., et al., *Aqp 9 and brain tumour stem cells.* The Scientific World Journal, 2012. **2012**.
117. Tan, G., S. Sun, and D. Yuan, *Expression of the water channel protein aquaporin-9 in human astrocytic tumours: correlation with pathological grade.* Journal of International Medical Research, 2008. **36**(4): p. 777-782.
118. Chen, Q., et al., *Effect of AQP9 Expression in Androgen-Independent Prostate Cancer Cell PC3.* International journal of molecular sciences, 2016. **17**(5): p. 738.
119. Vićovac, L. and J. Aplin, *Epithelial-mesenchymal transition during trophoblast differentiation.* Cells Tissues Organs, 1996. **156**(3): p. 202-216.
120. Thiery, J.P., *Epithelial–mesenchymal transitions in tumour progression.* Nature Reviews Cancer, 2002. **2**(6): p. 442-454.

121. Kalluri, R. and R.A. Weinberg, *The basics of epithelial-mesenchymal transition.* The Journal of clinical investigation, 2009. **119**(6): p. 1420.
122. Thiery, J.P., *Epithelial–mesenchymal transitions in development and pathologies.* Current opinion in cell biology, 2003. **15**(6): p. 740-746.
123. Cavallaro, U. and G. Christofori, *Cell adhesion and signalling by cadherins and Ig-CAMs in cancer.* Nature Reviews Cancer, 2004. **4**(2): p. 118-132.
124. van Zijl, F., G. Krupitza, and W. Mikulits, *Initial steps of metastasis: cell invasion and endothelial transmigration.* Mutation Research/Reviews in Mutation Research, 2011. **728**(1): p. 23-34.
125. Angst, B.D., C. Marcozzi, and A.I. Magee, *The cadherin superfamily: diversity in form and function.* Journal of cell science, 2001. **114**(4): p. 629-641.
126. Alizadeh, A.M., S. Shiri, and S. Farsinejad, *Metastasis review: from bench to bedside.* Tumor Biology, 2014. **35**(9): p. 8483-8523.
127. Cano, A., et al., *The transcription factor snail controls epithelial–mesenchymal transitions by repressing E-cadherin expression.* Nature cell biology, 2000. **2**(2): p. 76-83.
128. Chua, H., et al., *NF-κB represses E-cadherin expression and enhances epithelial to mesenchymal transition of mammary epithelial cells: potential involvement of ZEB-1 and ZEB-2.* Oncogene, 2007. **26**(5): p. 711-724.
129. Korpal, M., et al., *The miR-200 family inhibits epithelial-mesenchymal transition and cancer cell migration by direct targeting of E-cadherin transcriptional repressors ZEB1 and ZEB2.* Journal of Biological Chemistry, 2008. **283**(22): p. 14910-14914.
130. Miettinen, P.J., et al., *TGF-beta induced transdifferentiation of mammary epithelial cells to mesenchymal cells: involvement of type I receptors.* The Journal of cell biology, 1994. **127**(6): p. 2021-2036.
131. Xu, J., S. Lamouille, and R. Derynck, *TGF-β-induced epithelial to mesenchymal transition.* Cell research, 2009. **19**(2): p. 156-172.
132. Lo, H.-W., et al., *Epidermal growth factor receptor cooperates with signal transducer and activator of transcription 3 to induce epithelial-mesenchymal transition in cancer cells via up-regulation of TWIST gene expression.* Cancer research, 2007. **67**(19): p. 9066-9076.
133. Kong, D., et al., *miR-200 Regulates PDGF-D-Mediated Epithelial–Mesenchymal Transition, Adhesion, and Invasion of Prostate Cancer Cells.* Stem cells, 2009. **27**(8): p. 1712-1721.
134. Pagan, R., et al., *Effects of growth and differentiation factors on the epithelial-mesenchymal transition in cultured neonatal rat hepatocytes.* Journal of hepatology, 1999. **31**(5): p. 895-904.
135. Yang, J., et al., *Twist, a master regulator of morphogenesis, plays an essential role in tumor metastasis.* cell, 2004. **117**(7): p. 927-939.
136. Medici, D., E.D. Hay, and B.R. Olsen, *Snail and Slug promote epithelial-mesenchymal transition through β-catenin–T-cell factor-4-dependent expression of transforming growth factor-β3.* Molecular biology of the cell, 2008. **19**(11): p. 4875-4887.
137. Li, A., et al., *Critical role of aquaporin-3 in epidermal growth factor-induced migration of colorectal carcinoma cells and its clinical significance.* Oncology reports, 2013. **29**(2): p. 535-540.
138. Huang, Y., et al., *Critical role of aquaporin-3 in the human epidermal growth factor-induced migration and proliferation in the human gastric*

adenocarcinoma cells. Cancer biology & therapy, 2010. **9**(12): p. 1000-1007.
139. Liu, W., et al., *Epidermal growth factor enhances MPC-83 pancreatic cancer cell migration through the upregulation of aquaporin 3.* Molecular medicine reports, 2012. **6**(3): p. 607-610.
140. Chen, J., et al., *Aquaporin 3 promotes epithelial-mesenchymal transition in gastric cancer.* Journal of Experimental & Clinical Cancer Research, 2014. **33**(1): p. 38.
141. Yun, S., et al., *Aquaporin 1 Is an Independent Marker of Poor Prognosis in Lung Adenocarcinoma.* Journal of pathology and translational medicine, 2016. **50**(4): p. 251.
142. Ding, T., et al., *Role of aquaporin-4 in the regulation of migration and invasion of human glioma cells.* International journal of oncology, 2011. **38**(6): p. 1521-1531.
143. Li, Y., S. Sun, and X. Han, *Down-regulation of AQP4 Inhibits Proliferation, Migration and Invasion of Human Breast Cancer Cells.* Folia biologica, 2016. **62**(3): p. 131-137.
144. Nicchia, G.P., et al., *New possible roles for aquaporin-4 in astrocytes: cell cytoskeleton and functional relationship with connexin43.* The FASEB journal, 2005. **19**(12): p. 1674-1676.
145. McCoy, E. and H. Sontheimer, *Expression and function of water channels (aquaporins) in migrating malignant astrocytes.* Glia, 2007. **55**(10): p. 1034-43.
146. Zhang, H. and A. Verkman, *Evidence against involvement of aquaporin-4 in cell–cell adhesion.* Journal of molecular biology, 2008. **382**(5): p. 1136-1143.
147. Guarino, M., B. Rubino, and G. Ballabio, *The role of epithelial-mesenchymal transition in cancer pathology.* Pathology, 2007. **39**(3): p. 305-318.
148. Chen, C., et al., *Down-regulation of aquaporin 5-mediated epithelial-mesenchymal transition and anti-metastatic effect by natural product Cairicoside E in colorectal cancer.* Molecular carcinogenesis, 2017. **56**(12): p. 2692-2705.
149. Zhang, W.-g., et al., *Aquaporin 9 is down-regulated in hepatocellular carcinoma and its over-expression suppresses hepatoma cell invasion through inhibiting epithelial-to-mesenchymal transition.* Cancer letters, 2016. **378**(2): p. 111-119.
150. Li, C.-F., et al., *Aquaporin 9 inhibits hepatocellular carcinoma through up-regulating FOXO1 expression.* Oncotarget, 2016. **7**(28): p. 44161-44170.
151. Klausen, M., et al., *Involvement of bacterial migration in the development of complex multicellular structures in Pseudomonas aeruginosa biofilms.* Molecular microbiology, 2003. **50**(1): p. 61-68.
152. Friedl, P., Y. Hegerfeldt, and M. Tusch, *Collective cell migration in morphogenesis and cancer.* International Journal of Developmental Biology, 2004. **48**: p. 441-450.
153. Friedl, P. and B. Weigelin, *Interstitial leukocyte migration and immune function.* Nature immunology, 2008. **9**(9): p. 960-969.
154. Dittmar, T., et al., *Adhesion molecules and chemokines: the navigation system for circulating tumor (stem) cells to metastasize in an organ-specific manner.* Clinical & experimental metastasis, 2008. **25**(1): p. 11-32.

155. Roussos, E.T., J.S. Condeelis, and A. Patsialou, *Chemotaxis in cancer*. Nature Reviews Cancer, 2011. **11**(8): p. 573.
156. Hara-Chikuma, M., S. Watanabe, and H. Satooka, *Involvement of aquaporin-3 in epidermal growth factor receptor signaling via hydrogen peroxide transport in cancer cells.* Biochemical and biophysical research communications, 2016. **471**(4): p. 603-609.
157. Rhee, S.G., *H2O2, a necessary evil for cell signaling.* Science, 2006. **312**(5782): p. 1882-1883.
158. Thannickal, V.J. and B.L. Fanburg, *Reactive oxygen species in cell signaling.* American Journal of Physiology-Lung Cellular and Molecular Physiology, 2000. **279**(6): p. L1005-L1028.
159. Satooka, H. and M. Hara-Chikuma, *Aquaporin-3 controls breast cancer cell migration by regulating hydrogen peroxide transport and its downstream cell signaling.* Molecular and cellular biology, 2016. **36**(7): p. 1206-1218.
160. Hara-Chikuma, M., et al., *Chemokine-dependent T cell migration requires aquaporin-3–mediated hydrogen peroxide uptake.* Journal of Experimental Medicine, 2012. **209**(10): p. 1743-1752.
161. Hu, J. and A.S. Verkman, *Increased migration and metastatic potential of tumor cells expressing aquaporin water channels.* FASEB J, 2006. **20**(11): p. 1892-4.
162. Chen, J., et al., *Aquaporin 3 promotes prostate cancer cell motility and invasion via extracellular signal-regulated kinase 1/2-mediated matrix metalloproteinase-3 secretion.* Molecular medicine reports, 2015. **11**(4): p. 2882-2888.
163. Shi, Y.-H., et al., *Increased migration and local invasion potential of SiHa cervical cancer cells expressing Aquaporin 8.* Asian Pac J Cancer Prev, 2013. **14**(3): p. 1825-1828.
164. Drubin, D.G. and W.J. Nelson, *Origins of cell polarity.* Cell, 1996. **84**(3): p. 335-344.
165. Swaney, K.F., C.-H. Huang, and P.N. Devreotes, *Eukaryotic chemotaxis: a network of signaling pathways controls motility, directional sensing, and polarity.* Annual review of biophysics, 2010. **39**: p. 265.
166. Johnson, D.I. and J.R. Pringle, *Molecular characterization of CDC42, a Saccharomyces cerevisiae gene involved in the development of cell polarity.* The Journal of cell biology, 1990. **111**(1): p. 143-152.
167. Allen, W.E., et al., *A role for Cdc42 in macrophage chemotaxis.* The Journal of cell biology, 1998. **141**(5): p. 1147-1157.
168. Goldstein, B. and I.G. Macara, *The PAR proteins: fundamental players in animal cell polarization.* Developmental cell, 2007. **13**(5): p. 609-622.
169. Etienne-Manneville, S. and A. Hall, *Cell polarity: Par6, aPKC and cytoskeletal crosstalk.* Current opinion in cell biology, 2003. **15**(1): p. 67-72.
170. Papadopoulos, M., S. Saadoun, and A. Verkman, *Aquaporins and cell migration.* Pflug Arch Eur J Phy, 2008. **456**(4): p. 693-700.
171. Verkman, A., *More than just water channels: unexpected cellular roles of aquaporins.* Journal of cell science, 2005. **118**(15): p. 3225-3232.
172. Hara-Chikuma, M. and A.S. Verkman, *Aquaporin-1 facilitates epithelial cell migration in kidney proximal tubule.* J Am Soc Nephrol, 2006. **17**(1): p. 39-45.

173. Loitto, V.-M., et al., *Neutrophil leukocyte motility requires directed water influx.* Journal of leukocyte biology, 2002. **71**(2): p. 212-222.
174. Stroka, K.M., et al., *Water permeation drives tumor cell migration in confined microenvironments.* Cell, 2014. **157**(3): p. 611-623.
175. Schwab, A., et al., *Cells move when ions and water flow.* Pflug Arch Eur J Phy, 2007. **453**(4): p. 421-432.
176. Pollard, T.D. and G.G. Borisy, *Cellular motility driven by assembly and disassembly of actin filaments.* Cell, 2003. **112**(4): p. 453-465.
177. Wang, Y.-L., *Exchange of actin subunits at the leading edge of living fibroblasts: possible role of treadmilling.* The Journal of cell biology, 1985. **101**(2): p. 597-602.
178. Theriot, J.A. and T.J. Mitchison, *Actin microfilament dynamics in locomoting cells.* Nature, 1991. **352**(6331): p. 126-131.
179. Fletcher, S.J. and J.Z. Rappoport, *Moving forward: polarised trafficking in cell migration.* Trends in cell biology, 2010. **20**(2): p. 71-78.
180. Pierini, L.M., et al., *Oriented endocytic recycling of α5β1 in motile neutrophils.* Blood, 2000. **95**(8): p. 2471-2480.
181. Bretscher, M.S. and C. Aguado-Velasco, *Membrane traffic during cell locomotion.* Current opinion in cell biology, 1998. **10**(4): p. 537-541.
182. Cramer, L.P., M. Siebert, and T.J. Mitchison, *Identification of novel graded polarity actin filament bundles in locomoting heart fibroblasts: implications for the generation of motile force.* The Journal of cell biology, 1997. **136**(6): p. 1287-1305.
183. Mattila, P.K. and P. Lappalainen, *Filopodia: molecular architecture and cellular functions.* Nature reviews Molecular cell biology, 2008. **9**(6): p. 446-454.
184. Ridley, A.J., et al., *The small GTP-binding protein rac regulates growth factor-induced membrane ruffling.* Cell, 1992. **70**(3): p. 401-410.
185. Hall, A., *Rho GTPases and the actin cytoskeleton.* Science, 1998. **279**(5350): p. 509-514.
186. Allen, W.E., et al., *Rho, Rac and Cdc42 regulate actin organization and cell adhesion in macrophages.* Journal of cell science, 1997. **110**(6): p. 707-720.
187. Machesky, L.M., *Lamellipodia and filopodia in metastasis and invasion.* FEBS letters, 2008. **582**(14): p. 2102-2111.
188. Price, L.S., et al., *Activation of Rac and Cdc42 by integrins mediates cell spreading.* Molecular biology of the cell, 1998. **9**(7): p. 1863-1871.
189. Loitto, V.M., et al., *Filopodia are induced by aquaporin-9 expression.* Experimental cell research, 2007. **313**(7): p. 1295-1306.
190. Ibarra, N., A. Pollitt, and R. Insall, *Regulation of actin assembly by SCAR/WAVE proteins.* 2005, Portland Press Limited.
191. Weaver, A.M., *Invadopodia: specialized cell structures for cancer invasion.* Clinical & experimental metastasis, 2006. **23**(2): p. 97-105.
192. Condeelis, J., *Life at the leading edge: the formation of cell protrusions.* Annual review of cell biology, 1993. **9**(1): p. 411-444.
193. Diez, S., et al., *Subsecond reorganization of the actin network in cell motility and chemotaxis.* P Natl Acad Sci USA, 2005. **102**(21): p. 7601-7606.
194. Disanza, A., et al., *Actin polymerization machinery: the finish line of signaling networks, the starting point of cellular movement.* Cell Mol Life Sci, 2005. **62**(9): p. 955-970.

195. Monzani, E., et al., *AQP1 is not only a water channel: it contributes to cell migration through Lin7/beta-catenin.* PLoS One, 2009. **4**(7): p. e6167.
196. Pelagalli, A., et al., *Inhibition of AQP1 hampers osteosarcoma and hepatocellular carcinoma progression mediated by bone marrow-derived mesenchymal stem cells.* International journal of molecular sciences, 2016. **17**(7): p. 1102.
197. Klebe, S., et al., *Blockade of aquaporin 1 inhibits proliferation, motility, and metastatic potential of mesothelioma in vitro but not in an in vivo model.* Disease markers, 2015. **2015**.
198. Wei, X. and J. Dong, *Aquaporin 1 promotes the proliferation and migration of lung cancer cell in vitro.* Oncology reports, 2015. **34**(3): p. 1440-1448.
199. Jiang, Y. and Z.-B. Jiang, *Aquaporin 1-expressing MCF-7 mammary carcinoma cells show enhanced migration in vitro.* Journal of Biomedical Science and Engineering, 2010. **3**(01): p. 95.
200. Jiang, Y., *Aquaporin-1 activity of plasma membrane affects HT20 colon cancer cell migration.* IUBMB Life, 2009. **61**(10): p. 1001-9.
201. Yu, J., et al., *Mechanism of gating and ion conductivity of a possible tetrameric pore in aquaporin-1.* Structure, 2006. **14**(9): p. 1411-23.
202. Kourghi, M., et al., *Bumetanide Derivatives AqB007 and AqB011 Selectively Block the Aquaporin-1 ion Channel Conductance and Slow Cancer Cell Migration.* Molecular pharmacology, 2015: p. mol. 115.101618.
203. Sekine, S., et al., *Expression Analysis of Aquaporin-1 (Aqp-1) in Human Biliary Tract Carcinoma.* Journal of Cancer Therapy, 2016. **7**(01): p. 17.
204. Aishima, S., et al., *Down-regulation of aquaporin-1 in intrahepatic cholangiocarcinoma is related to tumor progression and mucin expression.* Human pathology, 2007. **38**(12): p. 1819-1825.
205. Sudo, K., et al., *Identification of a cell polarity-related protein, Lin-7B, as a binding partner for a Rho effector, Rhotekin, and their possible interaction in neurons.* Neuroscience research, 2006. **56**(4): p. 347-355.
206. McCoy, E.S., B.R. Haas, and H. Sontheimer, *Water permeability through aquaporin-4 is regulated by protein kinase C and becomes rate-limiting for glioma invasion.* Neuroscience, 2010. **168**(4): p. 971-981.
207. Mcferrin, M.B. and H. Sontheimer, *A role for ion channels in glioma cell invasion.* Neuron glia biology, 2006. **2**(1): p. 39-49.
208. Neely, J.D., et al., *Syntrophin-dependent expression and localization of Aquaporin-4 water channel protein.* Proceedings of the National Academy of Sciences, 2001. **98**(24): p. 14108-14113.
209. Kang, B.W., et al., *Expression of aquaporin-1, aquaporin-3, and aquaporin-5 correlates with nodal metastasis in colon cancer.* Oncology, 2015. **88**(6): p. 369-376.
210. Zhang, Z., et al., *Expression of aquaporin 5 increases proliferation and metastasis potential of lung cancer.* J Pathol, 2010. **221**(2): p. 210-20.
211. Kang, S.K., et al., *Role of human aquaporin 5 in colorectal carcinogenesis.* The American journal of pathology, 2008. **173**(2): p. 518-525.
212. Vicent, S., et al., *ERK1/2 is activated in non-small-cell lung cancer and associated with advanced tumours.* British journal of cancer, 2004. **90**(5): p. 1047.

213. Chen, Z., et al., *Impaired migration and cell volume regulation in aquaporin 5-deficient SPC-A1 cells.* Respiratory physiology & neurobiology, 2011. **176**(3): p. 110-117.
214. Curtis, A., *The mechanism of adhesion of cells to glass A study by interference reflection microscopy.* The Journal of cell biology, 1964. **20**(2): p. 199-215.
215. Vicente-Manzanares, M. and A.R. Horwitz, *Cell migration: an overview*, in *Cell Migration*. 2011, Springer. p. 1-24.
216. Ridley, A.J., et al., *Cell migration: integrating signals from front to back.* Science, 2003. **302**(5651): p. 1704-1709.
217. Geiger, B., et al., *Transmembrane crosstalk between the extracellular matrix and the cytoskeleton.* Nature Reviews Molecular Cell Biology, 2001. **2**(11): p. 793-805.
218. Martin, K.H., et al., *Integrin connections map: to infinity and beyond.* Science, 2002. **296**(5573): p. 1652-1653.
219. Meng, F., et al., *Aqp1 enhances migration of bone marrow mesenchymal stem cells through regulation of FAK and beta-catenin.* Stem Cells Dev, 2014. **23**(1): p. 66-75.
220. Schaller, M.D., et al., *pp125FAK a structurally distinctive protein-tyrosine kinase associated with focal adhesions.* Proceedings of the National Academy of Sciences, 1992. **89**(11): p. 5192-5196.
221. McLean, G.W., et al., *The role of focal-adhesion kinase in cancer—a new therapeutic opportunity.* Nature Reviews Cancer, 2005. **5**(7): p. 505.
222. Zhao, X. and J.-L. Guan, *Focal adhesion kinase and its signaling pathways in cell migration and angiogenesis.* Advanced drug delivery reviews, 2011. **63**(8): p. 610-615.
223. Chen, Y., et al., *Aquaporin 2 promotes cell migration and epithelial morphogenesis.* Journal of the American Society of Nephrology, 2012: p. ASN. 2012010079.
224. Brinckerhoff, C.E. and L.M. Matrisian, *Matrix metalloproteinases: a tail of a frog that became a prince.* Nature reviews Molecular cell biology, 2002. **3**(3): p. 207-214.
225. Mott, J.D. and Z. Werb, *Regulation of matrix biology by matrix metalloproteinases.* Current opinion in cell biology, 2004. **16**(5): p. 558-564.
226. Friedl, P. and K. Wolf, *Proteolytic interstitial cell migration: a five-step process.* Cancer and Metastasis Reviews, 2009. **28**(1-2): p. 129-135.
227. Wolf, K., et al., *Multi-step pericellular proteolysis controls the transition from individual to collective cancer cell invasion.* Nature cell biology, 2007. **9**(8): p. 893-904.
228. Netzel-Arnett, S., et al., *Membrane anchored serine proteases: a rapidly expanding group of cell surface proteolytic enzymes with potential roles in cancer.* Cancer and Metastasis Reviews, 2003. **22**(2-3): p. 237-258.
229. Nagase, H. and J.F. Woessner, *Matrix metalloproteinases.* Journal of Biological chemistry, 1999. **274**(31): p. 21491-21494.
230. Xu, H., et al., *Aquaporin-3 positively regulates matrix metalloproteinases via PI3K/AKT signal pathway in human gastric carcinoma SGC7901 cells.* Journal of Experimental & Clinical Cancer Research, 2011. **30**(1): p. 86.

231. Xiong, G., et al., *RNA interference influenced the proliferation and invasion of XWLC-05 lung cancer cells through inhibiting aquaporin 3.* Biochemical and Biophysical Research Communications, 2017. **485**(3): p. 627-634.
232. Xia, H., et al., *Aquaporin 3 knockdown suppresses tumour growth and angiogenesis in experimental non-small cell lung cancer.* Experimental physiology, 2014. **99**(7): p. 974-984.
233. Vicente-Manzanares, M., et al., *Non-muscle myosin II takes centre stage in cell adhesion and migration.* Nature reviews Molecular cell biology, 2009. **10**(11): p. 778-790.
234. Chrzanowska-Wodnicka, M. and K. Burridge, *Rho-stimulated contractility drives the formation of stress fibers and focal adhesions.* The Journal of cell biology, 1996. **133**(6): p. 1403-1415.
235. Huttenlocher, A., et al., *Regulation of cell migration by the calcium-dependent protease calpain.* Journal of Biological Chemistry, 1997. **272**(52): p. 32719-32722.
236. Palecek, S.P., et al., *Physical and biochemical regulation of integrin release during rear detachment of migrating cells.* Journal of Cell Science, 1998. **111**(7): p. 929-940.
237. Preston, G.M., et al., *The mercury-sensitive residue at cysteine 189 in the CHIP28 water channel.* Journal of Biological Chemistry, 1993. **268**(1): p. 17-20.
238. Martins, A.P., et al., *Aquaporin inhibition by gold (III) compounds: new insights.* ChemMedChem, 2013. **8**(7): p. 1086-1092.
239. Bing, M., et al., *Effects of acetazolamide and anordiol on osmotic water permeability in AQP1-cRNA injected Xenopus oocyte.* Acta Pharmacol Sin, 2004. **25**: p. 90-97.
240. Gao, J., et al., *Acetazolamide inhibits osmotic water permeability by interaction with aquaporin-1.* Analytical biochemistry, 2006. **350**(2): p. 165-170.
241. Brooks, H.L., J.W. Regan, and A.J. Yool, *Inhibition of aquaporin-1 water permeability by tetraethylammonium: involvement of the loop E pore region.* Mol Pharmacol, 2000. **57**(5): p. 1021-6.
242. Huber, V.J., et al., *Inhibition of aquaporin 4 by antiepileptic drugs.* Bioorganic & medicinal chemistry, 2009. **17**(1): p. 418-424.
243. Detmers, F.J., et al., *Quaternary ammonium compounds as water channel blockers. Specificity, potency, and site of action.* J Biol Chem, 2006. **281**(20): p. 14207-14.
244. Martins, A.P., et al., *Targeting aquaporin function: potent inhibition of aquaglyceroporin-3 by a gold-based compound.* PloS one, 2012. **7**(5): p. e37435.
245. Seeliger, D., et al., *Discovery of novel human aquaporin-1 blockers.* ACS chemical biology, 2012. **8**(1): p. 249-256.
246. Yool, A.J., *Functional domains of aquaporin-1: keys to physiology, and targets for drug discovery.* Curr Pharm Des, 2007. **13**(31): p. 3212-21.
247. Niemietz, C.M. and S.D. Tyerman, *New potent inhibitors of aquaporins: silver and gold compounds inhibit aquaporins of plant and human origin.* FEBS letters, 2002. **531**(3): p. 443-447.
248. Wu, B., et al., *A yeast-based phenotypic screen for aquaporin inhibitors.* Pflügers Archiv-European Journal of Physiology, 2008. **456**(4): p. 717-720.

249. Tanimura, Y., Y. Hiroaki, and Y. Fujiyoshi, *Acetazolamide reversibly inhibits water conduction by aquaporin-4.* Journal of structural biology, 2009. **166**(1): p. 16-21.
250. Yang, B., J.K. Kim, and A. Verkman, *Comparative efficacy of HgCl2 with candidate aquaporin-1 inhibitors DMSO, gold, TEA+ and acetazolamide.* FEBS letters, 2006. **580**(28-29): p. 6679-6684.
251. Søgaard, R. and T. Zeuthen, *Test of blockers of AQP1 water permeability by a high-resolution method: no effects of tetraethylammonium ions or acetazolamide.* Pflügers Archiv-European Journal of Physiology, 2008. **456**(2): p. 285-292.
252. Xiang, Y., et al., *Acetazolamide inhibits aquaporin-1 protein expression and angiogenesis.* Acta Pharmacologica Sinica, 2004. **25**: p. 812-816.
253. Xiang, Y., et al., *Acetazolamide suppresses tumor metastasis and related protein expression in mice bearing Lewis lung carcinoma.* Acta pharmacologica Sinica, 2002. **23**(8): p. 745-751.
254. Bin, K. and Z. Shi-Peng, *Acetazolamide inhibits aquaporin-1 expression and colon cancer xenograft tumor growth.* Hepato-gastroenterology, 2011. **58**(110-111): p. 1502-1506.
255. Bing, M., et al., *Inhibitory effect of topiramate on Lewis lung carcinoma metastasis and its relation with AQP1 water channel.* Acta Pharmacol Sin, 2004. **25**(1): p. 54-60.
256. Yool, A., et al., *Tetraethylammonium block of water flux in Aquaporin-1 channels expressed in kidney thin limbs of Henle's loop and a kidney-derived cell line.* BMC Physiology, 2002. **2**: p. 4.
257. Migliati, E., et al., *Inhibition of aquaporin-1 and aquaporin-4 water permeability by a derivative of the loop diuretic bumetanide acting at an internal pore-occluding binding site.* Mol Pharmacol, 2009. **76**(1): p. 105-12.
258. Dorward, H.S., et al., *Pharmacological blockade of aquaporin-1 water channel by AqB013 restricts migration and invasiveness of colon cancer cells and prevents endothelial tube formation in vitro.* Journal of Experimental & Clinical Cancer Research, 2016. **35**(1): p. 36.
259. Musa-Aziz, R., et al., *Relative CO2/NH3 selectivities of AQP1, AQP4, AQP5, AmtB, and RhAG.* Proceedings of the National Academy of Sciences, 2009. **106**(13): p. 5406-5411.
260. Tsunoda, S.P., et al., *Aquaporin-1, nothing but a water channel.* J Biol Chem, 2004. **279**(12): p. 11364-11367.
261. Yang, B., et al., *Carbon dioxide permeability of aquaporin-1 measured in erythrocytes and lung of aquaporin-1 null mice and in reconstituted proteoliposomes.* Journal of Biological Chemistry, 2000. **275**(4): p. 2686-2692.
262. Fang, X., et al., *Evidence against aquaporin-1-dependent CO2 permeability in lung and kidney.* The Journal of physiology, 2002. **542**(1): p. 63-69.
263. Agre, P., et al., *Aquaporins and ion conductance.* Science, 1997. **275**(5305): p. 1490; author reply 1492.
264. Saparov, S.M., et al., *Water and ion permeation of aquaporin-1 in planar lipid bilayers. Major differences in structural determinants and stoichiometry.* J Biol Chem, 2001. **276**(34): p. 31515-20.
265. Campbell, E.M., D.N. Birdsell, and A.J. Yool, *The activity of human aquaporin 1 as a cGMP-gated cation channel is regulated by tyrosine*

phosphorylation in the carboxyl-terminal domain. Mol Pharmacol, 2012. **81**(1): p. 97-105.
266. Kourghi, M., et al., *Identification of loop D domain amino acids in the human Aquaporin-1 channel involved in activation of the ionic conductance and inhibition by AqB011.* Frontiers in chemistry, 2018. **6**: p. 142.
267. Pei, J.V., et al., *Differential Inhibition of Water and Ion Channel Activities of Mammalian Aquaporin-1 by Two Structurally Related Bacopaside Compounds Derived from the Medicinal Plant Bacopa monnieri.* Molecular Pharmacology, 2016. **90**(4): p. 496-507.
268. Pan, X.Y., et al., *Ginsenoside Rg3 attenuates cell migration via inhibition of aquaporin 1 expression in PC-3M prostate cancer cells.* Eur J Pharmacol, 2012. **683**(1-3): p. 27-34.
269. Gupta, S.C., S. Patchva, and B.B. Aggarwal, *Therapeutic roles of curcumin: lessons learned from clinical trials.* The AAPS journal, 2013. **15**(1): p. 195-218.
270. Aggarwal, B.B., A. Kumar, and A.C. Bharti, *Anticancer potential of curcumin: preclinical and clinical studies.* Anticancer research, 2003. **23**(1/A): p. 363-398.
271. Preston, G.M., et al., *The mercury-sensitive residue at cysteine 189 in the CHIP28 water channel.* J Biol Chem, 1993. **268**(1): p. 17-20.
272. Zelenina, M., et al., *Nickel and extracellular acidification inhibit the water permeability of human aquaporin-3 in lung epithelial cells.* Journal of Biological Chemistry, 2003. **278**(32): p. 30037-30043.
273. Zelenina, M., et al., *Copper inhibits the water and glycerol permeability of aquaporin-3.* Journal of Biological Chemistry, 2004. **279**(50): p. 51939-51943.
274. Serna, A., et al., *Functional Inhibition of Aquaporin-3 With a Gold-Based Compound Induces Blockage of Cell Proliferation.* Journal of cellular physiology, 2014. **229**(11): p. 1787-1801.
275. Brooks, H.L., J.W. Regan, and A.J. Yool, *Inhibition of aquaporin-1 water permeability by tetraethylammonium: involvement of the loop E pore region.* Molecular pharmacology, 2000. **57**(5): p. 1021-1026.
276. Saadoun, S., et al., *Impairment of angiogenesis and cell migration by targeted aquaporin-1 gene disruption.* Nature, 2005. **434**(7034): p. 786-92.
277. Yool, A.J. and E.M. Campbell, *Structure, function and translational relevance of aquaporin dual water and ion channels.* Mol Aspects Med, 2012: p. in press.

Chapter 2: An Accurate and Cost-Effective Alternative Method for Measuring Cell Migration with the Circular Wound Closure Assay

Michael L De Ieso[1] and Jinxin Pei[1]

[1]Department of Physiology, Adelaide Medical School, University of Adelaide, Adelaide, SA, Australia

Chapter 2 is a methodology chapter that presents novel adaptations to existing protocols for measuring two-dimensional cell migration, as performed for work in this thesis. It incorporates a published paper: An Accurate and Cost-Effective Alternative Method for Measuring Cell Migration with the Circular Wound Closure Assay. **M. De Ieso** and Jinxin Pei. Bioscience Reports. Bioscience Reports 2018;38:5.

2.1 Abstract

Cell migration is important in many physiological and pathological processes. Mechanisms of two-dimensional cell migration have been investigated most commonly by evaluating rates of cell migration into linearly scratched zones on the surfaces of culture plates. Here, we present a detailed description of a simple adaptation for the well-known and popular wound closure assay, using a circular wound instead of a straight line. This method demonstrates improved precision, reproducibility, and sampling objectivity for measurements of wound sizes as compared to classic scratch assays, enabling more accurate calculations of migration rate. The added benefits of the method are simplicity and low cost as compared with commercially available assays for generating circular wounds.

2.2 Statement of Authorship

Statement of Authorship

Title of Paper	An accurate and cost-effective alternative method for measuring cell migration with the circular wound closure assay
Publication Status	☑ Published ☐ Accepted for Publication ☐ Submitted for Publication ☐ Unpublished and Unsubmitted work written in manuscript style
Publication Details	Bioscience Reports 2018; 38:5

Principal Author

Name of Principal Author (Candidate)	Michael Lucio De Ieso
Contribution to the Paper	First author and main contributor. Concept and methodological design. Investigation, formulation of initial draft, and incorporation of reviewer and coauthor comments and suggestions. Figure and table development.
Overall percentage (%)	60
Certification:	This paper reports on original research I conducted during the period of my Higher Degree by Research candidature and is not subject to any obligations or contractual agreements with a third party that would constrain its inclusion in this thesis. I am the primary author of this paper.
Signature	Date: 19th NOVEMBER 2018

Co-Author Contributions

By signing the Statement of Authorship, each author certifies that:

i. the candidate's stated contribution to the publication is accurate (as detailed above);
ii. permission is granted for the candidate in include the publication in the thesis; and
iii. the sum of all co-author contributions is equal to 100% less the candidate's stated contribution.

Name of Co-Author	Jinxin Victor Pei
Contribution to the Paper	Concept and methodological design. Contribution to the initial draft. Figure and table development. Project administration. Review of the final manuscript.
Signature	Date: 19th November 2018

2.3 Introduction

Cell migration is a multistep process that is essential for diverse life functions in multicellular and single-celled organisms, and includes both collective and individual cell movements across extracellular spaces or through tissues [1, 2]. In normal physiological processes, migration enables morphogenesis, immunity, and tissue repair [2, 3]; in pathological processes migration has been linked to cancer, atherosclerosis, rheumatoid arthritis, multiple sclerosis, and others [4-9]. Understanding the mechanisms of cell migration could facilitate development of therapeutic interventions for a wide range of diseases.

Existing literature provides a comprehensive comparison of advantages and disadvantages of approaches for measuring two-dimensional (2D) cell migration [10]. A technique commonly used for measuring 2D cell migration is the scratch wound assay. In brief, the 2D scratch wound assay involves creating a linear "scratch" or wound across a confluent monolayer of cultured cells, and capturing images to measure cell migration rate by the decrease in distance across the open wound as a function of time [11, 12]. Though useful, the 2D scratch wound assay has disadvantages (summarized in Table 2.1), stemming primarily from the fact that the scratch wound is usually longer (but not wider) than the field of view used during analysis. Without live-cell imaging facilities (to capture images in identical locations at repeated intervals), experimenters are faced with the challenge of recapturing the same position on the scratch at multiple time points without subjective error. This is especially difficult for high-throughput assays with multi-well plates, and is likely to result in reduced reproducibility of results. A second disadvantage is that typically scratch wound images are quantified by visually estimating the positions of the boundaries of the scratch, assuming lines to approximate the walls, and measuring the distances across the gap. Manually taking multiple measurements of the gap distances at various locations is intended to reduce variability by generating an average value of the distance across the scratch [13], but the reliability is handicapped by the fact that the boundary edges are ragged; the selected positions for the boundaries will vary between samples and within samples. Analyses with the classic scratch method must be done blinded to reduce the risk of unintentional bias in the acquisition of data. Improvements on

the method have used image analysis software to find lines of best fit to measure the boundaries or areas of wounds [14, 15], but the scratch method is still vulnerable to variability in the image locations selected at each time-point. The third consideration is that most studies with the 2D scratch wound assay have not accounted for the potentially confounding effects of cell proliferation on the apparent rate of closure of the wound, a factor that might not be addressed fully by a "serum-starvation" step prior to commencing the assay [16-18].

The concept for generating a circular wound for measuring 2D cell migration has been previously established [19-21]. The circular wound closure assay (CWCA) permits the analyst to easily relocate the wound at any time point, and it enables accurate analysis by calculating the area or the radius of the circular wound using image analysis software. Current techniques to generate circular wounds such as exclusion zone assays [22] involve growing the cells around circular barriers (poly-dimethylsiloxane micropillars, stoppers, or biocompatible gels) of uniform size [21], or using a stabilized, rotating, silicone-tipped drill press to create uniform, circular wounds in an intact confluent monolayer of cells (Tab. 2.1) [19]. One advantage to these techniques is that they can generate highly consistent initial wounds; however, they are more complex and costlier than the CWCA described here. The CWCA uses a sterile 10uL (P10) micropipette tip attached to an aspirator to remove a small circular area of cells (Fig 2.1). The complete wound can be reliably re-located for manual or automatic imaging at all subsequent time points. Processing images of circular wounds for analysis can be done with the freely available cross-platform Fiji (ImageJ) software [23]. Use of a mitotic inhibitor minimizes confounding effects of proliferation on apparent wound closure rates; this step is optional depending on cell type and assay duration. In summary, with this protocol easily relocatable, clean, sufficiently uniform circular wounds can be generated in diverse cell lines (Fig 2.2) that are amenable to streamlined computer-assisted data analysis, without costly equipment or reagents. These modifications reduce the cost and simplify the analysis of *in vitro* cell migration assays.

Table 2.1: Summary of assays used previously for measuring 2D cell migration, including advantages and disadvantages.

Assay	Method	Advantages/ Disadvantages	Diagram
Scratch wound assay	1. Generate confluent monolayer of cells 2. Use pipette tip to scratch a portion of cells away, leaving a "wound"	**Adv:** • Cost effective • Minimal equipment required **Dis:** • Difficult to relocate exact wound sites at sequential timepoints without expensive live-cell imaging facilities, reducing accuracy of results	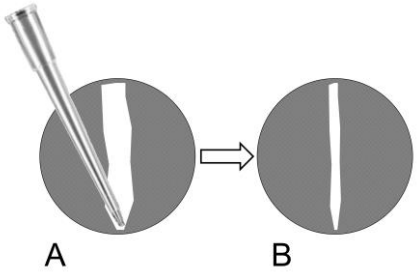
Cell exclusion zone assay with stopper	1. Insert stopper in well prior to seeding cells 2. Allow cells to grow around the stopper 3. Remove stopper to expose circular wound	**Adv:** • Consistent initial wound size • High throughput • Semi-automatic **Dis:** • High cost • Technically complex • Unknown effects of stopper-derived components on cell properties	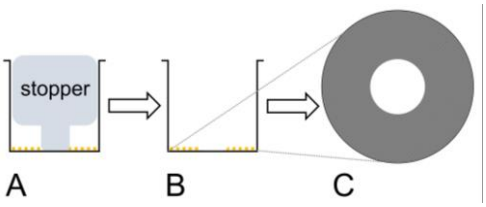
Cell exclusion zone assay with bio-compatible gel	1. Apply gel in the center of each well prior to seeding cells 2. Allow cells to grow around the gel 3. Remove gel to expose circular wound	**Adv:** • Consistent initial wound size **Dis:** • High cost • Gel needs to be manually removed, which may alter cell or substrate properties • Low throughput (24 wells per assay)	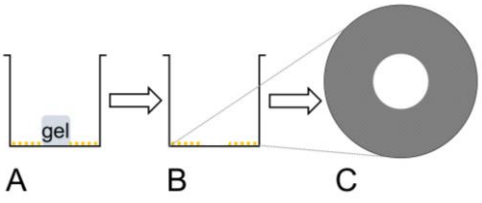

2.4 Materials and Methodology

2.4.1 Cell lines

Lines used for this study were: (1) human colorectal adenocarcinoma HT29 (supplied by the American Type Culture Collection (ATCC®), catalogue number HTB-38™) and SW480 (ATCC®, catalogue number CCL-228™); (2) Human glioblastoma cell line U251-MG (supplied by the European Collection of Cell Cultures (ECACC; Salisbury, United Kingdom), catalogue number 09063001 purchased from CellBank Australia (Westmead, NSW, Australia)); (3) Mammary adenocarcinoma MDA-MB-231 (ATCC®, catalogue number HTB-26™); and (4) human embryonic kidney HEK-293 (ATCC®, catalogue number CRL-1573™).

2.4.2 Reagents

- Cell culture medium and supplements appropriate for cell line.
- 5-Fluoro-2'-deoxyuridine (FUDR) (100 ng/mL final solution)
- Lifting solution, 0.25 mM EDTA with 0.25% trypsin (2.5%, Gibco)
- Phosphate buffer saline (PBS, Gibco)

2.4.3 Equipment

- Cell culture incubator at 37 °C with 5% CO_2
- Inverted light microscope with camera attachment
- Flat bottom 96 well plate
- Vacuum pump for molecular biology (Welch Laboratory, 2511B-01, 219 mmHg vacuum pressure)
- p10 pipette tips (Labcon, LC1038-290)
- Hemocytometer

2.4.4 Free software

- XnConvert version 1.73 (https://www.xnview.com/en/xnconvert/#downloads)
- Fiji (ImageJ) version 1.51h (http://imagej.nih.gov/ij/)

2.4.5 Procedure

Note: Perform assays under sterile conditions. See figure 2.1 for short summary and example of wound and outline appearance.

5. **Passage the cells.** When the cells to be used for the assay are approximately 70-80% confluent, detach the cells with trypsin and EDTA cell-lifting solution and centrifuge cells at 125G for 5 to 7 minutes. Re-suspend cells and perform a cell count using a hemocytometer. **Note:** *The CWCA can be used to generate wounds in diverse cell lines (Fig 2.2A).*
6. **Plate the cells.** Prepare an appropriate volume of working cell solution at $5x10^5$ cells/ml. Plate the working cell solution at 500 μl/well for 24-well plate or 100 μl/well for 96-well plate. Incubate the plate until cells reach 90% confluency. **Note:** *Incubation time will vary depending on the cell line.*
7. **Mitotic inhibitor and serum starvation.** When the cells reach 90% confluency, exchange the media with FUDR-containing reduced-serum medium (1-2% serum), and incubate overnight. Use FUDR at a concentration of 100ng/mL. **Note:** *The use of a mitotic inhibitor is not required although recommended to reduce potential overestimation of apparent migration due to cell proliferation (Supp. Fig 2.1).* The serum-starvation step is essential.
8. **Create wound using vacuum pump.** Attach a p10 pipette tip to the end of vacuum tube (to do this, it may be necessary to first attach a p200 pipette tip to the tubing, and then overlay a p10 pipette tip on the p200 pipette tip). With medium still in the well, position the pipette tip perpendicularly above the center of the well. Gently lower the tip and make brief contact with the base to aspirate off a circular layer of cells and create a circular wound (Fig 2.1). Figure 2.2B shows the consistency of initial wound sizes generated using this technique. *Note: Gentle perpendicular contact between the pipette tip and the cell monolayer is important for clean and consistent wounds. Practicing the technique in several wells prior to the first experiment is recommended (see Supp. Fig 2.2 for examples of good and bad wounds). Flat pipette tips from 2 different vendors (Labcon, LC1038-290 and Brand Z740066) and vacuum pumps with different pressure settings (219 mmHg and 449 mmHg) have been tested in our lab with no distinctive differences in wound quality.*

9. **Wash the wound.** Aspirate any remaining medium from the edge of the well, and wash with PBS. One wash is usually sufficient, but some cell lines will require an extra washing step to clear any residual cellular debris.
10. **Apply treatments.** Remove the PBS/media from wells and replace with culture medium containing the treatments or control samples that are being tested. Prepare treatments and controls in the same FUDR-containing reduced-serum medium as used previously. For example, if certain chemicals are being tested for their effect on cell migration, dissolve these chemicals at the appropriate final concentration in FUDR-containing reduced-serum medium.
11. **Imaging.** Using microscopy imaging facilities, capture images of each complete circular wound centered in the field of view. Once all wells have been imaged, return the plate back to the incubator until the next time point (if imaging is being performed manually). If desired, wound closure can be monitored over multiple time points (Fig 2.2C). The final time-point for imaging depends on the cell line, as some cells migrate faster than others. *Note: The maximal duration of the experiment should ensure the wounds do not fully close during the treatment period of interest.*
12. **XnConvert.** This software can be used for batch image processing to crop to regions of interest or to change resolution of pictures.
13. **Process images in ImageJ.** Use NIH ImageJ software to calculate the wound area and to generate an outline of the perimeter of the wound area. The following steps illustrate how to analyze the wound area on ImageJ, and also how to use the "macro" feature to semi-automate the analysis for each image, improving consistency and objectivity of measurements. The same macro settings should be used for all sampled images collected in an experiment.
    a. Download and open Fiji (ImageJ)
    b. Select **File>Open** and then select the image file to be analyzed
    c. Go to **Analyze>Set Scale** and input the scale information relative to your image.

d. To begin recording the macro to be used for all images, select **Plugins>Macro>Record…** A "Record" box will appear, and the macro will now begin to record all following selections.
e. Select **Image>Type>8-bit.** This will convert the image to binary image.
f. Select **Process>Find Edges**
g. Select **Process>Sharpen**
h. Select **Image>Adjust>Threshold…** Be sure the settings are set to "Default" and "B&W" and untick the "Dark background" and "Stack histogram" boxes.
i. Move the two bars until the best clarity and contrast is achieved for the image. See image below for how the image should look following adjustment.

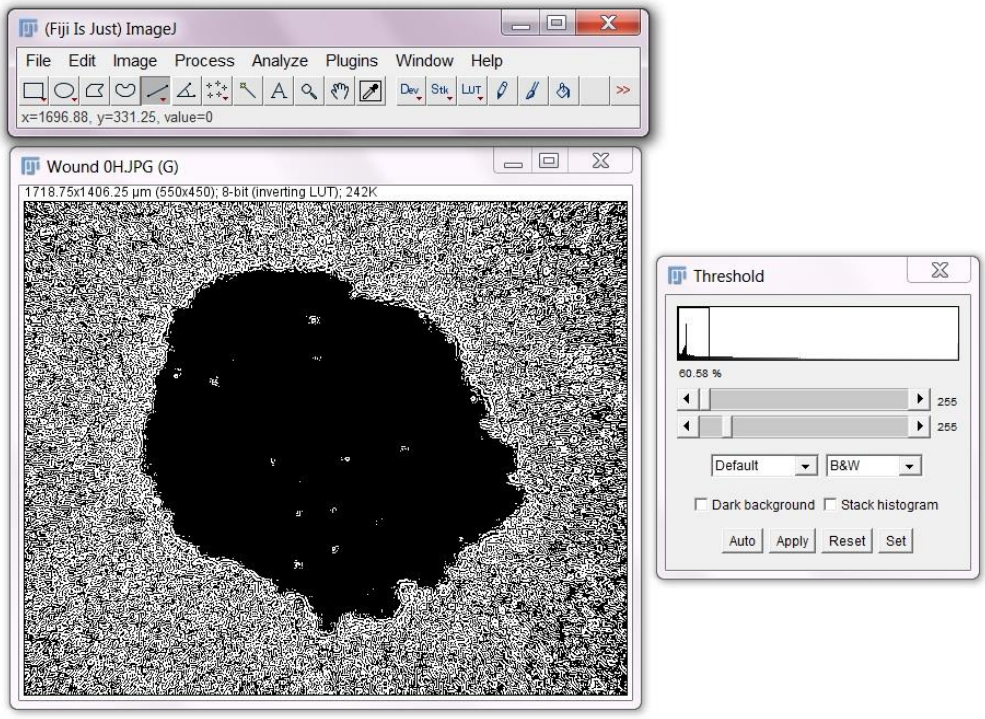

j. Select **Set** and a "Set Threshold Level" box should appear. Select **OK**
k. Now select **Apply** in "Threshold" box.
l. Select **Process>Find Edges**

m. Select **Image>Lookup Tables>Invert LUT.** See image below for how the image should look after LUT inversion.

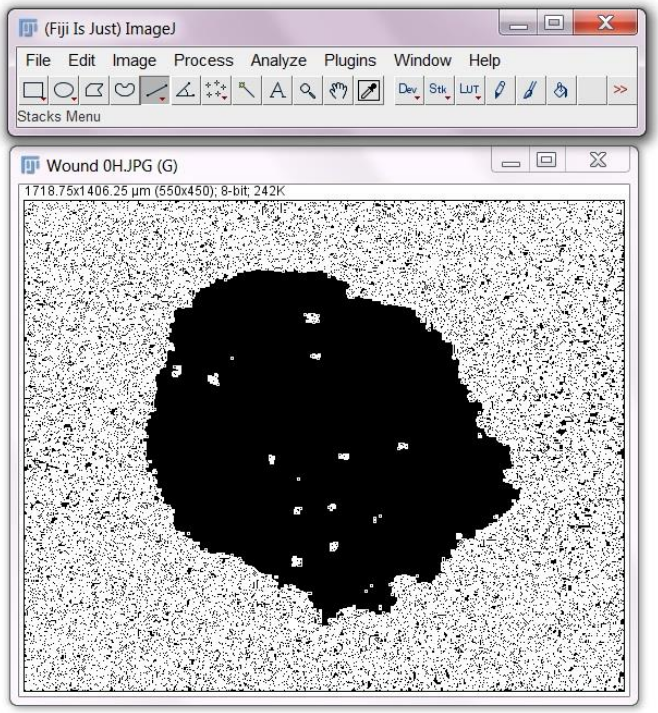

n. Select **Analyze>Analyze Particles…**
o. In the "Size (pixel^2)" section, select minimum and maximum pixel areas you would like the program to identify. For example, if there are artifacts ("holes") that are visible in the current image, and you do not want to program to mistake these "holes" for wounds, it is important to input the range of areas within which wounds are likely to fall. Try "2000-Infinity" to begin, and adjust accordingly. If the program is detecting "holes" that are not wounds, increase the first value. If the program is not detecting anything at all, including wounds, decrease the first value.
p. Set "Circularity" to "0.00-1.00".
q. In the "Show" section, choose "Bare Outlines" to generate an outline of the wound.
r. Be sure "Summarize" is ticked to generate data of the wound area.
s. Select **OK.**

t. A summary box will appear, which will include the area value of the wound to be used for further statistical analysis. An outline of the wound will also appear. See below image for summary and outline following this step.

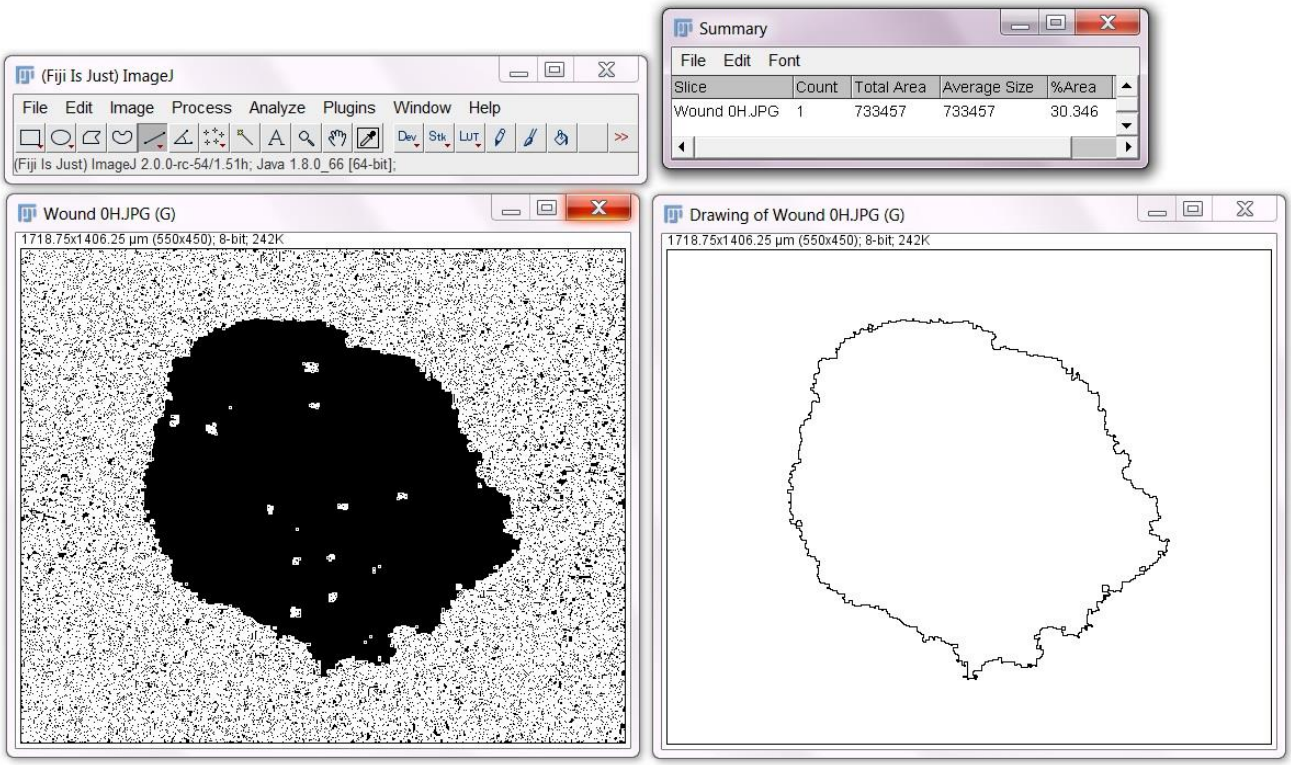

u. Find the “Record” box for the macro and select **Create.**

v. A new box will appear labelled, “Macro.ijm”. In this box, select **Save As**, and save as a .txt file.

w. Now go to **Plugins>Macros>Install…**

x. Find and select the .txt macro file from step v.

y. Open a new wound image for analysis.

z. Select **Plugins>Macros>“Your Macro”.** Your macro should be located at the bottom of the dropdown box.

14. **Check for initial wound size consistency.** Run an ANOVA statistical test to confirm the absence of significant differences between the initial wound areas across all the control and treatment groups in an experiment. This rules out the possibility that differences in wound closure observed between treatment groups were an indirect result of initial wound size.

15. **Analyze wound closure.** The wound area measured at time zero (the start of the treatment) serves as a reference point for standardization. Subsequent samples can be evaluated in different ways to estimate the magnitude of cell migration. One method is to calculate the radius of the initial wound minus the radius of the end wound. This method determines distance moved but assumes circularity of the wound shapes. A second method is to calculate the final wound area as a percentage of the initial wound area. This method requires consistency of initial wound sizes, but is more tolerant of non-circular wounds. The percent closure method has been the analysis of choice for published work [24, 25]; however, results from both methods show a robust correlation, demonstrating reliability (Fig 2.3).

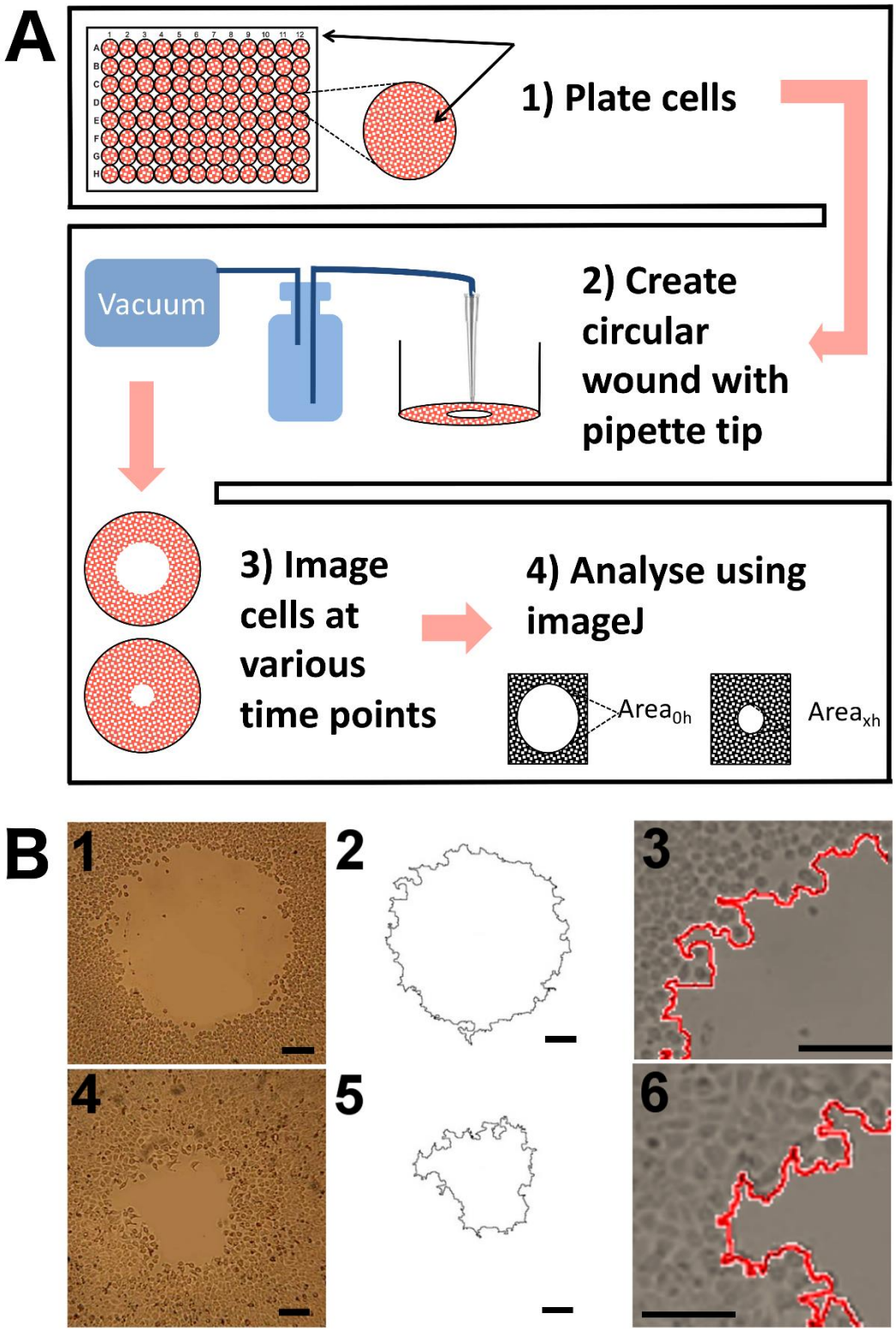

Figure 2.1: Schematic summary of procedures and examples of results for the circular wound closure assay in HT29 cells. (A) 1. Seed the cells in a 96-well plate, and grow to full confluence. 2. Connect a p10 pipette tip to a vacuum pump and gently press the end of the pipette tip perpendicularly down onto the cell monolayer (without lateral movement) to detach cells from the substratum, creating

a circular wound. 3. Image the wound at various time points. 4. Measure cell migration by calculating the percent change in wound area over time, standardised to the initial area at time zero. (B) Raw images of the same circular wound at 0 (B1) and 24 hours (B4). Outlines of circular wound perimeters at 0 (B2) and 24 (B5) hours were generated by ImageJ software. Magnified superimposed views of circular wounds show outlines at 0 (B3) and 24 (B6) hours, illustrating the precision of the data capture method. Black bars represent 100μm.

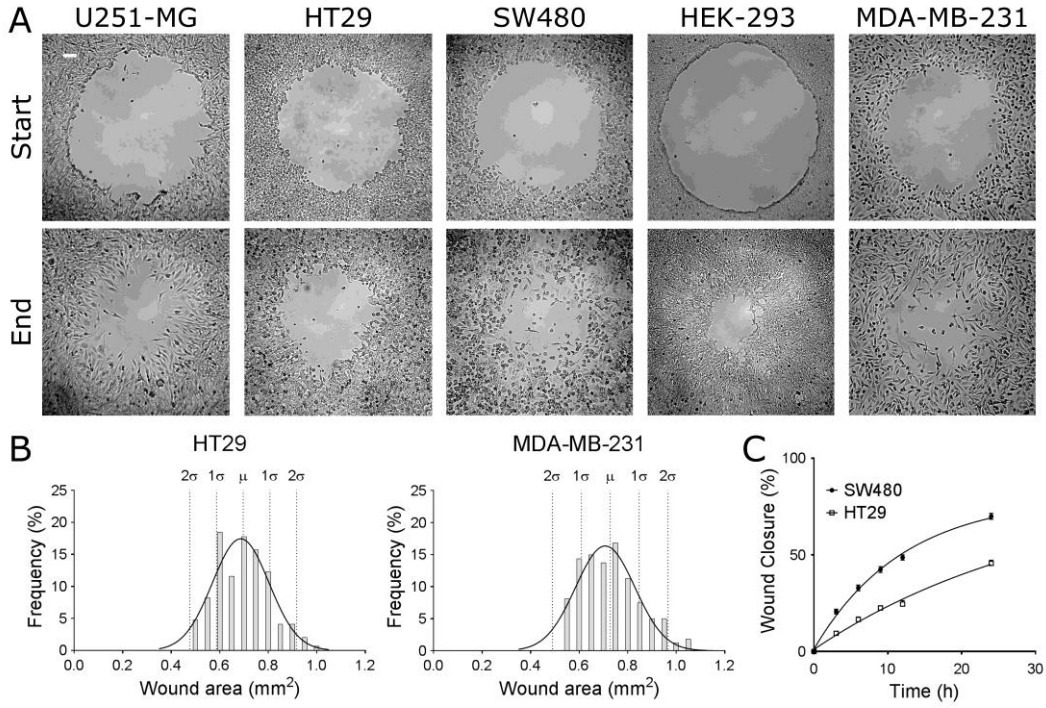

Figure 2.2: Wounds can be generated consistently for various cell lines using CWCA. (A) Start-point represents 0 hours and end-point represents various time points depending on the cell line. The end points for cell lines shown are: U251-MG 20 hours, HT29 24 hours, SW480 24 hours, HEK-293 24 hours, and MDA-MB-231 20 hours. White bar represents 100μm; the scale is consistent for all images. (B) Wounds were generated by two different experimenters (subjects) for two different cell lines (MDA-MB-231 and HT29), using the CWCA technique described here. The initial wound sizes were calculated (in mm^2), and the data sets from each subject were combined for each cell line. The plots depict Gaussian distributions of the resulting initial wound areas. For MDA-MB-231, the mean (μ) wound area is $0.728mm^2$ (standard deviation (σ) $\pm 0.119mm^2$). N-value is 160. For HT29, μ is $0.697mm^2$ ($\sigma \pm 0.110mm^2$). N-value is 146. (C) Wound closure was recorded as the percent change in wound area with time (3, 6, 9, 12 and 24 hours) in HT29 and SW480 cells. SW480 cells show a faster rate of migration than HT29 cells. Non-linear (sigmoidal) regression functions showed the best fit of wound closure as a function of time, yielding a correlation coefficient of $r^2 = 0.95$ for SW480 (n=16), and $r^2 = 0.94$ for HT29 (n=7).

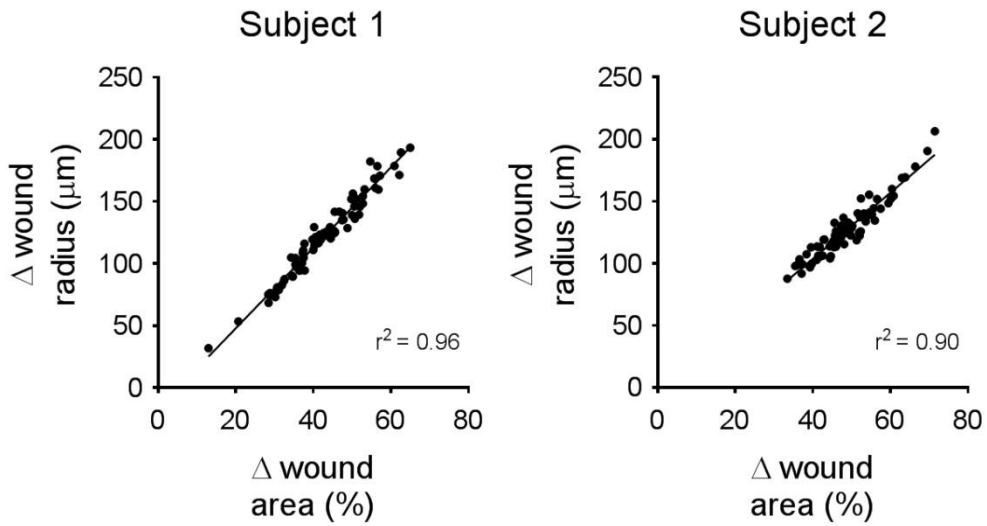

Figure 2.3: Results obtained from calculations of percent wound closure and wound radius decrease are strongly correlated. Plots generated from the experimental results obtained by two different experimenters (subjects). Each experiment had various treatment groups, with some treatments exhibiting inhibitory effects on cell migration (explaining that wide range of wound closure in both plots). Analysis was done by calculating both the percentage wound closure and the change in wound radius for each wound image. The results from each method were compared and linear regression yielded a correlation coefficient of r2=0.96 for subject 1, and r2=0.9 for subject 2. N-value is 73 for each subject. These results suggest that both techniques of analysis produce data that is strongly correlated.

2.5 Supplementary Figures

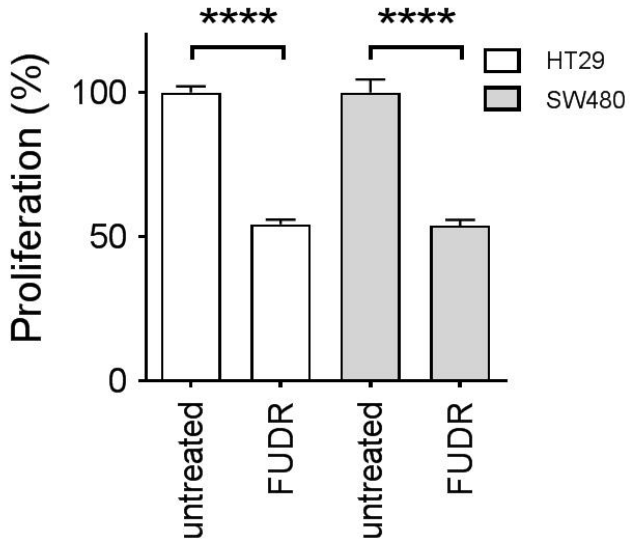

Supplementary Figure 2.1: Analyses of proliferation with and without mitotic inhibitor FUDR. For the proliferation assay, cells were plated at 10^5 cells/ml in a flat-bottom 96-well plate in 2% serum DMEM culture medium with and without 100ng/mL FUDR for 24 hours. Four images were acquired for each treatment (one image per well), standardised with XnConvert software, and used to count the total numbers of individual cells in each field of view. FUDR (100ng/mL) significantly reduced cell proliferation measured at 24 hours in HT29 and SW480 colorectal adenocarcinoma cells ($p<0.0001$, $n=4$).

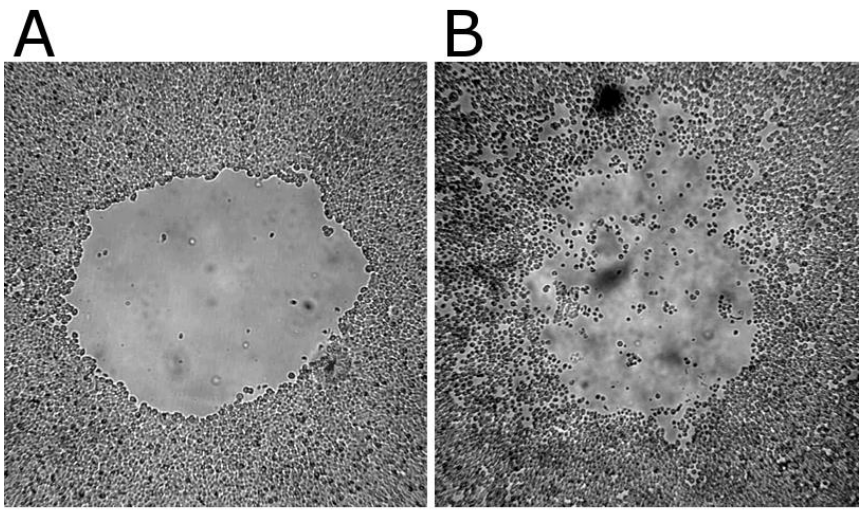

Supplementary Figure 2.2: **Examples of high and low-quality wounds.** Images of cultured HT29 cells in two wells of a 96-well plate, immediately after wounding. (A) A high-quality wound, with a clean wound area and well-defined border, in a uniform background of cells grown to near 100% confluence. (B) A low-quality wound (inadequate for further analysis) littered with cellular debris, ragged borders, and gaps in the cell monolayer, due to lack of confluency as well as inadequate contact with the suction p10 tip onto the well floor.

2.6 Conclusion

This CWCA technique provides a simple and reliable alternative method with distinct advantages over older methods such as the scratch wound assay or cell exclusion zone assays. Accurate data measurements enable straightforward objective computer-assisted analyses. This simple adaptation of a well-established protocol generates results that are comparable in consistency and quality to expensive commercial options, and supports relatively high throughput screening of novel therapeutic agents that regulate cell migration rates [24, 25]. The main limitation of CWCA is that manual wound generation can yield higher variability in initial wound sizes and shapes as compared to cell exclusion zone or silicone-tipped drill wounding methods; however, this limitation exists for any assays involving the manual generation of wounds. Variability is reduced with practice. Ruling out the potential impact of variability is addressed by running an ANOVA statistical test on initial wound sizes across all treatment groups in a given experiment. Absence of a significant difference rules out non-specific effects of initial wound sizes on measures of closure. Analyzing data by determining wound radius change, as opposed to percentage wound closure, is less sensitive to initial wound size, but more sensitive to the circularity of wound shape; however, both methods are reliable. In summary, this protocol offers a quality advance in methodology that is possible without specialized equipment or costly resources. Cutting edge research on cell migration can be carried out by laboratories, including those located in developing countries where research funding and facilities might be limited.

2.7 References

1. Klausen, M., et al., *Involvement of bacterial migration in the development of complex multicellular structures in Pseudomonas aeruginosa biofilms.* Molecular microbiology, 2003. **50**(1): p. 61-68.
2. Friedl, P., Y. Hegerfeldt, and M. Tusch, *Collective cell migration in morphogenesis and cancer.* International Journal of Developmental Biology, 2004. **48**: p. 441-450.
3. Friedl, P. and B. Weigelin, *Interstitial leukocyte migration and immune function.* Nature immunology, 2008. **9**(9): p. 960-969.
4. Yamaguchi, H., J. Wyckoff, and J. Condeelis, *Cell migration in tumors.* Curr Opin Cell Biol, 2005. **17**(5): p. 559-564.
5. Ross, R., *The pathogenesis of atherosclerosis: a perspective for the 1990s.* Nature, 1993. **362**(6423): p. 801.
6. McInnes, I.B., et al., *The role of interleukin–15 in T–cell migration and activation in rheumatoid arthritis.* Nature medicine, 1996. **2**(2): p. 175.
7. Leppert, D., et al., *Interferon beta-1b inhibits gelatinase secretion and in vitro migration of human T cells: A possible mechanism for treatment efficacy in multiple sclerosis.* Annals of neurology, 1996. **40**(6): p. 846-852.
8. Billuart, P., et al., *Oligophrenin-1 encodes a rhoGAP protein involved in X-linked mental retardation.* Nature, 1998. **392**(6679): p. 923.
9. De Ieso, M.L. and A.J. Yool, *Mechanisms of Aquaporin-Facilitated Cancer Invasion and Metastasis.* Frontiers in Chemistry, 2018. **6**.
10. Ascione, F., et al., *Comparison between fibroblast wound healing and cell random migration assays in vitro.* Experimental cell research, 2016. **347**(1): p. 123-132.
11. Liang, C.-C., A.Y. Park, and J.-L. Guan, *In vitro scratch assay: a convenient and inexpensive method for analysis of cell migration in vitro.* Nature protocols, 2007. **2**(2): p. 329.
12. Justus, C.R., et al., *In vitro cell migration and invasion assays.* JoVE (Journal of Visualized Experiments), 2014(88): p. e51046-e51046.
13. Dorward, H.S., et al., *Pharmacological blockade of aquaporin-1 water channel by AqB013 restricts migration and invasiveness of colon cancer cells and prevents endothelial tube formation in vitro.* Journal of Experimental & Clinical Cancer Research, 2016. **35**(1): p. 36.
14. Pan, X.Y., et al., *Ginsenoside Rg3 attenuates cell migration via inhibition of aquaporin 1 expression in PC-3M prostate cancer cells.* Eur J Pharmacol, 2012. **683**(1-3): p. 27-34.
15. Meng, F., et al., *Aqp1 enhances migration of bone marrow mesenchymal stem cells through regulation of FAK and beta-catenin.* Stem Cells Dev, 2014. **23**(1): p. 66-75.
16. Saxena, N.K., et al., *Concomitant activation of the JAK/STAT, PI3K/AKT, and ERK signaling is involved in leptin-mediated promotion of invasion and migration of hepatocellular carcinoma cells.* Cancer research, 2007. **67**(6): p. 2497-2507.
17. Hu, J. and A.S. Verkman, *Increased migration and metastatic potential of tumor cells expressing aquaporin water channels.* FASEB J, 2006. **20**(11): p. 1892-4.
18. Jiang, Y., *Aquaporin-1 activity of plasma membrane affects HT20 colon cancer cell migration.* IUBMB Life, 2009. **61**(10): p. 1001-9.

19. Kam, Y., et al., *A novel circular invasion assay mimics in vivo invasive behavior of cancer cell lines and distinguishes single-cell motility in vitro.* BMC cancer, 2008. **8**(1): p. 198.
20. Daniel, T.O., et al., *Thromboxane A2 is a mediator of cyclooxygenase-2-dependent endothelial migration and angiogenesis.* Cancer research, 1999. **59**(18): p. 4574-4577.
21. Li, D.S., J. Zimmermann, and H. Levine, *Modeling closure of circular wounds through coordinated collective motion.* Physical biology, 2016. **13**(1): p. 016006.
22. Hulkower, K.I. and R.L. Herber, *Cell migration and invasion assays as tools for drug discovery.* Pharmaceutics, 2011. **3**(1): p. 107-124.
23. Schindelin, J., et al., *Fiji: an open-source platform for biological-image analysis.* Nature methods, 2012. **9**(7): p. 676.
24. Kourghi, M., et al., *Bumetanide Derivatives AqB007 and AqB011 Selectively Block the Aquaporin-1 ion Channel Conductance and Slow Cancer Cell Migration.* Molecular pharmacology, 2015: p. mol. 115.101618.
25. Pei, J.V., et al., *Differential Inhibition of Water and Ion Channel Activities of Mammalian Aquaporin-1 by Two Structurally Related Bacopaside Compounds Derived from the Medicinal Plant Bacopa monnieri.* Molecular Pharmacology, 2016. **90**(4): p. 496-507.

Chapter 3: Pharmacological evidence that the AQP1 ion conductance is rate-limiting for cell migration and invasion in glioma, breast and colorectal cancers.

Michael L De Ieso[1], Saeed Nourmohammadi[1], Jinxin Pei[1], Pak Hin Chow[1] and Andrea J Yool[1]

[1]Department of Physiology, Adelaide Medical School, University of Adelaide, Adelaide, SA, Australia

3.1 Abstract

Aquaporin-1 (AQP1) is a dual water and ion channel that facilitates cancer cell migration and invasion, and in certain cancers, has been linked with metastasis which is a leading cause of cancer-related deaths. Other AQPs with water channel function are not able to substitute for AQP1 in facilitating cell migration, and there is a gap in knowledge regarding the properties of AQP1 that permit its migration-enhancing effect. We hypothesised that AQP1 ion channel activity facilitates cell migration in AQP1-expressing cancer cell lines. Cell lines derived from colorectal adenocarcinoma, glioblastoma, mammary adenocarcinoma, and embryonic kidney cells were analysed by western blot to determine presence or absence of AQP-1, -3, -4, and -5. Rates of cell migration were measured with two-dimensional circular wound closure and live cell imaging assays, and three-dimensional invasion was measured by transwell assay, with and without pharmacological inhibitors of AQP channels and ion transporters. siRNA-mediated knockdown of AQP1 and AQP5, as compared with scrambled control siRNA transfections, was confirmed with real-time polymerase chain reaction and western blot. Cell viability was measured with alamarBlue. The sodium-hydrogen-antiporter 1 inhibitor, ethylisopropylamiloride, inhibited HT29 colorectal cancer wound closure as did the AQP1 ion channel blockers AqB011, AqB007, and AqB006, suggesting multiple pathways for Na^+ entry are involved in enabling cell motility. AqB011 (80μM) produced the strongest block of wound closure (58 ± 3.1%) in HT29 cells as compared to vehicle-treated, and also significantly inhibited wound closure in glioblastoma lines U87-MG (36 ±

2.4%.) and U251-MG (25 ± 4.4%.), without cytotoxicity. AQP5-knockdown in HT29 colorectal carcinoma cells resulted in increased sensitivity of wound closure to inhibition by AqB011, suggesting AQP1 was recruited as a compensatory mechanism. Live cell imaging confirmed at the single cell level that the mean overall distance migrated by U87-MG cells in 24 hours (649 ± 27 μm) was significantly reduced by AqB011 (525 ± 27 μm). Invasiveness also was inhibited significantly by AqB011 in glioblastoma U87-MG (49 ± 7.1%) and U251-MG (63 ± 12%), and in breast cancer MDA-231-MB (40 ± 9.4%), as compared to vehicle-treated controls in the same lines. This is the first demonstration that the AQP1 ion channel blocker, AqB011, significantly inhibits cell migration and invasion in diverse AQP1-expressing cancer cell lines, including glioblastoma, breast, and colon cancers. This discovery highlights the AQP1 ion conductance as a new potential pharmacological target for cancer invasion and metastasis.

3.2 Statement of Authorship

Statement of Authorship

Title of Paper	Pharmacological evidence that the AQP1 ion conductance is rate-limiting for cell migration and invasion in glioma, breast and colorectal cancers.
Publication Status	☐ Published ☐ Accepted for Publication ☐ Submitted for Publication ☑ Unpublished and Unsubmitted w ork w ritten in manuscript style
Publication Details	N/A

Principal Author

Name of Principal Author (Candidate)	Michael Lucio De Ieso
Contribution to the Paper	First author and main contributor. Formulation of research question. Concept and methodological design. Performed experiments and data analysis. Generation of manuscript. Figure and table development. Incorporation of superviser comments and suggestions for manuscript.
Overall percentage (%)	90
Certification:	This paper reports on original research I conducted during the period of my Higher Degree by Research candidature and is not subject to any obligations or contractual agreements with a third party that would constrain its inclusion in this thesis. I am the primary author of this paper.
Signature	Date 19 / 11 / 2018

Co-Author Contributions

By signing the Statement of Authorship, each a

i. the candidate's stated contribution to the publication is accurate (as detailed above);
ii. permission is granted for the candidate in include the publication in the thesis; and
iii. the sum of all co-author contributions is equal to 100% less the candidate's stated contribution.

Name of Co-Author	Jinxin Victor Pei
Contribution to the Paper	Performed experimental procedures.
Signature	Date 19th November 2018

Name of Co-Author	Saeed Nourmohammadi
Contribution to the Paper	Performed experimental procedures.
Signature	Date 19/11/2018

Please cut and paste additional co-author panels here as required.

Name of Co-Author	Pak Hin Chow		
Contribution to the Paper	Performed experimental procedures.		
Signature		Date	19th November 2018

Name of Co-Author	Andrea J Yool		
Contribution to the Paper	Reviewed and edited the manuscript.		
Signature		Date	19 Nov 2018

Please cut and paste additional co-author panels here as required.

3.3 Introduction

Aquaporins (AQPs) are a family of water channels with functions including maintaining structure; regulating cell volume and osmotic membrane water permeability; enabling fluid flow across barrier tissues; and supporting metabolic demands and cellular migration [1, 2]. The first aquaporin to be cloned, aquaporin-1 (AQP1), was identified in red blood cells and renal proximal tubules [3, 4]. In the *Xenopus laevis* expression system, introduced AQP1 channels enabled high osmotic water flux across the plasma membrane as compared to non-AQP1 control oocytes [5], explaining the mechanism behind rapid transmembrane water flux in certain cell types. So far, fifteen classes of aquaporin genes have been discovered in mammals (AQP0-AQP14) [6-8]. The first thirteen aquaporins (AQP0-AQP12) have been separated into groups based on functional properties, including the classical aquaporins (AQP0, -1, -2, -4, -5, -6, -8), the aquaglyceroporins (AQP3, -7, -9 and -10), and the distantly related paralogs (AQP11 and AQP12) [9]. Aquaporins assemble as homo-tetramers, with monomers ranging 26 to 34kDa [2]. In most AQPs, each monomer is composed of six membrane spanning helices and five loops (A to E); the amino and carboxyl terminal domains are intracellular [10]. Each monomer has highly conserved asparagine-proline-alanine (NPA) motifs in cytoplasmic loop B and in extracellular loop E [10], which contribute to a monomeric pore configuration that facilitates bidirectional, selective, single-file transport of water in the classical aquaporins [11], and water and glycerol in aquaglyceroporins [12]. The classical aquaporins (AQP0, -1, -2, -4, -5, -6, -8) were originally thought to transport only water, though aquaporin-0, -1, and -6 have also been shown to conduct charged particles [13-15].

AQP1 ion conductance was first discovered in AQP1-expressing *Xenopus* oocytes stimulated with forskolin [16]; however, the forskolin response proved to be inconsistent when tested by other groups [17]. Further work showed the forskolin effect was indirect; the non-selective monovalent cation conductance is gated by cGMP [13, 18, 19]. It was later discovered that cGMP-gated ion conductance in AQP1 depends on the structural integrity of the loop D domain [20], and that monovalent cations permeate the central tetrameric pore [21, 22]. Conversely, AQP0 and AQP6 possess different physiological roles, and enable ion flow through

the monomeric pores and not the central tetrameric pore (see Box 3.1). It has been suggested that there is no physiological function of the AQP1 ion pore, as AQP1 ion channels have a low opening probability [23] or are not detectable in some expression systems [24]. However, the cGMP-mediated gating of AQP1 is subject to additional regulation including tyrosine phosphorylation [25], and the physiological relevance of AQP1 ion channel activity has been shown for fluid secretion across choroid plexus epithelium [26].

Dual water and ion conductance in AQP1 might play a role in AQP1-facilitated cancer cell migration and invasion. AQP1 is upregulated in certain aggressive cancers including colorectal cancer, glioma, breast cancer, lung adenocarcinoma, laryngeal cancer and cholangiocarcinoma [27-32], and contributes to tumour cell migration and metastasis [33]. This was demonstrated when AQP1 levels were increased by transfection into deficient lines (B16F10 melanoma, and 4T1 mammary gland tumour), resulting in accelerated cell migration *in vitro* and an increased likelihood of lung metastases in mice *in vivo* [34]. Moreover, AQP1 knockdown in cancer lines using small-interfering RNAs resulted in substantial impairment of cell migration *in vitro* [35, 36]. Interestingly, other mammalian water channels such as AQP4 did not substitute for AQP1 in facilitating cell migration in AQP1-dependent cell lines [37], suggesting that the migration-enhancing property of AQP1 in some cases relies on more than membrane water permeability. In addition to water, membrane ion permeability is also important in cell migration. The Na^+/H^+ exchanger (NHE1) plays an important role in cell migration by polarizing to the leading edge of migrating cells [38], maintaining the polarity and directionality of migrating cells [39, 40]; controlling cell adhesion [41]; and regulating uptake of Na^+ at the leading edge to create an osmotic gradient, which triggers the local influx of water via AQPs [42]. This local influx of water increases local hydrostatic pressure, causing the cell membrane to protrude at the leading edge, which makes room for actin polymerization and subsequently lamellipodial formation. Here, we hypothesise that AQP1 possesses a dual function of enabling the uptake of Na^+ and water at the leading edge, contributing to AQP1-facilitated cell migration in AQP1-expressing cancer cell lines. We aimed to test the role of the AQP1 ion conductance in cancer cell migration and invasion using small

molecule AQP1 ion channel inhibitors AqB011 and AqB007 [43], and compare the effects with compounds shown to inhibit AQP1 water flux; bacopaside II and acetazolamide. Bacopaside II is a derivative of the perennial herb, *Bacopa monnieri*, and was shown to block water flux through AQP1 but not AQP4 channels [44]. Acetazolamide is a carbonic anhydrase inhibitor that also has been suggested to inhibit AQP1-mediated water flux [45]. Results here demonstrate a physiological role for the AQP1 ion conductance in cell migration and invasion in AQP1-dependent cancer cell lines.

Box 3.1: Mechanisms and physiological roles of ion conductance in AQP0 and AQP6

AQP0

To date, AQP1, AQP0, and AQP6 have been uncovered as dual water and ion channels, however, AQP0 and AQP6 have different physiological roles and mechanisms of ion transport as compared to AQP1 (see Table 3.1). AQP0, once known as MIP or MIP26, is the most abundant intrinsic membrane protein of the ocular lens fibres [46], and is the major protein component of isolated lens junctions. AQP0 has been shown to function as a water channel exogenously in Xenopus oocytes [47, 48] and endogenously in membrane vesicles freshly isolated from mouse, frog and rabbit lens fibres [49-51]. However, compared to AQPs 1-5, AQP0 has the lowest water permeability [52] with single channel water permeability about 1/40th that of AQP1 [47]. It has been postulated that the primary functions of AQP0 in the lens are more than just increasing membrane water permeability. Liu et al. (2011) suggested that lens AQP0 functions in cell to cell adhesion of lens fibres, and regulation of gap junction channels [53]. Chepelinsky (2009) suggested AQP0 is required for maintaining the transparency and optical accommodation of the ocular lens [54]. AQP0-null humans and mice were found to have congenital cataracts [54, 55], and heterozygous loss of AQP0 in mice similarly triggered cataractogenesis [56].

AQP0 is thought to have ion channel pores in each monomer, unlike AQP1 which enables ion flow via the central tetrameric pore [15, 57-60]. In bilayer preparations, bovine AQP0 showed high single channel conductance that was voltage- and pH-

sensitive [15, 59]. Opening probability increased with increasing H^+ concentration, and was low at neutral pH showing a current amplitude similar to control bilayers [59]. Bovine AQP0 channels that were reconstituted in unilamellar vesicles had two preferred conductance states with amplitudes of 380 and 160 pS [15]. AQP0 displayed slight anion selectivity, symmetrical voltage dependence, and rapid opening and slow closing rates [59]. The water channel activity of AQP0 was shown to be regulated by pH and calcium [61], suggesting regulatory mechanisms control both the water and ion conductance of AQP0. Ehring et al. (1990) proposed that the role of AQP0 in maintaining optimal lens transparency was linked with its dual water and ion channel functions [15]. AQP0 might promote the uptake of Na^+ from the extracellular space, minimising extracellular fluid volume; this would act to reduce light scattering and improve optical transparency of the lens [15].

AQP6

Aquaporin-6 (AQP6) is unusual among mammalian AQPs in functioning more effectively as an ion channel than a water channel, and in being activated rather than blocked by mercuric chloride ($HgCl_2$) [14]. In the AQP6 tetramer, individual monomeric pores carry anion currents with a permeability sequence of NO_3>I>>Br>Cl>>F, showing minimal water permeability in standard conditions [62, 63]. Covalent modification of AQP6 by $HgCl_2$ (300µM) increased the ion conductance more than six-fold, and activated water permeability [14, 62, 64], in stark contrast to the potent blocking effect of mercurial compounds known for AQP1, AQP2, and AQP5 water channel activities. Activation of AQP6 ion conductance by $HgCl_2$ is due to the interaction of HgCl with two cysteines (C155 and C190), implicating these residues in the gating mechanism [65]. AQP6 water and anion fluxes were also reversibly potentiated by low pH, providing evidence for a possible physiological role [62]. In the broader MIP family, the insect AQP channel Big Brain (BIB) similarly functions as an ion channel, lacking water channel activity [66]

AQP6 is expressed in intracellular vesicles of renal collecting duct, colocalized with H^+/ATPase transporters in α-intercalated cells that function in urinary acid secretion [62, 65, 67]. A role in acid/base regulation in α-intercalated cells is supported by

evidence showing significant upregulation of AQP6 expression in rats exposed to chronic alkalosis or water loading, but not those with chronic acidosis [68, 69]. AQP6 might also function as a pH-sensitive chloride channel in kidney endosomes [70]. AQP6 is located in rat gastrointestinal epithelium near tight junctions, in secretory granule membranes of parotid acinar cells, and is expressed in some ovarian cancers [71-73], although its physiological roles in these tissues are not yet understood. Susceptibility to viral infection in host cell lines was decreased following overexpression of AQP6, suggesting a possible protective role. Molinas et al. (2016) found GFP-AQP6 transduced C3H10T1/2 chimeric cells showed reduced infectivity of Hazara virus (used as a model for Crimean–Congo haemorrhagic fever virus), and conversely that infection with the Hazara virus decreased AQP6 expression at protein and mRNA levels [74].

Table 3.1: A summary of gating mechanisms, selectivity, and physiological roles of ion channel functions in mammalian aquaporins

Aquaporin subtype	Mechanism(s) of ion permeation	Selectivity	Physiological role(s) of ion channel
AQP0	• Ion conductance is voltage- and pH-sensitive. • Ion channel closed at neutral pH • Ion permeation occurs through the monomeric pores	• Permeability sequence of $Cl^->K^+$	• Maintains optimal lens transparency by minimising extracellular fluid volume, which reduces light scattering
AQP1	• cGMP-gated, subject to additional regulation by tyrosine phosphorylation • Dependent on the structural integrity of the loop D domain • Ion permeation occurs through the central tetrameric pore	• Permeable to monovalent cations (Na^+, K^+, and Cs^+)	• Enables fluid secretion across choroid plexus epithelium • Enables cancer cell migration
AQP6	• Ion conductance potentiated by low pH and HgCl • Ion permeation occurs through the monomeric pores	• Permeability sequence of $NO_3^->I^->Br^->Cl^->F^-$	• Play a role in acid/base regulation in α-intercalated cells, which function in urinary acid secretion • pH-sensitive chloride channel in kidney endosomes • Possible protective role during Hazara virus infection

3.4 Materials and Methodology

3.4.1 Cell lines

Lines used for this study were: (1) human colorectal adenocarcinoma HT29 (from the American Type Culture Collection (ATCC), catalogue number HTB-38), and SW620 (ATCC; catalogue number CCL-227); (2) Human glioblastoma cell lines U251-MG (from the European Collection of Cell Cultures (ECACC; Salisbury, United Kingdom), catalogue number 09063001 purchased from CellBank Australia (Westmead, NSW, Australia)), A-172 (ECACC, catalogue number 88062428), and U87-MG (ECACC, catalogue number 89081402); (3) Mammary adenocarcinoma MDA-MB-231 (ATCC; catalogue number HTB-26); (4) Human embryonic cell line HEK-293 (ATCC; catalogue number CRL-1573). Cells were cultured in T-75 plates in Dulbecco's Modified Eagle Medium (DMEM; Life Technologies, Grand Island, NY, USA) supplemented with 10% fetal bovine serum (FBS), 1% Gibco GlutaMAX (all cells except MDA-MB-231 were treated with GlutaMAX) and 100 units/ml each of penicillin and streptomycin. Cell cultures were grown at 37°C in a humidified 5% CO_2 incubator.

3.4.2 Inhibitors

Bumetanide derivatives AqB011 (MW 434.9), AqB006 (MW 413.9), and AqB007 (MW 470.0) were synthesised by Dr Gary A. Flynn (SpaceFill Discovery LLC, West Yellowstone, MT, USA) [43] and dissolved in dimethyl sulfoxide (DMSO) to create 1000x stock solutions. 5-(N-Ethyl-N-isopropyl)amiloride (EIPA; catalogue number A3085; Sigma-Aldrich, St. Louis, MO) and acetazolamide (catalogue number A6011; Sigma-Aldrich) were also dissolved in DMSO to create 1000x stock solutions. Bacopaside II was purchased from Sigma-Aldrich (St. Louis, MO), solubilised in methanol to yield 100x stock solutions, and stored at -20°C in an airtight vial to minimize evaporation. Stock solutions were diluted in culture medium to final concentrations for testing in the circular wound closure [75], transwell invasion, live cell imaging, and alamarBlue assays.

3.4.3 Western Blot Analysis

Cells were seeded at 4-5x10^5 cells per well in 6-well tissue culture plates in normal growth medium, and incubated for 24 hours at 37°C in 5% CO_2. For siRNA experiments, transfection was initiated 48 hours before protein extraction. Once cultures reached 70-80% confluence, cells were washed with ice-cold Dulbecco's phosphate buffered saline, and incubated on ice for 5 minutes in radioimmunoprecipitation assay lysis and extraction buffer (Life Technologies) containing 1% Halt protease inhibitor (Thermo Scientific™). Cells were dislodged using a clean Corning® Cell Lifter, and homogenised with a 26-gauge needle and syringe. Homogenised lysates were collected into 1.5 mL centrifuge tubes, and centrifuged at 17,000 G for 10 minutes at 4°C. The cell debris pellet was discarded, and the supernatant was carefully transferred to a new 1.5 mL centrifuge tube. After Bradford protein estimation, 40 µg protein samples were prepared in 10 µL Novex™ 4X Bolt™ LDS Sample Buffer (Life Technologies; cat # B0007), 4 µL 10X Bolt™ Sample Reducing Agent (Invitrogen™; cat # B0009), with deionised water added to 40 µL total. After heating at 70°C for 10 minutes, samples were resolved by SDS-PAGE on Bolt 4-12% Bis-Tris Plus gel (Invitrogen™; cat # NW04122BOX), and transferred onto 0.2µm polyvinylidenefluoride membrane using the iBlot 2 Gel Transfer System (Invitrogen™; cat # IB21001). Immunodetection was performed with the iBind Western System using the iBind™ Western Device (Invitrogen™; cat # SLF1000), iBind™ cards (Invitrogen™; cat # SLF1010), and iBind™ Solution Kit (Invitrogen™; cat # SLF1020). Antibody details are as follows: Secondary antibody IRDye® anti-rabbit 800CW (1:2000; Abcam; ab216773) was used for the following primary antibodies: rabbit polyclonal AQP1 (1:1000; obtained from the Department of Ophthalmology, Duke University, Durham, NC, USA [76, 77]); rabbit polyclonal AQP3 (1:1000; Abcam; ab125219); rabbit polyclonal AQP4 (1:1000; Abcam; ab46182); rabbit monoclonal AQP5 (1:1000; Abcam; ab92320). Secondary antibody IRDye® anti-mouse 680RD (1:2000; Abcam; ab216778) was used for GAPDH antibody (1:200; Abcam; ab9484). Western blots were assessed using ImageStudio® Lite, version 5.2. Signal intensities were determined relative to local background. For siRNA experiments, data were standardised to the loading control (GAPDH). Band intensities from

CTRL siRNA-treated cells were used as the reference point for normalization of AQP1 and AQP5 siRNA-treated cells.

3.4.4 AQP1 and AQP5 siRNA knockdown

Cells were plated in a 96-well plate and incubated in normal growth conditions (37°C 5% CO_2) until 60-80% confluent. Transfection was performed as per manufacturer's instructions with Lipofectamine® RNAiMAX Reagent (Life Technologies, Grand Island, NY, USA). Ambion® Silencer Select Negative Control #1 siRNA (cat # 4390843), validated Ambion® Silencer Select AQP1 siRNA (cat # 4390824), and SMARTpool siGENOME AQP5 siRNA (Dharmacon™; cat # M-004520-01-0005) were used at a final concentration of 50 nM. BLOCK-iT™ Alexa Fluor® Red Fluorescent Oligo (cat # 14750100) was used to determine transfection efficiency. Experimental assays commenced at 48h post-transfection.

3.4.5 Real-time quantitative reverse-transcription polymerase chain reaction

Following siRNA transfection, PureLink™ RNA Mini Kit (Invitrogen™) was used to extract total RNA; cDNA synthesis required 1 µg total RNA. QuantiTect® Reverse Transcription Kit (Qiagen®) was used to synthesize cDNA. NanoDrop™ (Life Technologies) was used to quantify cDNA; 50 ng cDNA was used in the polymerase chain reaction. Real-time qRT-PCR analyses were performed using SYBR™ Green PCR Master Mix (Applied Biosystems™) in a final volume of 10 µl with StepOne Plus™ Real-Time PCR system (Applied Biosystems™). Data were analysed by StepOne Plus™ Real-Time PCR software v2.3. The primer sequences for AQP1 were forward: 5′-CGCAGAGTGTGGGCCACATCA- 3′, and reverse: 5′ -CCCGAGTTCACACCATCAGCC- 3′, amplifying a product of 217 bp. The primer sequences for AQP5 were forward: 5′ -CGTTTGGCCTGGCCATAGGCA- 3′, and reverse: 5′ -TGGCCCTGCGTTGTGTTGTTG- 3′, amplifying a product of 247 bp. *RPS13* was used as a standard and target mRNA levels relative to *RPS13* were calculated using the formula $2^{-\Delta CT}$ [78].

3.4.6 Circular wound closure assay

Two-dimensional (2D) collective cancer cell migration was measured with the circular wound closure assay as described by De Ieso and Pei (2018) [75]. Cells were seeded at 1 x 10^5 cells/ml in normal culture medium with 10% fetal bovine serum (FBS), and incubated at 37°C in 5% CO_2 in a 96-well plate. When cells reached 80-90% confluence, cells were incubated in reduced-serum (2% FBS) media and 400nM of the mitotic inhibitor 5-fluoro-2'-deoxyuridine (FUDR) overnight to achieve a confluent monolayer. Circular wounds were generated with a sterile p10 pipette tip; drug-treated media (with 2% FBS and FUDR) was applied following wounding. Complete wounds were imaged at 10x magnification with a Canon 6D camera on a Nikon inverted microscope. Images were standardised using XnConvert software, and wound areas were quantified using NIH ImageJ software (U.S. National Institutes of Health). Closure was calculated as a percentage of the initial wound area for the same well as a function of time. All experiments were repeated twice.

3.4.7 Live Cell Imaging

U87-MG cells were seeded on flat-bottomed 96-well plates at a density of 1x10^5 cells/mL. A confluent monolayer was achieved 2-3 days after plating. Cells were conditioned in low serum culture medium (2% FBS) in the presence of FUDR (400 nM) for 12-18 hours before wounding. A circular wound was created in each well using techniques described above for the wound closure assays. Plate was mounted on a Nikon Ti E Live Cell Microscope (Nikon, Tokyo, Japan) in an enclosed humidified chamber kept at 37°C with 5% CO_2. Images were taken at 30-minute intervals for 20 hours, using Nikon NIS-Elements software. AVI files were exported from NIS-Elements and converted into TIFF files using Fiji (ImageJ). Converted files were analyzed using Fiji software [80] with the Manual Tracking plug-in. Total distance per cell was calculated as the cumulative distance travelled over the full duration of the experiment.

3.4.8 Transwell Invasion Assay

Three-dimensional (3D) cancer cell invasion was measured with the transwell invasion assay, which was performed using 6.5 mm Corning® Transwell®

polycarbonate membrane cell culture inserts with 8μm pore size (cat #3422; Sigma-Aldrich). The upper surface of the filter was coated with 40 μL of water-diluted extracellular matrix (ECM) gel from Engelbreth-Holm-Swarm murine sarcoma (250 μg/mL for each cell line; Sigma-Aldrich, St. Louis, MO). The transwells with the ECM gel are left to dehydrate overnight, and rehydrated 2 hours prior to cell seeding with 50 μL of serum-free DMEM per transwell insert. Cells were grown to approximately 40% confluence under normal conditions, and transferred into reduced serum (2% FBS) medium for 12-18 hours prior to seeding. Cells were detached (at ≤80% confluency) and resuspended in serum-free culture media with and without pharmacological treatments at $5x10^4$ cells per well. Cells were then seeded in transwell inserts (total 150μL of cell suspension per transwell, including 50 μL of rehydration medium added earlier). 600 μL of culture medium with 10% serum (chemoattractant) and the pharmacological treatment was added to the lower chamber. Cells were incubated for 4 hours, at 37°C in 5% CO_2. Non-migrated cells were scraped from the upper surface of the membrane with a cotton swab; migrated cells remaining on the bottom surface were counted after staining with crystal violet [81].

3.4.9 Cell viability assay

Cell viability was quantified using an alamarBlue assay [82], as per the manufacturer's guidelines (Life Technologies). Cells were plated in FUDR-containing culture media with 2% FBS, at 10^5 cells/ml in a 96-well plate. Treatments were applied 12-18 hours after plating, and cells were incubated for 24 hours. At 24 hours, cells were treated with 10% alamarBlue in culture media as above, for 1-2 hours (this depends on the cell type). Fluorescence signal levels were measured with a FLUOstar Optima microplate reader for control and treatment groups. The mean signal obtained from the no-cell control group was subtracted from every value in each treatment to correct for background fluorescence. Mercuric chloride (HgCl) was used as a positive control for cytotoxicity. The assay for cell proliferation was the same as above, except without the addition of FUDR.

3.4.10 Statistical Analyses

Statistical analyses performed with GraphPad Prism 7.02 software involved one-way ANOVA and post-hoc Bonferroni tests. Statistically significant outcomes are represented as $p<0.05$ (*), $p<0.01$ (**), $p<0.001$ (***), or $p<0.0001$ (****); NS is not significant. All data are presented as mean ± standard error of the mean (SEM); *n* values for independent samples are indicated in italics above the x-axes in histogram figures.

3.5 Results

3.5.1 AQP-1, -3, -4 and -5 expression in cell lines

AQP protein was measured in seven cell lines by western blot (Fig 3.1). An equal amount of total protein was added in each lane (40 μg), as determined by Bradford protein estimation. AQP1 was present in all cell lines; the major bands near 37kD were consistent with glycosylated forms of the 28kD AQP1 monomer [83]. AQP3 and AQP4 were also present in all cell lines near 37kD and 75kD, thought to be monomers and dimers [84, 85]. AQP5 was present in HT29 and HEK-293, but not detected in MDA-231-MB, SW620, U87-MG, A172, and U251. AQP5 bands near 25kD and 37kD are thought to be non-glycosylated and glycosylated forms of AQP5 [86, 87]. Thus, expression patterns for various AQPs differed between cell lines; however, all cell lines expressed AQP1 and were therefore suitable for testing effects of AQP1 pharmacological agents on cell motility.

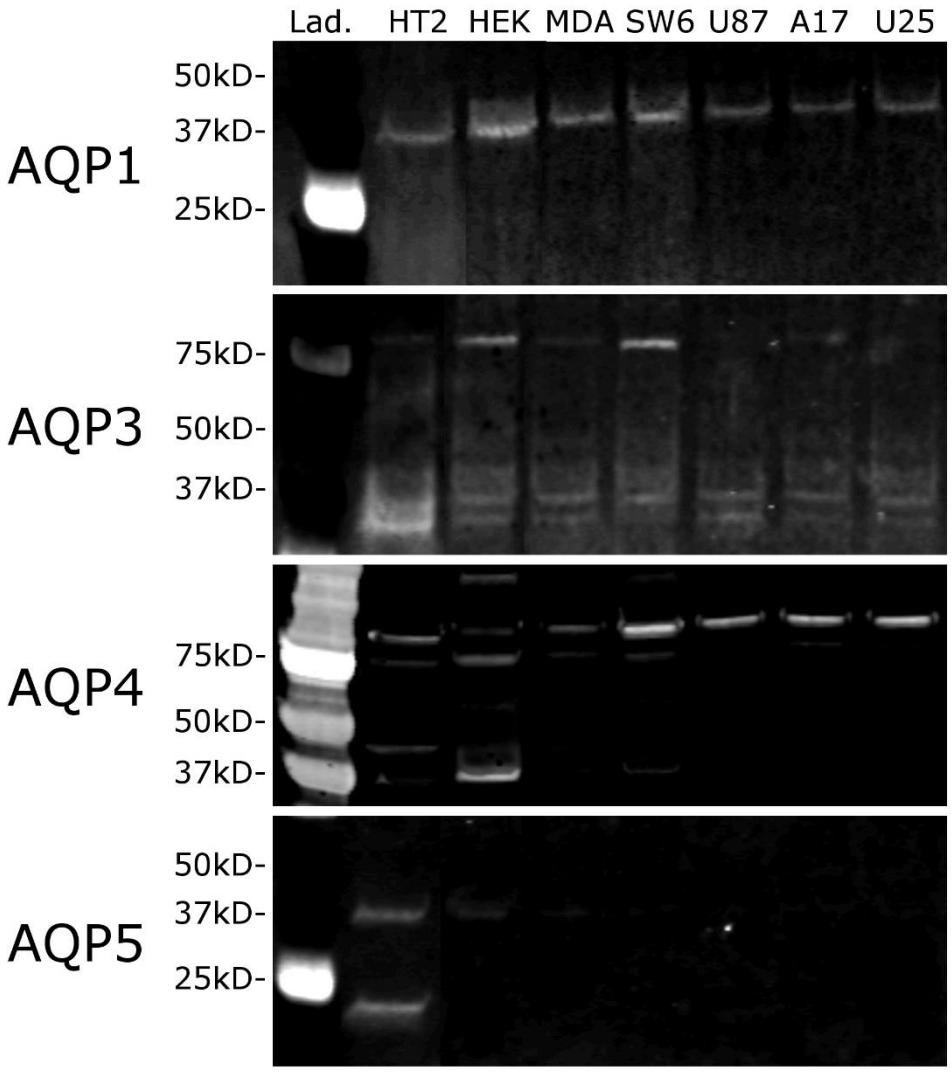

Figure 3.1 Western blot depicting bands for AQP-1, -3, -4, and -5 in each cell line. AQP-1, -3, and -4 protein were present in all cell lines. AQP5 was present only in HT29 and HEK-293. Definitions for abbreviations are as follows: protein ladder (Lad.); HT29 (HT2); HEK-293 (HEK); MDA-231-MB (MDA); SW620 (SW6); U87-MG (U87); A172 (A17); U251-MG (U25).

3.5.2 Ethylisopropylamiloride and bumetanide derivatives inhibited wound closure of AQP1-expressing cell lines

The dependence of cell migration on water and ion fluxes across the membrane was tested with antagonists of the AQP1 ion channel, AQP1 water channel, and a Na^+-dependent exchanger shown previously to influence motility [88]. The cell lines tested here were selected based on their positive AQP1 expression. As shown previously, bumetanide derivatives AqB011, AqB007, and AqB006 inhibited AQP1 ion currents in the oocyte expression system, and blocked 2D migration of HT29 cells (Fig 3.2A) [43]. Interestingly, the effectiveness of the bumetanide derivatives in blocking cell migration followed the same order of potency as measured for inhibition of the AQP1 ion channel conductance. AqB011 (50 μM) blocked wound closure by 60 ± 2.3%; AqB007 (50 μM) blocked wound closure by 29 ± 8.5%; AqB006 (50 μM) blocked wound closure by 27 ± 4.6%. The bumetanide derivatives were non-toxic at all doses tested, with the exception of 100μM AqB011 which resulted in 85 ± 1.4% cell viability, as referenced to 100% viability in untreated cells (Fig 3.2E). AqB011 was identified as the most potent of the bumetanide series of antagonists in reducing migration. To determine the possible contribution of NHE1 in HT29 and A172 cell migration, the antagonist EIPA was tested in wound closure assays (Fig 3.2B). EIPA (20μM) caused a small but significant block of wound closure in HT29 (by 33 ± 3.4%) in contrast to the strong block that was seen with AqB011 (Fig 3.2A). EIPA blocked A172 migration by 38 ± 3.4%. EIPA had no effect on cell viability at any of the doses tested (Fig 3.2E). These results indicated that membrane sodium flux is important for cell migration in both HT29 and A172, and that more than one transport mechanism is involved, though the relative contributions of each pathway depend on the cell type.

To determine whether AQP1 water conductance was physiologically important for cancer cell migration, we tested two agents shown to have antagonistic effects on AQP1 water conductance; acetazolamide and bacopaside II. Acetazolamide is a carbonic anhydrase inhibitor that has been shown to block AQP1 water flow in some preparations [89]. Bacopaside II has been shown to block AQP1 water flow but not AQP1 ion conductance in Xenopus oocytes [44]. Acetazolamide did not significantly reduce HT29 wound closure at any dose tested (1μM to 300μM; Fig

2C) and was non-toxic (Fig 3.2E). In contrast, bacopaside II (7.5μM) did significantly block wound closure in HT29 (27 ± 7.0%; Fig 3.2D), without evidence of cytotoxicity (Fig 3.2E). A172, HEK-293, and U87-MG cell migration were unaffected by bacopaside II (Fig 3.2D) at doses that had no effect on cell viability (Fig 3.2E). Thus, HT29 cell migration was reduced after treatment with bacopaside II and not acetazolamide, suggesting that acetazolamide and bacopaside II do not have similar pharmacological targets.

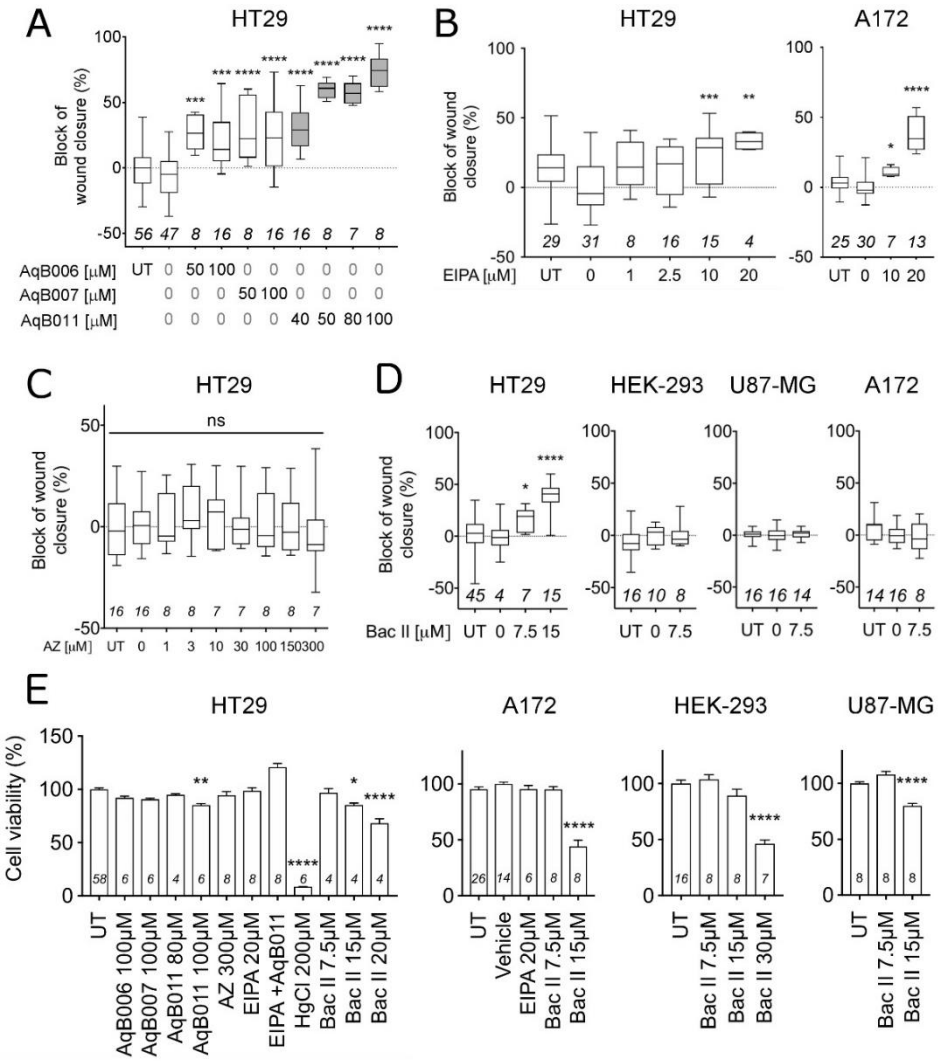

Figure 3.2 Effect of acetazolamide, EIPA, bacopaside II, and bumetanide derivatives on wound closure in AQP1-expressing cell lines. (A) Box and whisker plot depicting block of HT29 wound closure following treatment with bumetanide derivatives AqB006, AqB007, and AqB011. All treatments significantly blocked wound closure; AqB011 100μM produced the strongest block. (B) Box and whisker plots depicting block of HT29 and A172 wound closure following treatment with EIPA. EIPA significantly reduced wound closure at 10μM and 20μM for both cell lines. (C) Box and whisker plot depicting block of HT29 wound closure following acetazolamide treatment. Acetazolamide had no effect on wound closure for all doses tested. (D) Box and whisker plot depicting block of wound closure following bacopaside II treatment. Bacopaside II blocked wound closure in HT29 cells. (E) Histograms depicting cell viability following treatment with all of the above tested compounds. AqB011 100μM produced a slight but significant reduction in HT29 cell viability. Bacopaside II (≥15μM) reduced cell viability in all cell lines.

3.5.3 AqB011 inhibited wound closure in multiple AQP1-expressing cancer cell lines

To see whether AQP1 ion conductance played a role in cell migration across multiple AQP1-expressing cell lines, we tested AqB011 in AQP1-expressing U87-MG, A172, U251-MG, SW620, HEK-293, and MDA-231-MB. AqB011 inhibited wound closure in U87-MG (at 20 to 80μM), A172 (40 to 80μM), and U251-MG (80μM) (Fig 3.3A). AqB011 had no effect on wound closure for SW620, HEK-293, and MDA-231-MB cell lines (Fig 3.3A). AqB011 had no significant effect on cell viability in any cell lines other than A172 (Fig 3.3B). In A172, AqB011 (40μM) treatment resulted in 80 ± 3.3% cell viability as referenced to untreated. Therefore, inhibition of A172 wound closure by AqB011 might be partly attributable to reduction in cell viability. Overall, these data suggested that the presence of AQP1 protein did not guarantee inhibition of wound closure by AqB011.

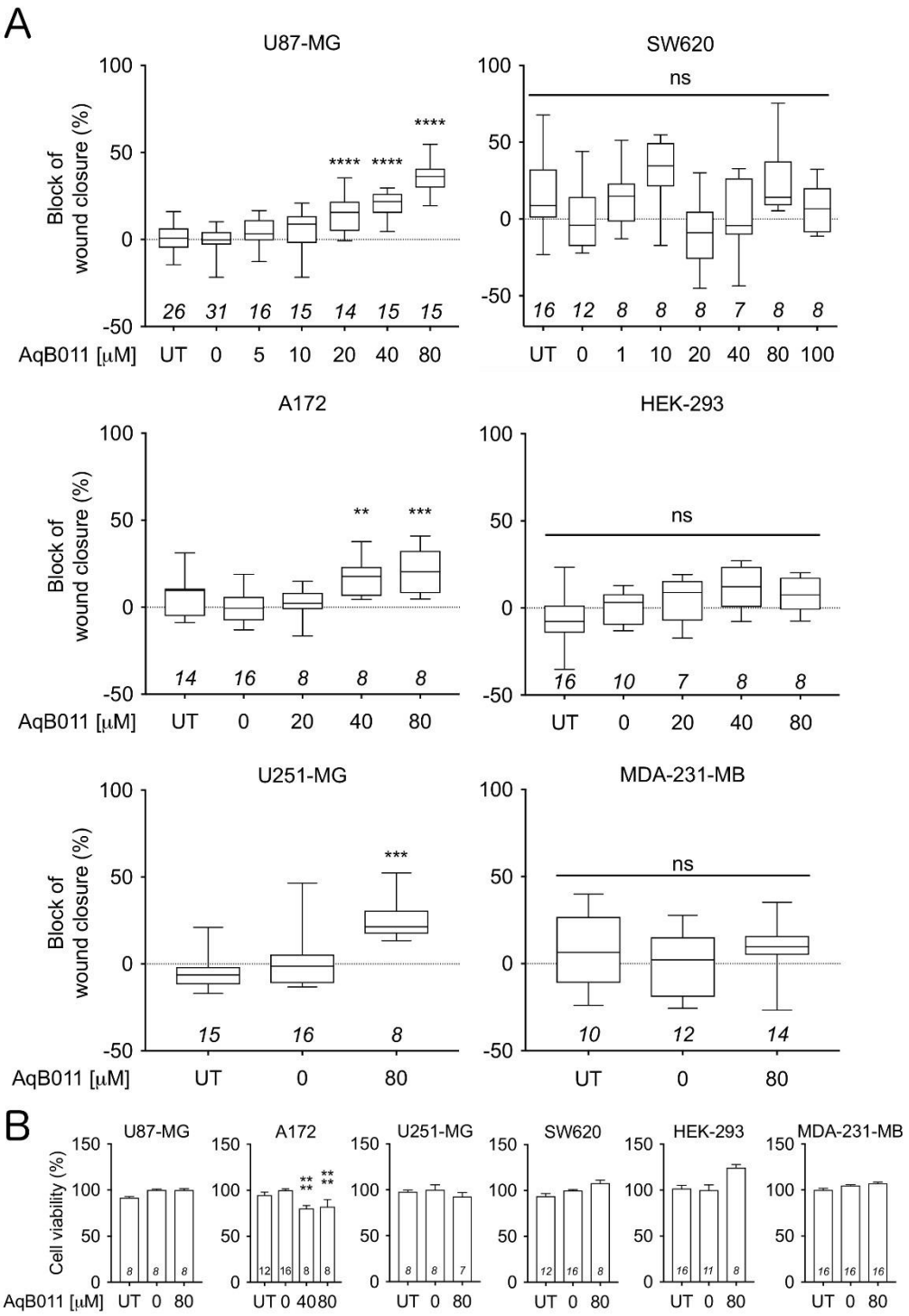

Figure 3.3 Effect of AqB011 on wound closure in other AQP1-expressing cell lines. (A) Box and whisker plots depicting block of wound closure following treatment with AqB011. Cell lines tested are glioblastoma cell lines U87-MG, A172, and U251-MG; colorectal adenocarcinoma cell line SW620; human embryonic cell line HEK-293; and breast cancer cell line MDA-231-MB. AqB011 produced a significant block in U87-MG, A172, and U251-MG. (B) Histogramss

depicting cell viability of each cell line following treatment with AqB011. AqB011 did not significantly reduce cell viability in any cell line except A172. AqB011 (40μM and 80μM) mildly but significantly reduced A172 cell viability (****).

3.5.4 AqB011 inhibited individual glioblastoma cell migration as assessed by live cell imaging

Important mechanisms of cancer invasion and metastasis are cell migration and disassociation of cell-cell adhesions [33]; these processes are not entirely captured in collective cell migration analyses such as the wound closure assay. Over 20 hours, U87-MG individual cell motility was measured following AqB011 and bacopaside II administration. The U87-MG cell line was selected for individual cell motility analysis based on the robust response to AqB011, which was depicted in figure 3.3A. Figure 3.4A illustrates 5-hour intervals of U87-MG cells treated with and without AqB011; there was a noticeable reduction in the distance covered by AqB011-treated cells as compared to vehicle treated cells. Impaired cell migration was evident from the shortened trajectories in the AqB011 (80μM) treatment group as compared with untreated and vehicle control (Fig 3.4B). Trajectory analysis showed that U87-MG cells treated with AqB011 80μM migrated significantly shorter total distances in 20 hours (525 ± 27 μm) than vehicle-treated cells (649 ± 27 μm) (Fig 3.4C). Bacopaside II (7.5μM) alone and combined with AqB011 (20μM) had no effect on U87-MG individual cell migration. Thus, AqB011 inhibited individual cell movement as well as collective cell migration in U87-MG glioblastoma cells.

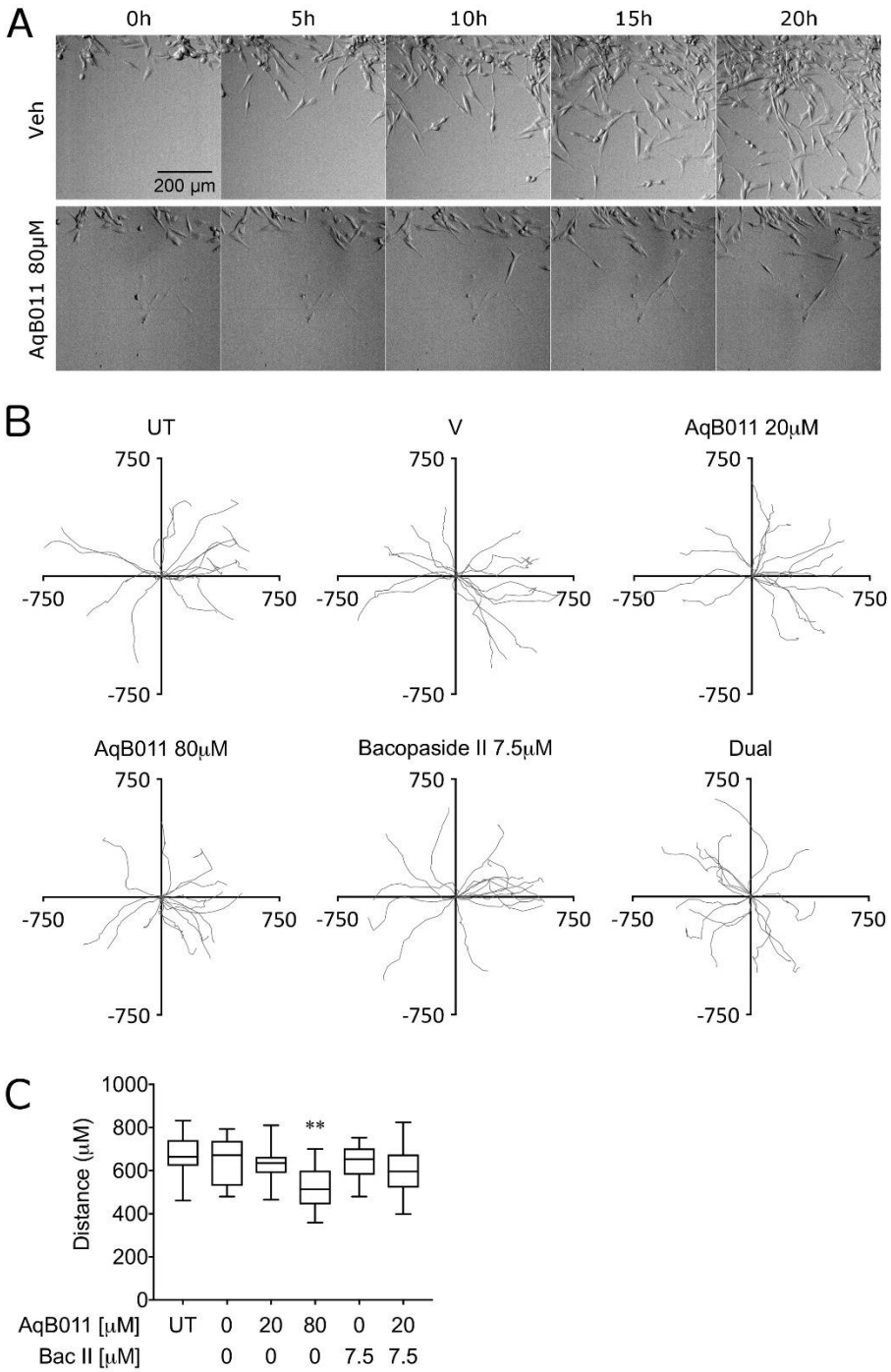

Figure 3.4 The effect of AqB011 on individual U87-MG glioblastoma cell migration. (A) Panels of five images each from time-lapse series are shown at 5-hour intervals. Vehicle and AqB011 80µM treatments are depicted. (B) Trajectory plots of individual cells (n=15) per treatment group, monitored by the position of the cell nucleus at 30 minute intervals over 20 hours; X and Y values are in µm. (C) Box and whisker plot depicting cell trajectory analysis; U87-MG cells treated with AqB011 80µM migrated significantly shorter total distances in 20 hours than vehicle-treated cells (**).

3.5.5 AQP5-knockdown in HT29 colorectal carcinoma cells resulted in increased sensitivity to inhibition of wound closure by AqB011

Results from the wound closure assay revealed that the presence of AQP1 protein did not guarantee inhibition of wound closure by AqB011, suggesting dependence on AQP1 ion conductance for rapid cell migration might vary between cell types. To determine the selectivity of AqB011 for AQP1, we tested AqB011 following mRNA knock-down of AQP1 and AQP5 in HT29 cells. Figure 3.5A depicted bands for western blot protein analysis following AQP1 and AQP5 siRNA treatments. Band intensities were standardised to the housekeeping protein, GAPDH. AQP5 bands were identified near 37kD and 25kD, and AQP1 bands were identified near 37kD, consistent with results in Figure 3.1. AQP1 protein expression was not significantly reduced following AQP1 siRNA transfection (Fig 3.5B); however, AQP5 protein expression was significantly reduced to $39 \pm 0.1\%$ of control siRNA-transfected cells following AQP5 siRNA transfection (Fig 3.5B). Interestingly, both AQP1 and AQP5 mRNA levels were significantly reduced following siRNA treatment (Fig 3.5C), suggesting the siRNAs had been effective in decreasing their targeted transcripts, but that a much slower turnover rate for AQP1 protein in HT29 allowed for persistence of the AQP1 channels. Figure 3.5D illustrates the high transfection efficiency achieved for HT29 cell lines. AQP1- and AQP5-siRNA-tranfected cells did not exhibit any significant reduction in wound closure as compared to control siRNA transfected cells (Fig 3.5E). Combined AQP1 and AQP5 siRNA treatments also did not produce any significant inhibition of wound closure as compared to control siRNA. Sensitivity to AqB011 in the inhibition of wound closure was not altered following AQP1 siRNA treatment (consistent with continued presence of AQP1 channels). The AQP1 siRNA treatment did not alter HT29 wound closure rates or AQP1 protein levels in HT29 cell lines, and thus served as an unintended control, showing that the experimental manipulations did not affect cell properties. In contrast, AQP5-siRNA treatment successfully reduced AQP5 protein levels, and the potency of AqB011 inhibition of wound closure was increased (Fig 3.5E), consistent with an amplified dependence on AQP1 for cell migration in the background of AQP5 knockdown.

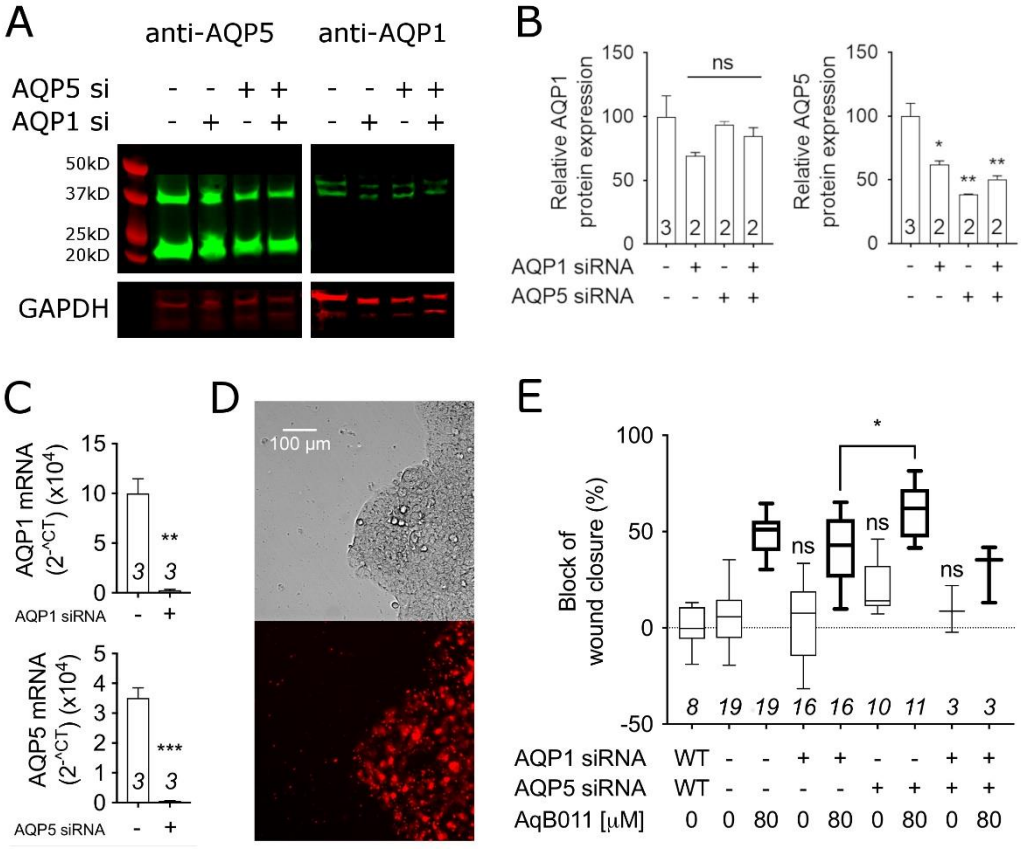

Figure 3.5 Effect of AQP1 and AQP5 knockdown on HT29 wound closure and AqB011 sensitivity. (A) Image depicting western blot analysis of AQP1 and AQP5 protein expression levels in HT29 cells following knockdown of AQP1, AQP5, or combined knockdown of AQP1 and AQP5. GAPDH is used as a reference protein for quantification. (B) Graphs depicting quantified AQP1 and AQP5 protein levels following knockdown. AQP5 protein levels were significantly reduced in AQP5 siRNA-transfected cells as compared to control siRNA-transfected cells (**). AQP1 siRNA-transfected cells did not show any significant reduction in AQP1 protein levels as compared to control siRNA-transfected cells. Control siRNA represented by double negative symbol. (C) Graphs depicting quantified AQP1 and AQP5 mRNA levels following respective siRNA knockdown. (D) Images depicting high transfection efficiency in HT29 cells. Top panel depicts brightfield image of cells, and bottom panel shows fluorescing (transfected) cells of the same image. (E) Graph depicting block of wound closure in AQP1- and AQP5-knockdown cells, following treatment with AqB011. AQP1- and AQP5-knockdown cells did not exhibit any significant reduction in wound closure as compared to control siRNA.

Cells with reduced AQP5 showed an increased sensitivity to AqB011 (*). WT is wild-type, meaning the cells have not been transfected.

3.5.6 AqB011 inhibited cell invasion in glioblastoma and breast cancer cell lines

In addition to cell motility, the process of cancer metastasis requires the movement of cells through extracellular matrix (ECM), an attribute not tested in standard 2D wound closure models. Thus, we aimed to test the role of AQP1 ion conductance in cancer invasiveness. The effects of AqB011 were tested on glioblastoma and breast cancer cell lines with transwell filter chambers in which cells migrated through an ECM layer towards a chemoattractant (FBS), and were stained and counted (Fig 3.6A). The cell lines were chosen based on their high invasive capacity and positive AQP1 expression. Moreover, the U87-MG and U251-MG cell lines were sensitive to block of wound closure by AqB011, whereas MDA-231-MB cells were not; this allowed for an investigation as to whether the effects of AqB011 were consistent in both 2D and 3D cell migration assays. AqB011 significantly inhibited cell invasion in U87-MG (40 to 100 μM), U251-MG (80 μM), and MDA-231-MB (80 μM) (Fig 3.6B). U87-MG cells treated with AqB011 at 80 μM invaded at 49 ± 7.1%; U251-MG cells treated with AqB011 80 μM invaded at 63 ± 12%; MDA-231-MB cells treated with AqB011 80 μM invaded at 40 ± 9.4%; as compared to vehicle. These results showed that AqB011 inhibited invasiveness in glioblastoma and breast cancer cells, in addition to impairing 2D cell migration in wound closure assays. Interestingly, these results also showed that MDA-231-MB cells were sensitive to block of invasion by AqB011, despite a lack of sensitivity to AqB011 when measuring wound closure. The effect of bacopaside II was tested on U87-MG invasiveness; U87-MG cells treated with bacopaside II at 7.5 μM invaded at 40 ± 3.9% compared to vehicle (Fig 3.6B). Combined treatment with bacopaside II and AqB011 did not result in any additional effect.

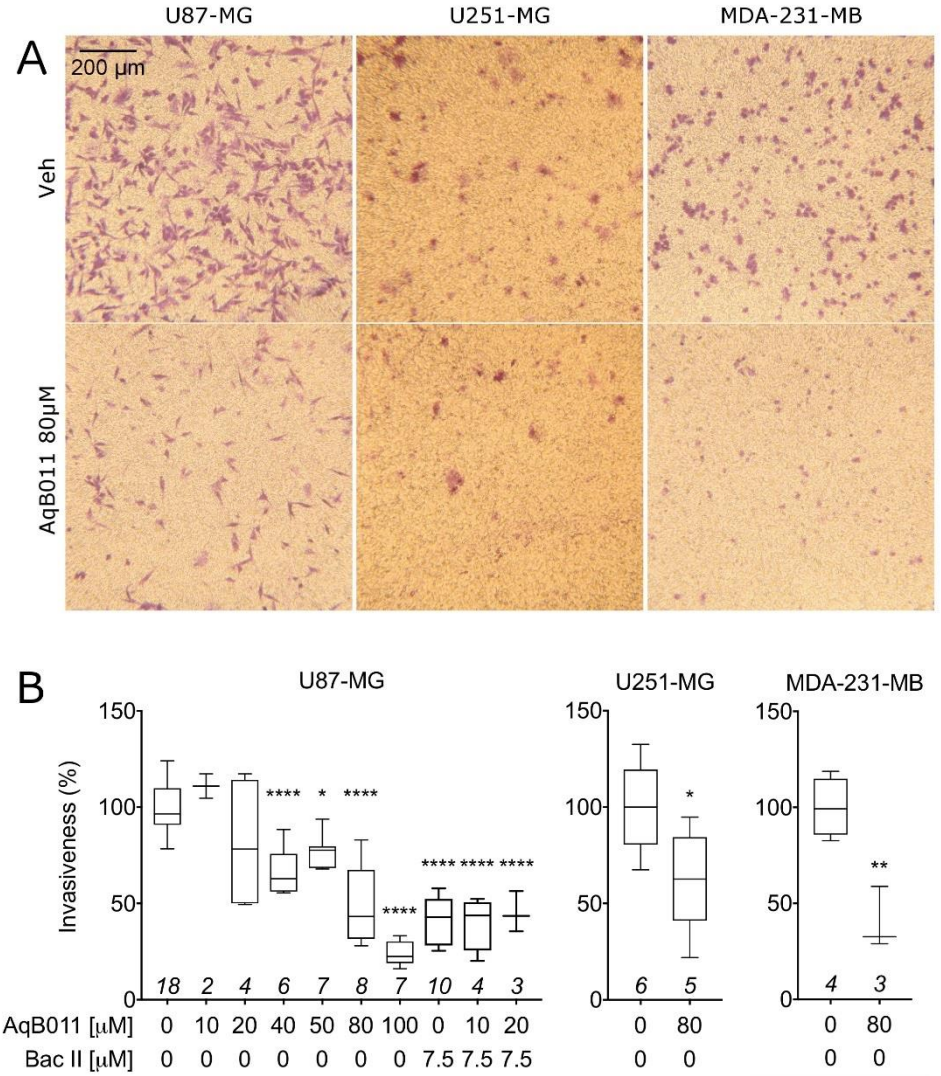

Figure 3.6 Invasive capacities of U87-MG, U251-MG, and MDA-231-MB cells following treatment with AqB011. (A) Images depicting cells that successfully crossed the ECM layer to reach the trans side of the transwell membrane in treatments with vehicle and AqB011 80µM (B) Box plots depicting U87-MG, U251-MG, and MDA-231-MB cell invasiveness after 4 hours with AqB011. AqB011 significantly inhibited cell invasiveness in all three cell lines.

3.5.7 AqB011 inhibited cell proliferation in U87-MG glioblastoma cell line

AQP1 enables proliferation in some cancer cells [90], so we proposed AQP1 ion conductance might play a role. Proliferation rate of U87-MG cells was measured with the alamarBlue assay, in the absence of FUDR. Over 24 hours, non-toxic doses (40 and 80μM) of AqB011 significantly inhibited cell growth; cells treated with AqB011 (80μM) proliferated at 83 ± 1.7% compared to vehicle treated cells. Bacopaside II 7.5μM had no effect on cell growth (Fig 3.7). Considering doses that reduced proliferation were not previously shown to be cytotoxic, it would be reasonable to assume that AqB011 inhibited glioblastoma cell proliferation, uncovering another possible role for AQP1 ion conductance. Alternatively, AqB011 might have other targets besides AQP1 ion conductance, which might play a role in cell proliferation. Although, AqB011 has not been shown to have any effect on cell motility in cells lacking AQP1 expression thus far, suggesting it is selective for AQP1 [43].

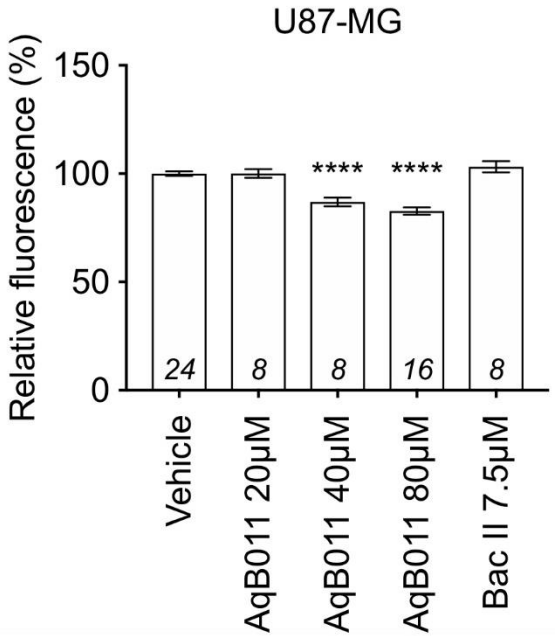

Figure 3.7 Graph depicting proliferation of U87-MG cells following treatment with AqB011 and bacopaside II. AqB011 significantly reduced cell proliferation over 24 hours.

3.6 Discussion

Pharmacological modulators of AQP1 are useful for investigating channel characteristics, gating mechanisms, and physiological roles of AQP1. The first AQP1 inhibitor to be discovered was mercuric chloride, which inhibited AQP1 water permeability through binding with a cysteine residue in loop E [91]. Despite high toxicity, mercuric chloride proved useful for uncovering novel AQP gating mechanisms [16, 92]. Tetraethylammonium (TEA) inhibited AQP1 water permeability in Xenopus ooctyes, playing a key role in revealing the involvement of loop E in AQP1 water conductance [93]. Acetazolamide reduced water permeability of AQP1 in Xenopus ooctyes [45], and AQP1-transfected HEK cells [89]. Both TEA and acetazolamide were not effective AQP1 blockers in some preparations [94], however they crucially indicated that pharmacological modification of AQP activity was possible. Later, the discovery of AQP1 inhibitors derived from bumetanide (the AqB compounds) enabled further investigation into physiological roles of AQP1. Proposed AQP1 blocker, AqB050, inhibited cancer cell motility and invasiveness *in vitro*, but not *in vivo* [95]. AqB013 also blocked the AQP1 water channel [96], and inhibited cancer cell migration, invasion, and angiogenesis *in vitro* [97]. AqB007 and AqB011 blocked AQP1 ion conductance [43], enabling investigation as to the role of AQP1 ion conductance in cancer motility. For the first time, we showed that AqB011 inhibited cell migration and invasion in AQP1-expressing glioblastoma, breast cancer, and colon cancer cell lines, suggesting AQP1 ion conductance might be a valuable pharmacological target for cancer therapy.

AQP1-enabled ion flux might contribute to cell migration via a similar mechanism as NHE1. NHE1 blocker, EIPA, was previously shown to inhibit cell migration in sarcoma and breast cancer cells [88], and for the first time we show that EIPA also inhibits cell migration in colon cancer and glioblastoma. During cell movement, process extension occurs via the reversible assembly of actin filaments [98-100], and local cell volume increases are enabled by water and ion influxes [42, 101, 102]. NHE1 plays an important role in cell migration by regulating uptake of Na^+ at the leading edge to create an osmotic gradient, which triggers the local influx of water via AQPs; this enables the generation of cell membrane protrusions at the

leading edge of a migrating cell [42, 88]. AQP1-facilitated Na^+ flux might also contribute to a local osmotic gradient driving simultaneous AQP1-mediated water influx at leading edges, leading to cell volume changes linked with process extension and cell migration [42, 88]. However, the physiological relevance of AQP1-mediated Na^+ transport over that of dedicated Na^+ channels is not understood. Future work will involve testing migration in cells transfected with AQP1 constructs that have been mutated so that AQP1 ion conductance is inactivated or activated without affecting water permeability. Additionally, AQP1 facilitates K^+ flux via the central pore [16, 21], and dedicated K^+ channels including the BK channel and inward rectifying K^+ channel-1 regulate cell migration [42, 103]. Therefore, AQP1-facilitated K^+ flux should not be excluded as an alternative mechanism underlying AQP1-facitated cell migration.

To determine the importance of AQP1-facilitated water permeability in cancer cell migration, we tested the effects of bacopaside II and acetazolamide on cancer cell migration and invasion. Acetazolamide has failed to inhibit AQP1 water channel activity in some preparations [94], which might explain why HT29 cell migration was unchanged following acetazolamide administration. Bacopaside II (7.5 μM) was non-toxic, and inhibited wound closure in HT29 colon cancer cells, and invasiveness in U87-MG glioblastoma cells, suggesting that AQP1 water flux plays a role in facilitating cell motility in these cell lines. However, bacopaside II (7.5μM) had no effect on 2D cell migration in every other cell line tested. IC_{50} for block of AQP1 water flux by bacopaside II in *Xenopus oocytes* is 18 μM [44]; bacopaside II started to exhibit toxicity beyond 7.5 μM (Fig 3E), and a limiting factor of the project was that higher doses could not be tested, which might have explained insensitivity to bacopaside II in some cell lines. It is also not known whether effects of bacopaside II on cell migration and invasion are due to AQP1 inhibition or off-target interactions; therefore, determining bacopaside II selectivity for AQP1 is crucial. This work highlights the importance of developing novel AQP1 water channel blockers with higher potency and reduced cytotoxicity in order to properly test the effect of AQP1 water channel inhibition in cancer cell migration and invasion.

Similar to bacopaside II, block of 2D cell migration by AqB011 was not consistent across all AQP1-expressing cell lines. HT29, U87-MG, A172, U251-MG were all sensitive to block by AqB011, but SW620, HEK-293, and MDA-231-MB were insensitive. Membrane localization of AQP1 has been shown to affect sensitivity to inhibitors [104], which might have accounted for the differences in sensitivity to block by AqB011 and bacopaside II. Moreover, sensitivity to AqB011 and bacopaside II was boosted during cell invasion. MDA-231-MB invasiveness was inhibited by AqB011, although wound closure was not. Additionally, U87-MG invasiveness was inhibited by bacopaside II, although wound closure was not. Unlike the wound closure assay, the transwell invasion assay encourages dynamic cell volume regulation to fit through narrow spaces. This might result in increased activity of AQP1 dual water and ion conductances, explaining increased sensitivity to AqB011. We also showed that AqB011 inhibited U87-MG cell proliferation, which could hint at another putative role for AQP1 ion conductance. However, more work is needed to elucidate the mechanisms of AqB011-induced reduction in cell proliferation, and to test the effects of AqB011 on cell proliferation in other lines used in this study.

A key element for establishing that AQP1-mediated ion conductance is important for cancer cell migration and invasion is to determine AqB011 selectivity for AQP1 over other ion channels. Recent work showed that AqB011 selectively inhibits AQP1 ion conductance in Xenopus oocytes via interaction with the loop D domain of AQP1 [20]; however more work is needed to confirm the specificity of AqB011 to AQP1 in cancer cells. To test this, we attempted to measure the effect of AqB011 after knocking down AQP1 in HT29 cells using siRNA. Unexpectedly, the AQP1 siRNA-transfection did not result in a concomitant reduction in sensitivity to AqB011; this was likely due to poor efficacy of AQP1 knock-down. In HT29, we successfully knocked down AQP5 protein, but not AQP1; this was despite the high transfection efficiency achieved (Fig 3.5D), the use of a validated AQP1 siRNA, and successful mRNA downregulation (Fig 3.5C). The failure to achieve significant knockdown of AQP1 protein might have been due to low AQP1 turnover in HT29 cells, which would explain why protein levels did not immediately decrease following a decrease in mRNA [105], and why HT29 wound closure was unchanged

between AQP1 and control siRNA-transfected cells. Rates of protein degradation can vary, which also could lead to differences in AQP1 and AQP5 turnover [8]. More work is needed to confirm the specificity of AqB011 for AQP1, and to test effects of AqB011 on other cell lines with endogenous AQP1 that are more amenable to knock-down. Other tests for selectivity might include electrophysiological analysis of AqB011 in an AQP expression system [106].

AQP5 promotes lymph node metastasis in patients with colon cancer [107], and colocalizes with ion channels such as NHE1 to enable local cell volume regulation at the leading edge of a migrating cell [88]. So, it was surprising that AQP5-knockdown cells did not exhibit any variation in wound closure as compared to cells treated with control siRNA. However, the AQP5-knockdown cells did exhibit a significantly increased sensitivity to block of wound closure by AqB011. HT29 cells might have compensated for loss of AQP5 by activating or upregulating AQP1, and subsequently becoming more sensitive to block by an AQP1-specific inhibitor such as AqB011. Future work should characterise effects of AQP1 and AQP5 knockdown in models of cell invasion and individual cell motility to rule out any additional effects that might not be apparent in the wound closure assay.

In conclusion, we demonstrated the efficacy of AQP1 ion channel blocker, AqB011, and AQP1 water channel blocker, bacopaside II, in blocking invasion and migration in various AQP1-expressing cancer types. This new discovery highlighted the importance of AQP1 ion conductance as a potential pharmacological target in cancer migration and invasion. Future directions involve testing whether AqB011 and bacopaside II can be administered in combination to inhibit dual AQP1 water and ion conductance for an amplified effect, and to test whether these compounds are effective blockers of metastasis and invasion in animal models of metastasis.

3.7 References

1. Kourghi, M., et al., *Fundamental structural and functional properties of Aquaporin ion channels found across the kingdoms of life.* Clinical and Experimental Pharmacology and Physiology, 2018. **45**(4): p. 401-409.
2. Verkman, A. and A.K. Mitra, *Structure and function of aquaporin water channels.* American Journal of Physiology-Renal Physiology, 2000. **278**(1): p. F13-F28.
3. Denker, B.M., et al., *Identification, purification, and partial characterization of a novel Mr 28,000 integral membrane protein from erythrocytes and renal tubules.* Journal of Biological Chemistry, 1988. **263**(30): p. 15634-15642.
4. Preston, G.M. and P. Agre, *Isolation of the cDNA for erythrocyte integral membrane protein of 28 kilodaltons: member of an ancient channel family.* Proceedings of the National Academy of Sciences, 1991. **88**(24): p. 11110-11114.
5. Preston, G.M., et al., *Appearance of water channels in Xenopus oocytes expressing red cell CHIP28 protein.* Science, 1992. **256**(5055): p. 385-387.
6. Ishibashi, K., S. Hara, and S. Kondo, *Aquaporin water channels in mammals.* Clinical and experimental nephrology, 2009. **13**(2): p. 107-117.
7. Finn, R.N. and J. Cerda, *Evolution and functional diversity of aquaporins.* The Biological Bulletin, 2015. **229**(1): p. 6-23.
8. Finn, R.N., et al., *The lineage-specific evolution of aquaporin gene clusters facilitated tetrapod terrestrial adaptation.* PLoS One, 2014. **9**(11): p. e113686.
9. Li, C. and W. Wang, *Molecular Biology of Aquaporins*, in *Aquaporins*. 2017, Springer. p. 1-34.
10. Jung, J.S., et al., *Molecular structure of the water channel through aquaporin CHIP. The hourglass model.* Journal of Biological Chemistry, 1994. **269**(20): p. 14648-14654.
11. Sui, H., et al., *Structural basis of water-specific transport through the AQP1 water channel.* Nature, 2001. **414**(6866): p. 872-878.
12. Jensen, M.Ø., E. Tajkhorshid, and K. Schulten, *The mechanism of glycerol conduction in aquaglyceroporins.* Structure, 2001. **9**(11): p. 1083-1093.
13. Anthony, T.L., et al., *Cloned human aquaporin-1 is a cyclic GMP-gated ion channel.* Mol Pharmacol, 2000. **57**(3): p. 576-88.
14. Hazama, A., et al., *Ion permeation of AQP6 water channel protein single-channel recordings after Hg2+ activation.* Journal of Biological Chemistry, 2002. **277**(32): p. 29224-29230.
15. Ehring, G.R., et al., *Properties of channels reconstituted from the major intrinsic protein of lens fiber membranes.* The Journal of General Physiology, 1990. **96**(3): p. 631-664.
16. Yool, A.J., W.D. Stamer, and J.W. Regan, *Forskolin stimulation of water and cation permeability in aquaporin-1 water channels.* Science, 1996. **273**(5279): p. 1216-8.
17. Agre, P., et al., *Aquaporins and ion conductance.* Science, 1997. **275**(5305): p. 1490; author reply 1492.
18. Boassa, D. and A.J. Yool, *Single amino acids in the carboxyl terminal domain of aquaporin-1 contribute to cGMP-dependent ion channel activation.* BMC Physiol, 2003. **3**: p. 12.

19. Zhang, W., et al., *Aquaporin-1 channel function is positively regulated by protein kinase C.* J Biol Chem, 2007. **282**(29): p. 20933-20940.
20. Kourghi, M., et al., *Identification of loop D domain amino acids in the human Aquaporin-1 channel involved in activation of the ionic conductance and inhibition by AqB011.* Frontiers in chemistry, 2018. **6**: p. 142.
21. Yu, J., et al., *Mechanism of gating and ion conductivity of a possible tetrameric pore in aquaporin-1.* Structure, 2006. **14**(9): p. 1411-23.
22. Yool, A.J. and E.M. Campbell, *Structure, function and translational relevance of aquaporin dual water and ion channels.* Mol Aspects Med, 2012. **33**(5-6): p. 553-561.
23. Saparov, S.M., et al., *Water and ion permeation of aquaporin-1 in planar lipid bilayers. Major differences in structural determinants and stoichiometry.* J Biol Chem, 2001. **276**(34): p. 31515-20.
24. Tsunoda, S.P., et al., *Aquaporin-1, nothing but a water channel.* J Biol Chem, 2004. **279**(12): p. 11364-7.
25. Campbell, E.M., D.N. Birdsell, and A.J. Yool, *The activity of human aquaporin 1 as a cGMP-gated cation channel is regulated by tyrosine phosphorylation in the carboxyl-terminal domain.* Mol Pharmacol, 2012. **81**(1): p. 97-105.
26. Boassa, D., W.D. Stamer, and A.J. Yool, *Ion channel function of aquaporin-1 natively expressed in choroid plexus.* J Neurosci, 2006. **26**(30): p. 7811-9.
27. Saadoun, S., et al., *Increased aquaporin 1 water channel expression in human brain tumours.* Br J Cancer, 2002. **87**(6): p. 621-3.
28. Moon, C., et al., *Involvement of aquaporins in colorectal carcinogenesis.* Oncogene, 2003. **22**(43): p. 6699-703.
29. Mazal, P.R., et al., *Diagnostic significance of aquaporin-1 in liver tumors.* Hum Pathol, 2005. **36**(11): p. 1226-31.
30. Hoque, M.O., et al., *Aquaporin 1 is overexpressed in lung cancer and stimulates NIH-3T3 cell proliferation and anchorage-independent growth.* Am J Pathol, 2006. **168**(4): p. 1345-53.
31. Guan, B., et al., *Expression and distribution of aquaporin 1 in laryngeal carcinoma.* Lin Chuang Er Bi Yan Hou Tou Jing Wai Ke Za Zhi, 2007. **21**(6): p. 269-272.
32. Shi, Z., et al., *Aquaporins in human breast cancer: identification and involvement in carcinogenesis of breast cancer.* Journal of surgical oncology, 2012. **106**(3): p. 267-272.
33. De Ieso, M.L. and A.J. Yool, *Mechanisms of Aquaporin-Facilitated Cancer Invasion and Metastasis.* Frontiers in Chemistry, 2018. **6**: p. 135.
34. Hu, J. and A.S. Verkman, *Increased migration and metastatic potential of tumor cells expressing aquaporin water channels.* FASEB J, 2006. **20**(11): p. 1892-4.
35. Saadoun, S., et al., *Impairment of angiogenesis and cell migration by targeted aquaporin-1 gene disruption.* Nature, 2005. **434**(7034): p. 786-92.
36. Nicchia, G.P., et al., *Inhibition of aquaporin-1 dependent angiogenesis impairs tumour growth in a mouse model of melanoma.* J Mol Med (Berl), 2013. **91**(5): p. 613-23.
37. McCoy, E. and H. Sontheimer, *Expression and function of water channels (aquaporins) in migrating malignant astrocytes.* Glia, 2007. **55**(10): p. 1034-43.

38. Grinstein, S., et al., *Focal localization of the NHE-1 isoform of the Na+/H+ antiport: assessment of effects on intracellular pH.* The EMBO Journal, 1993. **12**(13): p. 5209-5218.
39. Denker, S.P. and D.L. Barber, *Cell migration requires both ion translocation and cytoskeletal anchoring by the Na-H exchanger NHE1.* The Journal of cell biology, 2002. **159**(6): p. 1087-1096.
40. Patel, H. and D.L. Barber, *A developmentally regulated Na-H exchanger in Dictyostelium discoideum is necessary for cell polarity during chemotaxis.* The Journal of cell biology, 2005. **169**(2): p. 321-329.
41. Stock, C., et al., *Migration of human melanoma cells depends on extracellular pH and Na+/H+ exchange.* The Journal of physiology, 2005. **567**(1): p. 225-238.
42. Schwab, A., et al., *Cells move when ions and water flow.* Pflug Arch Eur J Phy, 2007. **453**(4): p. 421-432.
43. Kourghi, M., et al., *Bumetanide Derivatives AqB007 and AqB011 Selectively Block the Aquaporin-1 Ion Channel Conductance and Slow Cancer Cell Migration.* Molecular Pharmacology, 2016. **89**(1): p. 133-140.
44. Pei, J.V., et al., *Differential Inhibition of Water and Ion Channel Activities of Mammalian Aquaporin-1 by Two Structurally Related Bacopaside Compounds Derived from the Medicinal Plant Bacopa monnieri.* Molecular Pharmacology, 2016. **90**(4): p. 496-507.
45. Bing, M., et al., *Effects of acetazolamide and anordiol on osmotic water permeability in AQP1-cRNA injected Xenopus oocyte.* Acta Pharmacol Sin, 2004. **25**: p. 90-97.
46. Bloemendal, H. and O. Hockwin, *Lens protein.* Critical Reviews in Biochemistry, 1982. **12**(1): p. 1-38.
47. Chandy, G., et al., *Comparison of the water transporting properties of MIP and AQP1.* Journal of Membrane Biology, 1997. **159**(1): p. 29-39.
48. Kushmerick, C., et al., *Ion, water and neutral solute transport in Xenopus oocytes expressing frog lens MIP.* Experimental eye research, 1995. **61**(3): p. 351-362.
49. Varadaraj, K., et al., *Regulation of aquaporin water permeability in the lens.* Investigative ophthalmology & visual science, 2005. **46**(4): p. 1393-1402.
50. Varadaraj, K., S.S. Kumari, and R.T. Mathias, *Functional expression of aquaporins in embryonic, postnatal, and adult mouse lenses.* Developmental Dynamics, 2007. **236**(5): p. 1319-1328.
51. Varadaraj, K., et al., *The role of MIP in lens fiber cell membrane transport.* Journal of Membrane Biology, 1999. **170**(3): p. 191-203.
52. Yang, B. and A. Verkman, *Water and glycerol permeabilities of aquaporins 1–5 and MIP determined quantitatively by expression of epitope-tagged constructs inXenopus oocytes.* Journal of Biological Chemistry, 1997. **272**(26): p. 16140-16146.
53. Liu, J., et al., *Aquaporin 0 enhances gap junction coupling via its cell adhesion function and interaction with connexin 50.* J Cell Sci, 2011. **124**(2): p. 198-206.
54. Chepelinsky, A.B., *Structural function of MIP/aquaporin 0 in the eye lens; genetic defects lead to congenital inherited cataracts*, in *Aquaporins*. 2009, Springer. p. 265-297.

55. Berry, V., et al., *Missense mutations in MIP underlie autosomal dominant'polymorphic'and lamellar cataracts linked to 12q.* Nature genetics, 2000. **25**(1): p. 15.
56. Shiels, A., et al., *Optical dysfunction of the crystalline lens in aquaporin-0-deficient mice.* Physiological genomics, 2001. **7**(2): p. 179-186.
57. Modesto, E., L. Barcellos, and A. Campos-de-Carvalho, *MIP 28 forms channels in planar lipid bilayers.* Brazilian journal of medical and biological research= Revista brasileira de pesquisas medicas e biologicas/Sociedade Brasileira de Biofisica...[et al.], 1989. **23**(10): p. 1029-1032.
58. Shen, L., et al., *Channel reconstitution in liposomes and planar bilayers with HPLC-purified MIP26 of bovine lens.* Journal of Membrane Biology, 1991. **124**(1): p. 21-32.
59. Zampighi, G.A., J.E. Hall, and M. Kreman, *Purified lens junctional protein forms channels in planar lipid films.* Proceedings of the National Academy of Sciences, 1985. **82**(24): p. 8468-8472.
60. Ehring, G. and J. Hall. *Single channel properties of lens MIP 28 reconstituted into planar lipid bilayers*. in *Proceedings of the Western Pharmacology Society*. 1988.
61. Németh-Cahalan, K.L. and J.E. Hall, *pH and calcium regulate the water permeability of aquaporin 0.* Journal of Biological Chemistry, 2000. **275**(10): p. 6777-6782.
62. Yasui, M., et al., *Rapid gating and anion permeability of an intracellular aquaporin.* Nature, 1999. **402**(6758): p. 184-187.
63. Ikeda, M., et al., *Characterization of aquaporin-6 as a nitrate channel in mammalian cells requirement of pore-lining residue threonine 63.* Journal of Biological Chemistry, 2002. **277**(42): p. 39873-39879.
64. Ma, T., et al., *cDNA Cloning and Gene Structure of a Novel Water Channel Expressed Exclusively in Human Kidney: Evidence for a Gene Cluster of Aquaporins at Chromosome Locus 12q13.* Genomics, 1996. **35**(3): p. 543-550.
65. Yasui, M., et al., *Aquaporin-6: An intracellular vesicle water channel protein in renal epithelia.* Proceedings of the National Academy of Sciences, 1999. **96**(10): p. 5808-5813.
66. Yanochko, G.M. and A.J. Yool, *Regulated cationic channel function in Xenopus oocytes expressing Drosophila big brain.* J Neurosci, 2002. **22**(7): p. 2530-40.
67. Kwon, T.-H., et al. *Physiology and pathophysiology of renal aquaporins*. in *Seminars in nephrology*. 2001.
68. Carbrey, J.M. and P. Agre, *Discovery of the aquaporins and development of the field*, in *Aquaporins*, E. Beitz, Editor. 2009, Springer Berlin Heidelberg. p. 3-28.
69. Promeneur, D., et al., *Regulation of AQP6 mRNA and protein expression in rats in response to altered acid-base or water balance.* American Journal of Physiology-Renal Physiology, 2000. **279**(6): p. F1014-F1026.
70. Verkman, A., *Aquaporin water channels and endothelial cell function.* Journal of anatomy, 2002. **200**(6): p. 617-627.
71. Matsuki-Fukushima, M., et al., *Presence and localization of aquaporin-6 in rat parotid acinar cells.* Cell and Tissue Research, 2008. **332**(1): p. 73-80.

72. Laforenza, U., et al., *Aquaporin-6 is expressed along the rat gastrointestinal tract and upregulated by feeding in the small intestine.* BMC Physiology, 2009. **9**(1): p. 18.
73. Ma, J., et al., *Expression of AQP6 and AQP8 in epithelial ovarian tumor.* Journal of molecular histology, 2016. **47**(2): p. 129-134.
74. Molinas, A., et al., *Protective role of host aquaporin 6 against Hazara virus, a model for Crimean–Congo hemorrhagic fever virus infection.* FEMS microbiology letters, 2016. **363**(8): p. fnw058.
75. De Ieso, M.L. and J.V. Pei, *An Accurate and Cost-Effective Alternative Method for Measuring Cell Migration with the Circular Wound Closure Assay.* Bioscience Reports, 2018.
76. Stamer, W.D., et al., *Cultured human trabecular mesh work cells express aquaporin-1 water channels.* Current eye research, 1995. **14**(12): p. 1095-1100.
77. Stamer, W.D., R.W. Snyder, and J.W. Regan, *Characterization of the transmembrane orientation of aquaporin-1 using antibodies to recombinant fusion proteins.* Biochemistry, 1996. **35**(50): p. 16313-16318.
78. Jacob, F., et al., *Careful Selection of Reference Genes Is Required for Reliable Performance of RT-qPCR in Human Normal and Cancer Cell Lines.* PLOS ONE, 2013. **8**(3): p. e59180.
79. Kam, Y., et al., *A novel circular invasion assay mimics in vivo invasive behavior of cancer cell lines and distinguishes single-cell motility in vitro.* BMC cancer, 2008. **8**(1): p. 198.
80. Schindelin, J., et al., *Fiji: an open-source platform for biological-image analysis.* Nature methods, 2012. **9**(7): p. 676.
81. Shaw, L.M., *Tumor cell invasion assays*, in *Cell Migration*. 2005, Springer. p. 97-105.
82. Simpson, K.J., et al., *Identification of genes that regulate epithelial cell migration using an siRNA screening approach.* Nature cell biology, 2008. **10**(9): p. 1027-1038.
83. Devuyst, O., et al., *Aquaporin-1 and endothelial nitric oxide synthase expression in capillary endothelia of human peritoneum.* American Journal of Physiology-Heart and Circulatory Physiology, 1998. **275**(1): p. H234-H242.
84. Matsuzaki, T., et al., *Water channel protein AQP3 is present in epithelia exposed to the environment of possible water loss.* Journal of Histochemistry & Cytochemistry, 1999. **47**(10): p. 1275-1286.
85. Neely, J.D., et al., *Heterotetrameric composition of aquaporin-4 water channels.* Biochemistry, 1999. **38**(34): p. 11156-11163.
86. Raina, S., et al., *Molecular cloning and characterization of an aquaporin cDNA from salivary, lacrimal, and respiratory tissues.* Journal of Biological Chemistry, 1995. **270**(4): p. 1908-1912.
87. Yang, J.-H., et al., *Expression and localization of aquaporin-5 in the epithelial ovarian tumors.* Gynecologic oncology, 2006. **100**(2): p. 294-299.
88. Stroka, K.M., et al., *Water permeation drives tumor cell migration in confined microenvironments.* Cell, 2014. **157**(3): p. 611-623.
89. Gao, J., et al., *Acetazolamide inhibits osmotic water permeability by interaction with aquaporin-1.* Analytical biochemistry, 2006. **350**(2): p. 165-170.

90. Hoque, M.O., et al., *Aquaporin 1 is overexpressed in lung cancer and stimulates NIH-3T3 cell proliferation and anchorage-independent growth.* Am J Pathol, 2006. **168**(4): p. 1345-1353.
91. Preston, G.M., et al., *The mercury-sensitive residue at cysteine 189 in the CHIP28 water channel.* J Biol Chem, 1993. **268**(1): p. 17-20.
92. Yukutake, Y., et al., *Mercury chloride decreases the water permeability of aquaporin-4-reconstituted proteoliposomes.* Biology of the Cell, 2008. **100**(6): p. 355-363.
93. Brooks, H.L., J.W. Regan, and A.J. Yool, *Inhibition of aquaporin-1 water permeability by tetraethylammonium: involvement of the loop E pore region.* Mol Pharmacol, 2000. **57**(5): p. 1021-6.
94. Søgaard, R. and T. Zeuthen, *Test of blockers of AQP1 water permeability by a high-resolution method: no effects of tetraethylammonium ions or acetazolamide.* Pflügers Archiv-European Journal of Physiology, 2008. **456**(2): p. 285-292.
95. Klebe, S., et al., *Blockade of aquaporin 1 inhibits proliferation, motility, and metastatic potential of mesothelioma in vitro but not in an in vivo model.* Disease markers, 2015. **2015**.
96. Devuyst, O. and A.J. Yool, *Aquaporin-1: new developments and perspectives for peritoneal dialysis.* Perit Dial Int, 2010. **30**(2): p. 135-41.
97. Dorward, H.S., et al., *Pharmacological blockade of aquaporin-1 water channel by AqB013 restricts migration and invasiveness of colon cancer cells and prevents endothelial tube formation in vitro.* Journal of Experimental & Clinical Cancer Research, 2016. **35**(1): p. 36.
98. Pollard, T.D. and G.G. Borisy, *Cellular motility driven by assembly and disassembly of actin filaments.* Cell, 2003. **112**(4): p. 453-465.
99. Wang, Y.-L., *Exchange of actin subunits at the leading edge of living fibroblasts: possible role of treadmilling.* The Journal of cell biology, 1985. **101**(2): p. 597-602.
100. Theriot, J.A. and T.J. Mitchison, *Actin microfilament dynamics in locomoting cells.* Nature, 1991. **352**(6331): p. 126-131.
101. Stroka, K.M., et al., *Water permeation drives tumor cell migration in confined microenvironments.* Cell, 2014. **157**(3): p. 611-23.
102. Frede, J., et al., *Ovarian cancer: Ion channel and aquaporin expression as novel targets of clinical potential.* Eur J Cancer. **49**(10): p. 2331-44.
103. Schwab, A., et al., *Role of ion channels and transporters in cell migration.* 2012. **92**(4): p. 1865-1913.
104. Marinelli, R.A., et al., *Secretin Promotes Osmotic Water Transport in Rat Cholangiocytes by Increasing Aquaporin-1 Water Channels in Plasma Membrane EVIDENCE FOR A SECRETIN-INDUCED VESICULAR TRANSLOCATION OF AQUAPORIN-1.* Journal of Biological Chemistry, 1997. **272**(20): p. 12984-12988.
105. Wu, W., et al., *A novel approach for evaluating the efficiency of siRNAs on protein levels in cultured cells.* 2004. **32**(2): p. e17-e17.
106. Yool, A.J., et al., *AqF026 is a pharmacologic agonist of the water channel aquaporin-1.* J Am Soc Nephrol, 2013. **24**(7): p. 1045-1052.
107. Kang, B.W., et al., *Expression of aquaporin-1, aquaporin-3, and aquaporin-5 correlates with nodal metastasis in colon cancer.* Oncology, 2015. **88**(6): p. 369-376.

Chapter 4: Combined pharmacological administration of AQP1 ion channel blocker AqB011 and water channel blocker Bacopaside II amplifies inhibition of colon cancer cell migration

Michael L De Ieso[1], Saeed Nourmohammadi[1], Jinxin Pei[1], Eric Smith[2], Pak Hin Chow[1], Mohamad Kourghi[1], Jennifer Hardingham[2], and Andrea J Yool[1]

[1]Department of Physiology, Adelaide Medical School, University of Adelaide, Adelaide, SA, Australia

[2]Oncology Department, The Basil Hetzel Institute, The Queen Elizabeth Hospital, Woodville SA 5011 Australia

Chapter 4 has been submitted for publication to Scientific Reports.

4.1 Abstract

Aquaporin-1 (AQP1) is a transmembrane water and cation channel that is upregulated in some colorectal cancers and enhances cell migration rates; however, the mechanism remains unknown. AqB011 and bacopaside II selectively block human AQP1 ion and water pores, respectively. HT29 and SW480 colorectal adenocarcinoma cell lines showed expression of AQP1 as determined by quantitative PCR and western blot. 2D migration rates were quantified using circular wound closure assays and live-cell tracking. Invasiveness was measured using transwell filters coated with an extracellular matrix. AQP1 expression and subcellular localisation were confirmed by immunofluorescence. Combined treatment with both AqB011 and bacopaside II produced a greater inhibitory effect on cell 2D migration than either treatment alone in HT29 and SW480 cells. AqB011, but not bacopaside II, significantly inhibited invasiveness. The high efficacy of AqB011 in blocking HT29 cell motility correlated with high levels of AQP1 protein localisation in the plasma membrane, in contrast to AqB011-insensitive SW480 cells in which most AQP1 protein is intracellular. Results here are the first to demonstrate a key role for the AQP1 ion channel in the invasiveness

of colon cancer cells, and to show that the effectiveness of AQP1 pharmacological agents depends on membrane localization of the channel.

4.2 Statement of authorship

Statement of Authorship

Title of Paper	Combined pharmacological administration of AQP1 ion channel blocker AqB011 and water channel blocker Bacopaside II amplifies inhibition of colon cancer cell migration
Publication Status	☐ Published ☐ Accepted for Publication ☑ Submitted for Publication ☐ Unpublished and Unsubmitted w ork w ritten in manuscript style
Publication Details	Scientific Reports

Principal Author

Name of Principal Author (Candidate)	Michael Lucio De Ieso
Contribution to the Paper	First author and main contributor. Formulation of research question. Concept and methodological design. Performed experiments and data analysis. Generation of manuscript. Figure and table development. Incorporation of superviser comments and suggestions for manuscript.
Overall percentage (%)	90
Certification:	This paper reports on original research I conducted during the period of my Higher Degree by Research candidature and is not subject to any obligations or contractual agreements with a third party that would constrain its inclusion in this thesis. I am the primary author of this paper.
Signature	Date 22ND NOV 2018

Co-Author Contributions

By signing the Statement of Authorship, each author certifies that:

i. the candidate's stated contribution to the publication is accurate (as detailed above);
ii. permission is granted for the candidate in include the publication in the thesis; and
iii. the sum of all co-author contributions is equal to 100% less the candidate's stated contribution.

Name of Co-Author	Saeed Nourmohammadi
Contribution to the Paper	Performed experiments.
Signature	Date 22/11/2018

Name of Co-Author	Jinxin Victor Pei
Contribution to the Paper	Performed experiments and data analysis.
Signature	Date 23/11/2018

Please cut and paste additional co-author panels here as required.

Name of Co-Author	Eric Smith
Contribution to the Paper	Performed experiments and data analysis. Reviewed and edited final manuscript.
Signature	Date 22-11-'18

Name of Co-Author	Pak Hin Chow
Contribution to the Paper	Performed experiments.
Signature	Date 23/11/18

Name of Co-Author	Jennifer Hardingham
Contribution to the Paper	Concept and methodological design. Reviewed and edited final manuscript.
Signature	Date 22-11-18

Name of Co-Author	Andrea Yool
Contribution to the Paper	Concept and methodological design. Reviewed and edited final manuscript.
Signature	Date 22 Nov 2018

Please cut and paste additional co-author panels here as required.

Name of Co-Author	Mohamad Kourghi
Contribution to the Paper	Concept and methodological design.
Signature	Date 26-Nov-2018

4.3 Introduction

Cancer is a leading cause of death worldwide, accounting for 8.2 million deaths in 2012 according to the World Health Organization [1], primarily due to metastasis [2, 3]. Colorectal cancer is the second most common cancer in women and the third in men [1]. A link between colon cancer severity and upregulation of aquaporin-1 (AQP1) expression has been previously documented [4, 5]. In humans, AQP1 normally serves essential roles in fluid absorption and secretion in tissues including the kidney, brain, eye and vascular system of humans [6, 7]. However, AQP1 water channels also are upregulated in subtypes of aggressive cancer types including colorectal cancers, gliomas, lung adenocarcinoma, laryngeal cancer and cholangiocarcinoma [8-12]. Positive correlations have been demonstrated between levels of AQP1 and angiogenesis, tumour progression, growth, migration and metastasis [13]. Knockdown of AQP1 in cancer lines using small-interfering RNAs resulted in substantial impairment of cell migration *in vitro* [14, 15]. Conversely, increasing AQP1 levels by transfection into deficient lines (B16F10 melanoma, and 4T1 mammary gland tumour) accelerated cell migration *in vitro* and increased the likelihood of lung metastases in mice *in vivo* [16]. Colon cancer cells (HT20) transfected with AQP1 similarly exhibited increased cell migration rates and enhanced extravasation after injection via the tail vein in mice [17].

The water channel activity of AQP1 has been proposed to facilitate extension of the leading edges of migrating cells to speed the rate of movement [18]. Bacopaside II from the medicinal plant *Bacopa monnieri* was shown to bind deep in the cytoplasmic vestibule of the AQP1 water pore, inhibiting AQP1 water flux without affecting AQP1 ion conductance; bacopaside II also slowed cell migration in a colon cancer line highly expressing AQP1 [19]. Other AQP1 inhibitors such as AqB013 and proposed AQP1 inhibitor, AqB050, have also been shown to reduce cancer cell migration rates *in vitro* [20, 21]. Interestingly, other mammalian water channels such as AQP4 do not substitute for AQP1 in facilitating cell migration in AQP1-dependent cell lines [22], suggesting that the migration-enhancing property in some cases relies on more than transmembrane water permeability. There is a gap in knowledge regarding the properties of AQP1 that permit its migration-

enhancing effect, but both the ion and water channel activities appear to be involved [23]. AQP1 dual water and ion channels mediate osmotic water flow through individual subunit pores, and a cation conductance through the central pore of the tetramer [24-26]. The non-selective monovalent cation conductance is gated by cGMP, which depends on loop D domain structural integrity for channel activation [25, 27-30]. In some expression systems, AQP1 ion channels have a low opening probability [31] or are not detectable [32], suggesting cGMP-mediated gating of AQP1 is subject to additional regulation including tyrosine phosphorylation [33]. Physiological relevance of AQP1 ion channel activity has been proposed for fluid secretion across barrier epithelia, and local volume control in cell migration. Blocking native AQP1 ion channels in choroid plexus was shown to alter net cerebrospinal fluid transport [34]. AqB011 is a bumetanide derivative that selectively blocks the ion pore of AQP1, without affecting AQP1 water flux [35]. Mutation of the AQP1 intracellular loop D domain removed sensitivity to AqB011, suggesting that loop D is the likely binding site for AqB011 to AQP1 [30]. AqB011 was used to show that AQP1 ion channels are needed for rapid migration of AQP1-expressing cancer cells [35]. To date, pharmacological modulators for AQP1 ion conductance include cadmium [34], calcium [36] and pharmacological derivatives of bumetanide such as AqB007 and AqB011 [35]. Functional evidence indicates that the AQP1 cation pore at the four-fold axis of symmetry is separate from the individual water pores in each monomer [25, 33, 37], and the pathways differ in pharmacological sensitivities [31, 38].

This study tested the hypotheses that cancer cell invasiveness is reduced by inhibition of the AQP1 ion channel, and that combined treatment with bacopaside II and AqB011 enhances the inhibitory effect on cell motility. Results here show the efficacy of AQP1 inhibitors was dependent on localization of AQP1 protein in the plasma membrane, and that combined administration of AQP1 water and ion channel blockers produced an amplified block of colon cancer cell migration. Thus, AQP1 water and ion channels appear to exhibit a coordinated role in AQP1-facilitated cancer cell migration. The discovery of pharmacological modulators of AQP1 has allowed dissection of the mechanisms of action of AQP1 in cell migration at a level not possible previously. Results support AQP1 as a novel

potential target for developing treatments aimed at the prevention of cancer metastasis.

4.4 Materials and Methods

4.4.1 AQP1 Inhibitors

The bumetanide derivative AqB011 (*Aq*uaporin ligand; *B*umetanide derivative; number *11* in a series) was synthesized by Dr Gary A. Flynn (SpaceFill Discovery LLC, West Yellowstone, MT, USA) [35]. Powdered AqB011 was dissolved in dimethyl sulfoxide (DMSO) to create 1000x stock solutions and diluted in culture medium to final concentrations for testing in the circular wound closure [39], transwell invasion, live cell imaging, and alamarBlue assays. Bacopaside II was purchased from Sigma-Aldrich (St. Louis, MO), solubilized in methanol to yield 100x stock solutions, and stored at -20°C in an airtight vial to minimize evaporation. For experimental use, bacopaside II stocks were diluted at 1/100 in culture medium. A combination of DMSO (1 μL/mL) and methanol (10 μL/ml) in culture medium was used as the vehicle control.

4.4.2 Cell Lines

Human colorectal adenocarcinoma cell lines HT29 (ATCC HTB-38TM) and SW480 (ATCC CCL-228TM) were cultured in T-75 plates in Dulbecco's Modified Eagle Medium (DMEM; Life Technologies, Grand Island, NY, USA) supplemented with 10% fetal bovine serum (FBS; Life Technologies), 1% Gibco GlutaMAX (Life Technologies) and 100 units/ml each of penicillin and streptomycin (Life Technologies). Cell cultures were grown at 37°C in a humidified 5% CO_2 incubator.

4.4.3 Immunofluorescence

Cells were seeded 2-3 days prior to cell fixation on 8-well uncoated Ibidi® μ-Slides (Ibidi, Munich, Germany) at a density of $5x10^4$ cells/well. Once 80% confluent, cells were stained with MemBrite™ Fix Cell Surface Staining Kit (Biotium, Fremont, CA, USA; cat # 30093), and purchased from Gene Target Solutions (Dural, NSW, Australia). Membrane staining was performed prior to cell fixation,

as per manufacturer's instructions. Cells were fixed with 1:1 (v/v) acetone and methanol at -20°C and incubated for 15 min at room temperature. Immunofluorescence staining was conducted as previously described by Wardill et al. (2016) [40]. The AQP1 primary antibody used for immunofluorescence was H-55 rabbit polyclonal (Santa Cruz Biotechnology, Dallas, TX, USA). The secondary antibody was Goat anti-Rabbit IgG (H+L) Cross-Adsorbed Secondary Antibody, Alexa Fluor 568 (Life Technologies; cat# A-11011). For nuclear staining, cells were incubated for 10 minutes at room temperature in a 1:1000 dilution of Hoechst 33258 (cat # 861405; Sigma-Aldrich, St. Louis, MO). The µ-Slide was imaged using an Olympus FV3000 Confocal Microscope. For the signal emitted by Hoechst 33258, excitation (Ex=405nm) and emission (Em=461nm) settings were used. For Alexa Fluor 568, settings were Ex=561nm and Em=603nm. For MemBrite™, settings were Ex=488nm and Em=513nm. Fiji (ImageJ) software (U.S. National Institutes of Health) was used to measure relative intensities of AQP1 signal standardised to membrane marker signal as a function of cross-sectional distance per cell.

4.4.4 Western Blot Analysis

Cells were seeded at 4-5x10^5 cells per well in 6-well tissue culture plates in normal growth medium, and incubated for 24 hours at 37°C in 5% CO_2. Once cultures reached 70-80% confluence, cells were washed with ice-cold Dulbecco's phosphate buffered saline, and incubated on ice for 5 minutes in radioimmunoprecipitation assay lysis and extraction buffer (Life Technologies) containing 1% Halt protease inhibitor (Life Technologies). Cells were dislodged using a clean Corning® Cell Lifter, and homogenized with a 26-gauge needle and syringe. Homogenized lysates were collected into 1.5 mL centrifuge tubes, and centrifuged at 17,000G for 10 minutes at 4°C. The cell debris pellet was discarded, and the supernatant was carefully transferred to a new 1.5 mL centrifuge tube. After Bradford protein estimation, 40 µg protein samples were prepared in 10 µL Novex™ 4X Bolt™ LDS Sample Buffer (Life Technologies; cat # B0007), 4 µL 10X Bolt™ Sample Reducing Agent (Invitrogen™; cat # B0009), with deionized water added to 40 µL total. After heating at 70ºC for 10 minutes, samples were resolved by SDS-PAGE on Bolt 4-12% Bis-Tris Plus gel (Invitrogen™; cat # NW04122BOX), and

transferred onto 0.2 μm polyvinylidenefluoride membrane using the iBlot 2 Gel Transfer System (Invitrogen™; cat # IB21001). Immunodetection was performed with the iBind Western System using the iBind™ Western Device (Invitrogen™; cat # SLF1000), iBind™ cards (Invitrogen™; cat # SLF1010), and iBind™ Solution Kit (Invitrogen™; cat # SLF1020). Antibody details are as follows: Secondary antibody IRDye® anti-rabbit 800CW (1:2000; Abcam; ab216773) was used for polyclonal AQP1 primary antibody (1:1000; obtained from the Department of Ophthalmology, Duke University, Durham, NC, USA [41, 42]). Secondary antibody IRDye® anti-mouse 680RD (1:2000; Abcam; ab216778) was used for GAPDH antibody (1:200; Abcam; ab9484). Western blots were assessed using ImageStudio® Lite, version 5.2. Signal intensities were determined relative to local background. Expression of AQP1 protein was normalised using GAPDH as a loading control, and was relative to HT29.

4.4.5 Quantitative PCR analysis of AQP1 expression

Cells plated in triplicate wells at 4×10^5 cells/well were incubated at 37°C in a humidified 5% CO_2 incubator overnight. Total RNA was extracted using PureLink™ RNA Mini Kit (Invitrogen™); 1 μg total RNA was used for cDNA synthesis. cDNA was synthesized using QuantiTect® Reverse Transcription Kit (Qiagen®). cDNA was quantified using NanoDrop™ (Life Technologies); 50 ng cDNA was used in the polymerase chain reaction. Real-time qRT-PCR analyses were performed using SYBR™ Green PCR Master Mix (Applied Biosystems™) in a final volume of 10 μl with StepOne Plus™ Real-Time PCR system (Applied Biosystems™). Data were analysed by StepOne Plus™ Real-Time PCR software v2.3. The primer sequences for AQP1 were forward: 5′-CGCAGAGTGTGGGCCACATCA- 3′, and reverse: 5′ - CCCGAGTTCACACCATCAGCC - 3′, amplifying a product of 217 bp. *RPS13* was used as a standard and target mRNA levels relative to *RPS13* were calculated using the formula $2^{-\Delta CT}$ [43].

4.4.6 Circular Wound Closure Assay

Circular wound closure assays were performed using methods described by De Ieso and Pei (2018) [39]. In brief, cells were plated at 1 x 10^5 cells/mL in DMEM culture medium with GlutaMAX and antibiotics (as above), reduced serum (2% FBS), and 400nM of the mitotic inhibitor 5-fluoro-2'-deoxyuridine (FUDR). A confluent monolayer was achieved at 2-3 days following plating; circular wounds were created with a sterile p10 pipette tip. After washing two to three times with phosphate-buffered saline to remove cell debris, media were applied with and without AQP inhibitors or vehicle in low serum (2% FBS) DMEM with FUDR for the wound closure assay. Complete wounds were imaged at 10x magnification with a Canon 6D camera on a Nikon inverted microscope. Images were standardised using XnConvert software, and wound areas were quantified using Fiji software (ImageJ; version 1.51h; U.S. National Institutes of Health). Closure was calculated as a percentage of the initial wound area for the same well as a function of time. All experiments were repeated in duplicate wells.

4.4.7 Cytotoxicity Assay

Cell viability was quantified using an alamarBlue assay [45], following manufacturer's guidelines (Life Technologies). Cells were plated at 10^5 cells/mL in 96-well plates, in the same FUDR-containing low serum culture media as used in the migration assays. At 12-18 hours after plating, treatments were applied, and cells were incubated 24 hours. At 24 hours, cells were treated with 10% alamarBlue solution for 1-2 hours. Fluorescence signal levels were measured with a FLUOstar Optima microplate reader for control and treatment groups. Mercuric chloride ($HgCl_2$) served as a positive control for inducing cytotoxic cell death, and a no-cell control was included to confirm low background fluorescence.

4.4.8 Live Cell Imaging

Cells were seeded on eight-well uncoated Ibidi μ-Slides (Ibidi) at a density of 1x10^5 cells/mL. A confluent monolayer was achieved 2-3 days after plating. Cells were conditioned in low serum culture medium (2% FBS) in the presence of FUDR (400 nM) for 12-18 hours before wounding. Three circular wounds were created in each

well using techniques described above for the wound closure assays. Slides were mounted on a Nikon Ti E Live Cell Microscope (Nikon, Tokyo, Japan) in an enclosed humidified chamber kept at 37°C with 5% CO_2. Images were taken at 30-minute intervals for 24 hours, using Nikon NIS-Elements software. AVI files were exported from NIS-Elements and converted into TIFF files using Fiji (ImageJ). Converted files were analyzed using Fiji software [46] with the Manual Tracking plug-in. Total distance per cell was calculated as the cumulative distance travelled over the full duration of the experiment. Displacement was calculated as the net distance travelled between the first and last time points.

4.4.9 Transwell Invasion Assay

Assays were performed using 6.5 mm Corning® Transwell® polycarbonate membrane cell culture inserts with 8 μm pore size (cat #3422; Sigma-Aldrich, St. Louis, MO). The upper surface of the filter was coated with 40 μL of water-diluted extracellular matrix (ECM) gel from Engelbreth-Holm-Swarm murine sarcoma (final concentration 25 μg/mL; Sigma-Aldrich, St. Louis, MO), and left to dehydrate overnight, and rehydrated 2 hours prior to cell seeding with 50 μL of serum-free DMEM per transwell insert. Cells were grown to approximately 40% confluence under normal conditions, and transferred into reduced serum (2% FBS) medium for 32-34 hours prior to seeding. Cells were harvested, resuspended in serum-free DMEM, and 2.5 x 10^5 cells in 100 μL was added to the upper chamber (total 150 μL of cell suspension per transwell, including 50 μL of rehydration medium added earlier). To the lower chamber, 600 μL of pharmacological treatment in DMEM supplemented with 10% serum (chemoattractant) was added, and cells were incubated for 24 hours at 37°C in 5% CO_2. Non-migrated cells were scraped from the upper surface of the membrane with a cotton swab; migrated cells remaining on the bottom surface were counted after staining with crystal violet [47].

4.4.10 Statistical Analyses

Statistical analyses performed with GraphPad Prism 7.02 software involved one-way ANOVA and post-hoc Bonferroni tests. Statistically significant outcomes are represented as $p<0.05$ (*), $p<0.01$ (**), $p<0.001$ (***), or $p<0.0001$ (****); NS is

not significant; other characters indicating significance (# and +) use the same pattern for defining p values. All data are presented as mean ± standard error of the mean (SEM); *n* values for independent samples are indicated in italics above the x-axes in histogram figures.

4.5 Results

4.5.1 AQP1 expression levels in HT29 and SW480 cell lines.

Levels of AQP1 expression were quantified in HT29 and SW480 cell lines by western blot and real-time reverse-transcription polymerase chain reaction (qRT-PCR). Western blot analyses showed no significant difference (p=0.055) between total AQP1 protein levels in HT29 (1.0 ± 0.05; n=4), and SW480 cells (0.84 ± 0.05; n=4), normalised to a reference protein GAPDH (Fig 4.1A and 4.1B). A supplementary figure shows the full length gel depicting anti-AQP1 signal (see Supplementary figure 4.1) and anti-GAPDH signal (see Supplementary figure 4.2). Main bands were identified near 37kD, consistent with glycosylated forms of the 28kD AQP1 monomer [48]. AQP1 mRNA levels as determined by qRT-PCR were approximately 15-fold higher in HT29 than in SW480 cell lines (Fig 4.1C).

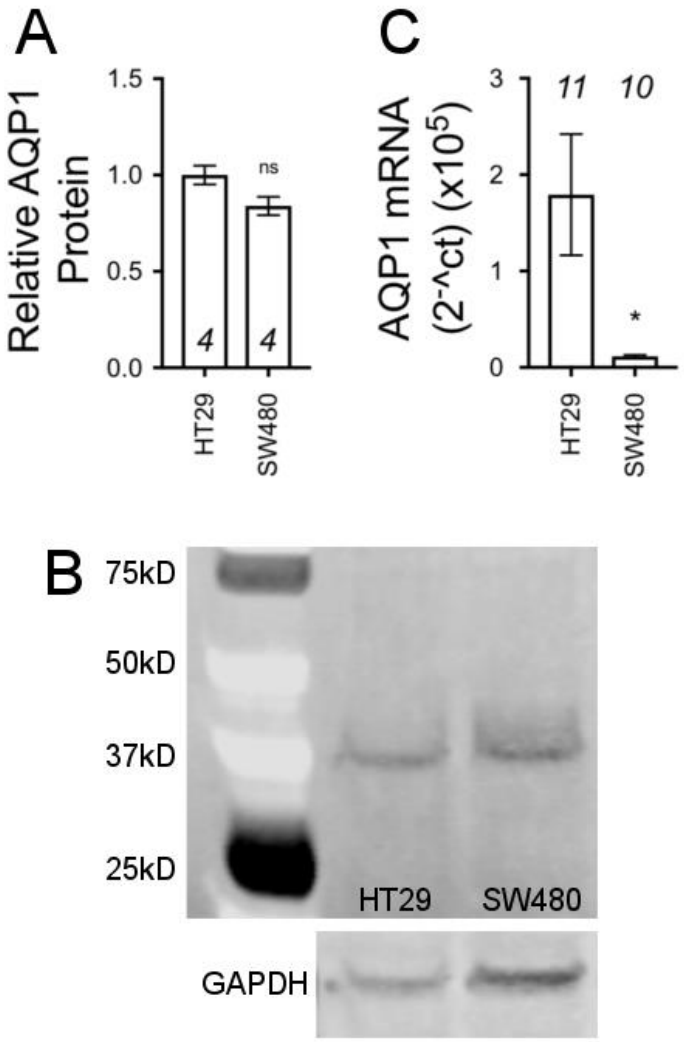

Figure 4.1 HT29 cells have comparable levels of AQP1 to SW480 cells. (A) AQP1 protein expression was determined by western blot, with GAPDH used as a reference protein. AQP1 protein levels were similar in HT29 (n=4) and SW480 (n=4) cell lines (p=0.055). AQP1 signal intensities were standardised to HT29 AQP1 level. (B) Western blot images of AQP1 and GAPDH in HT29 and SW480 cells. Main bands for AQP1 were located near 37kD. (C) AQP1 mRNA levels were higher in HT29 cells (n=11) than SW480 cells (n=10), as determined by qRT-PCR.

4.5.2 Combined treatment with bacopaside II and AqB011 produced additive block of wound closure in colon cancer cells.

The combined effects of AqB011 and bacopaside II on 2D cell migration of HT29 and SW480 colorectal cell lines were tested using circular wound closure (Fig 4.2). At 24 h, significant block of HT29 cell migration was observed with AqB011 alone (at 20 to 100 µM), and with bacopaside II alone (at 7.5 to 15 µM), as compared to vehicle control (Fig 4.2A), consistent with previous findings [19, 35]. While migration was reduced 38 ± 2.9% by AqB011 (at 20 µM), and 44 ± 3.1% by bacopaside II (at 15 µM), the combined treatment produced a block of 81 ± 1.3%, significantly greater than that seen with either agent alone. In contrast, SW480 cells showed no sensitivity to AqB011 or bacopaside II in 2D migration (Fig 4.2B), with no significant differences after 24 hours in AqB011 (at 1 to 100 µM) or bacopaside II (at 7.5 to 15 µM) as compared with vehicle-treated cells (Fig 4.2B). However, combined treatment of SW480 cells with AqB011 (20 µM) and bacopaside II (15 µM) blocked 2D migration by 50.4 ± 5.4%, which was significantly greater than bacopaside II or AqB011 alone. In summary, these results showed that AqB011 and bacopaside II additively block wound closure in both HT29 and SW480 cell lines, but that the efficacy of the AQP1 inhibitors was much lower in the SW480 cell line.

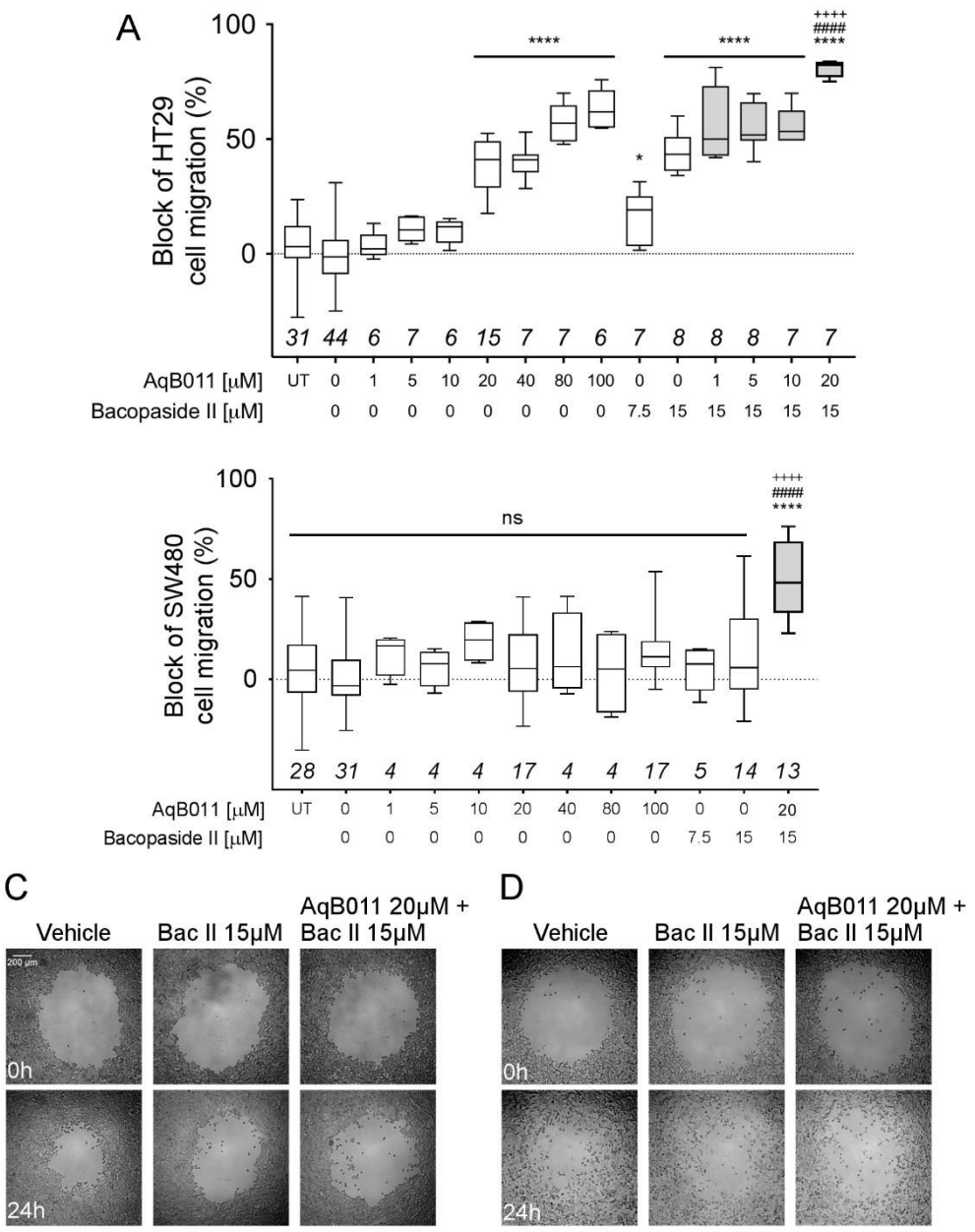

Figure 4.2 Wound closure assay showing the block of cell migration in HT29 cells with combined treatment (bacopaside II and AqB011), as compared with each compound alone. (A) Box plot depicting dose-dependent block (%) of HT29 wound closure after 24 hours. White bars represent single treatment; grey bars represent combined treatment with AqB011 and bacopaside II. AqB011 (20μM) and bacopaside II (15μM) treatment yielded block that was significantly greater than vehicle (****), AqB011 (20μM) alone (####), and bacopaside II (15μM) alone (++++), suggesting an additive interaction; n-values are in italics above the x-axis for A and B. (B) Box plot depicting wound closure block (%) of SW480 after 24 hours. White bars represent single treatment; grey bars represent combined

treatment with AqB011 and bacopaside II. SW480 cells were insensitive to block by AqB011 and bacopaside II. AqB011 (20μM) and bacopaside II (15μM) treatment yielded block that was significantly greater than vehicle (****), AqB011 (20μM) alone (####), and bacopaside II (15μM) alone (++++), suggesting an additive interaction. (C) Representative images showing HT29 cells treated with vehicle, bacopaside II (15μM), and combined treatment at 0 hours (upper row) and 24 hours (bottom row). Scale bar applies for both C and D. (D) Representative images showing SW480 cells treated with vehicle, bacopaside II (15μM), and combined treatment at 0 hours (upper row) and 24 hours (bottom row).

4.5.3 Effects of bacopaside II and AqB011 on individual colon cancer cell migration assessed by live cell imaging.

The effects of AQP1 modulators on single cell migration were measured by tracking individual cell trajectories over 24 hours in cultures of HT29 (Fig 4.3), and SW480 (Fig 4.4). The effects of the treatments on total distance travelled and net displacement were quantified from analyses of the live cell imaging results (Fig 4.5). In HT29 cells, impaired directional migration was evident from the short convoluted trajectories in each treatment group as compared with untreated and vehicle control (Fig 4.3B). HT29 cells treated with 20 µM AqB011 migrated significantly shorter total distances in 24 hours (162 ± 9 µm) than vehicle-treated cells (250 ± 13 µm) (Fig 4.5A). HT29 cells treated with bacopaside II at 15 µM also showed a significant reduction in total distance travelled (153 ± 7 µm) as compared to vehicle control. Interestingly, the HT29 cells treated with both AqB011 (20 µM) and bacopaside II (15 µM) displayed a mean total migration distance of 105 ± 6µm, which was significantly lower than with either agent alone. In contrast, SW480 cells showed comparable trajectories in all treatment groups (Fig 4.4B), and no effect of AqB011 at doses up to 100 µM. SW480 cells travelled a mean total distance of 379 ± 29 µm following treatment with 100 µM AqB011 which was not significantly different from vehicle treated cells at 451 ± 42 µm (Fig 4.5B). There were no significant differences in total distances travelled by SW480 cells treated with vehicle, bacopaside II (15 µM) alone (518 ± 39 µm), or combined AqB011 (20 µM) and bacopaside II (15 µM) treatment (347 ± 35 µm).

Net displacement (the linear distance between the start and end points for individual cells) in HT29 cells was significantly different from vehicle for all treatment groups (Fig 4.5C). The results of the treatment conditions closely paralleled those seen for total distance travelled (Fig 4.5A), in magnitude of block and dose dependence. Although migration trajectories were reduced, the directions of movement in successive intervals remained roughly oriented in the same direction for HT29 cells (Fig 4.3B). A significant decrease of net displacement in SW480 cells was seen only with the combined treatment (169 ± 19 µm), and not with bacopaside II alone (273 ± 31 µm) or AqB011 alone (349 ± 25 µm) as compared with vehicle-treated cells (296 ± 20 µm). This result contrasted with the absence of an effect of combined

treatment on the cumulative total distance travelled by SW480 cells. Although SW480 cells moved well, their failure to achieve a commensurate net displacement suggested that the directionality of movement (i.e., maintaining a consistent vector over successive intervals) was compromised by combined treatment. The reduction of HT29 displacement can be attributed to decreased total distance travelled, but the reduction of SW480 displacement appears to be due to reduced directionality. SW480 cells migrated significantly faster than HT29 cells (Fig 4.5E).

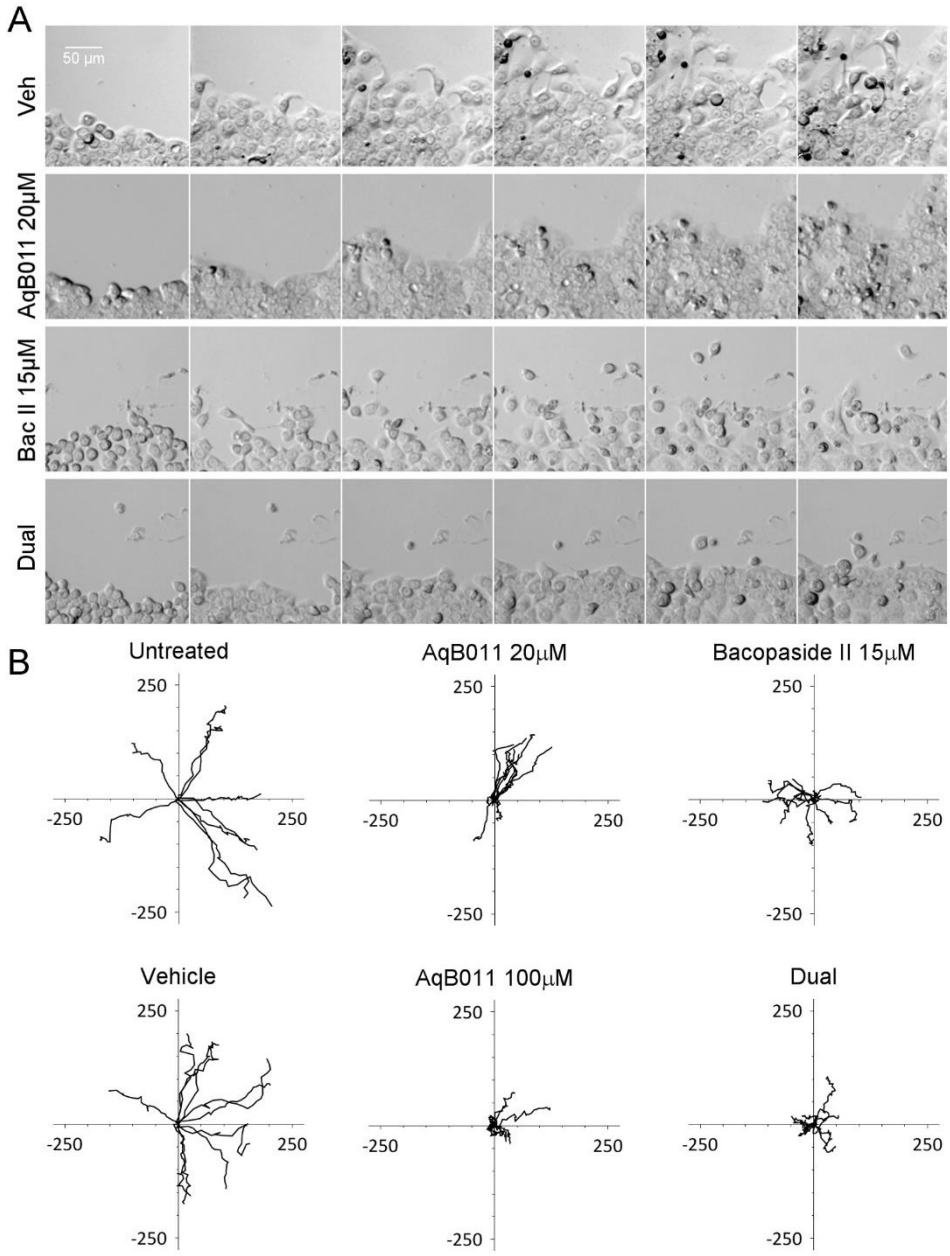

Figure 4.3 Live cell imaging of HT29 cell trajectories in treatments with bacopaside II and AqB011 alone, and in combination. Single cells at the boundaries of circular wounds were tracked with time-lapse images taken at 30 minute intervals for 24 hours at 37°C. (A) Panels of six images each from time-lapse series are shown at 4-hour intervals. Vehicle, AqB011 (20µM), bacopaside II (15µM), and combined (dual) treatment of AqB011 (20µM) and bacopaside II (15µM) are depicted. (B) Trajectory plots of individual cells (n=9-11 per treatment group), monitored by the position of the cell nucleus at 60 minute intervals over 24 hours. Data were referenced to the starting position at 0,0 on the graph axes; X and Y values are in µm.

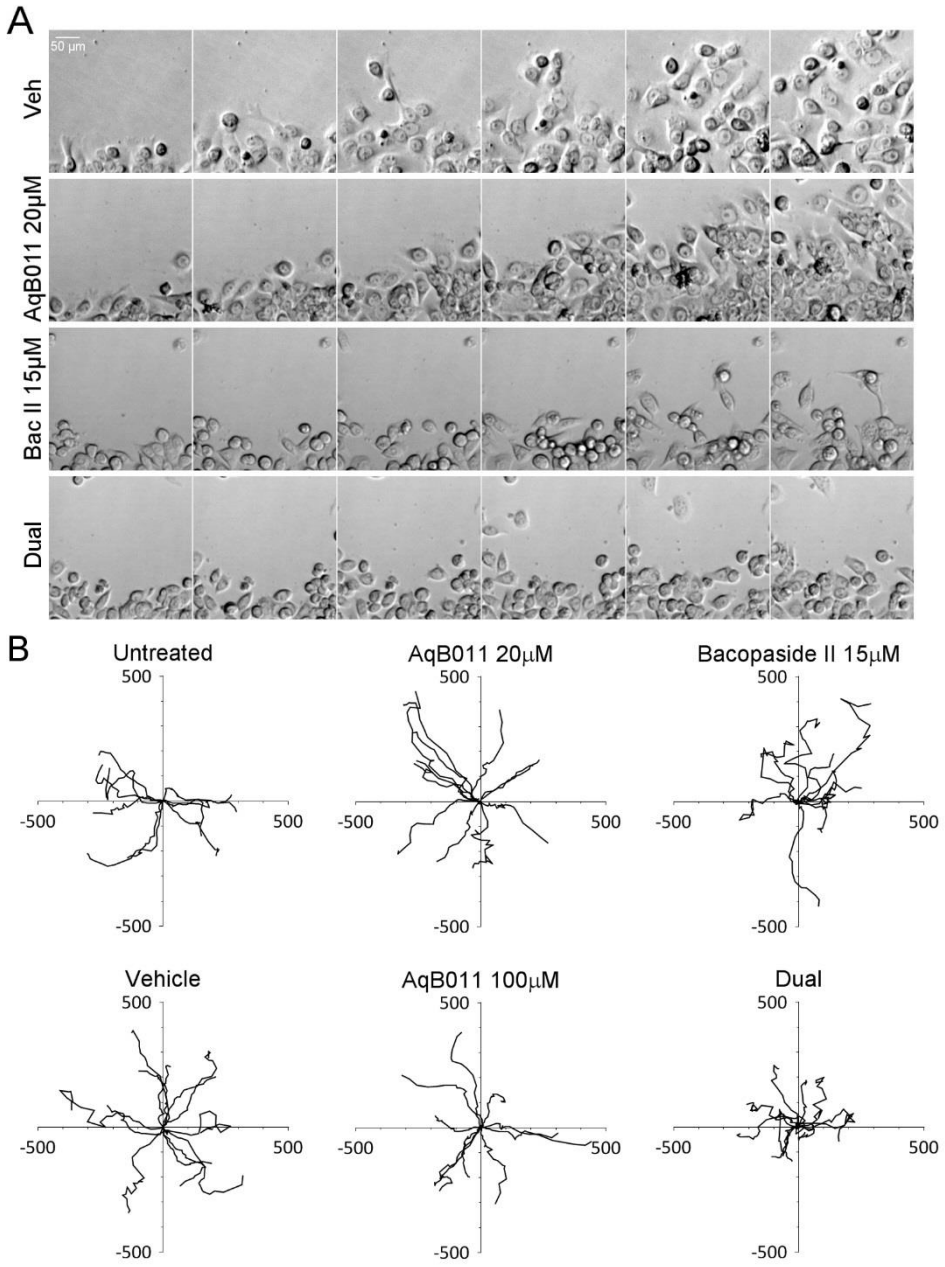

Figure 4.4 Live cell imaging of SW480 cell trajectories in treatments with bacopaside II and AqB011 alone, and in combination. Single cells at the boundaries of circular wounds were tracked with time-lapse images taken at 30-minute intervals for 24 hours at 37°C. (A) Panels of six images each from time-lapse series are shown at 4-hour intervals. Vehicle, AqB011 (20µM), bacopaside II (15µM), and combined (dual) treatments are depicted. (B) Trajectory plots of individual cells (n=10-12) per treatment group, monitored by the position of the cell nucleus at 60 minute intervals over 24 hours; X and Y values are in µm.

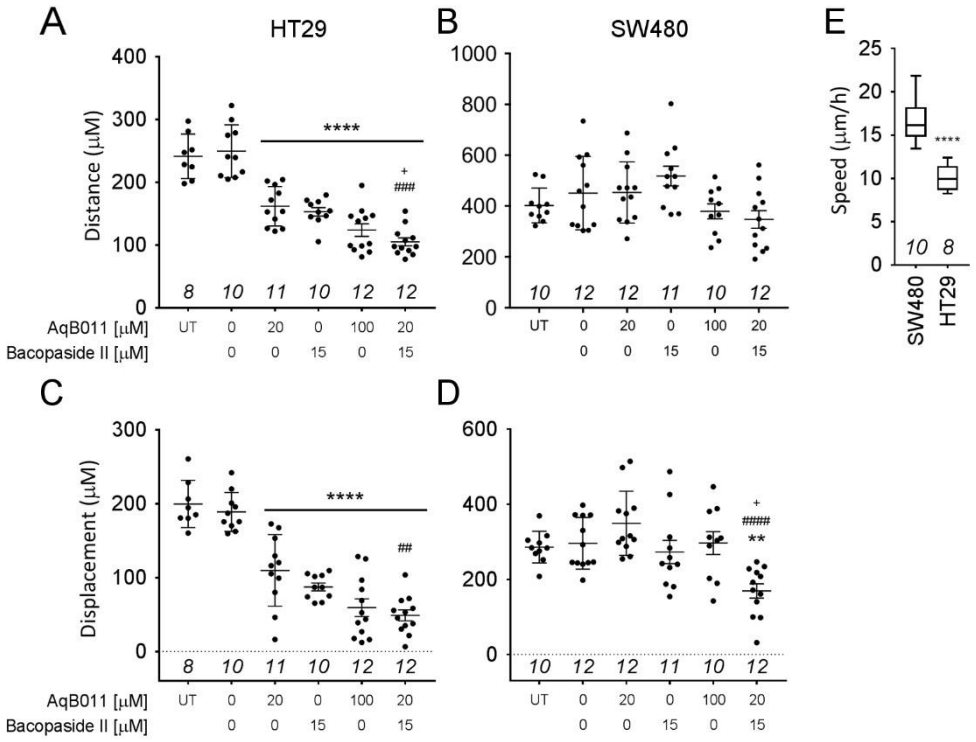

Figure 4.5 Summary plots of total distances travelled and net displacement of HT29 and SW480 cells in each treatment group, measured by live cell imaging. (A) 20µM AqB011 or 15µM bacopaside II treatments alone significantly reduced total distance migrated for HT29 cells as compared to vehicle treated. The level of inhibition was significantly enhanced by combined treatment as compared with either agent alone. (B) No significant block of SW480 total distance was seen in any treatment as compared with vehicle. (C) Net displacement in HT29 cells was reduced by all treatments as compared to vehicle. Combined treatment showed significantly greater block of HT29 net displacement than either treatment alone. (D) Only the combined treatment reduced SW480 net displacement as compared to vehicle. (E) SW480 mean migration velocity was significantly greater than that of HT29. *n*-values in italics are above the x-axis.

4.5.4 Effects of bacopaside II and AqB011 on lamellipodial formation

An important step in cell migration is protrusion formation [13]. Lamellipodia are broad, flat, actin-rich protrusions that extend in the direction of locomotion and provide a base on which the cell moves forward [49]. Loss of the elongated cell morphology associated with lamellipodial extension is an effect consistent with reduced rates of migration [50]. Figure 4.6 depicts cells that were representative of the ensemble behavior in each treatment group for HT29 and SW480 cell lines. Images of vehicle-treated cells illustrate the high proportion of migrating cells with membrane protrusions. Lamellipodia in HT29 cells normally appeared as flat sheet-like protrusions (Fig 4.6A; middle image in the vehicle treatment 'veh' row) or as "winged" processes (left and right images in 'veh'). All treatments resulted in reduced lengths of HT29 lamellipodial formations as compared to vehicle-treated cells (Fig 4.6A), and a lower proportion of cell population that possessed lamellipodial protrusions. A supplementary movie file shows this in more detail (see Supplementary video 4.1). Lamellipodia in SW480 cells were more slender and longer, with flattened sheet-like protrusions at the distal end of the extensions (Fig 4.6B; 'veh'), and showed no impairment of lamellipodial extensions with AqB011 treatment; however, protrusions appeared to be reduced in size and number in the bacopaside II alone, and combined treatment conditions (Fig 4.6B). A supplementary movie file shows this in more detail (see Supplementary video 4.2). The insensitivity of SW480 morphology to AqB011 was consistent with the lack of effect of AqB011 in 2D and 3D assays of SW480 cell motility. In summary, pharmacological treatment with the AQP1 ion channel blocker, AqB011, impaired process formation selectively in HT29, consistent with inhibition of cell motility observed in wound closure and live cell imaging assays. Treatment with bacopaside II impaired the generation of polarized cellular processes in HT29 and SW480 cells. In both HT29 and SW480 cells (Fig 4.3A and 4.4A), bacopaside II treatment interestingly also appeared to facilitate a decrease in intercellular adhesion, suggested by the increased proportion of individual cells at the wound edge that were separated away from neighbouring cells.

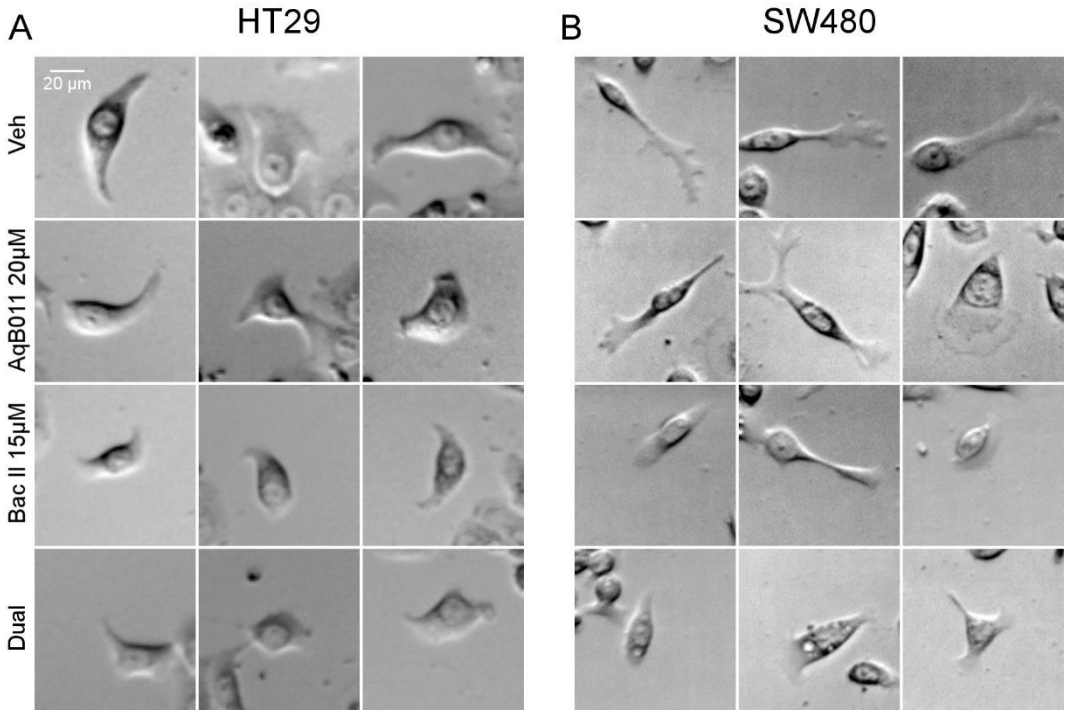

Figure 4.6 Images of actively migrating cells from different treatment groups for HT29 (A) and SW480 (B) cell lines, showing three representative examples each. Vehicle-treated cells (A and B; top row) showed distinct membrane protrusions in both cell lines. AqB011 and bacopaside II treated HT29 cells showed protrusions that were reduced in size as compared to vehicle in all treatment groups (A; rows 2-4). For SW480 cells, cellular protrusions appeared decreased in size in treatments containing bacopaside II (B; rows 3 and 4) but not with AqB011 (B; row 2).

4.5.5 AqB011, but not bacopaside II, inhibits colon cancer cell invasiveness.

An important aspect of cancer metastasis is the movement of cells in three-dimensional space, across tissue boundaries and through ECM, involving attributes that are not fully captured in a 2D wound closure model. The effects of AQP1 inhibitors were tested on colon cancer invasiveness using the transwell invasion analysis, in which cells migrated through an ECM layer and a semi-permeable membrane towards a chemoattractant (FBS), and were stained and counted (Fig 4.7C).

Treatment with AqB011 alone resulted in approximately 40% block of HT29 cell invasiveness at concentrations ≥10 μM (Fig 4.7A). For HT29 treated with AqB011 (10 μM), 63 ± 5.3% of cells invaded the lower chamber as compared to vehicle treated (Fig 4.7A). The highest dose of AqB011 (80 μM) also impaired SW480 cell invasiveness (49.7 ± 10%); lower doses had no significant effect (Fig 4.7B). Unexpectedly, application of bacopaside II alone at 15 μM potentiated colon cancer cell invasiveness in both cell lines. HT29 cells treated with bacopaside II showed a 2.7-fold increase in invasion, and SW480 cells showed a 4.5 fold increase. Interestingly, the potentiating effect in HT29 cells was negated in full by co-application of AqB011 (Fig 4.7A). In contrast, SW480 showed only a small effect of AqB011 co-application on the invasion-promoting effect of bacopaside II. Cell invasion responses required the presence of a chemotactic gradient (FBS), and an ECM gel layer (Fig 4.7D). HT29 cells were significantly more invasive (269 ± 16 cells per field of view; n=15) than SW480 (90 ± 8 cells per field of view; n=15) (Fig 4.7E). This work is the first to show the anti-invasive effects of AQP1 ion channel blocker AqB011 in colon cancer cells, suggesting a novel role for AQP1 ion conductance in facilitating cancer invasion. HT29 was more sensitive to the inhibitory effect of AqB011 than SW480, consistent with observations from 2D assays. In contrast, bacopaside II surprisingly enhanced cancer cell invasion in both cell lines, suggesting this agent is likely to have multiple targets of action.

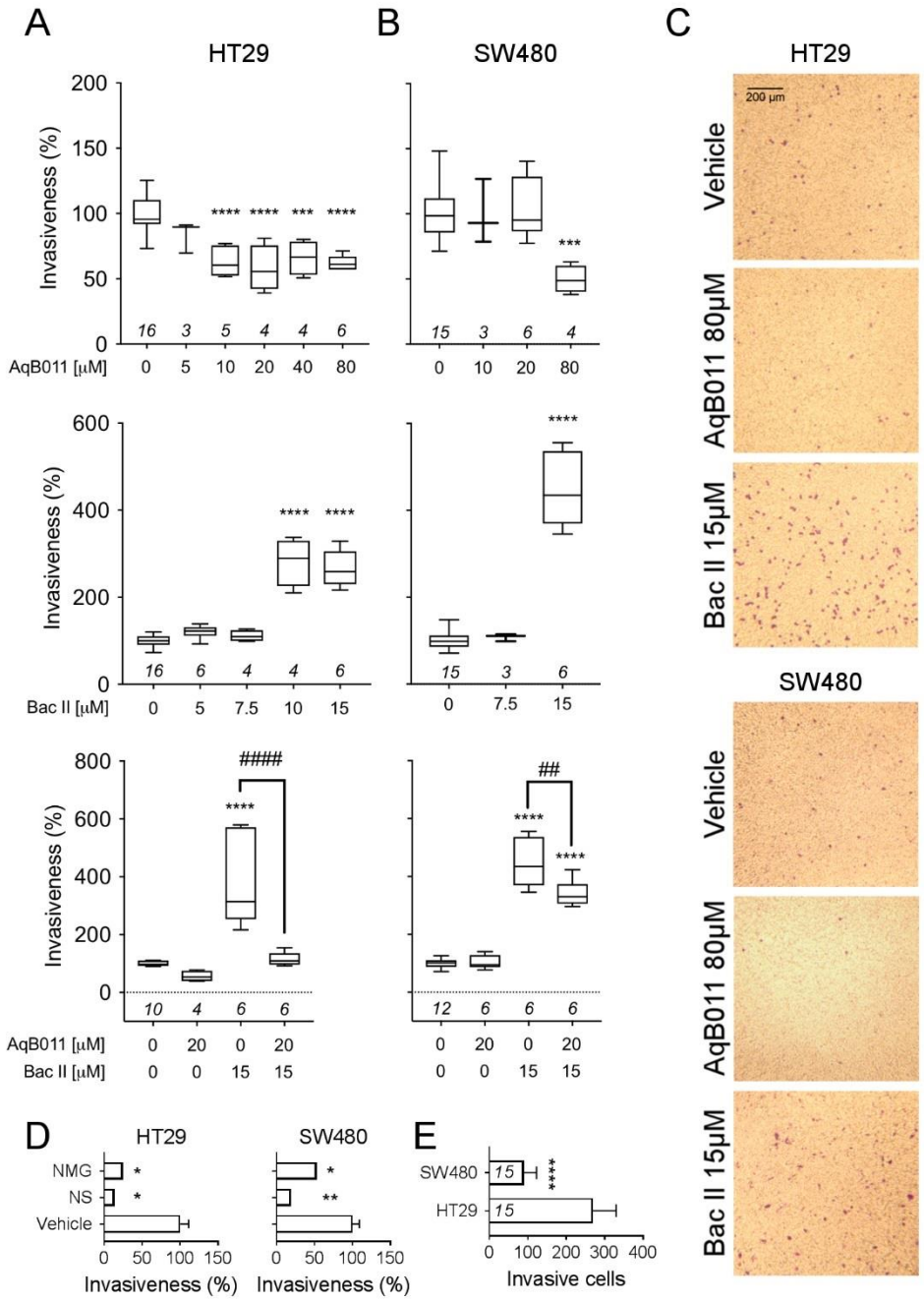

Figure 4.7 Invasive capacities of HT29 and SW480 cells during treatments with bacopaside II, AqB011, and both in combination, measured with transwell assays. Box plots depicting (A) HT29 and (B) SW480 cell invasiveness after 24 hours with AqB011 (top row), bacopaside II (row 2), or both (row 3). AqB011 significantly inhibited HT29 cell invasiveness at 10 to 80μM. Bacopaside II significantly potentiated HT29 invasiveness at 10 and 15μM. Combined treatment with AqB011 ablated the pro-invasive effect of bacopaside II in HT29 cells. AqB011 inhibited

SW480 cell invasiveness only at the highest dose tested (80μM). Bacopaside II significantly potentiated SW480 invasiveness at 15μM. AqB011 showed a small but significant reversal of the pro-invasive effect of bacopaside II in SW480. (C) Images depicting HT29 and SW480 cells that successfully crossed the ECM layer to reach the trans side of the transwell membrane in treatments with vehicle, AqB011 80μM, and bacopaside II 15μM. (D) Histograms summarizing the reduced invasiveness of HT29 and SW480 cells in the absence of ECM (no matrix gel (NMG)), or in the absence of a serum gradient (no serum (NS)), as compared with vehicle controls containing both serum gradient and ECM (vehicle). (E) HT29 cells were significantly more invasive than SW480 cells, except in the presence of bacopaside II. *n*-values are depicted in italics next to the y-axis.

4.5.6 Cell viability is not reduced by AqB011 or bacopaside II at doses that impair migration.

AqB011- and bacopaside II-mediated impairment of cell migration and invasion did not result indirectly from reduced cell viability. Cell viability was measured with the alamarBlue assay. Data were standardised to results for untreated groups in each cell line (Fig 4.8). HT29 cell viability was 99.6 ± 1.4% in AqB011 (100 µM); 94.5 ± 0.7% in combined treatment; and 3.1 ± 0.04% in mercuric chloride (5 µM). SW480 cell viability was 97.6 ± 0.2% in AqB011 (100 µM); 96.2 ± 0.6% in combined treatment; and 2.4 ± 0.04% in mercuric chloride (5 µM). These data showed that the AQP1 modulatory agents affected viability by less than 6%, demonstrating that cytotoxicity did not account indirectly for the substantial reductions observed for cell migration and invasion.

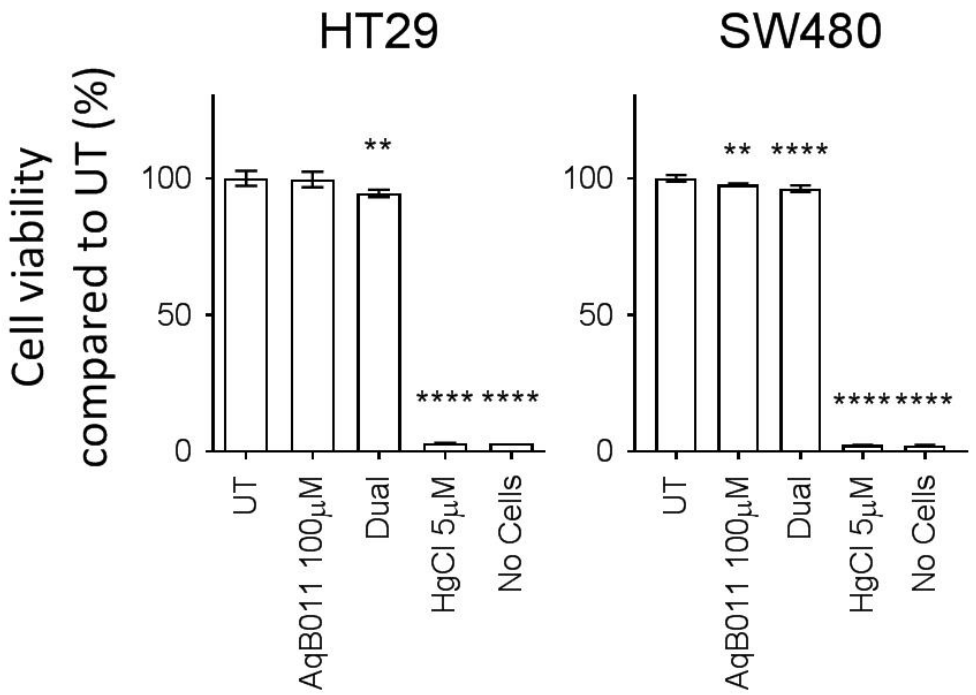

Figure 4.8 Summary histogram of cytotoxic effects of treatments, measured by alamarBlue assay for HT29 and SW480 cells. "Dual" indicates combined treatment with AqB011 (20 µM) and bacopaside II (15 µM). A slight but significant decrease in cell viability was observed for HT29 cells with the combined AQP1 inhibitor treatment and in SW480 cells in all treatments. Mercuric chloride served as a positive control causing cell death; 'no-cell' controls confirmed minimal background fluorescence. All treatments were *n*=4. Data are standardised to results for untreated (UT) cells.

4.5.7 Efficacy of AqB011 requires the plasma membrane localisation of AQP1.

AqB011 was not effective in blocking cell migration and invasion in SW480 as compared to HT29, even though total AQP1 protein levels were similar in both cell lines as determined by western analysis. Prior results showing SW480 cells were relatively insensitive to AqB011 had been attributed to low levels of AQP1 expression, presumed from the low levels of AQP1 transcript measured by quantitative PCR [35], as confirmed in Fig 4.1C. However, western blot analyses showed protein levels of AQP1 were comparable between HT29 and SW480 cell lines (Fig 4.1A and 4.1B). To test whether the difference in sensitivity resulted from differences in AQP1 protein localization, AQP1 signal intensity throughout the cell was assessed by immunofluorescent labelling of AQP1, in combination with a fluorogenic membrane dye (MemBrite™), and Hoechst nuclear stain (Fig 4.9A). We used Fiji (ImageJ) to analyse and compare intensity patterns of the AQP1 and membrane stains for each cell line (Fig 4.9B and C). Plasma membrane levels of AQP1 were significantly lower in SW480 (0.3802 ± 0.043; n=6) than in HT29 (1.046 ± 0.15; n=; p=0.0004) cell lines (Fig 4.9D), suggesting that efficacy of AQP1 modulators depends on AQP1 membrane localization.

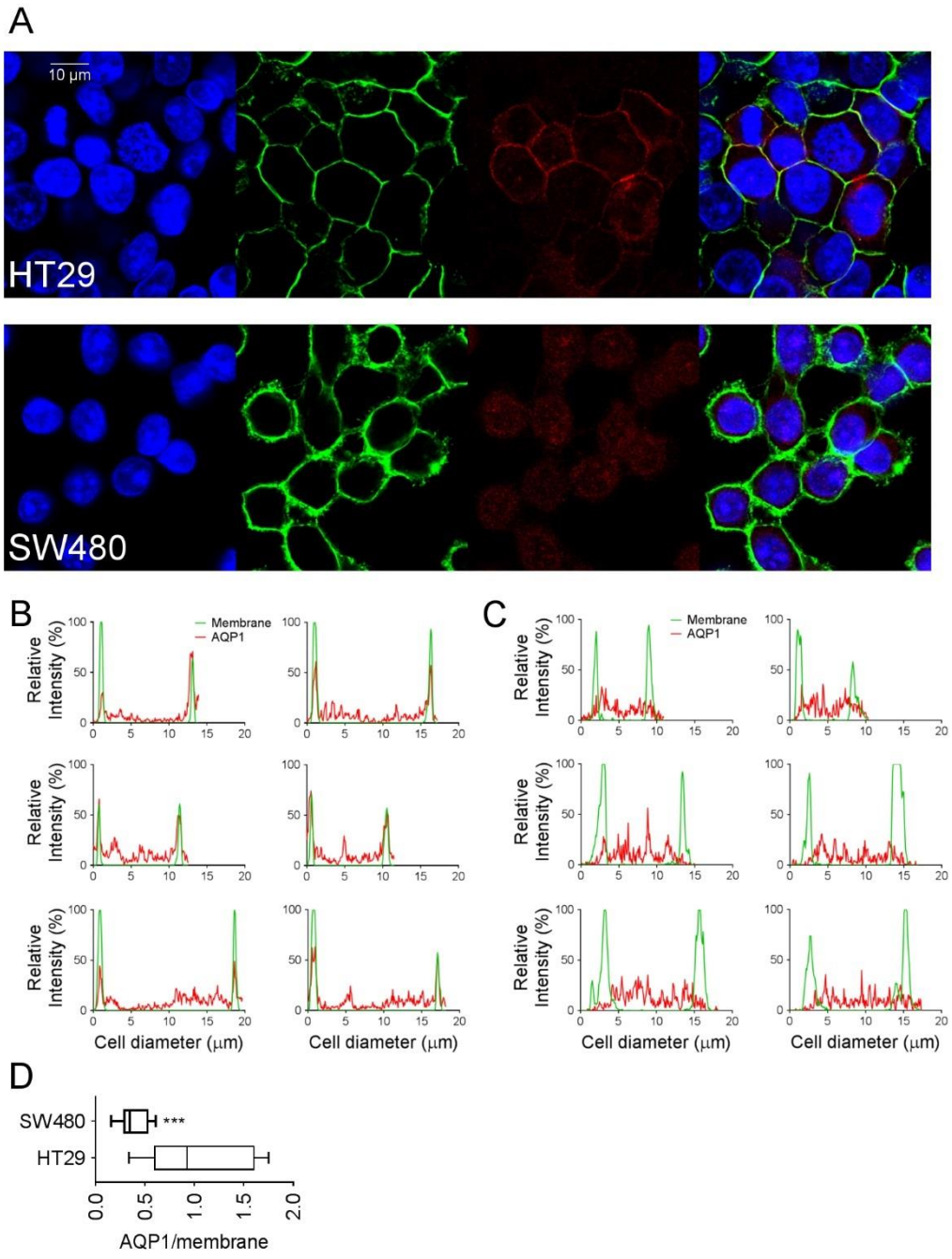

Figure 4.9 Confocal images and quantitative analyses of AQP1 subcellular localization measured by immunolabelling. (A) Confocal images of a single field of view for HT29 (top row) and SW480 (bottom row) cells. The panels in each row (from left to right) depict nuclear staining (blue); membrane staining (green); AQP1 signal (red); and an overlay of the three images. (B, C) Each graph shows the intensities (y-axis) of the membrane stain (green) and the AQP1 signal (red), as a function of distance across the diameters of three individual HT29 (B) or SW480

(C) cells. Two cross-sections per cell were measured. (D) Calculated as signal intensity ratios, HT29 cells showed strong colocalization of AQP1 and membrane staining that was not evident in SW480 cells.

4.6 Supplementary Figures

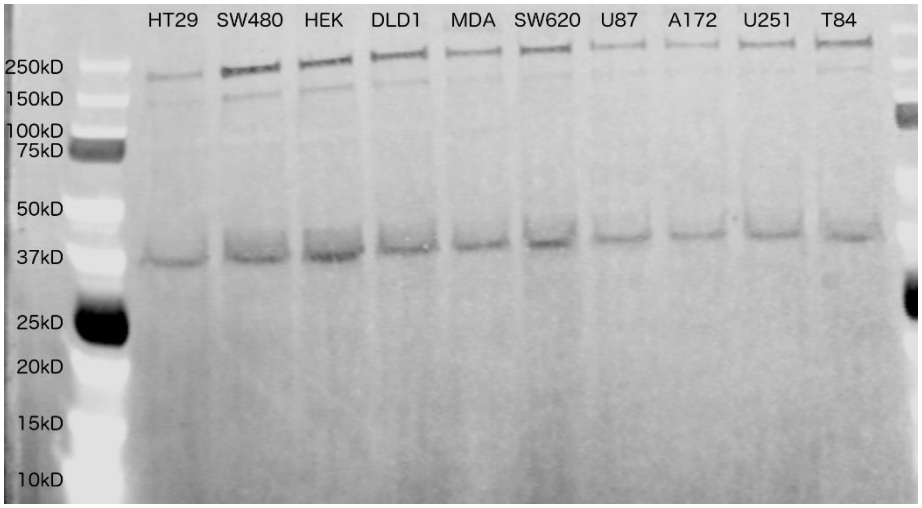

Supplementary Figure 4.1 Full-length western blot gel depicting signal for anti-AQP1 primary antibody. Other cell lines depicted were used for this experiment but results were not included as part of this chapter.

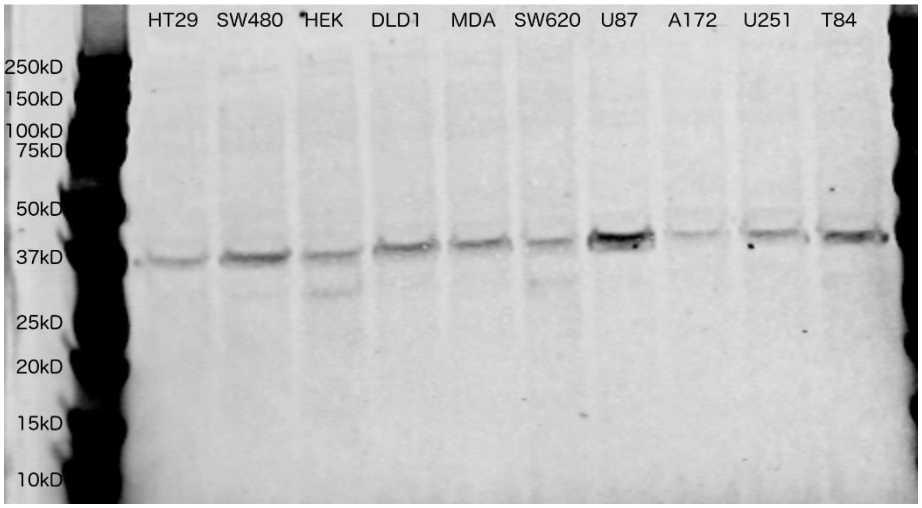

Supplementary Figure 4.2 Full-length western blot gel (the same gel as in supplementary figure 4.1) depicting signal for anti-GAPD primary antibody. Other cell lines depicted were used for this experiment but results were not included as part of this chapter.

Supplementary Video 4.1

Video animation showing HT29 cell wound closure over 24 hours. Panels (from left to right) represent cells treated with vehicle, AqB011 (20 μM), bacopaside II (15 μM), and combined treatment. All treatments significantly reduced HT29 cancer cell motility and collective cell migration, as compared to vehicle treated cells. Cellular extensions and lamellipodial formations were reduced in frequency and size in all treatment groups, as compared to vehicle.

Supplementary Video 4.2

Video animation showing SW480 cell wound closure over 24 hours. Panels (from left to right) represent cells treated with vehicle, AqB011 (20 μM), bacopaside II (15 μM), and combined treatment. Cellular extensions and lamellipodial formations were reduced in frequency and size in treatments with bacopaside II (with or without AqB011), as compared to vehicle.

4.7 Discussion

Cell migration and invasion are key pathological processes of cancer metastasis. AQP1 expression has been shown to enhance cell migration and metastasis in specific subtypes of cancers [14, 16, 17], and other channels such as AQP3, AQP4, and AQP5 have also been linked to cancers, affecting viability, proliferation and migration [13, 51-54]. In cell migration, process formation is thought to be driven by reversible assembly of actin filaments [55-57], and local cell volume increases facilitated by water and ion influxes [23, 58, 59]. AQPs that are upregulated in cancers can be co-localized with ion channels and transporters to support cell volume regulation and process extension. AQP5, not known to have an intrinsic ion channel function under the conditions tested [27], could work in some cases by colocalization with separate ion channels or transporters, such as the Na^+/H^+ exchanger in breast cancer cells [58]. AQP4 colocalizes with the chloride channel (ClC2) and the potassium-chloride co-transporter 1 (KCC1) in glioma cells, which are proposed to provide a driving force for water efflux leading to cell volume changes that could augment invasiveness [60, 61]. Results here confirmed that 2D migration of HT29 colon cancer cells was impaired by blockers of the AQP1 water pores (bacopaside II) or ion channel (AqB011), and provided new information that combined treatment enhanced inhibition of migration. A testable idea for future work is that ionic influx through AQP1 channels might contribute to a local osmotic gradient driving concomitant AQP1-mediated water influx at leading edges, leading to local volume changes associated with process extension and cell movement [23], thus enhancing cancer cell motility and invasion.

HT29 and SW480 exhibited comparable protein levels, however, AQP1 mRNA levels were significantly lower in SW480 than HT29. This is not unusual, as lack of correlation between mRNA and protein levels has previously been demonstrated in liver cells [62] and yeast [63]; some proteins expressed in lung cancer cells demonstrate strong negative correlation with their mRNA levels [64]. AQP1 has multiple isoforms, and one possible suggestion is that SW480 expresses a different AQP1 isoform than HT29; the isoform of AQP1 in SW480 may have been detected with western blot analysis, but not for RT-PCR. SW480 cells showed uniformly fast 2D migration as compared to HT29 cells (Fig 5E), but were unaffected by the

AQP1 modulator AqB011, suggesting that this class of cells employs mechanisms to achieve rapid motility that do not require AQP1 ion conductance. This idea fits with the observation that the AQP1 protein in SW480 was predominantly intracellular, where its functional relevance or potential regulation remains to be determined. SW480 cells have been shown to express high levels of AQP5 protein [65-67], which might be part of an alternative mechanism for enabling rapid cell motility in combination with co-expressed ion channels, since AQP5 is not known to have any ion channel function [27], but does colocalize with ion channels that enhance cell migration in other cancer cells [68].

The insensitivity of SW480 cells to inhibition of 2D cell migration by AqB011 showed that AqB011 does not cause non-specific effects on general channel or transporter function, viability, cytoskeletal structure regulation, or other essential processes, since SW480 cells were unaffected by the agent. Nevertheless, more investigation into selectivity of AqB011 for AQP1 in cancer cells is required. The insensitivity of SW480 cells to AqB011 showed that AQP1 ion channels are not essential for the migration mechanism in this cell line, and highlighted the point that functional contributions of AQP1 depend on its localization in the plasma membrane. Regulation of the membrane localization of AQP1 and its corresponding sensitivity to inhibitors has been previously explored. Secretin was shown to increase AQP1-mediated osmotic water permeability in rat cholangiocytes by stimulating vesicular translocation of AQP1 to the plasma membrane; osmotic water permeability of rat cholangiocytes gained sensitivity to block by mercuric chloride after stimulation by secretin [69]. The small increase in efficacy of combined treatment on inhibiting SW480 2D cell migration could suggest that the low levels of AQP1 present in the plasma membrane are partially contributing to an enhanced cell motility. Future work might identify signals analogous to secretin that induce trafficking of intracellular AQP1 to the membrane in SW480 cells to test if this affects migration rate, or increases sensitivity to block by AqB011.

Two-dimensional migration and three-dimensional invasiveness do not rely on the same set of mechanisms. Surprisingly, bacopaside II alone strongly increased the

invasiveness of both HT29 and SW480 cell lines (Fig 7), contradicting expectations based on 2D migration assays. AqB011 fully reversed the pro-invasive effects of bacopaside II in HT29 cells, and partially reversed the enhanced invasion in SW480, following a pattern consistent with the relative levels of AQP1 plasma membrane localization. Bacopaside II is a chemically complex molecule, unlikely to be selective for AQPs alone. The mechanism of the pro-invasive effect of bacopaside II is not known. However, bacopaside II appeared to reduce cell size and promote separation of individual cells from adjacent cells (Fig 3A and 4A; Fig 6), suggesting a boost in invasiveness might come from reduced cell-to-cell adhesion and decreased cell volumes, both of which could facilitate movement through narrow passages. The chemotactic gradient imposed by serum might restore the capacity for directional movement which appeared to be lost following bacopaside II treatment (Fig 5C and D). At high doses bacopaside II is cytotoxic; at non-toxic doses it inhibits colon cancer growth by inducing cell cycle arrest, apoptosis [70], and reduced angiogenesis [71]. Thus, bacopaside II and its metabolites *in vivo* are likely to affect a diverse array of processes, which could account for some of the observed effects of cell migration and invasion. These non-specific effects might complicate the interpretation of these results, as drug selectivity is key to understanding the role of AQP1 water and ion channel function in this study. Further tests to dissect the chemical moieties in bacopaside II and define their biological activities are needed to better identify candidates that are specific for pharmacological modulation of AQP1.

In summary, results here are the first to show that AQP1 ion channel blocker AqB011 reduces colon cancer cell invasiveness *in vitro*, and that sensitivity to this agent depends on AQP1 localization in the plasma membrane. AQP1 water fluxes and ion conductance appear to exhibit a coordinated role in facilitating cell migration in AQP1-dependent cancer cell lines. Combined pharmacological block of both the AQP1 water and ion channels in HT29 and SW480 colon cancer cells amplified the inhibition of 2D cell migration, as compared with effects of either inhibitor alone. The prospect of a cooperative role between the AQP1 water flux and ion conductance is promising, in that lower doses of two compounds when combined could produce a beneficial level of cell migration impairment. Combined

AQP1 inhibitors could act on target cells (such as migrating cancers) that require both the AQP1 water and ion channel activities, while minimising side effects as a result of being applied at lower concentrations on other cells and tissues. Future work is needed to explore effects of AQP1 inhibitors on other cancer cell types, optimize bacopaside-related compounds for modulating AQP1 water flow, and test the effectiveness of AQP1 agents in restraining metastasis *in vivo*.

4.8 References

1. Ferlay, J., et al., *GLOBOCAN 2012 v1.0, Cancer Incidence and Mortality Worldwide: IARC CancerBase No. 11*. 2013, Lyon, France: International Agency for Research on Cancer. .
2. Chaffer, C.L. and R.A. Weinberg, *A perspective on cancer cell metastasis.* Science, 2011. **331**(6024): p. 1559-1564.
3. Mehlen, P. and A. Puisieux, *Metastasis: a question of life or death.* Nature Reviews Cancer, 2006. **6**(6): p. 449-458.
4. Yoshida, T., et al., *Expression of aquaporin-1 is a poor prognostic factor for stage II and III colon cancer.* Molecular and clinical oncology, 2013. **1**(6): p. 953-958.
5. Kang, B.W., et al., *Expression of aquaporin-1, aquaporin-3, and aquaporin-5 correlates with nodal metastasis in colon cancer.* Oncology, 2015. **88**(6): p. 369-376.
6. Ishibashi, K., S. Hara, and S. Kondo, *Aquaporin water channels in mammals.* Clin Exp Nephrol, 2009. **13**(2): p. 107-17.
7. Finn, R.N., et al., *The lineage-specific evolution of aquaporin gene clusters facilitated tetrapod terrestrial adaptation.* PLoS One, 2014. **9**(11): p. e113686.
8. Saadoun, S., et al., *Increased aquaporin 1 water channel expression in human brain tumours.* Br J Cancer, 2002. **87**(6): p. 621-3.
9. Moon, C., et al., *Involvement of aquaporins in colorectal carcinogenesis.* Oncogene, 2003. **22**(43): p. 6699-703.
10. Mazal, P.R., et al., *Diagnostic significance of aquaporin-1 in liver tumors.* Hum Pathol, 2005. **36**(11): p. 1226-31.
11. Hoque, M.O., et al., *Aquaporin 1 is overexpressed in lung cancer and stimulates NIH-3T3 cell proliferation and anchorage-independent growth.* Am J Pathol, 2006. **168**(4): p. 1345-53.
12. Guan, B., et al., *Expression and distribution of aquaporin 1 in laryngeal carcinoma.* Lin Chuang Er Bi Yan Hou Tou Jing Wai Ke Za Zhi, 2007. **21**(6): p. 269-272.
13. De Ieso, M.L. and A.J. Yool, *Mechanisms of Aquaporin-Facilitated Cancer Invasion and Metastasis.* Frontiers in Chemistry, 2018. **6**: p. 135.
14. Saadoun, S., et al., *Impairment of angiogenesis and cell migration by targeted aquaporin-1 gene disruption.* Nature, 2005. **434**(7034): p. 786-92.
15. Nicchia, G.P., et al., *Inhibition of aquaporin-1 dependent angiogenesis impairs tumour growth in a mouse model of melanoma.* J Mol Med (Berl), 2013. **91**(5): p. 613-23.

16. Hu, J. and A.S. Verkman, *Increased migration and metastatic potential of tumor cells expressing aquaporin water channels.* FASEB J, 2006. **20**(11): p. 1892-4.
17. Jiang, Y., *Aquaporin-1 activity of plasma membrane affects HT20 colon cancer cell migration.* IUBMB Life, 2009. **61**(10): p. 1001-9.
18. Papadopoulos, M., S. Saadoun, and A. Verkman, *Aquaporins and cell migration.* Pflug Arch Eur J Phy, 2008. **456**(4): p. 693-700.
19. Pei, J.V., et al., *Differential Inhibition of Water and Ion Channel Activities of Mammalian Aquaporin-1 by Two Structurally Related Bacopaside Compounds Derived from the Medicinal Plant Bacopa monnieri.* Molecular Pharmacology, 2016. **90**(4): p. 496-507.
20. Klebe, S., et al., *Blockade of aquaporin 1 inhibits proliferation, motility, and metastatic potential of mesothelioma in vitro but not in an in vivo model.* Disease markers, 2015. **2015**.
21. Dorward, H.S., et al., *Pharmacological blockade of aquaporin-1 water channel by AqB013 restricts migration and invasiveness of colon cancer cells and prevents endothelial tube formation in vitro.* Journal of Experimental & Clinical Cancer Research, 2016. **35**(1): p. 36.
22. McCoy, E. and H. Sontheimer, *Expression and function of water channels (aquaporins) in migrating malignant astrocytes.* Glia, 2007. **55**(10): p. 1034-43.
23. Schwab, A., et al., *Cells move when ions and water flow*. Pflug Arch Eur J Phy, 2007. **453**(4): p. 421-432.
24. Yool, A.J. and E.M. Campbell, *Structure, function and translational relevance of aquaporin dual water and ion channels.* Mol Aspects Med, 2012: p. in press.
25. Yu, J., et al., *Mechanism of gating and ion conductivity of a possible tetrameric pore in aquaporin-1*. Structure, 2006. **14**(9): p. 1411-23.
26. Sui, H., et al., *Structural basis of water-specific transport through the AQP1 water channel.* Nature, 2001. **414**(6866): p. 872-878.
27. Anthony, T.L., et al., *Cloned human aquaporin-1 is a cyclic GMP-gated ion channel.* Mol Pharmacol, 2000. **57**(3): p. 576-88.
28. Boassa, D. and A.J. Yool, *Single amino acids in the carboxyl terminal domain of aquaporin-1 contribute to cGMP-dependent ion channel activation.* BMC Physiol, 2003. **3**: p. 12.
29. Zhang, W., et al., *Aquaporin-1 channel function is positively regulated by protein kinase C.* J Biol Chem, 2007. **282**(29): p. 20933-40.
30. Kourghi, M., et al., *Identification of loop D domain amino acids in the human Aquaporin-1 channel involved in activation of the ionic conductance and inhibition by AqB011*. Frontiers in chemistry, 2018. **6**: p. 142.
31. Saparov, S.M., et al., *Water and ion permeation of aquaporin-1 in planar lipid bilayers. Major differences in structural determinants and stoichiometry.* J Biol Chem, 2001. **276**(34): p. 31515-20.
32. Tsunoda, S.P., et al., *Aquaporin-1, nothing but a water channel.* J Biol Chem, 2004. **279**(12): p. 11364-7.
33. Campbell, E.M., D.N. Birdsell, and A.J. Yool, *The activity of human aquaporin 1 as a cGMP-gated cation channel is regulated by tyrosine phosphorylation in the carboxyl-terminal domain.* Mol Pharmacol, 2012. **81**(1): p. 97-105.

34. Boassa, D., W.D. Stamer, and A.J. Yool, *Ion channel function of aquaporin-1 natively expressed in choroid plexus.* J Neurosci, 2006. **26**(30): p. 7811-9.
35. Kourghi, M., et al., *Bumetanide Derivatives AqB007 and AqB011 Selectively Block the Aquaporin-1 Ion Channel Conductance and Slow Cancer Cell Migration.* Molecular Pharmacology, 2016. **89**(1): p. 133-140.
36. Kourghi, M., et al., *Divalent cations regulate the ion conductance properties of diverse classes of aquaporins.* International journal of molecular sciences, 2017. **18**(11): p. 2323.
37. Yool, A.J. and A.M. Weinstein, *New roles for old holes: Ion channel function in aquaporin-1.* News Physiological Sciences, 2002. **17**: p. 68-72.
38. Yool, A.J., et al., *Tetraethylammonium block of water flux in Aquaporin-1 channels expressed in kidney thin limbs of Henle's loop and a kidney-derived cell line.* BMC Physiol, 2002. **2**: p. 4.
39. De Ieso, M.L. and J.V. Pei, *An Accurate and Cost-Effective Alternative Method for Measuring Cell Migration with the Circular Wound Closure Assay.* Bioscience Reports, 2018.
40. Wardill, H.R., et al., *A novel in vitro platform for the study of SN38-induced mucosal damage and the development of Toll-like receptor 4-targeted therapeutic options.* Experimental Biology and Medicine, 2016. **241**(13): p. 1386-1394.
41. Stamer, W.D., et al., *Cultured human trabecular mesh work cells express aquaporin-1 water channels.* Current eye research, 1995. **14**(12): p. 1095-1100.
42. Stamer, W.D., R.W. Snyder, and J.W. Regan, *Characterization of the transmembrane orientation of aquaporin-1 using antibodies to recombinant fusion proteins.* Biochemistry, 1996. **35**(50): p. 16313-16318.
43. Jacob, F., et al., *Careful Selection of Reference Genes Is Required for Reliable Performance of RT-qPCR in Human Normal and Cancer Cell Lines.* PLOS ONE, 2013. **8**(3): p. e59180.
44. Kam, Y., et al., *A novel circular invasion assay mimics in vivo invasive behavior of cancer cell lines and distinguishes single-cell motility in vitro.* BMC cancer, 2008. **8**(1): p. 198.
45. Simpson, K.J., et al., *Identification of genes that regulate epithelial cell migration using an siRNA screening approach.* Nature cell biology, 2008. **10**(9): p. 1027-1038.
46. Schindelin, J., et al., *Fiji: an open-source platform for biological-image analysis.* Nature methods, 2012. **9**(7): p. 676.
47. Shaw, L.M., *Tumor cell invasion assays*, in *Cell Migration*. 2005, Springer. p. 97-105.
48. Devuyst, O., et al., *Aquaporin-1 and endothelial nitric oxide synthase expression in capillary endothelia of human peritoneum.* American Journal of Physiology-Heart and Circulatory Physiology, 1998. **275**(1): p. H234-H242.
49. Cramer, L.P., M. Siebert, and T.J. Mitchison, *Identification of novel graded polarity actin filament bundles in locomoting heart fibroblasts: implications for the generation of motile force.* The Journal of cell biology, 1997. **136**(6): p. 1287-1305.
50. Friedl, P. and K. Wolf, *Plasticity of cell migration: a multiscale tuning model.* The Journal of cell biology, 2009: p. jcb. 200909003.

51. Verkman, A.S., *Knock-out models reveal new aquaporin functions.* Handb Exp Pharmacol, 2009(190): p. 359-81.
52. Jung, H.J., et al., *Aquaporin-5: a marker protein for proliferation and migration of human breast cancer cells.* PloS one, 2011. **6**(12): p. e28492.
53. Cao, X.C., et al., *Aquaporin3 is required for FGF-2-induced migration of human breast cancers.* PLoS One, 2013. **8**(2): p. e56735.
54. Saadoun, S., et al., *Involvement of aquaporin-4 in astroglial cell migration and glial scar formation.* Journal of cell science, 2005. **118**(24): p. 5691-5698.
55. Pollard, T.D. and G.G. Borisy, *Cellular motility driven by assembly and disassembly of actin filaments.* Cell, 2003. **112**(4): p. 453-465.
56. Wang, Y.-L., *Exchange of actin subunits at the leading edge of living fibroblasts: possible role of treadmilling.* The Journal of cell biology, 1985. **101**(2): p. 597-602.
57. Theriot, J.A. and T.J. Mitchison, *Actin microfilament dynamics in locomoting cells.* Nature, 1991. **352**(6331): p. 126-131.
58. Stroka, K.M., et al., *Water permeation drives tumor cell migration in confined microenvironments.* Cell, 2014. **157**(3): p. 611-23.
59. Frede, J., et al., *Ovarian cancer: Ion channel and aquaporin expression as novel targets of clinical potential.* Eur J Cancer. **49**(10): p. 2331-44.
60. McCoy, E.S., B.R. Haas, and H. Sontheimer, *Water permeability through aquaporin-4 is regulated by protein kinase C and becomes rate-limiting for glioma invasion.* Neuroscience, 2010. **168**(4): p. 971-981.
61. Mcferrin, M.B. and H. Sontheimer, *A role for ion channels in glioma cell invasion.* Neuron glia biology, 2006. **2**(1): p. 39-49.
62. Anderson, L. and J. Seilhamer, *A comparison of selected mRNA and protein abundances in human liver.* Electrophoresis, 1997. **18**(3-4): p. 533-537.
63. Gygi, S.P., et al., *Correlation between protein and mRNA abundance in yeast.* Molecular and cellular biology, 1999. **19**(3): p. 1720-1730.
64. Chen, G., et al., *Discordant protein and mRNA expression in lung adenocarcinomas.* Molecular & cellular proteomics, 2002. **1**(4): p. 304-313.
65. Shan, T., et al., *Impact of AQP-5 on the growth of colorectal cancer cells and the underlying mechanism.* INTERNATIONAL JOURNAL OF CLINICAL AND EXPERIMENTAL PATHOLOGY, 2018. **11**(1): p. 58-67.
66. Shan, T., et al., *AQP5: a novel biomarker that predicts poor clinical outcome in colorectal cancer.* Oncology reports, 2014. **32**(4): p. 1564-1570.
67. Kang, S.K., et al., *Role of human aquaporin 5 in colorectal carcinogenesis.* The American journal of pathology, 2008. **173**(2): p. 518-525.
68. Stroka, K.M., et al., *Water permeation drives tumor cell migration in confined microenvironments.* Cell, 2014. **157**(3): p. 611-623.
69. Marinelli, R.A., et al., *Secretin Promotes Osmotic Water Transport in Rat Cholangiocytes by Increasing Aquaporin-1 Water Channels in Plasma Membrane EVIDENCE FOR A SECRETIN-INDUCED VESICULAR TRANSLOCATION OF AQUAPORIN-1.* Journal of Biological Chemistry, 1997. **272**(20): p. 12984-12988.
70. Smith, E., et al., *The Purified Extract from the Medicinal Plant Bacopa monnieri, Bacopaside II, Inhibits Growth of Colon Cancer Cells In Vitro by Inducing Cell Cycle Arrest and Apoptosis.* Cells, 2018. **7**(7): p. 81.

71. Palethorpe, H.M., et al., *The Aquaporin 1 Inhibitor Bacopaside II Reduces Endothelial Cell Migration and Tubulogenesis and Induces Apoptosis.* International journal of molecular sciences, 2018. **19**(3): p. 653.

Chapter 5: Discovery of a new pharmacological inhibitor of chemokine-activated invasiveness in glioblastoma cells

Michael L De Ieso[1], Saeed Nourmohammadi[1] and Andrea J Yool[1]

[1]Department of Physiology, Adelaide Medical School, University of Adelaide, Adelaide, SA, Australia

Chapter 5 describes observations pertaining to the anti-invasive qualities of (an) unknown compound(s) present in the mixture, fraction E. Fraction E is a by-product of an error in synthesis that led to the generation of a mixture of compounds (AqB051) including the target molecule (AqB050) and related derivatives. It is important to note that this chapter is a working progress, and the future purpose of this work is to clarify the structure of the active compound in fraction E.

5.1 Abstract

Glioblastoma (GBM) is the most lethal primary malignancy of the central nervous system, because of its high invasive capacity. Investigating therapies to reduce invasion is crucially important. The aim of this study was to isolate and characterise a novel pharmacological agent, fractionated from a mixture of synthetic arylsulfonamide compounds, that accounted for the strong inhibition of GBM invasiveness observed in transwell migration assays *in vitro*. During the intended re-synthesis of the proposed aquaporin-1 inhibitor, AqB050, an error led to generation of a mixture of compounds (AqB051) including the target molecule (AqB050) and related derivatives. This mixture was found to strongly block cancer transwell invasion, likely acting at sub-micromolar concentrations. Human colorectal adenocarcinoma, human glioblastoma, and mammary adenocarcinoma cell lines were used for this study. Two-dimensional rates of collective cancer cell migration were measured with the circular wound closure assay. Three-dimensional cancer cell invasion and chemotaxis were measured with the transwell invasion assay. Angiogenesis in human umbilical cord endothelial cells was measured with the Ibidi μ-plate angiogenesis assay. General matrix metalloproteinase activity was

measured using the fluorometric matrix metalloproteinase activity assay kit. Cell viability was quantified using an alamarBlue assay. The potent biologically active agent has thus far been narrowed to one of eight fractions (Fraction E) from AqB051. AqB051 and fraction E significantly inhibited invasiveness in all glioblastoma cell lines, and in one of the two colorectal adenocarcinoma cell lines. AqB051 (72 μg/mL) blocked wound closure by 60% in U87-MG, 43% in HT29, and 16% in A172 cells. AqB050 (40μM) blocked HT29 wound closure by 41%. Compared to vehicle, U87-MG cells treated with AqB051 (4.5 μg/mL) invaded at 5.2%; and fraction E (4.5 μg/mL) at 20%. AqB050 had minimal effect on glioblastoma invasiveness, however it strongly inhibited invasiveness in mammary carcinoma cell line. AqB051 and fraction E also blocked A172 transwell migration in the absence of extracellular matrix gel, suggesting these compounds do not affect matrix degrading enzymes. AqB051 (36 μg/mL) inhibited HUVEC tube formation by approximately 95%. AqB050 (20μM) decreased glioblastoma cell proliferation to 51% of vehicle over 48 hours. Fraction E had no effect on cell proliferation. A novel pharmacological agent (fraction E) appears to be a potent blocker of GBM invasiveness *in vitro*. The proposed AQP1 inhibitor, AqB050, blocks brain and breast cancer invasiveness, and glioblastoma proliferation. With further investigation, these pharmacological compounds with biological activity could lead to the discovery of an anti-invasive therapy that could enhance the effectiveness of existing treatments.

5.2 Statement of authorship

Statement of Authorship

Title of Paper	Discovery of a new pharmacological inhibitor of chemokine-activated invasiveness in glioblastoma cells
Publication Status	☐ Published ☐ Accepted for Publication ☐ Submitted for Publication ☑ Unpublished and Unsubmitted w ork w ritten in manuscript style
Publication Details	N/A

Principal Author

Name of Principal Author (Candidate)	Michael Lucio De Ieso
Contribution to the Paper	First author and main contributor. Formulaton of research question. Concept and methodological design. Performed experiments and data analysis. Generation of manuscript. Figure and table development. Incorporation of superviser comments and suggestions for manuscript.
Overall percentage (%)	90
Certification:	This paper reports on original research I conducted during the period of my Higher Degree by Research candidature and is not subject to any obligations or contractual agreements with a third party that would constrain its inclusion in this thesis. I am the primary author of this paper.
Signature	Date: 23 NOV 2018

Co-Author Contributions

By signing the Statement of Authorship, each author certifies that:

i. the candidate's stated contribution to the publication is accurate (as detailed above);
ii. permission is granted for the candidate in include the publication in the thesis; and
iii. the sum of all co-author contributions is equal to 100% less the candidate's stated contribution.

Name of Co-Author	Andrea Yool
Contribution to the Paper	Intellectual contribution to project design and research questions. Reviewed and edited final manuscript.
Signature	Date: 23 Nov 2018

Name of Co-Author	Saeed Nourmohammadi
Contribution to the Paper	Performed experimental procedures
Signature	Date: 23/11/2018

Please cut and paste additional co-author panels here as required.

5.3 Introduction

Glioblastoma (GBM) is the most common and aggressive primary malignancy of the central nervous system, classified as a grade IV glioma based on the World Health Organisation classification [1]. The average annual age-adjusted incidence rate of GBM per 100,000 persons ranges from 2.05 in England (1999-2003) [2], 3.19 in the United States of America (2006-2010) [3], to 3.4 in Australia (2000-2008) [4]. To date, the most effective treatment for GBM involves resection, followed by radiotherapy and temozolomide chemotherapy [5]. However, the invasive phenotype of GBM cells makes it difficult to treat, with a median prognosis of only 14.6 months [6-8]. Notably, current treatment is mainly focused on removal and destruction of the tumourous cells, despite the devastating consequences of GBM invasiveness. Anti-angiogenic therapies (such as anti-VEGF therapy) block GBM tumour growth in mice and humans, but result in a more invasive phenotype in the cancerous cells [9-11]. Thus, adjuvant anti-invasive therapy might improve effectiveness of current treatments.

Mechanisms involved in glioblastoma invasion include detachment from the tumour mass, adherence to the extracellular matrix (ECM), degradation of the ECM, migration, cell volume regulation, and chemotaxis [12-14]. The molecular bases of these mechanisms have been a logical research focus for anti-invasive therapies in glioblastoma, though with limited success thus far. Transforming growth factor-β (TGF-β) produced by microglia promotes glioblastoma invasion by inducing matrix metalloproteinase (MMP) expression, and by suppressing tissue inhibitor of metalloproteinase (TIMP), allowing for enhanced ECM degradation [15-18]. Administration of the TGF-β2 antisense oligonucleotide, trabedersen (AP12009; 10μM) in clinical trials increased median survival for patients to 39.1 months as compared with 21.7 months for standard chemotherapy; however, the difference was not statistically significant [19, 20]. Epidermal growth factor receptor (EGFR), often overexpressed in GBMs, promotes chemotaxis, invasion, and migration [21]. However, EGFR kinase inhibitors such as erlotinib and gefitinib proved to be effective only for a small subset of GBM patients [22, 23]. Focal adhesion kinase (FAK), which phosphorylates cytoskeleton-associated substrates such as Src, is upregulated in GBM. Src tyrosine kinases contribute to cell adhesion

formation and disassembly [12, 24], enabling detachment of cells from the tumour mass and interaction with ECM. Src inhibitors CGP76030 and CGP77675 *in vitro* reduced migration, invasion, and adhesion of GBM cell lines [25]. However, the multitargeted tyrosine kinase inhibitor, Dasatinib, in clinical trials was ineffective in recurring GBM [26]. Ion channel upregulation promotes GBM cell volume regulation and cell migration [13, 14, 27]. Blockade of GBM chloride channels by chlorotoxin (CTX), a scorpion-derived peptide, produced dose-dependent inhibition of tumour cell migration and invasion through a transwell membrane [27]. Further work is needed to assess the translational potential of CTX in clinical trials. Ultimately, a combination of clinically efficacious pharmacological treatments might be selected to inhibit GBM invasiveness. The aim of this study was to identify a novel pharmacological agent that strongly inhibits GBM invasiveness *in vitro*.

Aquaporin-1 (AQP1) is a member of the family of membrane-spanning water channels with diverse physiological functions including enhancing plasma membrane osmotic water permeability [28]. AQP1 also potentiates cell migration and invasion [29, 30]. A synthetic compound AqB050 is a proposed blocker of AQP1, shown to inhibit mesothelioma cell migration and invasiveness *in vitro*, but not *in vivo* [31, 32]. Here, we introduce a novel molecule that was serendipitously created during the intended re-synthesis of AqB050. An error in synthesis led to the generation of a mixture of compounds (nominally referred to as "AqB051"), including the target molecule (AqB050) and related derivatives which included an unknown compound (referred to nominally as “fraction E”, pending chemical characterisation) with high potency for block of GBM invasiveness. These findings introduce a new anti-invasive molecule with possible therapeutic potential in the treatment of GBM.

5.4 Materials and Methodology

5.4.1 Cell lines

Lines used for this study were: (1) human colorectal adenocarcinoma HT29 (supplied by the American Type Culture Collection (ATCC®), catalogue number

HTB-38™), and DLD1 (ATCC; catalogue number CCL-221™); (2) Human glioblastoma cell lines U251-MG (supplied by the European Collection of Cell Cultures (ECACC; Salisbury, United Kingdom), catalogue number 09063001 purchased from CellBank Australia (Westmead, NSW, Australia)), A-172 (ECACC, catalogue number 88062428), and U87-MG (ECACC, catalogue number 89081402); (3) Mammary adenocarcinoma MDA-MB-231 (ATCC; catalogue number HTB-26™); (4) human umbilical vein endothelial cells (HUVEC) (ATCC; catalogue number CRL-1730™). Cells were cultured in T-75 plates in Dulbecco's Modified Eagle Medium (DMEM; Life Technologies, Grand Island, NY, USA) supplemented with 10% fetal bovine serum (FBS), 1% Gibco GlutaMAX (all cells except MDA-MB-231 were treated with GlutaMAX) and 100 units/ml each of penicillin and streptomycin. Cell cultures were grown at 37°C in a humidified 5% CO_2 incubator.

5.4.2 Inhibitors

AqB051 mixture was separated into subsets of constituent components using thin layer chromatography (TLC). High resolution mass spectrometry was performed to evaluate the chemical components in each fraction and narrow the possible chemical compositions (Mass Spectrometry Facility, School of Chemistry, University of Sydney, NSW). TLC produced eight fractions. The intended molecule, AqB050, constituted the majority of one of the lower MW fractions. The higher MW fraction which showed striking potency in bioassays of cancer cell invasion (done in Adelaide by De Ieso) was in the fraction labelled "fraction E", still pending further refinement and chemical characterisation. The other six fractions were tested for biological activity; however, none exhibited any substantial effect in blocking migration (data not shown). Broad spectrum MMP inhibitor, batimastat, was purchased in powder form (cat # SML0041-5MG; Sigma-Aldrich). All agents were reconstituted in DMSO as 1000x stock solutions.

5.4.3 Circular wound closure assay

Two-dimensional cell migration was measured with the circular wound closure assay as described by De Ieso and Pei (2018) [33]. Cells were seeded at 1 x 10^5 cells/ml in normal culture medium with 10% foetal bovine serum (FBS), and

incubated at 37°C in 5% CO_2 in a 96-well plate. Once cells achieved 80-90% confluence, they were incubated in reduced-serum (2% FBS) media and 400 nM of the mitotic inhibitor 5-fluoro-2'-deoxyuridine (FUDR) overnight to achieve a confluent monolayer. A sterile p10 pipette tip was used to generate circular wounds; pharmacological compound-treated media (with 2% FBS and FUDR) was applied following wounding. The final time-point was dependent on cell line. Wounds were imaged at 10x magnification with a Canon 6D camera on a Nikon inverted microscope. Images were standardised using XnConvert software, and wound areas were quantified using NIH ImageJ software (U.S. National Institutes of Health). Closure was calculated as a percentage of the initial wound area for the same well as a function of time. All experiments were repeated twice.

5.4.4 Transwell invasion and chemotaxis assay

Three-dimensional cancer cell invasion and chemotaxis was measured with the transwell invasion assay, which was performed using 6.5mm Corning® Transwell® polycarbonate membrane cell culture inserts with 8μm pore size (cat #3422; Sigma-Aldrich). For the invasion assay, the upper surface of the filter was coated with 40μL of water-diluted extracellular matrix (ECM) gel from Engelbreth-Holm-Swarm murine sarcoma (250 μg/mL for each cell line; Sigma-Aldrich, St. Louis, MO). The transwells with the ECM gel are left to dehydrate overnight and rehydrated 2 hours prior to cell seeding with 50μL of serum-free DMEM per transwell insert. The chemotaxis assay does not include pre-coating the membrane with the ECM gel, and follows the same procedure as the invasion assay from this point onwards. Cells were grown to approximately 40% confluence under normal conditions, and transferred into reduced serum (2% FBS) medium for 12-18 hours prior to seeding. Cells were detached (at ≤80% confluency) and resuspended in serum-free culture media with and without pharmacological treatments at $5x10^4$ cells per well (for invasion assay) and $2x10^4$ cells per well (for chemotaxis assay). Cells were then seeded in transwell inserts (total 150 μL of cell suspension per transwell, including 50 μL of rehydration medium added earlier for invasion assay). 600 μL of culture medium with 10% serum (chemoattractant) and the pharmacological treatment was added to the lower chamber. All cells except HT29

and DLD1 were incubated for 4 hours (for invasion assay) and 2 hours (for chemotaxis assay), at 37°C in 5% CO_2. HT29 and DLD1 were incubated for 24 hours at 37°C in 5% CO_2. Non-migrated cells were scraped from the upper surface of the membrane with a cotton swab; migrated cells remaining on the bottom surface were counted after staining with crystal violet [35].

5.4.5 Angiogenesis assay

Ibidi® μ-plate angiogenesis assay was conducted as per manufacturer's instructions [36]. HUVECs were seeded onto a thin layer (12 μL) of matrigel in a 96-well angiogenesis μ-plate (Ibidi, Martinsried, Germany) at 1.5 x 10^4 cells per well either in vehicle (0.1% DMSO) or AqB051 at 9, 18 or 36 μg/mL, made in endothelial growth medium (HUVEC). The numbers of loops formed were counted at 20 h.

5.4.6 Fluorometric matrix metalloproteinase activity assay

General MMP activity was measured using the Fluorometric MMP Activity Assay Kit (Abcam; ab112146), as per the manufacturer's protocol [37]. In brief, A172 cells (10^4) were seeded into 6-well plates in FBS-free media and incubated in 37°C in 5% CO_2 for 18 h. Pharmacological compound treatments were then added to each well and cells were incubated for another 2 hours in the same conditions. The conditioned media was used to assay MMP activity; three 25 μL samples from each treatment were added to three wells in a 96-well plate to make triplicate wells for each treatment (one triplicate condition was FBS-free media that had not been conditioned by cells or treated with any pharmacological compounds). 25 μL of 4-aminophenylmercuric acetate (APMA; 2mM) working solution was added to each well and incubated at 37°C for another 3 hours to activate MMPs. Next, 50 μL of the green substrate solution was added to each well (to make a total of 100 μL solution in each well) and incubated for 1 hour in the dark at room temperature. Fluorescence was measured in the sample wells using a microplate reader with a filter set for excitation/emission of 490/525 nm. Background fluorescence (fluorescence detected in the unconditioned media) was subtracted from all other treatments.

5.4.7 Cell viability assay

Cell viability was quantified using an alamarBlue assay [38], following the manufacturer's guidelines (Life Technologies). Cells were plated in FUDR-containing culture media with 2% FBS, at 10^5 cells/ml in a 96-well plate. Treatments were applied 12-18 hours after plating, and cells were incubated for 24 hours. Cells were treated with 10% alamarBlue in culture media at 24 hours, and incubated for 1-2 hours (depending on the cell type). Fluorescence was measured with a FLUOstar Optima microplate reader for control and treatment groups. The mean signal obtained from the no-cell control group was subtracted from every value in each treatment to correct for background fluorescence. The proliferation assay followed the same procedure as above, except no FUDR was used and fluorescence was measured at the start and end points.

5.5 Results

5.5.1 AqB051 inhibits colon cancer and glioblastoma wound closure

AqB051 tested in five different cell lines showed variable effects on wound closure. No effect of AqB051 was seen for MDA-231-MB (at 9 μg/mL) or U251-MG (at 18 to 72 μg/mL). AqB051 (72 μg/mL) blocked wound closure by 60 ± 2.3% in U87-MG cells, 43 ± 1.8% in HT29 cells, and 16 ± 1.9% in A172 cells (Fig 5.1); U87-MG was most sensitive to inhibition by AqB051, with significant block recorded at 4.5 μg/mL (8.6 ± 1.3%). AqB050 blocked HT29 wound closure at 40 μM (41 ± 10%) and 80μM (45 ± 3.5%), but had no effect on MDA-MB-231 cells at doses tested. MDA-MB-231 cells also were insensitive to block by fraction E (9 μg/mL). Block of HT29 wound closure by AqB051 was consistent with the observation that migration of HT29 also was inhibited by AqB050, a constituent of AqB051. Data for AqB050 on block of U87-MG and A172 cell migration is still needed, and currently limits the possible interpretation.

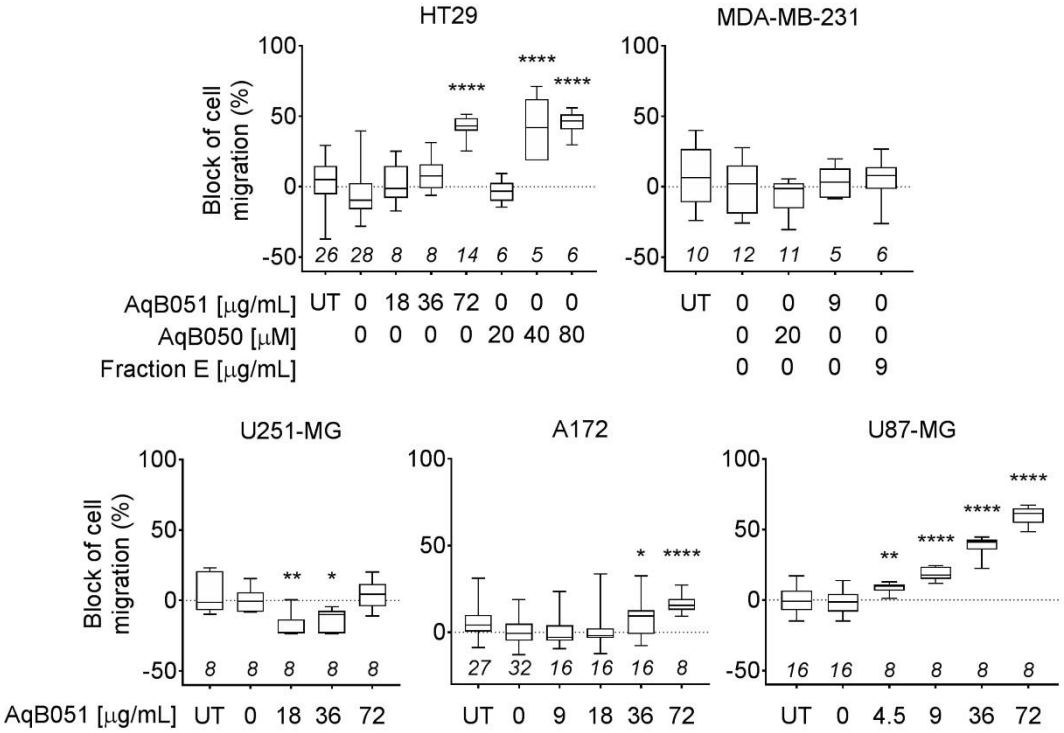

Figure 5.1 Effect of treatments on two-dimensional wound closure in various cancer cell lines. Box and whisker plots depicting percentage block of cell migration over 24h (HT29 and MDA-MB-231) and 20h (U251-MG, A172, and U87-MG) time points following treatment with AqB051, AqB050, and fraction E. AqB051 blocked wound closure in HT29, A172, and U87-MG cell lines, and had no effect in MDA-MB-231 and U251-MG. AqB050 was tested in HT29 and MDA-MB-231, and produced a significant block in HT29 cells (40-80μM). Fraction E was only tested in MDA-MB-231 and had no effect.

5.5.2 Effect of AqB051, AqB050, and fraction E on cancer invasiveness

Cancer invasiveness through extracellular matrix (ECM) utilizes mechanisms not completely captured in a 2D wound closure assay. Therefore, the effects of AqB050 at doses from 1 to 20μM, and AqB051 and fraction E at doses from 0.5 to 9 μg/mL, were measured with transwell invasion assays. In U87-MG cells, AqB051 (4.5 μg/mL) reduced invasion to 5.2 ± 1.5%, fraction E (4.5 μg/mL) limited invasion to 20 ± 5.6%, and AqB050 (20μM) reduced invasion to 66 ± 10% as compared with vehicle controls (Fig 5.2A). In HT29 cells, invasiveness was not affected by any of the treatments. In U251-MG cells, invasion was reduced to 36 ± 3.7% by fraction E (4.5 μg/mL), and to 24 ± 4.2% by AqB051 (4.5 μg/mL) as compared to vehicle; AqB050 had a small but significant effect (63 ± 20%) (Fig 5.2A). In contrast in MDA-231-MB cells, only the treatment with AqB050 (10μM) impaired invasion to 56 ± 8.4% of vehicle treated cells; AqB051 (4.5 μg/mL) or fraction E (4.5 μg/mL) were ineffective (Fig 5.2A). A172 cells were sensitive to block by AqB051 (2.3-9 μg/mL) and fraction E (4.5 and 9 μg/mL). A172 cells treated with fraction E (4.5 μg/mL) invaded at 47 ± 5.2% compared to vehicle (Fig 5.2A). DLD1 cells treated with AqB051 (9 μg/mL) invaded at 1.2 ± 1.2% compared to vehicle control (Fig 5.2A). AqB050 impaired invasion in some but not all cell lines, suggesting it is not the blocking agent of primary interest in the AqB051 mixture. Fraction E was a potent blocker of cancer invasion in all cell lines that were highly sensitive to block by AqB051, suggesting Fraction E is likely to contain the unknown component of AqB051 that strongly blocks invasiveness *in vitro*.

Environmental parameters influence transwell migration efficiency. The role of FBS in inducing chemotaxis was tested in invasion assays with and without FBS added to the lower chamber of the transwell. The presence of FBS was required for transwell migration in all cell lines tested (Fig 5.2B). Cancer invasion involves the degradation of local ECM by proteolysis, using surface proteases such as zinc-dependent MMPs [39]. Effects of a broad spectrum MMP blocker, batimastat, were measured for wound closure in A172 cells, and for transwell invasiveness with and without an ECM layer. Batimastat had no effect on 2D wound closure, and did not alter migration through a transwell membrane in the absence of an ECM layer (Fig

5.2C). However, batimastat effectively blocked invasion when the ECM barrier was present (Fig 5.2C).

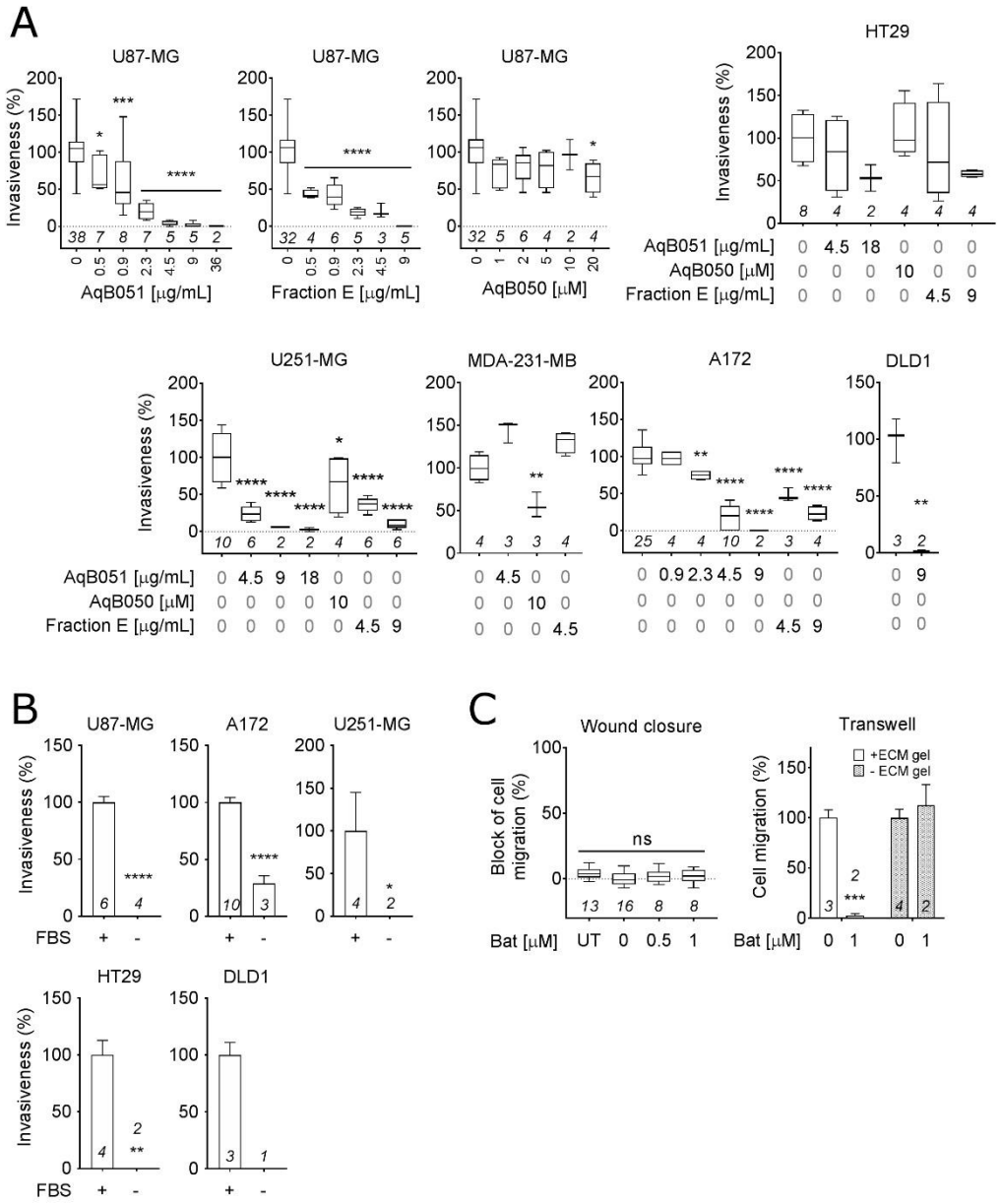

Figure 5.2 Effect of treatments on invasiveness of various cancer cell lines. (A) Box and whisker plots depicting cancer invasiveness as a factor of pharmacological compound treatment and dosage. Trends of block by AqB051 and fraction E were similar; both were strong blockers of invasiveness in all glioblastoma cell lines and DLD1. HT29 and MDA-MB-231 were both insensitive to block of invasion by AqB051 and fraction E. AqB050 inhibited invasion in U87-MG, U251-MG, and MDA-231-MB. (B) Histograms demonstrating the role of the serum (chemotactic) gradient in the transwell assays. All cell lines exhibited dramatically augmented invasiveness in the presence of a chemotactic gradient, suggesting the invasion assay was also a measure of chemotaxis. (C) Graphs depicting the effect of broad

spectrum MMP inhibitor, batimastat, on A172 two-dimensional wound closure, invasion through an uncoated transwell membrane, and invasion through and ECM-coated transwell membrane. Batimastat was only able to significantly reduce cell motility when the ECM barrier was present, suggesting that the invasion assay used here sufficiently measures ECM degrading ability and invasiveness.

5.5.3 AqB051 and fraction E inhibit chemokine-activated invasiveness

Cells activate MMPs to penetrate the ECM-coated transwell membrane. The effect of treatments on A172 invasiveness was tested in the absence of ECM to rule out pharmacological inhibition of MMP activity as a major mechanism of action (Fig 5.3A). Compared to vehicle, treatment with fraction E (9 μg/mL) impaired invasion to 44 ± 13%; AqB051 (9 μg/mL) impaired invasion to 9.9 ± 7.2%; AqB050 was ineffective (Fig 5.3B). The presence of FBS was required for transwell migration (Fig 5.3C). The fluorometric MMP activity assay was used to confirm effects of treatments on MMP activity. Batimastat was used as a positive control, and did not affect MMP activity as compared to untreated or vehicle. AqB051 increased MMP activity compared to untreated and batimastat (Fig 5.3D). These results suggest that AqB051 and fraction E did not inhibit invasiveness by inhibition of MMP activity. Instead, AqB051 and fraction E might impede invasiveness via inhibition of chemotactic receptors or stimuli.

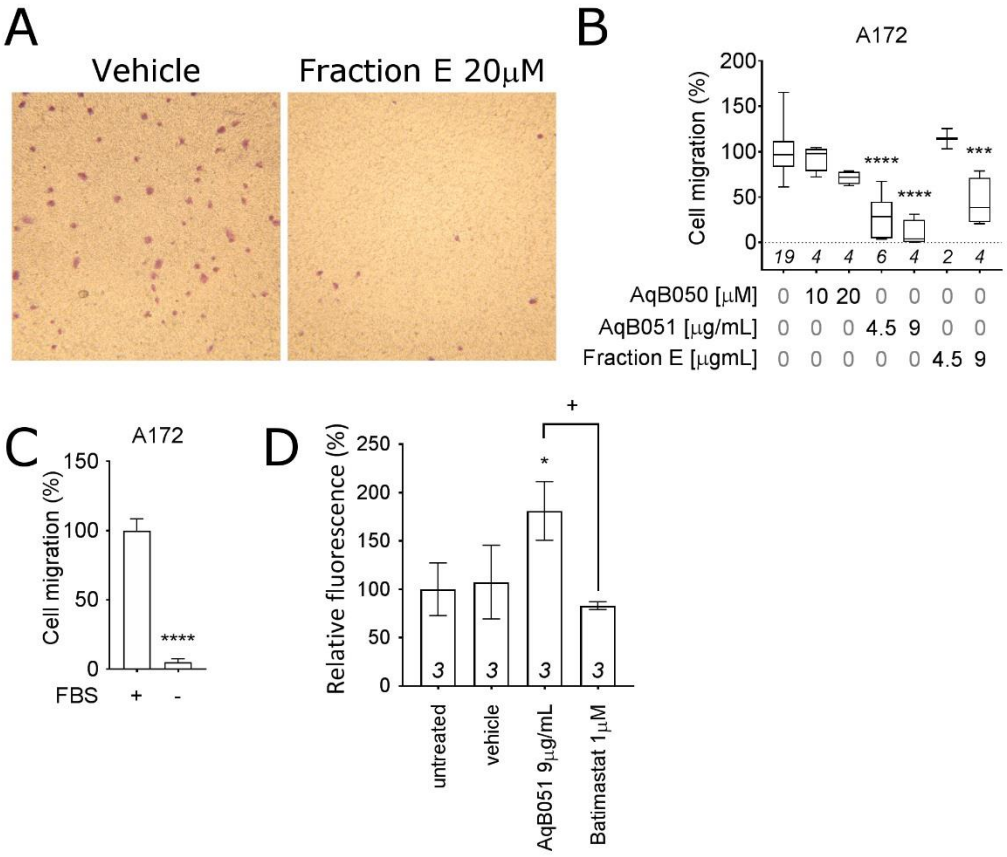

Figure 5.3 Anti-invasive effect of AqB051 and fraction E is not due to inhibition of ECM degradation. (A) Images depicting the number of invasive cells on the underside of the transwell membrane following treatment with vehicle or fraction E (20μM). (B) Box and whisker plot showing percentage cell migration across the transwell membrane (compared to vehicle) as a function of pharmacological compound treatments and doses. AqB051 and fraction E both inhibit A172 cell migration across the uncoated transwell membrane. AqB050 has no significant effect. (C) Histogram depicting cell migration across the uncoated membrane in the presence or absence of a chemotactic gradient; cells cannot sufficiently migrate in the absence of a chemotactic gradient. (D) Histogram representing normalised fluorescence intensity (relative to untreated) directly proportional to MMP activity. None of the treatments significantly reduce MMP activity as compared to untreated, however batimastat treatment significantly reduced MMP activity as compared to AqB051, suggesting AqB051 does not impede MMP activity.

5.5.4 AqB051 inhibits endothelial tube formation

We investigated whether AqB051 inhibited angiogenesis with the endothelial tube formation assay (Fig 5.4A). AqB051 (36 μg/mL) clearly inhibited HUVEC tube formation (2 ± 1 tubes) as compared to vehicle (39 ± 8 tubes) (Fig 5.4B). AqB051 (≤18 μg/mL) had no effect on tubule formation (Fig 5.4B). Many chemotactic factors also stimulate angiogenesis [40-42]. Further investigation might involve testing the hypothesis that AqB051 inhibits one or more angiogenic factors or receptors with dual roles in chemotaxis.

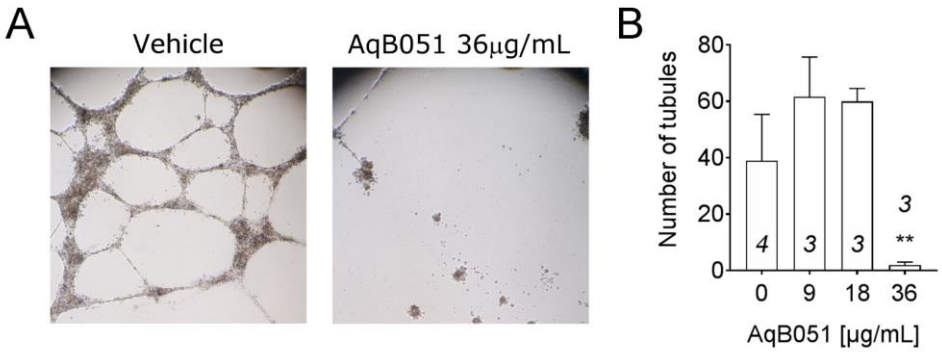

Figure 5.4 AqB051 inhibits endothelial tube formation. (A) Images representing endothelial tube formation in HUVECs treated with vehicle and AqB051 (36μg/mL). (B) Histogram depicting mean number of tubules formed in each treatment tested. AqB051 significantly inhibited tube formation at 36μg/mL concentration.

5.5.5 AqB051 and Fraction E were non-toxic at effective doses

AqB050-, AqB051-, and fraction E-mediated impairment of cell migration and invasion did not result indirectly from reduced cell viability, as measured with alamarBlue. Data were standardised to results for untreated groups in each cell line (Fig 5.5). AqB051 and fraction E were not cytotoxic; treatment with AqB050 did not reduce cell viability in any cell lines except A172. A172 cells treated with AqB050 (20μM) showed 50 ± 3.4% cell viability as referenced to untreated.

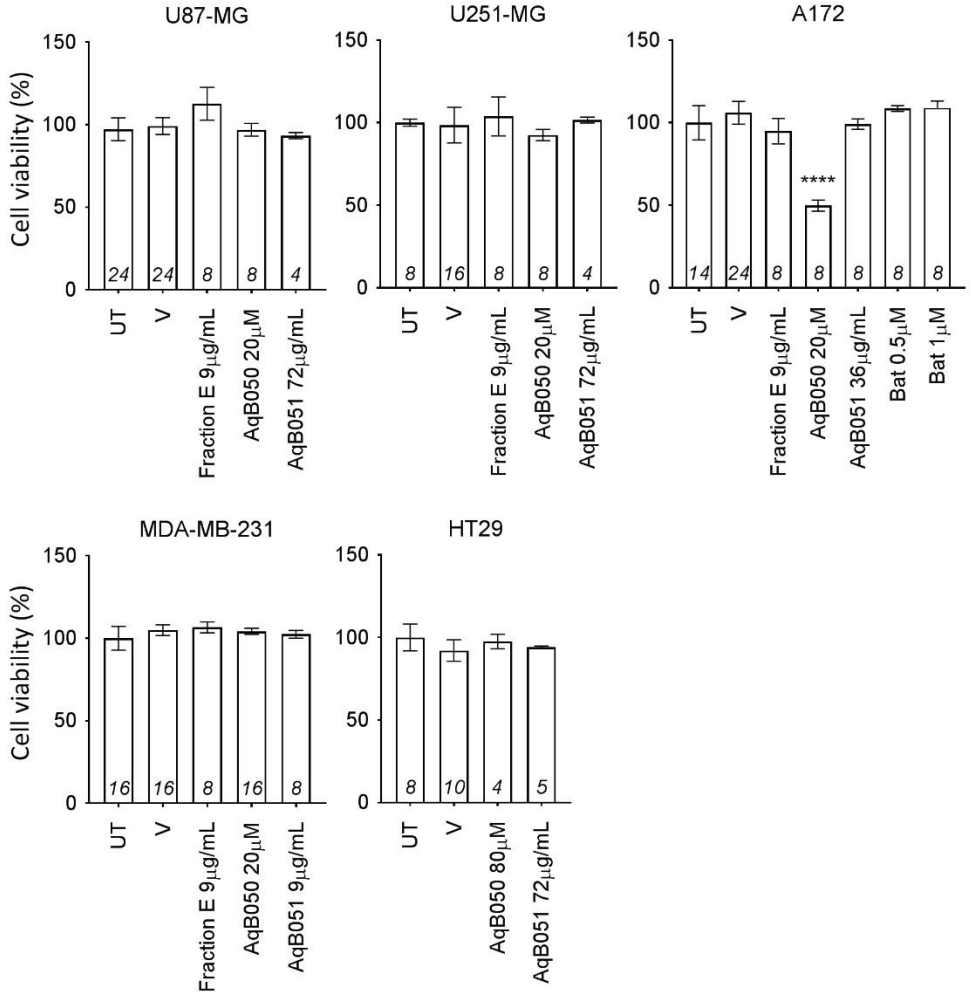

Fig 5.5. Histograms showing pharmacological compound effects on cell viability in each cell line (cells treated with mitotic inhibitor), as determined by alamarBlue. AqB051 and fraction E had no effect on cell viability as compared to untreated in each cell line. AqB050 was non-toxic in all cell lines except A172.

5.5.6 Effect of AqB051, fraction E, and AqB050 on cancer cell growth

Many chemotactic factors also stimulate cell growth [40-42]. In the absence of a mitotic inhibitor, we measured effects of AqB051, fraction E, and AqB050 on U87-MG cell proliferation using the alamarBlue assay. Readings were taken at 0 and 48 hours, and proliferation was measured in the presence (Fig 5.6A) and absence (Fig 5.6B) of FBS; cell proliferation rate was normalised to the vehicle control of the corresponding timepoint (0 or 48 hours). In the absence of FBS, fraction E (9 μg/mL) potentiated growth from 99 ± 5.4% of vehicle (0 hours), to 118 ± 2.2% of vehicle (48 hours); AqB050 (20μM) decreased growth from 140 ± 8.2% of vehicle (0 hours) to 50.9 ± 1.6% of vehicle (48 hours); AqB051 (9 μg/mL) decreased growth from 113 ± 4.6% of vehicle (0 hours) to 85 ± 2.1% of vehicle (48 hours). In the presence of FBS (2%), fraction E and AqB051 had no effect on cell growth; AqB050 (20μM) inhibited cell growth from 122 ± 7.7% of vehicle (0 hours) to 51 ± 3.2% of vehicle (48 hours). Thus, fraction E does not inhibit cell proliferation. AqB050 strongly inhibits proliferation and might account for the inhibitory effect of AqB051 in the absence of FBS.

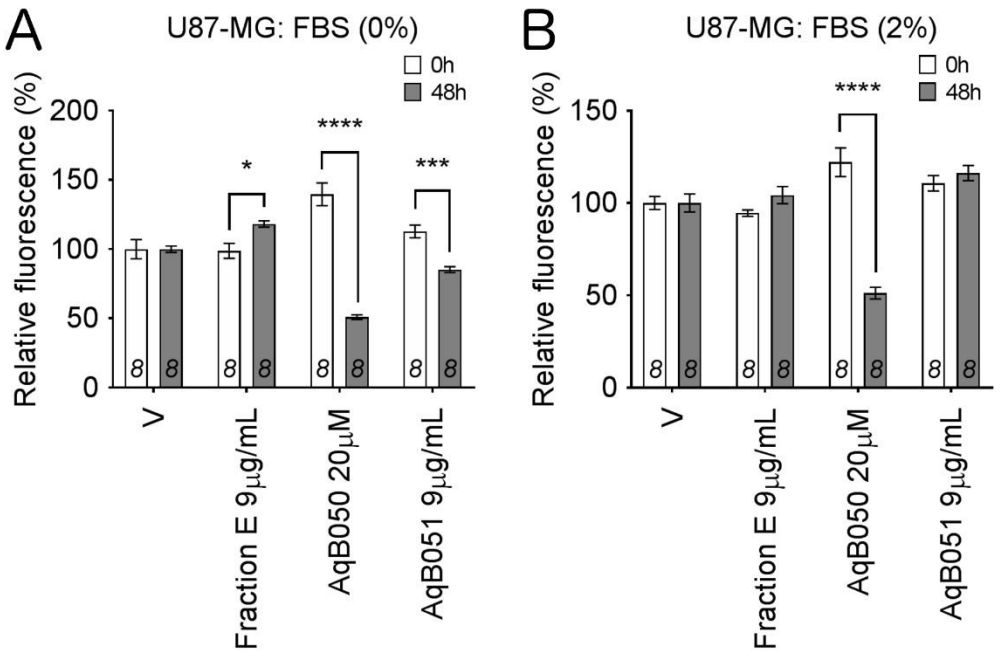

Figure 5.6 Histograms depicting fluorescence intensity (normalised to untreated; as determined by alamarBlue) that is directly proportional to U87-MG cell number, as a function of treatment. (A) Cells were incubated without serum over 48 hours. Fraction E significantly potentiated cell growth in the absence of serum; AqB050 and AqB051 significantly inhibited cell growth. (B) Cells incubated with 2% FBS for 48 hours. AqB050 significantly inhibits U87-MG cell proliferation in the presence of serum; no other treatments have any effect.

5.6 Discussion

The highly invasive phenotype of GBM cells enables them to evade localised therapies such as surgical resection and radiotherapy. Additionally, invasive GBM cells exhibit lower proliferation rate and higher apoptotic resistance, making them more resistant to chemotherapy [43]. Despite progress in the development of new molecular markers for GBM, the overall survival of responsive patients has only minimally improved in the past 20 years [44], and there is great need for an anti-invasive therapy in GBM. In the present study, we introduce a novel pharmacological agent (fraction E), which is a potent blocker of GBM invasiveness *in vitro*. We also show that proposed AQP1 inhibitor, AqB050 [45], inhibits brain, colon, and breast cancer migration, invasion, and growth.

From all the fractions of AqB051 tested, fraction E exhibited pharmacological characteristics most similar to those of AqB051. In all GBM cell lines, ≥75% block of invasiveness was observed for cells treated with fraction E (9 μg/mL), and ≥94% block of invasiveness was observed for AqB051 (9 μg/mL). Other fractions were ineffective (data not shown), so fraction E likely contained the anti-invasive compound from AqB051. AQP1-expressing cell lines MDA-231-MB, U87-MG, and U251-MG were sensitive to block of invasion by AqB050 (see figure 3.2, chapter 3) [46]. It is reasonable to propose that the AqB050-mediated component of block of invasiveness occurs at least in part via AQP1 inhibition [14]. Interestingly, fraction E was less potent than AqB051 in blocking invasion of U251-MG and A172 cells. This might have been due to the presence of AqB050 in the AqB051 mixture, producing an additive block in these cell lines.

GBM cell invasiveness was highly sensitive to AqB051 at doses that had a very low or no effect on GBM wound closure capacity. In all GBM cell lines and the DLD1 cell line, ≥94% block of invasiveness was observed for AqB051 9 μg/mL. This same dose had no effect on U251-MG and A172 wound closure, and only blocked U87-MG wound closure by 18.6 ± 4.6%. This would suggest that the AqB051 mixture is likely to be inhibiting GBM invasion in part via mechanisms that are not necessary for 2D wound closure such as chemotaxis and ECM degradation. The fluorometric MMP activity assay tested the effect of the pharmacological

compounds on ECM degrading proteases. AqB051 enhanced MMP activity compared to batimastat (positive control), but batimastat did not inhibit MMP activity compared to vehicle, suggesting a false negative result. The fluorometric reagent produced high background fluorescence (data not shown), which might have reduced precision of the measurement. This was a limitation of the study as the result was inconclusive. Nevertheless, we determined that the mechanism of action of the target compound in fraction E was unlikely to involve modulation of adhesion to, or degradation of adjacent ECM fibres, as glioblastoma invasiveness was still heavily constrained by AqB051 and fraction E in the absence of the ECM layer. Instead, the unknown target compound in fraction E might inhibit chemotactic machinery.

AqB051 significantly inhibited endothelial tube formation in HUVECs. Many ligands that stimulate chemotaxis in cancer have also been linked with angiogenesis, including epidermal growth factor (EGF), vascular endothelial growth factor (VEGF), transforming growth factor alpha (TGFα), transforming growth factor beta (TGFβ) and fibroblast growth factor (FGF) [40-42]. Therefore, future studies might involve testing the hypothesis that the target compound in AqB051 and fraction E reduces cancer invasiveness via block of one of the above dual chemotactic and angiogenic factors. The high potency of AqB051 in blocking invasion particularly in glioblastoma lines, not in HT29 colon and MDA-231-MB breast cancer lines, indicates other biologically active components in the AqB051 mixture must influence invasion differentially across the diverse cell lines, and suggests potential targeted therapies could be possible.

AqB051 and AqB050, but not fraction E, inhibited GBM proliferation. AQP1 overexpression stimulates lung cancer cell proliferation [47], so the inhibition of AQP1 activity by AqB050 might explain the decrease in GBM proliferation observed following treatment with AqB050 in both serum-treated and serum-free conditions. Moreover, dose-dependent block of cell proliferation by AqB050 was also observed in malignant mesothelioma (MM) cells where ≥20% of the MM population expressed AQP1; AqB050 had no effect when ≤20% of the MM population expressed AQP1, suggesting AQP1 as a target for AqB050 [32].

Fraction E has no effect on cell proliferation or cell viability, suggesting the anti-invasive effects of fraction E are not a result of cytotoxicity or reduced cell growth. Considering fraction E does not inhibit GBM cell proliferation, the inhibition of proliferation by AqB051 observed in the serum free condition might be due to the AqB050 compound present in AqB051. The anti-proliferative effect of AqB051 is nullified in the presence of serum, likely due to the effect of constituent growth factors.

In summary, prognoses for patients with GBM have improved only minimally in the past 20 years [44], largely due to the survival mechanisms of GBM cells that are in the invasive phenotype. We are identifying a novel pharmacological agent (in fraction E of AqB051), which appears to be a potent blocker of GBM invasiveness *in vitro*. We also show that AQP1 inhibitor, AqB050, blocks breast cancer invasiveness, and GBM proliferation. With further investigation, these pharmacological compounds with biological activity could lead to the discovery of an anti-invasive therapy that could augment the effectiveness of currently available treatments.

5.7 References

1. Louis, D.N., et al., *The 2016 World Health Organization classification of tumors of the central nervous system: a summary.* Acta neuropathologica, 2016. **131**(6): p. 803-820.
2. Arora, R.S., et al., *Age–incidence patterns of primary CNS tumors in children, adolescents, and adults in England.* Neuro-oncology, 2009. **11**(4): p. 403-413.
3. Ostrom, Q.T., et al., *CBTRUS statistical report: Primary brain and central nervous system tumors diagnosed in the United States in 2006-2010.* Neuro-oncology, 2013. **15**(suppl_2): p. ii1-ii56.
4. Dobes, M., et al., *Increasing incidence of glioblastoma multiforme and meningioma, and decreasing incidence of Schwannoma (2000–2008): findings of a multicenter Australian study.* Surgical neurology international, 2011. **2**.
5. Stupp, R., et al., *Radiotherapy plus concomitant and adjuvant temozolomide for glioblastoma.* New England Journal of Medicine, 2005. **352**(10): p. 987-996.
6. Koshy, M., et al., *Improved survival time trends for glioblastoma using the SEER 17 population-based registries.* Journal of neuro-oncology, 2012. **107**(1): p. 207-212.
7. Tamimi, A.F. and M. Juweid, *Epidemiology and Outcome of Glioblastoma.* 2017.
8. Nakada, M., et al., *Molecular targets of glioma invasion.* Cellular and Molecular Life Sciences, 2007. **64**(4): p. 458.
9. de Groot, J.F., et al., *Tumor invasion after treatment of glioblastoma with bevacizumab: radiographic and pathologic correlation in humans and mice.* Neuro-oncology, 2010. **12**(3): p. 233-242.
10. Lucio-Eterovic, A.K., Y. Piao, and J.F. de Groot, *Mediators of glioblastoma resistance and invasion during antivascular endothelial growth factor therapy.* Clinical cancer research, 2009. **15**(14): p. 4589-4599.
11. Lamszus, K., P. Kunkel, and M. Westphal, *Invasion as limitation to anti-angiogenic glioma therapy*, in *Local Therapies for Glioma Present Status and Future Developments*. 2003, Springer. p. 169-177.
12. Drappatz, J., A.D. Norden, and P.Y. Wen, *Therapeutic strategies for inhibiting invasion in glioblastoma.* Expert review of neurotherapeutics, 2009. **9**(4): p. 519-534.
13. McCoy, E.S., B.R. Haas, and H. Sontheimer, *Water permeability through aquaporin-4 is regulated by protein kinase C and becomes rate-limiting for glioma invasion.* Neuroscience, 2010. **168**(4): p. 971-981.
14. McCoy, E. and H. Sontheimer, *Expression and function of water channels (aquaporins) in migrating malignant astrocytes.* Glia, 2007. **55**(10): p. 1034-43.
15. Nakano, A., et al., *Matrix metalloproteinases and tissue inhibitors of metalloproteinases in human gliomas.* Journal of neurosurgery, 1995. **83**(2): p. 298-307.
16. Wick, W., M. Platten, and M. Weller, *Glioma cell invasion: regulation of metalloproteinase activity by TGF-β.* Journal of neuro-oncology, 2001. **53**(2): p. 177-185.

17. Lindholm, D., et al., *Transforming growth factor-beta 1 in the rat brain: increase after injury and inhibition of astrocyte proliferation.* The Journal of cell biology, 1992. **117**(2): p. 395-400.
18. Wesolowska, A., et al., *Microglia-derived TGF-β as an important regulator of glioblastoma invasion—an inhibition of TGF-β-dependent effects by shRNA against human TGF-β type II receptor.* Oncogene, 2007. **27**: p. 918.
19. Hau, P., et al., *Inhibition of TGF-β 2 with ap 12009 in recurrent malignant gliomas: from preclinical to phase I/II studies.* Oligonucleotides, 2007. **17**(2): p. 201-212.
20. Bogdahn, U., et al., *Targeted therapy for high-grade glioma with the TGF-β2 inhibitor trabedersen: results of a randomized and controlled phase IIb study.* Neuro-oncology, 2011. **13**(1): p. 132-142.
21. Mellinghoff, I.K., et al., *Molecular determinants of the response of glioblastomas to EGFR kinase inhibitors.* New England Journal of Medicine, 2005. **353**(19): p. 2012-2024.
22. Rich, J.N., et al., *Phase II trial of gefitinib in recurrent glioblastoma.* Journal of Clinical Oncology, 2004. **22**(1): p. 133-142.
23. Prados, M., et al., *33 Phase I study of OSI-774 alone or with temozolomide in patients with malignant glioma.* EJC Supplements, 2003. **5**(1): p. S14.
24. Webb, D.J., et al., *FAK–Src signalling through paxillin, ERK and MLCK regulates adhesion disassembly.* Nature cell biology, 2004. **6**(2): p. 154.
25. Angers-Loustau, A., et al., *Src Regulates Actin Dynamics and Invasion of Malignant Glial Cells in Three Dimensions11Alex Pavanel and Franco Di Giovanni Funds for Brain Tumor Research (RF Del Maestro), Canadian Cancer Society and National Cancer Institute of Canada (DR Kaplan), National Cancer Institute of Canada Terry Fox Studentship (A. Angers-Loustau), Canadian Institute for Health Research doctoral research award (TE Werbowetski), Harold Johns and Canadian Cancer Society research scientist award and Canada Research Chair (DR Kaplan), Montreal Neurological Institute Killam Scholarship, and William Feindel Chair in Neuro-Oncology (RF Del Maestro). Note: A. Angers-Loustau was cosupervised by RF Del Maestro and DR Kaplan.* Molecular Cancer Research, 2004. **2**(11): p. 595-605.
26. Lassman, A.B., et al., *Phase 2 trial of dasatinib in target-selected patients with recurrent glioblastoma (RTOG 0627).* Neuro-Oncology, 2015. **17**(7): p. 992-998.
27. Soroceanu, L., T.J. Manning, and H. Sontheimer, *Modulation of glioma cell migration and invasion using Cl− and K+ ion channel blockers.* Journal of Neuroscience, 1999. **19**(14): p. 5942-5954.
28. Hu, J. and A.S. Verkman, *Increased migration and metastatic potential of tumor cells expressing aquaporin water channels.* FASEB J, 2006. **20**(11): p. 1892-4.
29. Kourghi, M., et al., *Fundamental structural and functional properties of Aquaporin ion channels found across the kingdoms of life.* Clinical and Experimental Pharmacology and Physiology, 2018. **45**(4): p. 401-409.
30. Verkman, A. and A.K. Mitra, *Structure and function of aquaporin water channels.* American Journal of Physiology-Renal Physiology, 2000. **278**(1): p. F13-F28.

31. Pulford, E., et al., *The Effect of Aquaporin 1-Inhibition on Vasculogenic Mimicry in Malignant Mesothelioma.* International journal of molecular sciences, 2017. **18**(11): p. 2293.
32. Klebe, S., et al., *Blockade of aquaporin 1 inhibits proliferation, motility, and metastatic potential of mesothelioma in vitro but not in an in vivo model.* Disease markers, 2015. **2015**.
33. De Ieso, M.L. and J.V. Pei, *An Accurate and Cost-Effective Alternative Method for Measuring Cell Migration with the Circular Wound Closure Assay.* Bioscience Reports, 2018.
34. Kam, Y., et al., *A novel circular invasion assay mimics in vivo invasive behavior of cancer cell lines and distinguishes single-cell motility in vitro.* BMC cancer, 2008. **8**(1): p. 198.
35. Shaw, L.M., *Tumor cell invasion assays*, in *Cell Migration*. 2005, Springer. p. 97-105.
36. Palethorpe, H.M., et al., *The Aquaporin 1 Inhibitor Bacopaside II Reduces Endothelial Cell Migration and Tubulogenesis and Induces Apoptosis.* International journal of molecular sciences, 2018. **19**(3): p. 653.
37. Khajah, M.A., et al., *Extracellular alkaline pH leads to increased metastatic potential of estrogen receptor silenced endocrine resistant breast cancer cells.* PLoS One, 2013. **8**(10): p. e76327.
38. Simpson, K.J., et al., *Identification of genes that regulate epithelial cell migration using an siRNA screening approach.* Nature cell biology, 2008. **10**(9): p. 1027-1038.
39. Wolf, K., et al., *Multi-step pericellular proteolysis controls the transition from individual to collective cancer cell invasion.* Nature cell biology, 2007. **9**(8): p. 893-904.
40. Roussos, E.T., J.S. Condeelis, and A. Patsialou, *Chemotaxis in cancer.* Nature Reviews Cancer, 2011. **11**(8): p. 573.
41. Ferrara, N., *VEGF and the quest for tumour angiogenesis factors.* Nature Reviews Cancer, 2002. **2**: p. 795.
42. Folkman, J. and M. Klagsbrun, *Angiogenic factors.* Science, 1987. **235**(4787): p. 442-447.
43. Giese, A., et al., *Cost of migration: invasion of malignant gliomas and implications for treatment.* Journal of clinical oncology, 2003. **21**(8): p. 1624-1636.
44. Wen, P.Y. and S. Kesari, *Malignant gliomas in adults.* New England Journal of Medicine, 2008. **359**(5): p. 492-507.
45. Migliati, E., et al., *Inhibition of aquaporin-1 and aquaporin-4 water permeability by a derivative of the loop diuretic bumetanide acting at an internal pore-occluding binding site.* Mol Pharmacol, 2009. **76**(1): p. 105-12.
46. Pei, J.V., et al., *Differential Inhibition of Water and Ion Channel Activities of Mammalian Aquaporin-1 by Two Structurally Related Bacopaside Compounds Derived from the Medicinal Plant Bacopa monnieri.* Molecular Pharmacology, 2016. **90**(4): p. 496-507.
47. Hoque, M.O., et al., *Aquaporin 1 is overexpressed in lung cancer and stimulates NIH-3T3 cell proliferation and anchorage-independent growth.* Am J Pathol, 2006. **168**(4): p. 1345-1353.

Chapter 6: Thesis General Discussion and Future Considerations

6.1 Thesis main findings and innovative contributions

Aquaporin-1 (AQP1) is an intrinsic protein well known as a pathway for water flux across cell membranes [1], and plays an important role in fluid absorption and secretion in some epithelia, including kidney tubules, choroid plexus and ciliary epithelium of the eye [2]. AQP1 also enhances cell migration and metastasis in a subset of aggressive cancers [3-6]. AQP1 knockdown impairs cancer cell migration *in vitro* [7-9], and increasing AQP1 levels by transfection into deficient lines accelerates cell migration *in vitro* and increases the probability of lung metastases in murine models [4]. AQP1 is also an ion channel [10-12], and the physiological role of AQP1 ion conductance is not yet fully understood. Like AQP1, AQP4 is a pathway for water flux but does not substitute for AQP1 in enabling cell migration, suggesting that the migration-enhancing property of AQP1 relies on more than membrane water permeability [13]. There is a gap in knowledge regarding the exclusive properties of AQP1 that enable its migration-enhancing effect, but both ion and water fluxes appear to be involved [14]. During cell movement, water and ion influxes establish local cell volume changes that enable process extension [14-16]. A testable prediction is that AQP1-facilitated Na^+ flux might contribute to the local osmotic gradient driving concurrent AQP1-mediated water influx at leading edges, leading to cell volume changes that enable process extension and cell migration [14, 17]. Therefore, part of the focus of this thesis was to test two hypotheses: (1) that AQP1 water and ion channels exhibit a coordinated role in AQP1-facilitated cancer cell motility; and (2) that the efficacy of AQP1 inhibitors depends on plasma membrane localisation of AQP1. To test these hypotheses we used a novel inhibitor of AQP1 ion conductance, AqB011 [18]; and the AQP1 water channel inhibitor bacopaside II [19] on AQP1-expressing human cancer cell lines.

For the first time, work presented in this thesis showed that AqB011 inhibited migration and invasion in brain, colon, and breast cancer cells *in vitro*, and that dual pharmacological block of AQP1 water flux and ion conductance enhanced the magnitude of block of cell motility as compared to effects of AqB011 alone. This work suggested a novel role for the AQP1 ion conductance in enabling AQP1-facilitated cell motility, supporting the first hypothesis. Cells expressing AQP1 on

the membrane were more sensitive to block by AQP1 inhibitors than cells with AQP1 localised intracellularly, which supported the second hypothesis. These findings revealed that AQP1 ion conductance is a putative pharmacological target for anti-invasive therapy. Pharmacologically targeting both AQP1 water and ion channels could yield potential for lower dosage requirements to produce an efficient block of cell migration; additionally, side effects might be reduced in cells that do not require both AQP1 water and ion channel properties to function normally. Therapeutically inhibiting AQP1 is unlikely to produce many debilitating side effects *in vivo*. Studies on AQP1-knockout mice, and humans lacking endogenous AQP1 have reported symptoms of defective urine-concentrating function exclusive of any other debilitating abnormalities [20, 21], and the clinical benefits would likely outweigh this side effect. Additionally, determining AQP1 cell membrane localization could be an important screening tool for identifying cancer subtypes likely to respond to AQP1 inhibitors.

Work from this thesis also identified a novel pharmacological modulator of glioblastoma (GBM) invasiveness *in vitro*. AqB050 is a bumetanide derivative that has been described as an AQP1 inhibitor [22]. During the intended re-synthesis of AqB050, an error resulted in the formulation of a mixture of compounds (AqB051) including the target molecule (AqB050) and related derivatives. The AqB051 mixture strongly blocked GBM transwell invasion at doses that had no effect on cell growth or viability. Therefore, the third hypothesis for this thesis was that (3) the biologically active component of the AqB051 mixture inhibits chemokine-dependent GBM invasiveness, independently of interactions with local extracellular matrix. The AqB051 mixture was fractionated into eight constituent mixtures via thin layer chromatography and chemical components in each fraction were characterised using high resolution mass spectrometry (work done by Mass Spectrometry Facility, School of Chemistry, University of Sydney, NSW). Of the eight fractions, AqB050 constituted the majority of one of the lower MW fractions, and a higher MW fraction labelled “fraction E” demonstrated biological activity that was most similar to the effects of the AqB051 mixture. My analyses thus far have revealed that AqB050 reduced invasiveness in GBM and breast cancer cells, and reduced GBM cell proliferation, suggesting AQP1 as a potential target for

treating GBM invasiveness and growth. Moreover, a novel pharmacological compound present in fraction E strongly inhibited chemokine-dependent GBM invasion in multiple GBM cell lines *in vitro*, with and without ECM, in support of the third hypothesis. Current treatment for GBM is mainly focused on removal and destruction of the tumourous cells [23, 24]. Identifying the pharmacological compound with biological activity in fraction E might have potential to be an adjuvant anti-invasive treatment, improving effectiveness of current treatments for GBM.

Finally, work here provided an innovative approach for measuring net 2D cell migration via the wound closure assay, using a circular wound instead of a straight line. This method demonstrated improved reproducibility, precision, and sampling objectivity for measurements of wound sizes as compared to classic scratch assays. Other benefits of the method include simplicity and low cost as compared with commercially available assays for generating circular wounds.

6.2 Future considerations

6.2.1 Role of AQP1 ion conductance in cancer invasion and metastasis

AQP1 ion conductance has been previously reported to be important for fluid regulation in the choroid plexus [25]; and colon cancer cell migration [18]. Work from this thesis revealed a potential coordinated function for AQP1 water and ion conductance in cancer cell migration and invasion, involving synchronised water and ion influx to generate cellular processes on the leading edge of migrating cells. AqB011 inhibited AQP1 ion conductance in Xenopus oocytes [18] and also attenuated 2D wound closure and 3D transwell invasion in colon, breast, and brain cancer. Future work might include investigating pharmacological sensitivity to AqB011 in non-AQP1-expressing cell lines following wild-type AQP1 transfection. The prediction would be that AQP1-trasfected cell lines would be more sensitive to block of migration by AqB011. It would also be intriguing to transfect AQP1-null cancer cell lines with AQP1 constructs that have been mutated so that AQP1 ion conductance is inactivated or activated without affecting water permeability. The structural conformation of cytoplasmic loop D is important for

AQP1 ion channel gating and does not affect water permeability. Site-directed mutagenesis could be carried out using primers designed to introduce selected mutations in the loop D domain that reduce AQP1 ion conductance, such as alanines substituted for two arginines (R159A+R160A); aspartic acid for proline (D158P); or threonine for proline (T157P) [26]. We predict that cancer cells expressing AQP1 R159A+R160A, D158P, or T157P mutants would migrate slower than control cells transfected with wild type AQP1, and would be insensitive to AqB011. Alternatively, mutagenesis could be carried out to introduce selected mutations in the loop D domain that enhance AQP1 ion conductance, such as glycine substituted for proline (G166P) [26]; we would predict that cancer cells expressing this mutant would migrate faster than control cells transfected with wild type AQP1, and would be more sensitive to AqB011.

6.2.2 Targeting AQP1 channels in glioblastoma

AQP1 is upregulated in GBM [27-29] and enhances GBM invasiveness; however pharmacologically targeting AQP1 channels to reduce growth and invasiveness in GBM has not been previously tested. In 9L gliosarcoma cells, simultaneous upregulation of AQP1, lactate dehydrogenase, and cathepsin B is stimulated by increased glucose metabolism at the tumour periphery [30]. It has been proposed that simultaneous upregulation of these proteins enhances invasiveness via acidification and enzymatic degradation of the extracellular matrix; AQP1 might enable this by shuttling water and CO_2 into the extracellular environment, thus promoting a more acidic extracellular space. Work from this thesis showed that AQP1 blockers, bacopaside II and AqB05, inhibited 3D invasion through an ECM barrier in several GBM cell lines, which might be partly explained by inhibition of AQP1-facilitated acidification of the extracellular environment. However, there is still a gap in knowledge as to the mechanisms of action by bacopaside II and AqB050, as these compounds also inhibited cell migration in the absence of ECM. Moreover, AqB011 inhibited GBM cell migration and invasion, and the role of AQP1 ion conductance in GBM cell motility is yet to be determined. Notably, GBM cell migration requires the movement of water and ions at the leading edge [31-33]. Therefore, a testable prediction might be that AQP1 inhibitors work by attenuating the AQP1-facilitated water and ion fluxes at the leading edge of a migrating GBM

cell, which contribute to both extracellular acidification and cell volume changes that enable process extension and cell migration. Future investigation might test the effect of AQP1 inhibitors on acidification of the GBM extracellular environment with the lactate assay [30]. Additionally, a limitation of the work done for this thesis was that AQP1 knockdown studies were inconclusive in colorectal cancer cell line HT29. Further work might also involve performing AQP1 gene transfection or knockdown in GBM cells to determine whether presence or absence of AQP1 affects sensitivity to AQP1 inhibitors.

Interestingly, AqB050 and AqB011 also inhibited GBM cell proliferation, and reduced cell viability at higher doses; these effects might be connected to inhibition of AQP1-facilitated alkalisation of the GBM cell cytoplasm. GBM intracellular environment is more alkaline than normal brain cells [34], and Hayashi and colleagues (2007) proposed that AQP1 maintains 9L gliosarcoma cell viability by regulating intracellular pH levels [30]. As AQP1-facilitated CO_2 efflux might be important for maintaining a favourable alkaline intracellular environment in GBM, it would be intriguing to investigate whether AqB011 or AqB050 also inhibit AQP1-enabled CO_2 transport, which might explain why AqB050 and AqB011 blocked GBM cell proliferation at low doses, and cell viability at higher doses. Transfection of AQP1 cDNA into NIH-3T3 lung cancer cells increased cell proliferation, as determined by the MTT assay [35]. Future work might include investigation into the role of AQP1 in regulating intracellular pH in lung cancer, and whether these cells would also be sensitive to reduced invasiveness and proliferation following treatment with AqB050 or AqB011. Finally, it would be useful to test these inhibitors in murine models of GBM to see if their anti-proliferative and anti-invasive effects translate to beneficial outcomes *in vivo*.

6.2.3 Identification of the biologically active compound in fraction E, and implications for glioblastoma treatment

GBM cells with an invasive phenotype have low rates of proliferation and apoptosis, providing improved resistance to chemotherapy and radiotherapy [36]. An invasive phenotype allows GBM cells to evade surgical resection, making GBM difficult to treat. With the overall survival for patients with GBM improving only

minimally in the past 20 years [37], new anti-invasive therapies in GBM are needed. Refinement and chemical characterisation of the biologically active compound in fraction E could offer insight into a new class of compounds with potent anti-invasive properties in GBM, if proven in animal models *in vivo* and eventually in clinical trials. The pharmacological characteristics and molecular targets of the biologically active compound(s) in AqB051 are not yet known. The AqB051 mixture also strongly inhibited invasiveness in the DLD1 colorectal adenocarcinoma cell line, but not in HT29 colorectal or MDA-231-MB breast cancer cell lines (see Figure 5.2, chapter 5). The variable efficacy of the AqB051 mixture across different cell lines might suggest specific molecular target(s) of the active compound in AqB051, as opposed to many targets likely to have non-specific or unfavourable side effects. Genomic and transcriptomic analyses comparing AqB051-sensitive and -insensitive cell lines could identify classes of molecular targets for further characterisation.

Work in this thesis showed that fraction E and AqB051 more potently inhibited cell migration in the presence of a chemotactic gradient, as opposed to no gradient. This might suggest that fraction E and AqB051 inhibit chemotactic machinery. Although there are many mechanisms involved in the invasiveness of glioma cells [24, 38], chemotaxis plays an important role in enabling directional migration and invasion of the tumour cells into healthy brain tissue [39]. Chemotaxis is mediated by chemokines, chemotactic receptors, growth factors, and growth factor receptors [39]. There are many chemokines and growth factors that have been attributed to enabling GBM chemotaxis and invasiveness, including the stromal cell-derived factor 1, also known as C-X-C motif chemokine 12 [40]; epidermal growth factor [41, 42]; scatter factor, also known as hepatocyte growth factor [43]; transforming growth factor alpha [43]; and fibroblast growth factor 1 [43]. Future work might investigate the effect of down-regulating receptors for these chemotactic factors in GBM cells and testing whether AqB051 or fraction E are still able to inhibit invasiveness. If the inhibitors lose sensitivity in any of the knockdown conditions, it would suggest that the target receptor in that condition might be the pharmacological target for the inhibitor. It would also be interesting to evaluate the effects of AqB051 and fraction E in another assay that tests chemotaxis without

requiring the cells to undergo dynamic cell volume changes to pass through very narrow pores, such as the ibidi μ-Slide Chemotaxis assay (catalogue number 80326) [44]. If the inhibitors were less effective in the μ-Slide chemotaxis assay, it could mean that the enhanced potency of inhibitors in the transwell invasion assay was due to the requirement to traverse narrow very narrow pores, which is not necessary in the wound closure assay. Overall, continued research into the identification and pharmacological properties of the biologically active compound in AqB051 and fraction E is crucial to potentially uncovering new pharmacological therapies and molecular targets for GBM.

6.2.4 Targeting AQP1 channels to regulate angiogenesis

Angiogenesis occurs in cancer when tissue hypoxia stimulates the formation of new vasculature, enabling tumours to better obtain nutrients and metastasize to distant organs [45]. Endothelial cell proliferation, differentiation and migration are crucial for angiogenesis [46]. AQP1 is expressed in peripheral vascular endothelial cells and is upregulated in low oxygen conditions [47, 48]. AQP1 is thought to contribute to angiogenesis by enabling endothelial cell migration [9, 49, 50], so pharmacological inhibition of AQP1-enabled endothelial cell migration might impede angiogenesis in cancer, and consequently restrict cancer growth and metastasis. Acetazolamide inhibited tumour growth and metastasis in mice with Lewis lung carcinoma [51, 52], perhaps as a result of reduced AQP1 expression [53]. Alternatively, this agent is known to be a broad spectrum carbonic anhydrase (CA) inhibitor [54, 55] and might cause effects by inhibition of CA activity, since expression of CA IX has been associated with poor prognosis in nasopharyngeal carcinoma [56], oesophageal and gastric adenocarcinoma [57], breast cancer [58], and lung cancer [59]. Bacopaside II was shown to inhibit angiogenesis and endothelial cell migration *in vitro* [60], which might be due in part to AQP1 water channel inhibition, although bacopaside II is likely to have non-specific effects including induction of cell cycle arrest and apoptosis [61], inhibition of acetylcholinesterase activity, or reduction of intracellular oxidative stress [62]. Future studies might use AqB011 to investigate the effects of AQP1 ion conductance on endothelial cell migration and angiogenesis. If endothelial cells

express AQP1 on the membrane, a prediction would be that AqB011 inhibits angiogenesis by restricting endothelial cell migration.

6.2.5 AQP1 pharmacological modulators for the treatment of non-neoplastic pathologies

In addition to cancer invasion and metastasis, AQP1 has been implicated in several other pathologies. For example, AQP1 modulators might be useful for the treatment of elevated intracranial pressure (ICP). Elevated ICP is a potentially lethal condition that occurs following stroke or traumatic brain injury, and is largely due to fluid build-up within the brain, also known as cerebral oedema [63, 64]. AQP1-null mice exhibited significantly reduced ICP following acute brain trauma as compared to wild type mice. This was largely due to reduced central venous pressure (CVP), as AQP1-null mice are unable to concentrate their urine, so more fluid is excreted [20, 65]. AQP1 is highly expressed in the choroid plexus epithelium [66, 67], and the reduction in ICP was also determined to be due to reduced secretion of cerebrospinal fluid from the choroid plexus in the AQP1-null mice, although to a lesser extent [65]. Thus, AQP1 inhibitors could be useful for the treatment of elevated ICP, although it is important to consider the blood brain barrier as an obstacle for drug bioavailability. Considering the significance of AQP1 ion conductance for fluid regulation in the choroid plexus [25], it would be intriguing to test AqB011 and other AQP1 inhibitors such as AqB050 and Bacopaside II in models that simulate choroid plexus fluid secretion *in vitro*, or models of acute brain injury *in vivo*.

AQP1 inhibitors might also be a useful treatment for reducing non-cerebral oedema. Conditions such as nephrotic syndrome (NS), cirrhosis, and congestive heart failure (CHF) often lead to various forms of oedema that range from low severity such as swollen eyelids and limbs, to higher severity such as pulmonary oedema, increased body weight, and ascites [68-71]. One of the main therapeutic targets for treating these forms of oedema involve restriction of reabsorption of salts in the kidney, resulting in higher water content in the urine [68]. Common pharmacological therapies for oedema include thiazide diuretics, which block the sodium-chloride transporter in the distal convoluted tubules (DCTs) of the kidney, and loop diuretics

that inhibit the sodium-potassium-chloride cotransporter in the ascending limb of the loop of Henle [72]. These agents are generally effective in restricting reabsorption of water and salts in the kidney, however some patients with more advanced conditions are resistant to DCT diuretics or loop diuretics [73]. Thus, there is a need for a combination therapy that can be used with current diuretics. AQP1 is highly expressed in the kidney proximal tubule and descending loop of Henle [74], enabling water reabsorption into the blood. Renal water reabsorption in mice lacking AQP1 was significantly reduced [75] due to dysfunctional proximal tubule water resorption [76], and reduced water permeability in the descending loop of Henle [77]. Therefore, future work might involve testing AQP1 blockers AqB050 or bacopaside II in combination with loop or DCT diuretics in a mouse model to test effects on urinary concentration ability. A prediction would be that combined treatment with the AQP1 inhibitor would cause a stronger reduction in urinary concentration than treatment with a DCT or loop diuretic alone.

Glaucoma is a pathology of the eye in which impaired outflow of aqueous humour leads to elevated intraocular pressure, and eventually blindness [78]. AQP1 is highly expressed in cells of the conventional outflow pathways for aqueous humour such as the trabecular meshwork (TM) and Schlemm's canal endothelial cells [79-81]. AQP1 improves TM cell viability during mechanical strain [82], and facilitates TM-mediated aqueous humour outflow [83]. Additionally, AQP1 is highly expressed in the ocular ciliary epithelium of the eye [80], where it enables secretion of aqueous humour [84]. AQP1 deletion in mice reduces aqueous humour secretion and intraocular pressure, so pharmacological inhibition of AQP1 might treat glaucoma by decreasing secretion of and outflow resistance to aqueous humour, thus reducing intraocular pressure.

AQP1 is expressed in the plasma membrane of dorsal root ganglion (DRG) neurons and nociceptive C-fibres [85-87], contributing to the perception of inflammatory thermal pain and cold pain in part by interaction with $Na_v1.8$ sodium channels [88]. AQP1 also enables DRG axonal growth and regeneration [89], which was proposed to be due to AQP1-facilitated plasma membrane extension of the DRG axons. Thus,

AQP1 might be a novel pharmacological target for treatment of inflammatory pain, or to accelerate neural regeneration.

In addition to investigating the effects of AQP1 antagonists, there is also benefit in searching for agonists of AQP1 that enhance osmotic membrane water permeability. For example, AQP1 agonists might be able to enhance the efficacy of peritoneal dialysis (PD) for patients with end-stage renal disease. The ability for water to traverse the peritoneal membrane via osmosis is a crucial predictor of outcome for patients that require peritoneal dialysis [90]. AQP1 is expressed in the capillary and venule endothelium of the peritoneum [91], and is critical for ultrafiltration and osmotically driven water transport across the peritoneal membrane during PD [92, 93]. AQP1 agonist AqF026 directly and specifically enhanced AQP1-facilitated osmotically driven water transport across the peritoneal membrane in a mouse model [94], so it would be fascinating to investigate the effect of AqF026 in a clinical setting of peritoneal dialysis.

6.3 Thesis Conclusion

This thesis supported the hypotheses that AQP1 ion conductance plays a role in AQP1-facilitated cancer cell motility, that the efficacy of AQP1 inhibitors depends on plasma membrane localisation of AQP1, and that the biologically active component of AqB051 inhibits GBM invasiveness independently of interaction with extracellular matrix. Findings revealed new biological activities for previously described AQP1 inhibitors such as bacopaside II, AqB011, and AqB050, and potentially new pharmacological modulators that potently inhibit GBM invasion. Work here has paved the way for improving methods utilized for measuring cell migration, investigating the role of AQP1 ion conductance and subcellular localisation in cancer migration and growth, and testing the effects of AQP1 modulators in treating glaucoma; cerebral oedema; oedema associated with CHF, cirrhosis, and nephrotic syndrome; pain perception and neuronal regeneration; and end-stage renal disease. Future investigations should utilise the findings produced from this thesis to further explore pharmacological modulators of AQP1 and novel therapeutics for the treatment of invasive and metastatic cancer.

6.4 References

1. Verkman, A. and A.K. Mitra, *Structure and function of aquaporin water channels.* American Journal of Physiology-Renal Physiology, 2000. **278**(1): p. F13-F28.
2. Verkman, A.S., *Aquaporins at a glance.* Journal of cell science, 2011. **124**(13): p. 2107-2112.
3. Papadopoulos, M., S. Saadoun, and A. Verkman, *Aquaporins and cell migration.* Pflug Arch Eur J Phy, 2008. **456**(4): p. 693-700.
4. Hu, J. and A.S. Verkman, *Increased migration and metastatic potential of tumor cells expressing aquaporin water channels.* FASEB J, 2006. **20**(11): p. 1892-4.
5. Verkman, A.S., M. Hara-Chikuma, and M.C. Papadopoulos, *Aquaporins--new players in cancer biology.* J Mol Med (Berl), 2008. **86**(5): p. 523-9.
6. Preston, G.M., et al., *Appearance of water channels in Xenopus oocytes expressing red cell CHIP28 protein.* Science, 1992. **256**(5055): p. 385-387.
7. Hara-Chikuma, M. and A.S. Verkman, *Aquaporin-1 facilitates epithelial cell migration in kidney proximal tubule.* J Am Soc Nephrol, 2006. **17**(1): p. 39-45.
8. Meng, F., et al., *Aqp1 enhances migration of bone marrow mesenchymal stem cells through regulation of FAK and beta-catenin.* Stem Cells Dev, 2014. **23**(1): p. 66-75.
9. Saadoun, S., et al., *Impairment of angiogenesis and cell migration by targeted aquaporin-1 gene disruption.* Nature, 2005. **434**(7034): p. 786-92.
10. Yool, A.J. and E.M. Campbell, *Structure, function and translational relevance of aquaporin dual water and ion channels.* Mol Aspects Med, 2012: p. in press.
11. Yu, J., et al., *Mechanism of gating and ion conductivity of a possible tetrameric pore in aquaporin-1.* Structure, 2006. **14**(9): p. 1411-23.
12. Sui, H., et al., *Structural basis of water-specific transport through the AQP1 water channel.* Nature, 2001. **414**(6866): p. 872-878.
13. McCoy, E. and H. Sontheimer, *Expression and function of water channels (aquaporins) in migrating malignant astrocytes.* Glia, 2007. **55**(10): p. 1034-43.
14. Schwab, A., et al., *Cells move when ions and water flow.* Pflug Arch Eur J Phy, 2007. **453**(4): p. 421-432.
15. Stroka, K.M., et al., *Water permeation drives tumor cell migration in confined microenvironments.* Cell, 2014. **157**(3): p. 611-23.
16. Frede, J., et al., *Ovarian cancer: Ion channel and aquaporin expression as novel targets of clinical potential.* Eur J Cancer. **49**(10): p. 2331-44.
17. Stroka, K.M., et al., *Water permeation drives tumor cell migration in confined microenvironments.* Cell, 2014. **157**(3): p. 611-623.
18. Kourghi, M., et al., *Bumetanide Derivatives AqB007 and AqB011 Selectively Block the Aquaporin-1 Ion Channel Conductance and Slow Cancer Cell Migration.* Molecular Pharmacology, 2016. **89**(1): p. 133-140.
19. Pei, J.V., et al., *Differential Inhibition of Water and Ion Channel Activities of Mammalian Aquaporin-1 by Two Structurally Related Bacopaside Compounds Derived from the Medicinal Plant Bacopa monnieri.* Molecular Pharmacology, 2016. **90**(4): p. 496-507.

20. Ma, T., et al., *Severely impaired urinary concentrating ability in transgenic mice lacking aquaporin-1 water channels.* J Biol Chem, 1998. **273**(8): p. 4296-9.
21. King, L.S., et al., *Defective urinary concentrating ability due to a complete deficiency of aquaporin-1.* New Engl J Med, 2001. **345**(3): p. 175-179.
22. Klebe, S., et al., *Blockade of aquaporin 1 inhibits proliferation, motility, and metastatic potential of mesothelioma in vitro but not in an in vivo model.* Disease markers, 2015. **2015**.
23. Koshy, M., et al., *Improved survival time trends for glioblastoma using the SEER 17 population-based registries.* Journal of neuro-oncology, 2012. **107**(1): p. 207-212.
24. Nakada, M., et al., *Molecular targets of glioma invasion.* Cellular and Molecular Life Sciences, 2007. **64**(4): p. 458.
25. Boassa, D., W.D. Stamer, and A.J. Yool, *Ion channel function of aquaporin-1 natively expressed in choroid plexus.* J Neurosci, 2006. **26**(30): p. 7811-9.
26. Kourghi, M., et al., *Identification of loop D domain amino acids in the human Aquaporin-1 channel involved in activation of the ionic conductance and inhibition by AqB011.* Frontiers in chemistry, 2018. **6**: p. 142.
27. Saadoun, S., et al., *Increased aquaporin 1 water channel expression inhuman brain tumours.* Brit J Cancer, 2002. **87**(6): p. 621-623.
28. Endo, M., et al., *Water channel (aquaporin 1) expression and distribution in mammary carcinomas and glioblastomas.* Microvascular research, 1999. **58**(2): p. 89-98.
29. Oshio, K., et al., *Expression of the aquaporin-1 water channel in human glial tumors.* Neurosurgery, 2005. **56**(2): p. 375-381.
30. Hayashi, Y., et al., *Regulation and function of aquaporin-1 in glioma cells.* Neoplasia, 2007. **9**(9): p. 777-787.
31. Soroceanu, L., T.J. Manning, and H. Sontheimer, *Modulation of glioma cell migration and invasion using Cl− and K+ ion channel blockers.* Journal of Neuroscience, 1999. **19**(14): p. 5942-5954.
32. Sciaccaluga, M., et al., *CXCL12-induced glioblastoma cell migration requires intermediate conductance Ca2+-activated K+ channel activity.* American Journal of Physiology-Cell Physiology, 2010. **299**(1): p. C175-C184.
33. Ding, T., et al., *Role of aquaporin-4 in the regulation of migration and invasion of human glioma cells.* International journal of oncology, 2011. **38**(6): p. 1521-1531.
34. Cadoux-Hudson, T., et al., *Human primary brain tumour metabolism in vivo: a phosphorus magnetic resonance spectroscopy study.* British journal of cancer, 1989. **60**(3): p. 430.
35. Hoque, M.O., et al., *Aquaporin 1 is overexpressed in lung cancer and stimulates NIH-3T3 cell proliferation and anchorage-independent growth.* Am J Pathol, 2006. **168**(4): p. 1345-1353.
36. Giese, A., et al., *Cost of migration: invasion of malignant gliomas and implications for treatment.* Journal of clinical oncology, 2003. **21**(8): p. 1624-1636.
37. Wen, P.Y. and S. Kesari, *Malignant gliomas in adults.* New England Journal of Medicine, 2008. **359**(5): p. 492-507.

38. Giesexs, A. and M. Westphal, *Glioma invasion in the central nervous system.* Neurosurgery, 1996. **39**(2): p. 235-252.
39. Roussos, E.T., J.S. Condeelis, and A. Patsialou, *Chemotaxis in cancer.* Nature Reviews Cancer, 2011. **11**(8): p. 573.
40. Ehtesham, M., et al., *CXCR4 expression mediates glioma cell invasiveness.* Oncogene, 2006. **25**(19): p. 2801.
41. Huang, J., et al., *Transactivation of the epidermal growth factor receptor by formylpeptide receptor exacerbates the malignant behavior of human glioblastoma cells.* Cancer research, 2007. **67**(12): p. 5906-5913.
42. Penar, P.L., et al., *Inhibition of Epidermal Growth Factor Receptor-associated Tyrosine Kinase Blocks Glioblastoma Invasion of the Brain: Experimental Studies.* Neurosurgery, 1997. **40**(1): p. 141-151.
43. Brockmann, M.-A., et al., *Glioblastoma and cerebral microvascular endothelial cell migration in response to tumor-associated growth factors.* Neurosurgery, 2003. **52**(6): p. 1391-1399.
44. Braig, S., et al., *Indirubin derivative 6BIO suppresses metastasis.* Cancer research, 2013.
45. Nishida, N., et al., *Angiogenesis in Cancer.* Vascular Health and Risk Management, 2006. **2**(3): p. 213-219.
46. Clapp, C. and G.M. de la Escalera, *Aquaporin-1: a novel promoter of tumor angiogenesis.* Trends in Endocrinology & Metabolism, 2006. **17**(1): p. 1-2.
47. Abreu-Rodríguez, I., et al., *Functional and transcriptional induction of aquaporin-1 gene by hypoxia; analysis of promoter and role of Hif-1α.* PLoS One, 2011. **6**(12): p. e28385.
48. Nielsen, S., et al., *Distribution of the aquaporin CHIP in secretory and resorptive epithelia and capillary endothelia.* Proceedings of the National Academy of Sciences, 1993. **90**(15): p. 7275-7279.
49. Monzani, E., et al., *AQP1 is not only a water channel: it contributes to cell migration through Lin7/beta-catenin.* PLoS One, 2009. **4**(7): p. e6167.
50. El Hindy, N., et al., *Correlation of aquaporin-1 water channel protein expression with tumor angiogenesis in human astrocytoma.* Anticancer Res, 2013. **33**(2): p. 609-13.
51. Xiang, Y., et al., *Acetazolamide inhibits aquaporin-1 protein expression and angiogenesis.* Acta Pharmacologica Sinica, 2004. **25**: p. 812-816.
52. Xiang, Y., et al., *Acetazolamide suppresses tumor metastasis and related protein expression in mice bearing Lewis lung carcinoma.* Acta pharmacologica Sinica, 2002. **23**(8): p. 745-751.
53. Bin, K. and Z. Shi-Peng, *Acetazolamide inhibits aquaporin-1 expression and colon cancer xenograft tumor growth.* Hepato-gastroenterology, 2011. **58**(110-111): p. 1502-1506.
54. Maren, T.H., E. Mayer, and B. Wadsworth, *Carbonic anhydrase inhibition. I. The pharmacology of diamox 2-acetylamino-1, 3, 4-thiadiazole-5-sulfonamide.* Bulletin of the Johns Hopkins Hospital, 1954. **95**(5): p. 199.
55. Supuran, C.T., *Carbonic anhydrases: novel therapeutic applications for inhibitors and activators.* Nature reviews Drug discovery, 2008. **7**(2): p. 168.
56. Hui, E.P., et al., *Coexpression of hypoxia-inducible factors 1α and 2α, carbonic anhydrase IX, and vascular endothelial growth factor in nasopharyngeal carcinoma and relationship to survival.* Clinical Cancer Research, 2002. **8**(8): p. 2595-2604.

57. Driessen, A., et al., *Expression of carbonic anhydrase IX (CA IX), a hypoxia-related protein, rather than vascular-endothelial growth factor (VEGF), a pro-angiogenic factor, correlates with an extremely poor prognosis in esophageal and gastric adenocarcinomas.* Annals of surgery, 2006. **243**(3): p. 334.
58. Chia, S.K., et al., *Prognostic significance of a novel hypoxia-regulated marker, carbonic anhydrase IX, in invasive breast carcinoma.* Journal of Clinical Oncology, 2001. **19**(16): p. 3660-3668.
59. Giatromanolaki, A., et al., *Expression of hypoxia-inducible carbonic anhydrase-9 relates to angiogenic pathways and independently to poor outcome in non-small cell lung cancer.* Cancer research, 2001. **61**(21): p. 7992-7998.
60. Palethorpe, H.M., et al., *The Aquaporin 1 Inhibitor Bacopaside II Reduces Endothelial Cell Migration and Tubulogenesis and Induces Apoptosis.* International journal of molecular sciences, 2018. **19**(3): p. 653.
61. Smith, E., et al., *The Purified Extract from the Medicinal Plant Bacopa monnieri, Bacopaside II, Inhibits Growth of Colon Cancer Cells In Vitro by Inducing Cell Cycle Arrest and Apoptosis.* Cells, 2018. **7**(7): p. 81.
62. Limpeanchob, N., et al., *Neuroprotective effect of Bacopa monnieri on beta-amyloid-induced cell death in primary cortical culture.* Journal of ethnopharmacology, 2008. **120**(1): p. 112-117.
63. Greve, M.W. and B.J. Zink, *Pathophysiology of traumatic brain injury.* Mount Sinai Journal of Medicine: A Journal of Translational and Personalized Medicine: A Journal of Translational and Personalized Medicine, 2009. **76**(2): p. 97-104.
64. Ropper, A.H., *Brain edema after stroke: clinical syndrome and intracranial pressure.* Archives of neurology, 1984. **41**(1): p. 26-29.
65. Oshio, K., et al., *Reduced cerebrospinal fluid production and intracranial pressure in mice lacking choroid plexus water channel Aquaporin-1.* The FASEB journal, 2005. **19**(1): p. 76-78.
66. Speake, T., L.J. Freeman, and P.D. Brown, *Expression of aquaporin 1 and aquaporin 4 water channels in rat choroid plexus.* Biochimica et Biophysica Acta (BBA)-Biomembranes, 2003. **1609**(1): p. 80-86.
67. Longatti, P., et al., *Choroid plexus and aquaporin-1: a novel explanation of cerebrospinal fluid production.* Pediatric neurosurgery, 2005. **40**(6): p. 277-283.
68. Qavi, A.H., R. Kamal, and R.W. Schrier, *Clinical Use of Diuretics in Heart Failure, Cirrhosis, and Nephrotic Syndrome.* International journal of nephrology, 2015. **2015**: p. 975934-975934.
69. Doucet, A., G. Favre, and G. Deschênes, *Molecular mechanism of edema formation in nephrotic syndrome: therapeutic implications.* Pediatric Nephrology, 2007. **22**(12): p. 1983-1990.
70. Warren, J.V. and E.A. STEAD, *Fluid dynamics in chronic congestive heart failure: an interpretation of the mechanisms producing the edema, increased plasma volume and elevated venous pressure in certain patients with prolonged congestive failure.* Archives of internal medicine, 1944. **73**(2): p. 138-147.
71. Ginès, P., et al., *Management of cirrhosis and ascites.* New England Journal of Medicine, 2004. **350**(16): p. 1646-1654.

72. Aronson, J.K., *Meyler's side effects of drugs: the international encyclopedia of adverse drug reactions and interactions*. 2015: Elsevier.
73. Elwell, R.J., A.P. Spencer, and G. Eisele, *Combined furosemide and human albumin treatment for diuretic-resistant edema.* Annals of Pharmacotherapy, 2003. **37**(5): p. 695-700.
74. Maunsbach, A.B., et al., *Aquaporin-1 water channel expression in human kidney.* Journal of the American Society of Nephrology, 1997. **8**(1): p. 1-14.
75. Ma, T., et al., *Severely impaired urinary concentrating ability in transgenic mice lacking aquaporin-1 water channels.* Journal of Biological Chemistry, 1998. **273**(8): p. 4296-4299.
76. Schnermann, J., et al., *Defective proximal tubular fluid reabsorption in transgenic aquaporin-1 null mice.* Proceedings of the National Academy of Sciences, 1998. **95**(16): p. 9660-9664.
77. Chou, C.-L., et al., *Reduced water permeability and altered ultrastructure in thin descending limb of Henle in aquaporin-1 null mice.* The Journal of clinical investigation, 1999. **103**(4): p. 491-496.
78. Johnstone, M.A. and W.M. Grant, *Pressure-dependent changes in structures of the aqueous outflow system of human and monkey eyes.* American journal of ophthalmology, 1973. **75**(3): p. 365-383.
79. Stamer, W.D., et al., *Cultured human trabecular mesh work cells express aquaporin-1 water channels.* Current eye research, 1995. **14**(12): p. 1095-1100.
80. Stamer, W.D., et al., *Localization of aquaporin CHIP in the human eye: implications in the pathogenesis of glaucoma and other disorders of ocular fluid balance.* Investigative ophthalmology & visual science, 1994. **35**(11): p. 3867-3872.
81. Hamann, S., et al., *Aquaporins in complex tissues: distribution of aquaporins 1–5 in human and rat eye.* American Journal of Physiology-Cell Physiology, 1998. **274**(5): p. C1332-C1345.
82. Baetz, N.W., et al., *Role of aquaporin-1 in trabecular meshwork cell homeostasis during mechanical strain.* Exp Eye Res, 2009. **89**(1): p. 95-100.
83. Stamer, W.D., et al., *Expression of aquaporin-1 in human trabecular meshwork cells: role in resting cell volume.* Investigative ophthalmology & visual science, 2001. **42**(8): p. 1803-1811.
84. Zhang, D., L. Vetrivel, and A. Verkman, *Aquaporin deletion in mice reduces intraocular pressure and aqueous fluid production.* The Journal of general physiology, 2002. **119**(6): p. 561-569.
85. Solenov, E., et al., *Optical measurement of swelling and water transport in spinal cord slices from aquaporin null mice.* Journal of neuroscience methods, 2002. **113**(1): p. 85-90.
86. Oshio, K., et al., *Impaired pain sensation in mice lacking Aquaporin-1 water channels.* Biochemical and biophysical research communications, 2006. **341**(4): p. 1022-1028.
87. Shields, S.D., et al., *Anatomical and functional analysis of aquaporin 1, a water channel in primary afferent neurons.* Pain, 2007. **131**(1-2): p. 8-20.
88. Zhang, H. and A.S. Verkman, *Aquaporin-1 tunes pain perception by interaction with Nav1. 8 Na+ channels in dorsal root ganglion neurons.* Journal of Biological Chemistry, 2010. **285**(8): p. 5896-5906.

89. Zhang, H. and A. Verkman, *Aquaporin-1 water permeability as a novel determinant of axonal regeneration in dorsal root ganglion neurons.* Experimental neurology, 2015. **265**: p. 152-159.
90. Brimble, K.S., et al., *Meta-analysis: peritoneal membrane transport, mortality, and technique failure in peritoneal dialysis.* Journal of the American Society of Nephrology, 2006. **17**(9): p. 2591-2598.
91. Devuyst, O., et al., *Aquaporin-1 and endothelial nitric oxide synthase expression in capillary endothelia of human peritoneum.* American Journal of Physiology-Heart and Circulatory Physiology, 1998. **275**(1): p. H234-H242.
92. Ni, J., et al., *Aquaporin-1 plays an essential role in water permeability and ultrafiltration during peritoneal dialysis.* Kidney Int, 2006. **69**(9): p. 1518-25.
93. Yang, B., et al., *Reduced osmotic water permeability of the peritoneal barrier in aquaporin-1 knockout mice.* American Journal of Physiology-Cell Physiology, 1999. **276**(1): p. C76-C81.
94. Yool, A.J., et al., *AqF026 is a pharmacologic agonist of the water channel aquaporin-1.* J Am Soc Nephrol, 2013. **24**(7): p. 1045-1052.

Appendix I: First-Author Publications as PDFs Arising from This Thesis

frontiers in Chemistry

REVIEW
published: 25 April 2018
doi: 10.3389/fchem.2018.00135

Mechanisms of Aquaporin-Facilitated Cancer Invasion and Metastasis

*Michael L. De Ieso and Andrea J. Yool**

Department of Physiology, Adelaide Medical School, University of Adelaide, Adelaide, SA, Australia

Cancer is a leading cause of death worldwide, and its incidence is rising with numbers expected to increase 70% in the next two decades. The fact that current mainline treatments for cancer patients are accompanied by debilitating side effects prompts a growing demand for new therapies that not only inhibit growth and proliferation of cancer cells, but also control invasion and metastasis. One class of targets gaining international attention is the aquaporins, a family of membrane-spanning water channels with diverse physiological functions and extensive tissue-specific distributions in humans. Aquaporins−1,−2,−3,−4,−5,−8, and−9 have been linked to roles in cancer invasion, and metastasis, but their mechanisms of action remain to be fully defined. Aquaporins are implicated in the metastatic cascade in processes of angiogenesis, cellular dissociation, migration, and invasion. Cancer invasion and metastasis are proposed to be potentiated by aquaporins in boosting tumor angiogenesis, enhancing cell volume regulation, regulating cell-cell and cell-matrix adhesions, interacting with actin cytoskeleton, regulating proteases and extracellular-matrix degrading molecules, contributing to the regulation of epithelial-mesenchymal transitions, and interacting with signaling pathways enabling motility and invasion. Pharmacological modulators of aquaporin channels are being identified and tested for therapeutic potential, including compounds derived from loop diuretics, metal-containing organic compounds, plant natural products, and other small molecules. Further studies on aquaporin-dependent functions in cancer metastasis are needed to define the differential contributions of different classes of aquaporin channels to regulation of fluid balance, cell volume, small solute transport, signal transduction, their possible relevance as rate limiting steps, and potential values as therapeutic targets for invasion and metastasis.

Keywords: aquaporin, cell migration, metastasis, cancer, invasion, pharmacology, drug

OPEN ACCESS

Edited by:
Graça Soveral,
Universidade de Lisboa, Portugal

Reviewed by:
Ali Mobasheri,
University of Surrey, United Kingdom
Miriam Echevarria Irusta,
Universidad de Sevilla, Spain

****Correspondence:***
Andrea J. Yool
andrea.yool@adelaide.edu.au

Specialty section:
This article was submitted to Chemical Biology, a section of the journal Frontiers in Chemistry

Received: *15 February 2018*
Accepted: *09 April 2018*
Published: *25 April 2018*

Citation:
De Ieso ML and Yool AJ (2018) Mechanisms of Aquaporin-Facilitated Cancer Invasion and Metastasis. Front. Chem. 6:135. doi: 10.3389/fchem.2018.00135

INTRODUCTION

Aquaporins

Aquaporins (AQPs) are a family of water channels that also include a subset of classes shown to mediate transport of glycerol, ions, and other molecules (Li and Wang, 2017). The first aquaporin to be cloned, aquaporin-1 (AQP1), was identified in red blood cells and renal proximal tubules (Denker et al., 1988; Preston and Agre, 1991). In the *Xenopus laevis* expression system, introduced AQP1 channels enabled high osmotic water flux across the plasma membrane as compared to non-AQP control oocytes (Preston et al., 1992), explaining the mechanism enabling rapid transmembrane passage of water in certain

types of cells. To date, 15 classes of aquaporin genes have been identified in mammals (AQP0–AQP14), with AQPs 13 and 14 found in older lineages of mammals (Metatheria and Prototheria) (Ishibashi et al., 2009; Finn et al., 2014; Finn and Cerda, 2015). The first 13 aquaporins (AQP0–AQP12) have been divided into categories based on functional properties (Li and Wang, 2017). One comprises the classical aquaporins (AQP0,−1,−2,−4,−5,−6,−8), which were thought initially to transport only water, though some also transport gases, urea, hydrogen peroxide, ammonia, and charged particles (Ehring and Hall, 1988; Preston et al., 1992; Fushimi et al., 1993; Hasegawa et al., 1994; Raina et al., 1995; Ma et al., 1996, 1997a; Chandy et al., 1997; Ishibashi et al., 1997b; Yasui et al., 1999; Anthony et al., 2000; Nakhoul et al., 2001; Bienert et al., 2007; Herrera and Garvin, 2011; Almasalmeh et al., 2014; Rodrigues et al., 2016). A second category consists of the aquaglyceroporins (AQP3,−7,−9, and−10), which are permeable to water and glycerol, with some also exhibiting urea, arsenite, and hydrogen peroxide permeability (Ishibashi et al., 1997a, 1998, 2002; Yang and Verkman, 1997; Liu et al., 2002; Lee et al., 2006; Rojek et al., 2008; Miller et al., 2010; Watanabe et al., 2016). A possible third category consists of AQP11 and AQP12, distantly related paralogs with only 20% homology with other mammalian AQPs (Ishibashi, 2009), which appear to carry both water and glycerol (Yakata et al., 2011; Bjørkskov et al., 2017). The permeability of AQP11 to glycerol could be important for its function in human adipocytes, in which it is natively expressed (Madeira et al., 2014). Aquaporins assemble as homo-tetramers, with monomers ranging 26–34 kDa (Verkman and Mitra, 2000). In most AQPs, each monomer is composed of six transmembrane domains and intracellular amino and carboxyl termini, with highly conserved asparagine-proline-alanine (NPA) motifs in cytoplasmic loop B and in extracellular loop E (Jung et al., 1994). The NPA motifs in loops B and E contribute to a monomeric pore structure that mediates selective, bidirectional, single-file transport of water in the classical aquaporins (Sui et al., 2001), and water and glycerol in aquaglyceroporins (Jensen et al., 2001).

Intracellular signaling processes regulate AQP channels by altering functional activity, intracellular localization, and levels of expression in different cells and tissues. For example, the peptide hormone vasopressin regulates excretion of water in the kidney by augmenting water permeability of collecting duct cells. Vasopressin induces phosphorylation of AQP2 (Hoffert et al., 2006), stimulating the reversible translocation of AQP2 from intracellular vesicles to the apical plasma membrane (Nielsen et al., 1995). Guanosine triphosphate (GTP) stimulates AQP1-induced swelling of secretory vesicles in the exocrine pancreas (Cho et al., 2002), with functional implications in pancreatic exocrine secretions. Additionally, AQP1 ion channel activity is activated by intracellular cGMP (Anthony et al., 2000), and phosphorylation of Y253 in the carboxyl terminal domain regulates responsiveness of AQP1 ion channels to cGMP (Campbell et al., 2012). Given the diverse array of functional properties, mechanisms of regulation, and tissue-specific distributions being discovered for aquaporins, it is not surprising that different classes of aquaporins (AQP-1,−2,−3,−4,−5,−8, and−9) have been implicated specifically in the complex steps associated with cancer invasion and metastasis (**Table 1**), suggesting specialized roles for these channels have been arrogated into the pathological processes.

Cancer Invasion and Metastasis

Cancer is a leading cause of death worldwide, accounting for 8.2 million deaths in 2012 (Ferlay et al., 2015). The incidence of cancer is rising steadily in an aging population, with numbers expected to increase 70% in the next two decades (Ferlay et al., 2015). Current treatments involve chemotherapy, radiation therapy, and surgery (Miller et al., 2016), associated with an array of side effects including nausea (Koeller et al., 2002), impaired fertility and premature menopause (Howard-Anderson et al., 2012; Wasilewski-Masker et al., 2014), painful neuropathy (Gamelin et al., 2002; Rivera and Cianfrocca, 2015), increased risk of cardiovascular disease (Monsuez et al., 2010; Willemse et al., 2013), and loss of bone density (Gralow et al., 2013). Inhibiting proliferation remains the primary focus of cancer treatments, although the predominant cause of death is cancer metastasis (Yamaguchi et al., 2005; Spano et al., 2012). Less devastating cancer therapies might be achievable via a combination of strategies that not only inhibit proliferation, but also control metastasis of tumor cells from their primary site to distant organs (Friedl and Wolf, 2003). Cancer cell migration through the body exploits pathways including blood stream, lymphatic system, and transcoelomic movement across body cavities (Wyckoff et al., 2000; Pepper et al., 2003; Tan et al., 2006). The hierarchical nature of the metastatic cascade suggests it should be vulnerable to intervention at multiple levels including angiogenesis, detachment of cells from the primary tumor, and infiltration of dissociated tumor cells into and out of circulatory pathways via intravasation and extravasation, respectively (**Figure 1**). AQPs that serve as rate-limiting steps in the metastatic cascade should have substantial value as prognostic markers and pharmacological targets for treatments.

ANGIOGENESIS

Both cancer invasion and metastasis are enhanced by angiogenesis. Angiogenesis, activated in response to inadequate oxygen perfusion, triggers extracellular matrix breakdown; endothelial cell proliferation, differentiation, and migration; and recruitment of periendothelial cells (Clapp and de la Escalera, 2006) which form discontinuous layers around vessels and exert developmental and homeostatic control (Njauw et al., 2008). Under physiological conditions, angiogenesis is seen in the proliferative phase of the menstrual cycle (Demir et al., 2010), development of fetal and placental vasculature (Demir et al., 2007), and skeletal muscle following physical activity (Egginton, 2009). In pathological scenarios such as tumorigenesis, tissue hypoxia stimulates the formation of new vasculature, enabling tumors to better obtain nutrients, exchange gases, and excrete waste (Nishida et al., 2006). Folkman et al. (1966) showed that tumors up to 2 mm in diameter could survive via passive diffusion from surrounding tissue; but angiogenesis was essential for support of larger tumors.

TABLE 1 | Key roles of AQPs involved in cancer invasion and metastasis.

AQP	Permeable to:	Key physiological role(s)	Cancer(s) up-regulated	Key role(s) in cancer invasion and metastasis
AQP1	• Water (Preston et al., 1992), monovalent cations (Anthony et al., 2000), CO_2 (Nakhoul et al., 1998), H_2O_2 (Almasalmeh et al., 2014), NO (Herrera et al., 2006), and NH_3 (Nakhoul et al., 2001)	• Water reabsorption in proximal tubule of the kidney for concentrating urine (Ma et al., 1998; Schnermann et al., 1998) • Secretion of aqueous fluid from ciliary epithelium in the eye, and cerebrospinal fluid from the choroid plexus (Zhang et al., 2002; Oshio et al., 2005) • Perception of thermal inflammatory pain and cold-induced pain (Zhang and Verkman, 2010)	Glioma (Saadoun et al., 2002a; El Hindy et al., 2013), mammary carcinoma (Endo et al., 1999), lung adenocarcinoma (Hoque et al., 2006), colorectal carcinoma (Moon et al., 2003), hemangioblastoma (Chen et al., 2006), and multiple myeloma (microvessels) (Vacca et al., 2001)	• Upregulated in response to tumor tissue hypoxia. Enables recruitment of new tumor vasculature by enhancing endothelial cell migration • Polarizes to leading and trailing edge of migrating cell, and enhances tumor cell migration and invasion by enabling rapid membrane protrusion formation via cell volume regulation and interaction with cytoskeletal dynamics • Enhances mesenchymal stem cell migration via FAK and β-catenin pathways • Might contribute to EMT • Possible interaction with ECM-degrading proteases
AQP2	• Water (Fushimi et al., 1993)	• Water reabsorption in collecting duct of the kidney to concentrate urine (Rojek et al., 2006)	Endometrial carcinoma (Zou et al., 2011)	• Enables "traction" for migrating cell by contributing to the regulation and recycling of focal adhesion proteins (e.g., integrin) • Necessary in estradiol-induced invasion and adhesion of endometrial carcinoma cells, through reorganization of F-actin
AQP3	• Water (Echevarria et al., 1994), glycerol, urea (Ishibashi et al., 1994), H_2O_2 (Miller et al., 2010), arsenite (Lee et al., 2006), and NH_3 (Holm et al., 2005)	• Water reabsorption in collecting duct of the kidney to concentrate urine (Ma et al., 2000) • Skin hydration (Ma et al., 2002) • Skin wound healing (Hara-Chikuma and Verkman, 2008a)	Lung cancer (Liu et al., 2007), hepatocellular carcinoma (Guo et al., 2013), gastric cancer (Shen et al., 2010), prostate cancer (Hwang et al., 2012), oesophageal and oral squamous cell carcinoma (Kusayama et al., 2011), colorectal carcinoma (Moon et al., 2003), skin squamous cell carcinoma (Hara-Chikuma and Verkman, 2008b), ovarian cancer (Ji et al., 2008), pancreatic cancer (Direito et al., 2017), and breast cancer (Mobasheri and Barrett-Jolley, 2014)	• Upregulated by EGF, and contributes to EGF-induced EMT and cancer migration • Contributes to chemokine-dependent cancer migration via enabling H_2O_2 influx and its downstream cell signaling • Interacts with ECM-degrading proteases • Might enhance tumor cell migration and invasion via regulation of cell protrusion formation
AQP4	• Water (Hasegawa et al., 1994)	• Water reabsorption in collecting duct of the kidney to concentrate urine (Ma et al., 1997b) • Transport of water into and out of the brain and spinal cord via blood-brain barrier (Manley et al., 2000) • Neuroexcitation (Binder et al., 2006) • Enables astrocyte cell migration following injury (Saadoun et al., 2005b)	Glioma (Saadoun et al., 2002b) and meningioma (Ng et al., 2009)	• Co-localizes with ion channels at leading and trailing edges of migrating cancer cells • Enhances tumor cell migration and invasion by enabling rapid membrane protrusion formation via cell volume regulation and interaction with cytoskeletal dynamics • Might interact with ECM-degrading proteases
AQP5	• Water (Raina et al., 1995) and H_2O_2 (Rodrigues et al., 2016)	• Secretion of saliva (Ma et al., 1999) and airway mucus (Song and Verkman, 2001)	Prostate cancer (Li et al., 2014), chronic myelogenous leukemia (Chae et al., 2008a), colorectal carcinoma (Wang et al., 2012), hepatocellular carcinoma (Guo et al., 2013), lung cancer (Chae et al., 2008b), cervical cancer (Zhang et al., 2012), pancreatic cancer (Direito et al., 2017), and breast cancer (Jung et al., 2011)	• Promotes EMT • Co-localizes with ion channels at leading and trailing edges of migrating cancer cells • Enhances tumor cell migration and invasion by enabling rapid membrane protrusion formation via cell volume regulation • Might interact with EGFR/ERK1/2 signaling pathway
AQP8	• Water, urea (Ma et al., 1997a), H_2O_2 (Bienert et al., 2007), and NH_3 (Holm et al., 2005; Saparov et al., 2007)	• Canalicular bile water secretion (Calamita et al., 2005) • Colonic water reabsorption (Yamamoto et al., 2007)	Cervical cancer (Shi et al., 2012, 2014)	• Not yet known

(Continued)

TABLE 1 | Continued

AQP	Permeable to:	Key physiological role(s)	Cancer(s) up-regulated	Key role(s) in cancer invasion and metastasis
AQP9	• Water, urea (Ishibashi et al., 1998), glycerol (Tsukaguchi et al., 1998), arsenite (Liu et al., 2002), and H_2O_2 (Watanabe et al., 2016)	• Hepatic glycerol uptake and metabolism for glucose production (Kuriyama et al., 2002; Rojek et al., 2007; Maeda et al., 2009) • Route for excretion of arsenic by the liver (Carbrey et al., 2009) and modulates arsenic sensitivity in leukemia (Bhattacharjee et al., 2004; Leung et al., 2007)	Glioblastoma (Fossdal et al., 2012), astrocytoma (Tan et al., 2008), prostate cancer (Chen et al., 2016)	• Overexpression might correspond with reduced EMT and growth in hepatocellular carcinoma • Might interact with ERK1/2 and MMP9 to enhance prostate cancer invasion and migration

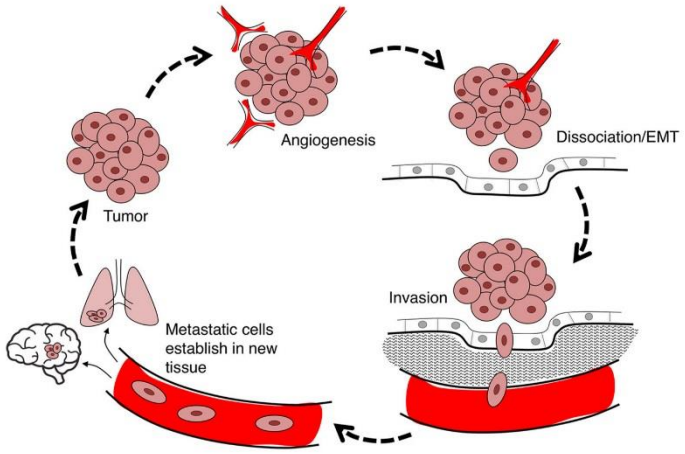

FIGURE 1 | Flow diagram summarizing the steps in cancer metastasis. Metastasis involves the migration of cells from the primary tumor to distant organs. Large tumors with tissue hypoxia rely on angiogenesis for vascular exchange of nutrients and waste. Primary tumor cells undergo phenotypic changes including loss of cell-cell adhesions which enables cells to dissociate from primary tumor, invade the adjacent extracellular matrix (ECM), and intravasate into the blood or lymph systems. Circulating tumor cells extravasate to seed secondary sites at which the process can reoccur.

AQP1, expressed in peripheral vascular endothelial cells, is involved in tumor angiogenesis (Nielsen et al., 1993; Endo et al., 1999; Saadoun et al., 2002a; El Hindy et al., 2013; Verkman et al., 2014). AQP1 knock-down in chick embryo chorioallantoic membrane resulted in a dramatic inhibition of angiogenesis (Camerino et al., 2006). Saadoun et al. (2005a) found AQP1-deficient mice exhibited reduced tumor growth and angiogenesis as compared to wild type, following subcutaneous or intracranial B16F10 melanoma cell implantation. Their work showed AQP1-null endothelial cells from mouse aorta had reduced motility as compared to wild-type, suggesting AQP1 was needed to facilitate cell migration for angiogenesis. Monzani et al. (2009) confirmed a reduced migration capacity in human microvascular endothelial cells (HMEC-1) after AQP1 knockdown by siRNA. AQP1 mRNA and protein levels are increased in response to tissue hypoxia (Kaneko et al., 2008; Abreu-Rodríguez et al., 2011). AQP1 facilitates hypoxia-induced angiogenesis by enhancing endothelial cell migration.

Angiogenesis is regulated by growth factors such as vascular endothelial growth factor (VEGF), which stimulates endothelial cell proliferation and angiogenesis in response to hypoxia (Suzuki et al., 2006), through processes that could augment AQP1 activity indirectly. Pan et al. (2008) found a positive correlation between levels of AQP1 expression, intratumoral microvascular density, and VEGF in endometrial adenocarcinoma. Similarly, AQP1 gene deletion correlated with reduced VEGF receptor expression in mouse primary breast tumor cells (Esteva-Font et al., 2014), and knockdown of AQP1 in human retinal vascular endothelial cells with concurrent inhibition of VEGF caused an additive inhibition of hypoxia-induced angiogenesis (Kaneko et al., 2008). However, application of VEGF-neutralizing antibodies did not alter AQP1 expression (Kaneko et al., 2008), and levels of VEGF in primary breast tumors were not different between AQP1-null

and wild-type mice (Esteva-Font et al., 2014), supporting the idea that VEGF is regulated independently of AQP1 expression or activity.

Other angiogenic factors, such as hypoxia-inducible factor 1-alpha (HIF-1α), induce AQP1 expression in low oxygen conditions (Abreu-Rodríguez et al., 2011). The AQP1 gene promoter carries a HIF-1α binding site which drives AQP1 expression in response to hypoxia in cultured human retinal vascular endothelial cells (HRVECs) (Tanaka et al., 2011), and involves phosphorylation of p38 mitogen-activated protein kinase (MAPK) (Tie et al., 2012). Estrogen signaling also targets the promoter region of the AQP1 gene to increase transcription, inducing enhanced tubulogenesis of vascular endothelial cells as a model for angiogenesis (Zou et al., 2013). In summary, AQP1 is upregulated by angiogenic factors in response to hypoxia, and necessary for endothelial cell migration and angiogenesis. Therapies aimed at blocking transcriptional activation of AQP1 could impede cancer angiogenesis, if the treatment could be spatially limited to the tumor site without impacting normal cell functions.

CELLULAR DISSOCIATION AND EPITHELIAL-MESENCHYMAL TRANSITION

Epithelial-mesenchymal transition (EMT) occurs in normal physiological conditions such as implantation, embryogenesis, and organ development, as well as pathological processes such as cancer invasion and metastasis (Vićovac and Aplin, 1996; Thiery, 2002). During EMT, polarized epithelial cells undergo biochemical changes to adopt a mesenchymal phenotype, characterized by a loss of cell polarity, reduced cell-cell adhesiveness, and enhanced invasive capacity (Thiery, 2002, 2003; Cavallaro and Christofori, 2004; Kalluri and Weinberg, 2009; van Zijl et al., 2011). Epithelial cadherin (E-cadherin), a transmembrane glycoprotein, enables calcium-dependent tight adhesions between epithelial cells and links to cytoskeletal elements (Angst et al., 2001; Alizadeh et al., 2014). Downregulation of E-cadherin is a hallmark feature of EMT (Cano et al., 2000; Chua et al., 2007; Korpal et al., 2008). EMT in cancer is induced by signals from the tumor-associated stroma, including epidermal growth factor (EGF), platelet-derived growth factor (PDGF), hepatocyte-derived growth factor (HGF), and transforming growth factor beta (TGF-β) (Miettinen et al., 1994; Pagan et al., 1999; Lo et al., 2007; Kong et al., 2009; Xu et al., 2009). These signals stimulate transcription factors such as SNAI1 (SNAIL), SNAI2 (SLUG), zinc finger E-box binding homeobox 1 (ZEB1), Mothers against decapentaplegic homolog 2 (SMAD-2) and Twist, which are all E-cadherin transcription repressors (Yang et al., 2004; Medici et al., 2008).

Classes of aquaporins such as AQP3 have been implicated in the EMT process. AQP3 up-regulation in response to EGF in colorectal, gastric, and pancreatic cancers, is associated with augmented cell migration, invasion, and metastasis (Huang et al., 2010; Liu et al., 2012; Li et al., 2013). In gastric cancer, EGF-induced AQP3 upregulation enhances the mesenchymal transformation (Chen et al., 2014). Chen et al. (2014) determined that mRNA and protein levels of vimentin and fibronectin (proteins associated with mesenchymal phenotype) were significantly increased in cells with high levels of AQP3 expression but decreased in AQP3-deficient cells. Conversely, E-cadherin expression was significantly lower in cells with high AQP3 and increased in AQP3-knockdown cells. The mechanisms for AQP3-facilitated pancreatic and colorectal cancer cell migration have not yet been determined. It will be interesting to investigate whether AQP3 promotes EMT in these cancers.

In addition to AQP3, AQPs 1, 4, 5, and 9 also have been linked to EMT in different types of cancer cells. In lung adenocarcinoma cells, AQP1 overexpression correlated with the down-regulation of E-cadherin, and up-regulation of vimentin (Yun et al., 2016). AQP4 knockdown in human breast cancer was associated with increased levels of E-cadherin, and in glioma cells with increased β-catenin (involved in actin reorganization and cell-cell adhesion) and connexin-43 (a gap junction protein that contributes to cell-cell signaling and adhesion) (Ding et al., 2011; Li Y. et al., 2016), suggesting AQP4 might enhance cell detachment from primary tumors. However, opposing evidence showed knockdown of AQP4 in primary human astrocytes correlated with down-regulation of connexin-43 (Nicchia et al., 2005); and transfection of wild type AQP4 into glioma cell lines caused enhanced adhesion (McCoy and Sontheimer, 2007). In primary glial cells, AQP4 expression levels had no appreciable effect on cell-cell adhesion under the conditions tested (Zhang and Verkman, 2008). In human non-small cell lung cancer cells (NSCLCs), AQP5 increased invasiveness; conversely, expression of AQP5 mutant channels lacking membrane targeting signals or the S156 phosphorylation site did not augment invasiveness (Chae et al., 2008b). Overexpression of AQP5 in NSCLCs was associated with a reduction in epithelial cell markers such as E-cadherin, α-catenin, and γ-catenin, and an increase in mesenchymal cell markers such as fibronectin and vimentin, concomitant with a mesenchymal change in morphology. Similarly, AQP3 and AQP5 overexpression in pancreatic ductal adenocarcinoma is accompanied by downregulation of E-cadherin and upregulation of vimentin (Direito et al., 2017). The invasion-promoting properties of AQP5 expression appear to depend on the c-Src signaling pathway, a potent trigger of EMT (Guarino et al., 2007; Chae et al., 2008b). High AQP5 expression correlated with an increase in phosphorylated SMAD2, promoting EMT in colorectal cancer, whereas AQP5 silencing was associated with a down-regulation of phosphorylated SMAD2, and a repressed EMT response (Chen et al., 2017). AQP9 is downregulated in hepatocellular carcinoma; overexpression corresponds to reduced growth and EMT, thus reducing cancer invasion and metastasis (Li C. F et al., 2016; Zhang et al., 2016). Evidence suggests that AQPs have different effects depending on the type of cancer. Moreover, the state of cancer progression, environmental factors, and the types of assays used will be complicating factors; nevertheless, AQPs have clear potential as diagnostic and prognostic

biomarkers, and as therapeutic targets for modulation of EMT, cell-cell adhesion, and dissociation phases of cancer progression.

INVASION AND CELL MIGRATION

Cell migration involves the translocation of individual and collective groups of cells through fluid or tissues, relevant for survival in multicellular and single-celled organisms (Klausen et al., 2003; Friedl et al., 2004). Migration enables physiological morphogenesis, immunity, and tissue repair (Friedl et al., 2004; Friedl and Weigelin, 2008). In most mammalian cells, migration is highest during development and morphogenesis and decreases after terminal differentiation. In pathological circumstances such as cancer, migration machinery can be reactivated. AQPs−1,−3,−4, and−5,−8, and−9 are known to contribute to cancer cell migration and invasion. Translocation of cancer cells can be initiated by chemokines released from host tissues, and growth factors such as EGF secreted by stromal cells (Dittmar et al., 2008; Roussos et al., 2011).

AQP3 has been suggested to increase EGF-induced cancer growth and migration by mediating H_2O_2 flux (Miller et al., 2010; Hara-Chikuma et al., 2016). H_2O_2 is known as an oxidative stressor, but is also a second messenger in cell proliferation, differentiation and migration (Thannickal and Fanburg, 2000; Rhee, 2006). AQP3 knockdown in skin and lung cancer cell lines reduced EGF-induced H_2O_2 influx, and attenuated EGF signaling cascades (Hara-Chikuma et al., 2016), reducing migration and growth. H_2O_2 also influenced chemokine-dependent migration of T-cells and breast cancer cells (Hara-Chikuma et al., 2012; Satooka and Hara-Chikuma, 2016). AQP1,−3,−5,−8, and−9 have all been suggested to transport H_2O_2 (Bienert et al., 2007; Miller et al., 2010; Almasalmeh et al., 2014; Rodrigues et al., 2016; Watanabe et al., 2016). All of these classes also have been linked with cancer cell migration (Hu and Verkman, 2006; Shi et al., 2013; Li et al., 2014; Chen et al., 2015; Zhang et al., 2016); however, H_2O_2 transport has thus far been linked only to AQP3 as a control mechanism in cancer cell migration. Further work might show H_2O_2 transport in other classes of AQPs regulates cell motility and invasion.

Polarization

Key molecular and cellular events involved in cell migration can be classified into five inter-dependent stages, which are polarization, protrusion, cell-matrix adhesion, extracellular matrix (ECM) degradation and retraction (**Figure 2**). Cell polarization provides functionally specialized domains in the membrane and cytoplasm (Drubin and Nelson, 1996), typified by asymmetric distributions of organelles, signaling mechanisms, and membrane channels, transporters and receptors (Swaney et al., 2010). In movement, changes in cell polarization generate leading and trailing edges, predominantly regulated by small GTPases such as CDC42 (Johnson and Pringle, 1990; Allen et al., 1998), which controls the recruitment of partitioning-defective (PAR) proteins, atypical protein kinase C (aPKC), and actin polymerization machinery (Etienne-Manneville and Hall, 2003; Goldstein and Macara, 2007). AQPs−1,−4,−5, and−9 have been shown to show polarized localization at the leading edges of migrating cells. Specific co-distributions with ion transporters such as the Na^+/H^+ exchanger, the Cl^-/HCO_3^- exchanger, and the Na^+/-HCO_3 co-transporter, suggest sophisticated mechanisms for regulation of fluid influx and efflux (Loitto et al., 2002; Verkman, 2005; Hara-Chikuma and Verkman, 2006; Papadopoulos et al., 2008; Stroka et al., 2014), potentially driving membrane protrusions for cell locomotion (Schwab et al., 2007).

Protrusion

A migrating cell extends its leading edge into the ECM by assembling a branched network of intracellular actin filaments, predicted to yield a physical force that dynamically pushes the membrane out, alternating with relaxation and actin depolymerization (Wang, 1985; Theriot and Mitchison, 1991; Pollard and Borisy, 2003). Membrane expansion requires the vesicle fusion to support the increase in surface area (Bretscher and Aguado-Velasco, 1998; Pierini et al., 2000; Fletcher and Rappoport, 2010). Three types of protrusions found in motile cells are lamellipodia, filopodia, and invadopodia. Lamellipodia are broad, flat, actin-rich protrusions that extend in the direction of locomotion and provide a foundation on which the cell moves forward (Cramer et al., 1997). Filopodia are long, thin protrusions of the membrane thought to be exploratory, "sensing" the local environment (Mattila and Lappalainen, 2008). Lamellipodial and filopodial formations are modulated by small GTPases in the Rho family, such as Rac1 and CDC42 (Ridley et al., 1992; Allen et al., 1997; Hall, 1998; Machesky, 2008), which stimulate actin polymerization in response to growth factor (Hall, 1998) and integrin receptor activations (Price et al., 1998). Interestingly, AQP9-facilitated water flux appears to critical for filopodial protrusion formation in fibroblasts, via the CDC42 pathway (Loitto et al., 2007). The Arp2/3 (actin-related protein 2/3) complex regulates the formation of new actin filaments in migrating cancer cells, and is regulated by Scar/WAVE complex (otherwise known as WANP), which interacts with the small GTPase Rac1 for lamellipodial assembly (Ibarra et al., 2005). Invadopodia are actin-rich, matrix-degrading protrusions that appear when ECM degradation and cell adhesion are needed to create space for movement, involving proteases such as MMP2, MMP9, and MT1-MMP and src tyrosine kinase (Weaver, 2006). Changes in cell volume during protrusion are assumed to require rapid water flow (Condeelis, 1993), and could occur in part in response to osmotic gradients governed by ion transport and actin polymerization state (Diez et al., 2005; Disanza et al., 2005; Schwab et al., 2007).

AQPs at the leading edges of migrating cells are well positioned to facilitate cell volume changes and cytoskeletal modifications during protrusion formation (Monzani et al., 2009; Jiang and Jiang, 2010; Klebe et al., 2015; Wei and Dong, 2015; Pelagalli et al., 2016). AQP1 overexpression in B16F10 melanoma cells and 4T1 mammary gland tumor cells enhanced cell migration and lamellipodial width *in vitro*, and augmented metastasis in a mouse model (Hu and Verkman, 2006). AQP1 is proposed to enhance lamellipodial formation by increasing membrane osmotic water permeability (Verkman, 2005; Hu

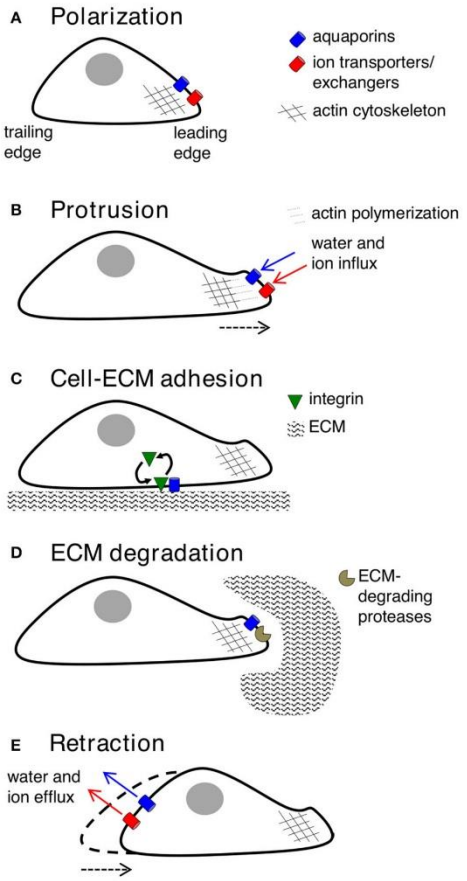

FIGURE 2 | Key contributions of aquaporins in cell migration. **(A)** Forward movement is preceded by establishing specialized loci within the cell, with redistribution of aquaporins, ion transporters/exchangers, and actin polymerization machinery to the leading edge. AQP-1,−4,−5, or−9 can be found on leading edges of migrating cancer cells. **(B)** Protrusions of the membrane might use water influx (down an osmotic gradient established by ion transporters/exchangers) and actin polymerization beneath the plasma membrane to dynamically push the membrane forward. AQP-1,−4, and−5 are implicated in water influx for protrusion extension in cancer cells; AQPs-1 and−4 also appear to interact with actin cytoskeleton. **(C)** Protrusions adhere to the ECM using integrin to generate "traction" for cellular movement. AQP2 might modulate turnover of integrin at adhesion sites, enabling forward cellular movement. **(D)** ECM degradation by enzymes can widen gaps through which the cell body can penetrate. AQP-1,−3,−4 and−9 are suggested to interact with ECM-degrading enzymes. **(E)** The final step is retraction of the cell trailing edge, thought to use aquaporins for water efflux following by K^+ export.

and Verkman, 2006; Jiang, 2009), allowing water entry at the leading edge to impose hydrostatic pressure, drive membrane extension, and create space for actin polymerization. In addition to water channel activity, AQP1 is also thought to be an ion channel, proposed to allow gated conduction of monovalent cations through the central tetrameric pore (Anthony et al., 2000; Yu et al., 2006). The dual water and ion conductance of AQP1 is essential for colon cancer cell migration *in vitro* (Kourghi et al., 2015). Conversely, in clinical cases of cholangiocarcinoma, high AQP1 expression has been correlated with low metastasis (Aishima et al., 2007; Sekine et al., 2016), suggesting that AQP1 might play different roles in different types of cancers.

Other classes of AQP water channels are not necessarily interchangeable with AQP1 in facilitating cell migration (McCoy and Sontheimer, 2007), suggesting features of AQP1 other than simple osmotic water permeability are involved. AQP1-enhanced cell migration might also be due to interactions with cytoskeletal proteins. For example, Monzani et al. (2009) demonstrated that AQP1 knockdown dramatically impeded actin cytoskeletal organization in migrating human melanoma and endothelial cell lines via interaction with Lin-7/β-catenin. The Lin-7/β-catenin complex enables asymmetrical organization of filamentous actin (F-actin). AQP1 might act as a scaffolding protein at the leading edges. Jiang (2009) found that knocking down AQP1 was associated with re-localization of actin in migrating HT20 colon cancer cells, and a reduction in the activity of actin regulatory factors RhoA and Rac. A PDZ domain in Lin-7 could mediate interaction with rhotekin protein, which inhibits Rho GTPase signaling that is involved in cell migration, invasion, and cytoskeletal reorganization (Sudo et al., 2006). Rhotekin merits further evaluation in models of AQP1-dependent cytoskeletal organization.

A role for AQP4 in glioma cell migration has similarly been proposed to occur through regulation of cell volume and cytoskeletal interactions. Protein kinase C (PKC)-mediated phosphorylation of AQP4 at serine 180 correlated with a decreased glioma cell invasion (McCoy et al., 2010). AQP4-facilitated glioma invasion is dependent on co-expression of chloride channels (ClC2) and the potassium-chloride co-transporter 1 (KCC1) in invadopodia, which could provide the ionic driving force for water efflux leading to cell shrinkage that could augment invasiveness through ECM (Mcferrin and Sontheimer, 2006; McCoy et al., 2010). AQP4 effects on actin cytoskeleton suggest a role for α-syntrophin, interacting with the C-terminal domain of AQP4 at a PDZ-binding site (Neely et al., 2001). In human glioma and primary astrocytes, reduced AQP4 expression correlated with dramatic morphological elongation, reduced invasiveness, and impaired F-actin polymerization (Nicchia et al., 2005; Ding et al., 2011).

AQP5 facilitates protrusion formation, volume regulation, cell migration, and metastasis. AQP5 expression is correlated with cell invasiveness and metastasis of human prostate cancer (Li et al., 2014), lymph node metastasis in patients with colon cancer (Kang et al., 2015), and metastatic potential of lung cancer cells (Zhang et al., 2010). Moreover, Jung et al. (2011) showed that a shRNA-induced reduction in AQP5 expression in MCF7 breast cancer cells was associated with significantly reduced cell proliferation and migration. The mechanism of AQP5-facilitated cancer cell invasion and metastasis might be due to its direct or indirect interaction with the epidermal growth factor receptor/extracellular signal-regulated kinase (ERK1/2)

pathway (Kang et al., 2008; Zhang et al., 2010), known to be important in cancer metastasis and aggressiveness (Vicent et al., 2004). Additionally, AQP5 mediates lung cancer cell membrane osmotic water permeability, and has been suggested to contribute to cancer cell migration and invasion by enabling rapid cell volume regulation and subsequent protrusion formation (Chen et al., 2011). The complementary role of ion transport for migration in AQP5-expressing cells was supported by Stroka et al. (2014), who found that cell migration through physically confined spaces occurred despite block of actin polymerization and myosin contraction, but relied on co-expression of the Na^+/H^+ exchanger with AQP5, supporting AQP5-induced cell volume regulation and its importance in cell motility.

AQP8 expression influences migration and invasion of cervical cancer cells, and AQP3 expression enhances pancreatic and colorectal cancer cell invasion and metastasis (Liu et al., 2012; Li et al., 2013; Shi et al., 2013). Further work is needed to investigate whether mechanisms of AQP3- and AQP8-facilitated cancer cell migration and invasion involve cell volume regulation, protrusion formation, cytoskeletal interaction, or other functional properties of the AQP channels that remain to be defined.

Cell-Matrix Adhesion

Cell-matrix adhesions, first observed in cultured fibroblasts, connect the extracellular matrix to the actin cytoskeleton (Curtis, 1964). During migration, contacts with substratum must form to facilitate extension, and must detach to allow forward displacement of the cell. Insufficient anchoring causes protrusions to collapse, leading to a "membrane ruffling" phenomenon (Vicente-Manzanares and Horwitz, 2011). Protrusions adhere to ECM via integrin receptors, in turn linked to intracellular actin filaments (Ridley et al., 2003). The extracellular binding of integrin receptors to ECM ligands initiates integrin clustering, and activates protein tyrosine kinases and small GTPases. The organization of actin cytoskeleton and cell polarity controls the positions of focal adhesions for cell locomotion (Geiger et al., 2001; Martin et al., 2002). Cell-matrix adhesions create the focal points for generation of traction to pull the cell forward over the substratum.

Classes of aquaporins (AQP1-4) have been shown to interact with adhesion molecules and to influence adhesive properties of migrating cells. Increased AQP1 in mesenchymal stem cells enhances migration by a mechanism involving β-catenin and the focal adhesion kinase (FAK) (Meng et al., 2014), which regulates integrin signaling at focal adhesion sites (Schaller et al., 1992; McLean et al., 2005; Zhao and Guan, 2011). Whether AQP1 and FAK also interact in cancer cell migration remains to be tested. AQP2 appears to promote cell migration by modulating integrin β1 at focal adhesion sites, by a mechanism thought to involve an arginine-glycine-aspartate (RGD) motif in the second extracellular loop of AQP2 (Chen et al., 2012). When AQP2 is absent, integrin β1 is retained at focal adhesion sites, delaying recycling of focal adhesions, thus reducing migration rate. AQP2 also enables estradiol-induced migration and adhesion of endometrial carcinoma cells by mechanisms involving annexin-2 and reorganization of F-actin (Zou et al., 2011). Knockdown of AQP3 in human esophageal and oral squamous cell carcinoma with siRNA correlated with reduced phosphorylation of FAK, impaired cell adhesion and cell death (Kusayama et al., 2011); these effects would be predicted to impair cancer cell migration. AQP4 expression has been suggested to enhance cell-matrix adhesion in cancer cells (McCoy and Sontheimer, 2007). More research is needed to identify the intracellular signaling mechanisms and to determine whether other AQP classes alter cell migration via modulation of cell adhesion.

ECM Degradation

Extracellular matrix degradation widens pathways through which cells can penetrate tissues, and reduces the distortion of the rounded cell body needed for physical progress (Brinckerhoff and Matrisian, 2002; Mott and Werb, 2004). Invadopodia sprout from leading edge filopodia, extending through tiny channels in the ECM, and adhere to ECM collagen fibers (Weaver, 2006; Friedl and Wolf, 2009). To accommodate displacement of the cell body, constraining ECM fibers are cleared by local proteolysis, using surface proteases such as zinc-dependent matrix metalloproteinases (MMP) and serine proteases (Nagase and Woessner, 1999; Netzel-Arnett et al., 2003; Wolf et al., 2007). AQPs−1,−3,−4, and−9 have been shown to interact with specific MMPs to facilitate ECM degradation and invasion.

In lung cancer cells, migration was facilitated by AQP1 expression, linked to expression of MMP2 and MMP9 (Wei and Dong, 2015). In gastric cancer cells (SGC7901), AQP3 levels were correlated with MMP2, MMP9, and MT1-MMP levels, and enhanced invasiveness via phosphoinositide 3-kinase signaling (Xu et al., 2011). Positive correlations between AQP3, MMP2, and MMP9 and cancer invasiveness also occur in lung cancer (Xia et al., 2014; Xiong et al., 2017). In prostate cancer, AQP3 expression is correlated with up-regulation of MMP3 via ERK1/2 signaling, with increased cell motility and invasion (Chen et al., 2015). In glioma, AQP4 levels correlated with migration and invasiveness *in vitro* and *in vivo* through a mechanism involving MMP2 (Ding et al., 2011). AQP9 upregulation in prostate cancer could enhance growth, migration, and invasion involving ERK1/2 signaling; reduced levels of phosphorylated ERK1/2 and MMP9 were observed in AQP9-deficient cell lines (Chen et al., 2016). These studies suggest one of the key components of AQP-mediated facilitation of cancer cell invasion is the regulation of MMP proteases needed for degradation of ECM.

Retraction

Following integrin-ligand binding, cross-linking proteins such as myosin II contract the actin filament strands (Vicente-Manzanares et al., 2009), developing tension against the intact adhesion points (Chrzanowska-Wodnicka and Burridge, 1996). The final step in the cycle of cell movement is retraction of the trailing edge. A working model is that membrane tension opens stretch-activated Ca^{2+} channels, activating calpain and triggering disassembly of focal adhesion proteins on the trailing edge, while concurrent K^+ efflux drives volume loss at the cell rear, resulting in detachment and net translocation along the substrate. In this model, the role of AQP channels is to facilitate osmotic water efflux in response to K^+ efflux (Huttenlocher et al., 1997; Palecek

et al., 1998; Schwab et al., 2007) presumably in parallel with electroneutral efflux of chloride ions.

AQP PHARMACOLOGY AND THERAPEUTIC IMPLICATIONS IN CANCER INVASION AND METASTASIS

Aquaporin pharmacological agents have attracted keen interest for their potential therapeutic uses in diseases involving impaired fluid homeostasis. Aquaporins in cancer metastasis are new translational targets for AQP modulators. Known and proposed inhibitors of AQPs include cysteine-reactive metals such as mercury (II) chloride ($HgCl_2$) (Preston et al., 1993), gold-based compounds (Martins et al., 2013), carbonic anhydrase inhibitor acetazolamide (Ma et al., 2004a; Gao et al., 2006), and small molecule inhibitors such as tetraethylammonium (TEA^+) (Brooks et al., 2000), although the small molecule blockers vary in efficacy between preparations. The pharmacological panel for AQPs has been expanding steadily, with new compounds being discovered around the world, including for example the University of Niigata, Japan (Huber et al., 2009), Radboud University, Netherlands (Detmers et al., 2006), the Faculty of Pharmacy, University of Lisbon, Portugal (Martins et al., 2012), the Institute of Food and Agricultural Research and Technology, Barcelona, Spain (Seeliger et al., 2012), the University of Adelaide, Australia (Niemietz and Tyerman, 2002; Yool, 2007), the University of Groningen, Netherlands (Martins et al., 2013), the University of Kiel, Germany (Wu et al., 2008), and others. This review focuses specifically on selected AQP pharmacological agents that to date have been tested in models of cancer cell migration and metastasis (**Table 2**).

Acetazolamide and Topiramate

Acetazolamide and topiramate are FDA-approved drugs that inhibit carbonic anhydrase. Acetazolamide at 100 μM was reported to inhibit water channel activity by 39% for AQP1 expressed in human embryonic kidney (HEK293) cells (Gao et al., 2006), and by 81% at 10 μM in the *Xenopus* oocyte expression system (Ma et al., 2004a). AQP4 activity was inhibited by 47% at 1,250 μM in proteoliposomes (Tanimura et al., 2009). However, acetazolamide (at doses up to 10,000 μM) did not block water flux in erythrocytes with native AQP1 expression, or epithelial cells transfected with AQP1 (Yang et al., 2006; Søgaard and Zeuthen, 2008). Acetazolamide inhibited angiogenesis in a chick chorioallantoic membrane assay, and tumor growth and metastasis in mice with Lewis lung carcinoma (Xiang et al., 2002, 2004), perhaps as a result of reduced AQP1 expression (Bin and Shi-Peng, 2011). Topiramate reduces Lewis lung carcinoma growth and metastasis, with effects similarly attributed to suppression of AQP1 expression (Ma et al., 2004b). It will be of interest to compare the effects of acetazolamide and topiramate on angiogenesis, tumor growth, and metastasis with those of AQP1 channel inhibitors.

Tetraethylammonium

TEA^+ is an inhibitor of voltage-gated potassium channels, calcium-dependent potassium channels, the nicotinic acetylcholine receptor, and it has also been shown to block AQP-1,−2, and−4 water permeability in *Xenopus laevis* oocytes and kidney derived cell lines (Brooks et al., 2000; Yool et al., 2002; Detmers et al., 2006). However, inhibition of AQP1 water permeability by TEA^+ is variable, having been confirmed by some groups (Detmers et al., 2006), and challenged by others (Søgaard and Zeuthen, 2008). Yang et al. (2006) reported no block of water flux by TEA^+ in erythrocytes with native AQP1, or in epithelial cells transfected with AQP1, and suggested previous positive results might have been due to inhibition of K^+ channels and altered baseline cell volume; however, the observation that site-directed mutation of AQP1 altered TEA sensitivity (Brooks et al., 2000) ruled out this alternative explanation. TEA^+ block of AQP1 water permeability reduced cell migration and invasion in *in vitro* models of osteosarcoma and hepatocellular carcinoma (Pelagalli et al., 2016), with outcomes interpreted as consistent with action of TEA^+ as a possible AQP1 inhibitor. However, given the variability in efficacy and cross-talk with other channels, TEA^+ is not an ideal candidate for clinical development, although the targets causing the observed block of cancer cell migration and invasion might merit further investigation.

Bumetanide Derivatives

Bumetanide is a sulfamoylanthranilic acid derivative used clinically to increase diuresis by blocking sodium cotransporter activity at the loop of Henle in the nephron. Molecular derivatives of bumetanide have been synthesized and found to exhibit inhibitory effects on classes of AQP channels. For example, the bumetanide derivative AqB013 blocks osmotic water fluxes mediated by mammalian AQP1 and AQP4 channels expressed in *Xenopus laevis* oocytes (Migliati et al., 2009). The water channel blocker AqB013 was shown to inhibit endothelial tube formation and colon cancer cell migration and invasion *in vitro* (Dorward et al., 2016). Other bumetanide derivatives, AqB011 and AqB007, block the AQP1 ion conductance, but not water flux (Kourghi et al., 2015). In AQP1, the central tetrameric pore is thought to be permeable to monovalent cations, CO_2, and NO (Nakhoul et al., 1998; Herrera et al., 2006; Yu et al., 2006; Musa-Aziz et al., 2009), although some work questioned AQP1-mediated CO_2 and cation transport properties (Yang et al., 2000; Fang et al., 2002; Tsunoda et al., 2004). An ionic conductance in AQP1-expressing *Xenopus* oocytes stimulated with forskolin was first reported in 1996 (Yool et al., 1996); however, the forskolin response proved to be inconsistent when repeated by other groups (Agre et al., 1997). Further work showed the forskolin effect was indirect; the direct regulation of the AQP1 cation conductance depended on cGMP binding (Anthony et al., 2000). The reason that AQP1 cation channels have low opening probability (Saparov et al., 2001) or are not detectable (Tsunoda et al., 2004) reflects the availability of AQP1 to be gated by cGMP, which depends on tyrosine phosphorylation status of the carboxyl terminal domain, suggesting the AQP1 ion channel function is highly regulated (Campbell et al., 2012). With the discovery of AQP1

TABLE 2 | Summary of AQP pharmacology used in cancer invasion and metastasis.

Molecule name	Molecular structure	AQP activity	Effect
TEA^+	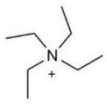	• Inhibits AQP1, AQP2, and AQP4 water flux (Brooks et al., 2000; Yool et al., 2002; Detmers et al., 2006)	• Inhibits osteosarcoma and hepatocellular carcinoma cell migration and invasion (*in vitro*) (Pelagalli et al., 2016)
Acetazolamide	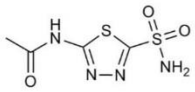	• Inhibits AQP1 and AQP4 water flux (Ma et al., 2004a; Tanimura et al., 2009) • Suppresses AQP1 expression (Xiang et al., 2004)	• Inhibits angiogenesis and metastasis in Lewis lung carcinoma (*in vivo*) (Xiang et al., 2002, 2004) • Suppresses tumor growth in colon cancer (*in vivo*) (Bin and Shi-Peng, 2011)
Topiramate	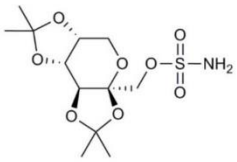	• Suppresses AQP1 expression (Ma et al., 2004b)	• Suppresses Lewis lung carcinoma growth and metastasis (*in vivo*) (Ma et al., 2004b)
AqB007	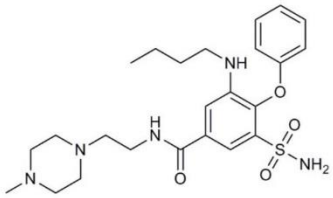	• Inhibits AQP1 ion flux (Kourghi et al., 2015)	• Inhibits colon cancer cell migration (*in vitro*) (Kourghi et al., 2015)
AqB011		• Inhibits AQP1 ion flux (Kourghi et al., 2015)	• Inhibits colon cancer cell migration (*in vitro*) (Kourghi et al., 2015)
AqB013	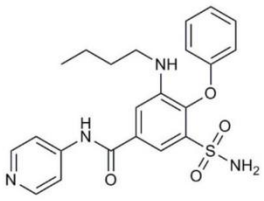	• Inhibits AQP1 and AQP4 water flux (Migliati et al., 2009)	• Inhibits endothelial tube formation and colon cancer cell migration (*in vitro*) (Dorward et al., 2016)

(Continued)

TABLE 1 | Continued

Molecule name	Molecular structure	AQP activity	Effect
Bacopaside I	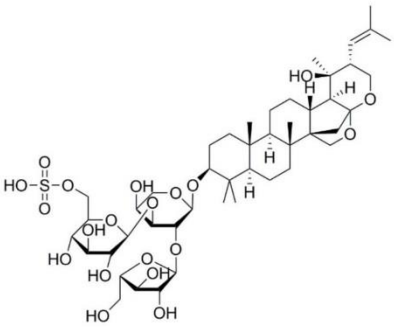	• Inhibits AQP1 water flux (Pei et al., 2016)	• Inhibits colon cancer cell migration (*in vitro*) (Pei et al., 2016)
Curcumin	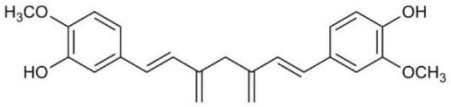	• Inhibits EGF-induced AQP3 upregulation (Ji et al., 2008)	• Inhibits ovarian cancer cell migration (*in vitro*) (Ji et al., 2008)
Bacopaside II	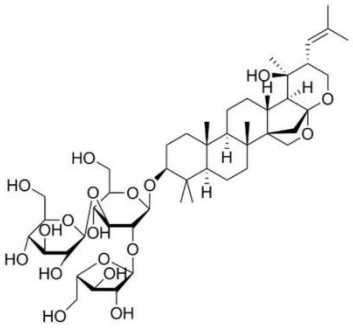	• Inhibits AQP1 water flux (Pei et al., 2016)	• Inhibits colon cancer cell migration (*in vitro*) (Pei et al., 2016)
Ginsenoside Rg3	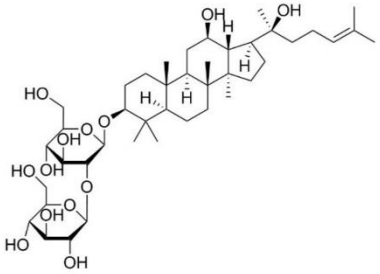	• Suppresses AQP1 expression (Pan et al., 2012)	• Inhibits prostate cancer cell migration (*in vitro*) (Pan et al., 2012)

ion blocking agents, AqB011 and AqB007, the physiological function of the ion channel activity could finally be addressed. When applied to AQP1-expressing HT29 colon cancer cells, these inhibitory compounds significantly reduced cancer cell motility (Kourghi et al., 2015), suggesting a physiological role of AQP1 ion conductance in cell migration. Mutation of the candidate binding site in the AQP1 intracellular loop D domain removed sensitivity to AqB011, showing that the inhibitory mechanism directly involved the AQP1 channel and could not readily be attributed to off-target actions on other channels or transporters (Kourghi et al., 2018). Another bumetanide derivative AqB050 was shown to inhibit mesothelioma cell motility and metastatic potential *in vitro*, but not *in vivo* (Klebe et al., 2015). The mechanism of action of AqB050 in blocking mesothelioma cell motility *in vitro* remains to be determined.

Plant-Based Derivatives

Plant-based derivatives that reduce cancer cell migration and invasion include agents that have also have been found to inhibit AQPs. Bacopa monnieri is a perennial herb native to the wetlands of India that is used in alternative medicinal therapies. Chemical constituents bacopaside-I and bacopaside-II, were shown to block AQP1 but not AQP4 water channels (Pei et al., 2016). Pei and colleagues also found that bacopaside-I and bacopaside-II attenuated migration of colon cancer cell lines expressing high levels of AQP1, but had no effect on lines with low AQP1, suggesting the inhibitory effects were AQP1-specific. Ginsenoside Rg3 from a traditional Asian medicinal plant Panax ginseng is an intriguing candidate for possible anti-metastatic therapies. Ginsenoside Rg3 inhibited prostate cancer cell migration and was associated with downregulation of AQP1 expression via the p38 MAPK pathway and transcription factors (Pan et al., 2012). Effects of Ginsenoside Rg3 directly on water channel activity, or on expression levels of other aquaporins, remain unknown. Curcumin is a naturally occurring ingredient in turmeric, used as therapeutic tool for pathologies including cancer (Gupta et al., 2013). Curcumin was found to inhibit EGF-induced upregulation of AQP3 and migration in human ovarian cancer cells, via inhibition of AKT/ERK and PI3K pathways (Ji et al., 2008); however, curcumin affects a number of biochemical pathways and might not be suited when AQP-specific modulation is required (Aggarwal et al., 2003). Research on the effects of curcumin in other cancers such as gastric cancer, in which EGF-induced AQP3 up-regulation occurs, might further understanding of the role of AQP3 in cell migration and invasion (Huang et al., 2010).

Metal-Based Inhibitors

Mercury has classically been used as an AQP1 inhibitor. In the human AQP1 monomer, the NPA motif in loop E is near cysteine 189, which is the site at which mercury inhibits osmotic water permeability (Preston et al., 1993). Lack of a cysteine in the corresponding position is consistent with mercury insensitivity in mammalian AQP4 (Preston et al., 1993). However, mercury is not a promising candidate for AQP-specific modulation or therapeutic application due to its toxicity and non-specific side-effects. Metal-based inhibitors that have been tested in models of cancer include AQP3 inhibitors such as $NiCl_2$ (Zelenina et al., 2003) and $CuSO_4$ (Zelenina et al., 2004), which inhibited EGF-induced cell migration in human ovarian cancer cells. Auphen is a gold-based compound which, when administered at concentrations of 100 μM, blocks AQP3 glycerol transport by 90%, and water transport by 20% in human red blood cells (Martins et al., 2012). Auphen also blocks proliferation in various mammalian cell lines, including human epidermoid carcinoma, by inhibiting AQP3 glycerol transport (Serna et al., 2014). This merits more research into the importance of AQP3-facilitated glycerol transport in cancer invasiveness, and whether gold-based compounds such as auphen can also be used to suppress cancer invasion and metastasis.

CONCLUSION

Aquaporin-dependent mechanisms serve as key steps throughout the process of metastasis, in angiogenesis, cellular dissociation, cell migration and invasion. AQPs−1,−2,−3,−4,−5,−8, and−9 contribute to one or more processes, generally potentiating cancer invasion and metastasis by boosting tumor angiogenesis, enhancing cell volume regulation, regulating cell-cell and cell-matrix adhesions, interacting with the actin cytoskeleton, regulating proteases and ECM degrading molecules, contributing to the regulation of epithelial-mesenchymal transition in cancer cells, and interacting with specific signaling pathways important in cancer cell motility and invasions. Pharmacological agents for aquaporin channels have therapeutic promise for improving cancer treatment, and include derivatives of bumetanide, organic metal compounds, plant medicinal agents, and other small molecule compounds. Although conflicting evidence has been raised for some compounds, there is nevertheless a compelling need to continue identifying novel candidates for AQP-specific modulators relevant not only for the treatment of cancer, but other pathological conditions. In conclusion, although much remains to be defined for molecular mechanisms in cancer invasion and metastasis, the roles of AQP channel function in cancer progression will inspire new therapeutic targets for improving treatment of malignant and invasive carcinomas.

AUTHOR CONTRIBUTIONS

MD: wrote the manuscript; AY: reviewed and edited the manuscript.

FUNDING

This work was supported by a Discovery Project grant from Australian Research Council (ARC DP160104641).

ACKNOWLEDGMENTS

Thanks to Dr. Jinxin Pei for assisting with molecular structure diagrams (**Table 2**).

REFERENCES

Abreu-Rodríguez, I., Silva, R. S., Martins, A. P., Soveral, G., Toledo-Aral, J. J., López-Barneo, J., et al. (2011). Functional and transcriptional induction of aquaporin-1 gene by hypoxia; analysis of promoter and role of Hif-1α. *PLoS ONE* 6:e28385. doi: 10.1371/journal.pone.0028385

Aggarwal, B. B., Kumar, A., and Bharti, A. C. (2003). Anticancer potential of curcumin: preclinical and clinical studies. *Anticancer Res.* 23, 363–398.

Agre, P., Lee, M. D., Devidas, S., and Guggino, W. B. (1997). Aquaporins and ion conductance. *Science* 275:1490; author reply 1492. doi: 10.1126/science.275.5305.1490

Aishima, S., Kuroda, Y., Nishihara, Y., Taguchi, K., Iguchi, T., Taketomi, A., et al. (2007). Down-regulation of aquaporin-1 in intrahepatic cholangiocarcinoma is related to tumor progression and mucin expression. *Hum. Pathol.* 38, 1819–1825. doi: 10.1016/j.humpath.2007.04.016

Alizadeh, A. M., Shiri, S., and Farsinejad, S. (2014). Metastasis review: from bench to bedside. *Tumor Biol.* 35, 8483–8523. doi: 10.1007/s13277-014-2421-z

Allen, W. E., Jones, G. E., Pollard, J. W., and Ridley, A. J. (1997). Rho, Rac and Cdc42 regulate actin organization and cell adhesion in macrophages. *J. Cell Sci.* 110, 707–720.

Allen, W. E., Zicha, D., Ridley, A. J., and Jones, G. E. (1998). A role for Cdc42 in macrophage chemotaxis. *J. Cell Biol.* 141, 1147–1157. doi: 10.1083/jcb.141.5.1147

Almasalmeh, A., Krenc, D., Wu, B., and Beitz, E. (2014). Structural determinants of the hydrogen peroxide permeability of aquaporins. *FEBS J.* 281, 647–656. doi: 10.1111/febs.12653

Angst, B. D., Marcozzi, C., and Magee, A. I. (2001). The cadherin superfamily: diversity in form and function. *J. Cell Sci.* 114, 629–641.

Anthony, T. L., Brooks, H. L., Boassa, D., Leonov, S., Yanochko, G. M., Regan, J. W., et al. (2000). Cloned human aquaporin-1 is a cyclic GMP-gated ion channel. *Mol. Pharmacol.* 57, 576–588. doi: 10.1124/mol.57.3.576

Bhattacharjee, H., Carbrey, J., Rosen, B. P., and Mukhopadhyay, R. (2004). Drug uptake and pharmacological modulation of drug sensitivity in leukemia by AQP9. *Biochem. Biophys. Res. Commun.* 322, 836–841. doi: 10.1016/j.bbrc.2004.08.002

Bienert, G. P., Møller, A. L., Kristiansen, K. A., Schulz, A., Møller, I. M., Schjoerring, J. K., et al. (2007). Specific aquaporins facilitate the diffusion of hydrogen peroxide across membranes. *J. Biol. Chem.* 282, 1183–1192. doi: 10.1074/jbc.M603761200

Bin, K., and Shi-Peng, Z. (2011). Acetazolamide inhibits aquaporin-1 expression and colon cancer xenograft tumor growth. *Hepatogastroenterology* 58, 1502–1506. doi: 10.5754/hge11154

Binder, D. K., Yao, X., Zador, Z., Sick, T. J., Verkman, A. S., and Manley, G. T. (2006). Increased seizure duration and slowed potassium kinetics in mice lacking aquaporin-4 water channels. *Glia* 53, 631–636. doi: 10.1002/glia.20318

Bjørkskov, F. B., Krabbe, S. L., Nurup, C. N., Missel, J. W., Spulber, M., Bomholt, J., et al. (2017). Purification and functional comparison of nine human Aquaporins produced in *Saccharomyces cerevisiae* for the purpose of biophysical characterization. *Sci. Rep.* 7:16899. doi: 10.1038/s41598-017-17095-6

Bretscher, M. S., and Aguado-Velasco, C. (1998). Membrane traffic during cell locomotion. *Curr. Opin. Cell Biol.* 10, 537–541. doi: 10.1016/S0955-0674(98)80070-7

Brinckerhoff, C. E., and Matrisian, L. M. (2002). Matrix metalloproteinases: a tail of a frog that became a prince. *Nat. Rev. Mol. Cell Biol.* 3, 207–214. doi: 10.1038/nrm763

Brooks, H. L., Regan, J. W., and Yool, A. J. (2000). Inhibition of aquaporin-1 water permeability by tetraethylammonium: involvement of the loop E pore region. *Mol. Pharmacol.* 57, 1021–1026.

Calamita, G., Ferri, D., Bazzini, C., Mazzone, A., Botta, G., Liquori, G. E., et al. (2005). Expression and subcellular localization of the AQP8 and AQP1 water channels in the mouse gall-bladder epithelium. *Biol. Cell* 97, 415–423. doi: 10.1042/BC20040137

Camerino, G., Nicchia, G., Dinardo, M., Ribatti, D., Svelto, M., and Frigeri, A. (2006). *In vivo* silencing of aquaporin-1 by RNA interference inhibits angiogenesis in the chick embryo chorioallantoic membrane assay. *Cell. Mol. Biol.* 52, 51–56.

Campbell, E. M., Birdsell, D. N., and Yool, A. J. (2012). The activity of human aquaporin 1 as a cGMP-gated cation channel is regulated by tyrosine phosphorylation in the carboxyl-terminal domain. *Mol. Pharmacol.* 81, 97–105. doi: 10.1124/mol.111.073692

Cano, A., Pérez-Moreno, M. A., Rodrigo, I., Locascio, A., Blanco, M. J., del Barrio, M. G., et al. (2000). The transcription factor snail controls epithelial–mesenchymal transitions by repressing E-cadherin expression. *Nat. Cell Biol.* 2, 76–83. doi: 10.1038/35000025

Carbrey, J. M., Song, L., Zhou, Y., Yoshinaga, M., Rojek, A., Wang, Y., et al. (2009). Reduced arsenic clearance and increased toxicity in aquaglyceroporin-9-null mice. *Proc. Natl. Acad. Sci. U.S.A.* 106, 15956–15960. doi: 10.1073/pnas.0908108106

Cavallaro, U., and Christofori, G. (2004). Cell adhesion and signalling by cadherins and Ig-CAMs in cancer. *Nat. Rev. Cancer* 4, 118–132. doi: 10.1038/nrc1276

Chae, Y. K., Kang, S. K., Kim, M. S., Woo, J., Lee, J., Chang, S., et al. (2008a). Human AQP5 plays a role in the progression of chronic myelogenous leukemia (CML). *PLoS ONE* 3:e2594. doi: 10.1371/journal.pone.0002594

Chae, Y. K., Woo, J., Kim, M.-J., Kang, S. K., Kim, M. S., Lee, J., et al. (2008b). Expression of aquaporin 5 (AQP5) promotes tumor invasion in human non small cell lung cancer. *PLoS ONE* 3:e2162. doi: 10.1371/journal.pone.0002162

Chandy, G., Zampighi, G. A., Kreman, M., and Hall, J. E. (1997). Comparison of the water transporting properties of MIP and AQP1. *J. Membr. Biol.* 159, 29–39. doi: 10.1007/s002329900266

Chen, C., Ma, T., Zhang, C., Zhang, H., Bai, L., Kong, L., et al. (2017). Down-regulation of aquaporin 5-mediated epithelial-mesenchymal transition and anti-metastatic effect by natural product Cairicoside E in colorectal cancer. *Mol. Carcinog.* 56, 2692–2705. doi: 10.1002/mc.22712

Chen, J., Wang, T., Zhou, Y.-C., Gao, F., Zhang, Z.-H., Xu, H., et al. (2014). Aquaporin 3 promotes epithelial-mesenchymal transition in gastric cancer. *J. Exp. Clin. Cancer Res.* 33:38. doi: 10.1186/1756-9966-33-38

Chen, J., Wang, Z., Xu, D., Liu, Y., and Gao, Y. (2015). Aquaporin 3 promotes prostate cancer cell motility and invasion via extracellular signal-regulated kinase 1/2-mediated matrix metalloproteinase-3 secretion. *Mol. Med. Rep.* 11, 2882–2888. doi: 10.3892/mmr.2014.3097

Chen, Q., Zhu, L., Zheng, B., Wang, J., Song, X., Zheng, W., et al. (2016). Effect of AQP9 expression in androgen-independent prostate cancer cell PC3. *Int. J. Mol. Sci.* 17:738. doi: 10.3390/ijms17050738

Chen, Y., Rice, W., Gu, Z., Li, J., Huang, J., Brenner, M. B., et al. (2012). Aquaporin 2 promotes cell migration and epithelial morphogenesis. *J. Am. Soc. Nephrol.* 23, 1506–1517. doi: 10.1681/ASN.2012010079

Chen, Y., Tachibana, O., Oda, M., Xu, R., Hamada, J.-I, Yamashita, J., et al. (2006). Increased expression of aquaporin 1 in human hemangioblastomas and its correlation with cyst formation. *J. Neurooncol.* 80, 219–225. doi: 10.1007/s11060-005-9057-1

Chen, Z., Zhang, Z., Gu, Y., and Bai, C. (2011). Impaired migration and cell volume regulation in aquaporin 5-deficient SPC-A1 cells. *Respir. Physiol. Neurobiol.* 176, 110–117. doi: 10.1016/j.resp.2011.02.001

Cho, S.-J., Sattar, A. A., Jeong, E.-H., Satchi, M., Cho, J. A., Dash, S., et al. (2002). Aquaporin 1 regulates GTP-induced rapid gating of water in secretory vesicles. *Proc. Natl. Acad. Sci. U.S.A.* 99, 4720–4724. doi: 10.1073/pnas.072083499

Chrzanowska-Wodnicka, M., and Burridge, K. (1996). Rho-stimulated contractility drives the formation of stress fibers and focal adhesions. *J. Cell Biol.* 133, 1403–1415. doi: 10.1083/jcb.133.6.1403

Chua, H., Bhat-Nakshatri, P., Clare, S., Morimiya, A., Badve, S., and Nakshatri, H. (2007). NF-κB represses E-cadherin expression and enhances epithelial to mesenchymal transition of mammary epithelial cells: potential involvement of ZEB-1 and ZEB-2. *Oncogene* 26, 711–724. doi: 10.1038/sj.onc.1209808

Clapp, C., and de la Escalera, G. M. (2006). Aquaporin-1: a novel promoter of tumor angiogenesis. *Trends Endocrinol. Metab.* 17, 1–2. doi: 10.1016/j.tem.2005.11.009

Condeelis, J. (1993). Life at the leading edge: the formation of cell protrusions. *Annu. Rev. Cell Biol.* 9, 411–444. doi: 10.1146/annurev.cb.09.110193.002211

Cramer, L. P., Siebert, M., and Mitchison, T. J. (1997). Identification of novel graded polarity actin filament bundles in locomoting heart fibroblasts: implications for the generation of motile force. *J. Cell Biol.* 136, 1287–1305. doi: 10.1083/jcb.136.6.1287

Curtis, A. (1964). The mechanism of adhesion of cells to glass A study by interference reflection microscopy. *J. Cell Biol.* 20, 199–215. doi: 10.1083/jcb.20.2.199

Demir, R., Seval, Y., and Huppertz, B. (2007). Vasculogenesis and angiogenesis in the early human placenta. *Acta Histochem.* 109, 257–265. doi: 10.1016/j.acthis.2007.02.008

Demir, R., Yaba, A., and Huppertz, B. (2010). Vasculogenesis and angiogenesis in the endometrium during menstrual cycle and implantation. *Acta Histochem.* 112, 203–214. doi: 10.1016/j.acthis.2009.04.004

Denker, B. M., Smith, B. L., Kuhajda, F. P., and Agre, P. (1988). Identification, purification, and partial characterization of a novel Mr 28,000 integral membrane protein from erythrocytes and renal tubules. *J. Biol. Chem.* 263, 15634–15642.

Detmers, F. J., de Groot, B. L., Müller, E. M., Hinton, A., Konings, I. B., Sze, M., et al. (2006). Quaternary ammonium compounds as water channel blockers. Specificity, potency, and site of action. *J. Biol. Chem.* 281, 14207–14214. doi: 10.1074/jbc.M513072200

Diez, S., Gerisch, G., Anderson, K., Müller-Taubenberger, A., and Bretschneider, T. (2005). Subsecond reorganization of the actin network in cell motility and chemotaxis. *Proc. Natl. Acad. Sci. U.S.A.* 102, 7601–7606. doi: 10.1073/pnas.0408546102

Ding, T., Ma, Y., Li, W., Liu, X., Ying, G., Fu, L., et al. (2011). Role of aquaporin-4 in the regulation of migration and invasion of human glioma cells. *Int. J. Oncol.* 38, 1521–1531. doi: 10.3892/ijo.2011.983

Direito, I., Paulino, J., Vigia, E., Brito, M. A., and Soveral, G. (2017). Differential expression of aquaporin-3 and aquaporin-5 in pancreatic ductal adenocarcinoma. *J. Surg. Oncol.* 115, 980–996. doi: 10.1002/jso.24605

Disanza, A., Steffen, A., Hertzog, M., Frittoli, E., Rottner, K., and Scita, G. (2005). Actin polymerization machinery: the finish line of signaling networks, the starting point of cellular movement. *Cell. Mol. Life Sci.* 62, 955–970. doi: 10.1007/s00018-004-4472-6

Dittmar, T., Heyder, C., Gloria-Maercker, E., Hatzmann, W., and Zänker, K. S. (2008). Adhesion molecules and chemokines: the navigation system for circulating tumor (stem) cells to metastasize in an organ-specific manner. *Clin. Exp. Metastasis* 25, 11–32. doi: 10.1007/s10585-007-9095-5

Dorward, H. S., Du, A., Bruhn, M. A., Wrin, J., Pei, J. V., Evdokiou, A., et al. (2016). Pharmacological blockade of aquaporin-1 water channel by AqB013 restricts migration and invasiveness of colon cancer cells and prevents endothelial tube formation *in vitro*. *Nat. Rev. Cancer* 35:36. doi: 10.1186/s13046-016-0310-6

Drubin, D. G., and Nelson, W. J. (1996). Origins of cell polarity. *Cell* 84, 335–344. doi: 10.1016/S0092-8674(00)81278-7

Echevarria, M., Windhager, E. E., Tate, S. S., and Frindt, G. (1994). Cloning and expression of AQP3, a water channel from the medullary collecting duct of rat kidney. *Proc. Natl. Acad. Sci. U.S.A.* 91, 10997–11001. doi: 10.1073/pnas.91.23.10997

Egginton, S. (2009). Invited review: activity-induced angiogenesis. *Pflügers Arch. Eur. J. Physiol.* 457:963. doi: 10.1007/s00424-008-0563-9

Ehring, G. R., and Hall, J. E. (1988). "Single channel properties of lens MIP 28 reconstituted into planar lipid bilayers," in *Proceedings of the Western Pharmacology Society*, 251.

El Hindy, N., Bankfalvi, A., Herring, A., Adamzik, M., Lambertz, N., Zhu, Y., et al. (2013). Correlation of aquaporin-1 water channel protein expression with tumor angiogenesis in human astrocytoma. *Anticancer Res.* 33, 609–613.

Endo, M., Jain, R. K., Witwer, B., and Brown, D. (1999). Water channel (aquaporin 1) expression and distribution in mammary carcinomas and glioblastomas. *Microvasc. Res.* 58, 89–98. doi: 10.1006/mvre.1999.2158

Esteva-Font, C., Jin, B.-J., and Verkman, A. S. (2014). Aquaporin-1 gene deletion reduces breast tumor growth and lung metastasis in tumor-producing MMTV-PyVT mice. *FASEB J.* 28, 1446–1453. doi: 10.1096/fj.13-245621

Etienne-Manneville, S., and Hall, A. (2003). Cell polarity: Par6, aPKC and cytoskeletal crosstalk. *Curr. Opin. Cell Biol.* 15, 67–72. doi: 10.1016/S0955-0674(02)00005-4

Fang, X., Yang, B., Matthay, M. A., and Verkman, A. (2002). Evidence against aquaporin-1-dependent CO2 permeability in lung and kidney. *J. Physiol.* 542, 63–69. doi: 10.1113/jphysiol.2001.013813

Ferlay, J., Soerjomataram, I., Dikshit, R., Eser, S., Mathers, C., Rebelo, M., et al. (2015). Cancer incidence and mortality worldwide: sources, methods and major patterns in GLOBOCAN 2012. *Int. J.Cancer* 136, E359–E386. doi: 10.1002/ijc.29210

Finn, R. N., and Cerdà, J. (2015). Evolution and functional diversity of aquaporins. *Biol. Bull.* 229, 6–23. doi: 10.1086/BBLv229n1p6

Finn, R. N., Chauvign,é, F., Hlidberg, J. B., Cutler, C. P., and Cerdà J. (2014). The lineage-specific evolution of aquaporin gene clusters facilitated tetrapod terrestrial adaptation. *PLoS ONE* 9:e113686. doi: 10.1371/journal.pone.0113686

Fletcher, S. J., and Rappoport, J. Z. (2010). Moving forward: polarised trafficking in cell migration. *Trends Cell Biol.* 20, 71–78. doi: 10.1016/j.tcb.2009.11.006

Folkman, J., Cole, P., and Zimmerman, S. (1966). Tumor behavior in isolated perfused organs: *in vitro* growth and metastases of biopsy material in rabbit thyroid and canine intestinal segment. *Ann. Surg.* 164:491. doi: 10.1097/00000658-196609000-00012

Fossdal, G., Vik-Mo, E. O., Sandberg, C., Varghese, M., Kaarbø, M., Telmo, E., et al. (2012). Aqp 9 and brain tumour stem cells. *Sci. World J.* 2012:915176. doi: 10.1100/2012/915176

Friedl, P., and Weigelin, B. (2008). Interstitial leukocyte migration and immune function. *Nat. Immunol.* 9, 960–969. doi: 10.1038/ni.f.212

Friedl, P., and Wolf, K. (2003). Tumour-cell invasion and migration: diversity and escape mechanisms. *Nat. Rev. Cancer* 3, 362–374. doi: 10.1038/nrc1075

Friedl, P., and Wolf, K. (2009). Proteolytic interstitial cell migration: a five-step process. *Cancer Metastasis Rev.* 28, 129–135. doi: 10.1007/s10555-008-9174-3

Friedl, P., Hegerfeldt, Y., and Tusch, M. (2004). Collective cell migration in morphogenesis and cancer. *Int. J. Dev. Biol.* 48, 441–450. doi: 10.1387/ijdb.041821pf

Fushimi, K., Uchida, S., Hara, Y., Hirata, Y., Marumo, F., and Sasaki, S. (1993). Cloning and expression of apical membrane water channel of rat kidney collecting tubule. *Nature* 361:549. doi: 10.1038/361549a0

Gamelin, E., Gamelin, L., Bossi, L., and Quasthoff, S. (2002). Clinical aspects and molecular basis of oxaliplatin neurotoxicity: current management and development of preventive measures. *Semin. Oncol.* 29(5Suppl. 15), 21–33. doi: 10.1053/sonc.2002.35525

Gao, J., Wang, X., Chang, Y., Zhang, J., Song, Q., Yu, H., et al. (2006). Acetazolamide inhibits osmotic water permeability by interaction with aquaporin-1. *Anal. Biochem.* 350, 165–170. doi: 10.1016/j.ab.2006.01.003

Geiger, B., Bershadsky, A., Pankov, R., and Yamada, K. M. (2001). Transmembrane crosstalk between the extracellular matrix and the cytoskeleton. *Nat. Rev. Mol. Cell Biol.* 2, 793–805. doi: 10.1038/35099066

Goldstein, B., and Macara, I. G. (2007). The PAR proteins: fundamental players in animal cell polarization. *Dev. Cell* 13, 609–622. doi: 10.1016/j.devcel.2007.10.007

Gralow, J. R., Biermann, J. S., Farooki, A., Fornier, M. N., Gagel, R. F., Kumar, R., et al. (2013). NCCN task force report: bone health in cancer care. *J. Natl. Comp. Cancer Netw.* 11, S1–S50. doi: 10.6004/jnccn.2013.0215

Guarino, M., Rubino, B., and Ballabio, G. (2007). The role of epithelial-mesenchymal transition in cancer pathology. *Pathology* 39, 305–318. doi: 10.1080/00313020701329914

Guo, X., Sun, T., Yang, M., Li, Z., Li, Z., and Gao, Y. (2013). Prognostic value of combined aquaporin 3 and aquaporin 5 overexpression in hepatocellular carcinoma. *Biomed Res. Int.* 2013:206525. doi: 10.1155/2013/206525

Gupta, S. C., Patchva, S., and Aggarwal, B. B. (2013). Therapeutic roles of curcumin: lessons learned from clinical trials. *AAPS J.* 15, 195–218. doi: 10.1208/s12248-012-9432-8

Hall, A. (1998). Rho GTPases and the actin cytoskeleton. *Science* 279, 509–514. doi: 10.1126/science.279.5350.509

Hara-Chikuma, M., and Verkman, A. (2008a). Aquaporin-3 facilitates epidermal cell migration and proliferation during wound healing. *J. Mol. Med.* 86, 221–231. doi: 10.1007/s00109-007-0272-4

Hara-Chikuma, M., and Verkman, A. (2008b). Prevention of skin tumorigenesis and impairment of epidermal cell proliferation by targeted aquaporin-3 gene disruption. *Mol. Cell. Biol.* 28, 326–332. doi: 10.1128/MCB.01482-07

Hara-Chikuma, M., and Verkman, A. S. (2006). Aquaporin-1 facilitates epithelial cell migration in kidney proximal tubule. *J. Am. Soc. Nephrol.* 17, 39–45. doi: 10.1681/ASN.2005080846

Hara-Chikuma, M., Chikuma, S., Sugiyama, Y., Kabashima, K., Verkman, A. S., Inoue, S., et al. (2012). Chemokine-dependent T cell migration requires aquaporin-3–mediated hydrogen peroxide uptake. *J. Exp. Med.* 209, 1743–1752. doi: 10.1084/jem.20112398

Hara-Chikuma, M., Watanabe, S., and Satooka, H. (2016). Involvement of aquaporin-3 in epidermal growth factor receptor signaling via hydrogen peroxide transport in cancer cells. *Biochem. Biophys. Res. Commun.* 471, 603–609. doi: 10.1016/j.bbrc.2016.02.010

Hasegawa, H., Ma, T., Skach, W., Matthay, M. A., and Verkman, A. (1994). Molecular cloning of a mercurial-insensitive water channel expressed in selected water-transporting tissues. *J. Biol. Chem.* 269, 5497–5500.

Herrera, M., and Garvin, J. L. (2011). Aquaporins as gas channels. *Pflügers Arch. Eur. J. Physiol.* 462:623. doi: 10.1007/s00424-011-1002-x

Herrera, M., Hong, N. J., and Garvin, J. L. (2006). Aquaporin-1 transports NO across cell membranes. *Hypertension* 48, 157–164. doi: 10.1161/01.HYP.0000223652.29338.77

Hoffert, J. D., Pisitkun, T., Wang, G., Shen, R.-F., and Knepper, M. A. (2006). Quantitative phosphoproteomics of vasopressin-sensitive renal cells: regulation of aquaporin-2 phosphorylation at two sites. *Proc. Natl. Acad. Sci. U.S.A.* 103, 7159–7164. doi: 10.1073/pnas.0600895103

Holm, L. M., Jahn, T. P., Møller, A. L., Schjoerring, J. K., Ferri, D., Klaerke, D. A., et al. (2005). NH3 and NH4+ permeability in aquaporin-expressing Xenopus oocytes. *Pflügers Arch.* 450, 415–428. doi: 10.1007/s00424-005-1399-1

Hoque, M. O., Soria, J.-C., Woo, J., Lee, T., Lee, J., Jang, S. J., et al. (2006). Aquaporin 1 is overexpressed in lung cancer and stimulates NIH-3T3 cell proliferation and anchorage-independent growth. *Am. J. Pathol.* 168, 1345–1353. doi: 10.2353/ajpath.2006.050596

Howard-Anderson, J., Ganz, P. A., Bower, J. E., and Stanton, A. L. (2012). Quality of life, fertility concerns, and behavioral health outcomes in younger breast cancer survivors: a systematic review. *J. Natl. Cancer Inst.* 104, 386–405. doi: 10.1093/jnci/djr541

Hu, J., and Verkman, A. S. (2006). Increased migration and metastatic potential of tumor cells expressing aquaporin water channels. *FASEB J.* 20, 1892–1894. doi: 10.1096/fj.06-5930fje

Huang, Y., Zhu, Z., Sun, M., Wang, J., Guo, R., Shen, L., et al. (2010). Critical role of aquaporin-3 in the human epidermal growth factor-induced migration and proliferation in the human gastric adenocarcinoma cells. *Cancer Biol. Ther.* 9, 1000–1007. doi: 10.4161/cbt.9.12.11705

Huber, V. J., Tsujita, M., Kwee, I. L., and Nakada, T. (2009). Inhibition of aquaporin 4 by antiepileptic drugs. *Bioorg. Med. Chem.* 17, 418–424. doi: 10.1016/j.bmc.2007.12.038

Huttenlocher, A., Palecek, S. P., Lu, Q., Zhang, W., Mellgren, R. L., Lauffenburger, D. A., et al. (1997). Regulation of cell migration by the calcium-dependent protease calpain. *J. Biol. Chem.* 272, 32719–32722. doi: 10.1074/jbc.272.52.32719

Hwang, I., Jung, S.-I., Hwang, E.-C., Song, S. H., Lee, H.-S., Kim, S.-O., et al. (2012). Expression and localization of aquaporins in benign prostate hyperplasia and prostate cancer. *Chonnam Med. J.* 48, 174–178. doi: 10.4068/cmj.2012.48.3.174

Ibarra, N., Pollitt, A., and Insall, R. (2005). Regulation of actin assembly by SCAR/WAVE proteins. *Biochem. Soc. Trans.* 33(Pt 6), 1243–1246. doi: 10.1042/BST0331243

Ishibashi, K. (2009). New members of mammalian aquaporins: AQP10–AQP12. *Aquaporins* 190, 251–262. doi: 10.1007/978-3-540-79885-9_13

Ishibashi, K., Hara, S., and Kondo, S. (2009). Aquaporin water channels in mammals. *Clin. Exp. Nephrol.* 13, 107–117. doi: 10.1007/s10157-008-0118-6

Ishibashi, K., Kuwahara, M., Gu, Y., Kageyama, Y., Tohsaka, A., Suzuki, F., et al. (1997a). Cloning and functional expression of a new water channel abundantly expressed in the testis permeable to water, glycerol, and urea. *J. Biol. Chem.* 272, 20782–20786. doi: 10.1074/jbc.272.33.20782

Ishibashi, K., Kuwahara, M., Gu, Y., Tanaka, Y., Marumo, F., and Sasaki, S. (1998). Cloning and functional expression of a new aquaporin (AQP9) abundantly expressed in the peripheral leukocytes permeable to water and urea, but not to glycerol. *Biochem. Biophys. Res. Commun.* 244, 268–274. doi: 10.1006/bbrc.1998.8252

Ishibashi, K., Kuwahara, M., Kageyama, Y., Tohsaka, A., Marumo, F., and Sasaki, S. (1997b). Cloning and functional expression of a second new aquaporin abundantly expressed in testis. *Biochem. Biophys. Res. Commun.* 237, 714–718. doi: 10.1006/bbrc.1997.7219

Ishibashi, K., Morinaga, T., Kuwahara, M., Sasaki, S., and Imai, M. (2002). Cloning and identification of a new member of water channel (AQP10) as an aquaglyceroporin. *Biochim. Biophys. Acta* 1576, 335–340. doi: 10.1016/S0167-4781(02)00393-7

Ishibashi, K., Sasaki, S., Fushimi, K., Uchida, S., Kuwahara, M., Saito, H., et al. (1994). Molecular cloning and expression of a member of the aquaporin family with permeability to glycerol and urea in addition to water expressed at the basolateral membrane of kidney collecting duct cells. *Proc. Natl. Acad. Sci. U.S.A.* 91, 6269–6273. doi: 10.1073/pnas.91.14.6269

Jensen, M. Ø., Tajkhorshid, E., and Schulten, K. (2001). The mechanism of glycerol conduction in aquaglyceroporins. *Structure* 9, 1083–1093. doi: 10.1016/S0969-2126(01)00668-2

Ji, C., Cao, C., Lu, S., Kivlin, R., Amaral, A., Kouttab, N., et al. (2008). Curcumin attenuates EGF-induced AQP3 up-regulation and cell migration in human ovarian cancer cells. *Cancer Chemother. Pharmacol.* 62, 857–865. doi: 10.1007/s00280-007-0674-6

Jiang, Y. (2009). Aquaporin-1 activity of plasma membrane affects HT20 colon cancer cell migration. *IUBMB Life* 61, 1001–1009. doi: 10.1002/iub.243

Jiang, Y., and Jiang, Z.-B. (2010). Aquaporin 1-expressing MCF-7 mammary carcinoma cells show enhanced migration *in vitro*. *J. Biomed. Sci. Eng.* 3:95. doi: 10.4236/jbise.2010.31014

Johnson, D. I., and Pringle, J. R. (1990). Molecular characterization of CDC42, a Saccharomyces cerevisiae gene involved in the development of cell polarity. *J. Cell Biol.* 111, 143–152. doi: 10.1083/jcb.111.1.143

Jung, H. J., Park, J.-Y., Jeon, H.-S., and Kwon, T.-H. (2011). Aquaporin-5: a marker protein for proliferation and migration of human breast cancer cells. *PLoS ONE* 6:e28492. doi: 10.1371/journal.pone.0028492

Jung, J. S., Preston, G. M., Smith, B. L., Guggino, W. B., and Agre, P. (1994). Molecular structure of the water channel through aquaporin CHIP. The hourglass model. *J. Biol. Chem.* 269, 14648–14654.

Kalluri, R., and Weinberg, R. A. (2009). The basics of epithelial-mesenchymal transition. *J. Clin. Invest.* 119:1420. doi: 10.1172/JCI39104

Kaneko, K., Yagui, K., Tanaka, A., Yoshihara, K., Ishikawa, K., Takahashi, K., et al. (2008). Aquaporin 1 is required for hypoxia-inducible angiogenesis in human retinal vascular endothelial cells. *Microvasc. Res.* 75, 297–301. doi: 10.1016/j.mvr.2007.12.003

Kang, B. W., Kim, J. G., Lee, S. J., Chae, Y. S., Jeong, J. Y., Yoon, G. S., et al. (2015). Expression of aquaporin-1, aquaporin-3, and aquaporin-5 correlates with nodal metastasis in colon cancer. *Oncology* 88, 369–376. doi: 10.1159/000369073

Kang, S. K., Chae, Y. K., Woo, J., Kim, M. S., Park, J. C., Lee, J., et al. (2008). Role of human aquaporin 5 in colorectal carcinogenesis. *Am. J. Pathol.* 173, 518–525. doi: 10.2353/ajpath.2008.071198

Klausen, M., Aaes-Jørgensen, A., Molin, S., and Tolker-Nielsen, T. (2003). Involvement of bacterial migration in the development of complex multicellular structures in Pseudomonas aeruginosa biofilms. *Mol. Microbiol.* 50, 61–68. doi: 10.1046/j.1365-2958.2003.03677.x

Klebe, S., Griggs, K., Cheng, Y., Driml, J., Henderson, D. W., and Reid, G. (2015). Blockade of aquaporin 1 inhibits proliferation, motility, and metastatic potential of mesothelioma *in vitro* but not in an *in vivo* model. *Dis. Markers* 2015:286719. doi: 10.1155/2015/286719

Koeller, J. M., Aapro, M. S., Gralla, R. J., Grunberg, S. M., Hesketh, P. J., Kris, M. G., et al. (2002). Antiemetic guidelines: creating a more practical treatment approach. *Support. Care Cancer* 10, 519–522. doi: 10.1007/s00520-001-0335-y

Kong, D., Li, Y., Wang, Z., Banerjee, S., Ahmad, A., Kim, H. R. C., et al. (2009). miR-200 Regulates PDGF-D-mediated epithelial–mesenchymal transition, adhesion, and invasion of prostate cancer cells. *Stem Cells* 27, 1712–1721. doi: 10.1002/stem.101

Korpal, M., Lee, E. S., Hu, G., and Kang, Y. (2008). The miR-200 family inhibits epithelial-mesenchymal transition and cancer cell migration by direct targeting of E-cadherin transcriptional repressors ZEB1 and ZEB2. *J. Biol. Chem.* 283, 14910–14914. doi: 10.1074/jbc.C800074200

Kourghi, M., De Ieso, M. L., Nourmohammadi, S., Pei, J. V., and Yool, A. J. (2018). Identification of loop D domain amino acids in the human Aquaporin-1 channel involved in activation of the ionic conductance and inhibition by AqB011. *Front. Chem.* 6:142. doi: 10.3389/fchem.2018.00142

Kourghi, M., Pei, J. V., De Ieso, M. L., Flynn, G., and Yool, A. J. (2015). Bumetanide derivatives AqB007 and AqB011 selectively block the Aquaporin-1 ion channel conductance and slow cancer cell migration. *Mol. Pharmacol.* 115:101618. doi: 10.1124/mol.115.101618

Kuriyama, H., Shimomura, I., Kishida, K., Kondo, H., Furuyama, N., Nishizawa, H., et al. (2002). Coordinated regulation of fat-specific and liver-specific

glycerol channels, aquaporin adipose and aquaporin 9. *Diabetes* 51, 2915–2921. doi: 10.2337/diabetes.51.10.2915

Kusayama, M., Wada, K., Nagata, M., Ishimoto, S., Takahashi, H., Yoneda, M., et al. (2011). Critical role of aquaporin 3 on growth of human esophageal and oral squamous cell carcinoma. *Cancer Sci.* 102, 1128–1136. doi: 10.1111/j.1349-7006.2011.01927.x

Lee, T.-C., Ho, I.-C., Lu, W.-J., and Huang, J.-D. (2006). Enhanced expression of multidrug resistance-associated protein 2 and reduced expression of aquaglyceroporin 3 in an arsenic-resistant human cell line. *J. Biol. Chem.* 281, 18401–18407. doi: 10.1074/jbc.M601266200

Leung, J., Pang, A., Yuen, W.-H., Kwong, Y.-L., and Tse, E. W. C. (2007). Relationship of expression of aquaglyceroporin 9 with arsenic uptake and sensitivity in leukemia cells. *Blood* 109, 740–746. doi: 10.1182/blood-2006-04-019588

Li, A., Lu, D., Zhang, Y., Li, J., Fang, Y., Li, F., et al. (2013). Critical role of aquaporin-3 in epidermal growth factor-induced migration of colorectal carcinoma cells and its clinical significance. *Oncol. Rep.* 29, 535–540. doi: 10.3892/or.2012.2144

Li, C., and Wang, W. (2017). Molecular biology of aquaporins. *Adv. Exp. Med. Biol.* 969, 1–34. doi: 10.1007/978-94-024-1057-0_1

Li, C.-F., Zhang, W.-G., Liu, M., Qiu, L.-W., Chen, X.-F., Lv, L., et al. (2016). Aquaporin 9 inhibits hepatocellular carcinoma through up-regulating FOXO1 expression. *Oncotarget* 7, 44161–44170. doi: 10.18632/oncotarget.10143

Li, J., Wang, Z., Chong, T., Chen, H., Li, H., Li, G., et al. (2014). Over-expression of a poor prognostic marker in prostate cancer: AQP5 promotes cells growth and local invasion. *World J. Surg. Oncol.* 12:284. doi: 10.1186/1477-7819-12-284

Li, Y. B., Sun, S. R., and Han, X. H. (2016). Down-regulation of AQP4 inhibits proliferation, migration and invasion of human breast cancer cells. *Folia Biol.* 62, 131–137.

Liu, W., Wang, K., Gong, K., Li, X., and Luo, K. (2012). Epidermal growth factor enhances MPC-83 pancreatic cancer cell migration through the upregulation of aquaporin 3. *Mol. Med. Rep.* 6, 607–610. doi: 10.3892/mmr.2012.966

Liu, Y. L., Matsuzaki, T., Nakazawa, T., Murata, S., Nakamura, N., Kondo, T., et al. (2007). Expression of aquaporin 3 (AQP3) in normal and neoplastic lung tissues. *Hum. Pathol.* 38, 171–178. doi: 10.1016/j.humpath.2006.07.015

Liu, Z., Shen, J., Carbrey, J. M., Mukhopadhyay, R., Agre, P., and Rosen, B. P. (2002). Arsenite transport by mammalian aquaglyceroporins AQP7 and AQP9. *Proc. Natl. Acad. Sci. U.S.A.* 99, 6053–6058. doi: 10.1073/pnas.092131899

Lo, H.-W., Hsu, S.-C., Xia, W., Cao, X., Shih, J.-Y., Wei, Y., et al. (2007). Epidermal growth factor receptor cooperates with signal transducer and activator of transcription 3 to induce epithelial-mesenchymal transition in cancer cells via up-regulation of TWIST gene expression. *Cancer Res.* 67, 9066–9076. doi: 10.1158/0008-5472.CAN-07-0575

Loitto, V. M., Huang, C., Sigal, Y. J., and Jacobson, K. (2007). Filopodia are induced by aquaporin-9 expression. *Exp. Cell Res.* 313, 1295–1306. doi: 10.1016/j.yexcr.2007.01.023

Loitto, V.-M., Forslund, T., Sundqvist, T., Magnusson, K.-E., and Gustafsson, M. (2002). Neutrophil leukocyte motility requires directed water influx. *J. Leukoc. Biol.* 71, 212–222. doi: 10.1189/jlb.71.2.212

Ma, B., Xiang, Y., Mu, S.-M., Li, T., Yu, H.-M., and Li, X.-J. (2004a). Effects of acetazolamide and anordiol on osmotic water permeability in AQP1-cRNA injected Xenopus oocyte. *Acta pharmacol. Sin.* 25, 90–97.

Ma, B., Xiang, Y., Li, T., Yu, H.-M., and Li, X.-J. (2004b). Inhibitory effect of topiramate on Lewis lung carcinoma metastasis and its relation with AQP1 water channel. *Acta pharmacol. Sin.* 25, 54–60.

Ma, T., Hara, M., Sougrat, R., Verbavatz, J.-M., and Verkman, A. (2002). Impaired stratum corneum hydration in mice lacking epidermal water channel aquaporin-3. *J. Biol. Chem.* 277, 17147–17153. doi: 10.1074/jbc.M200925200

Ma, T., Song, Y., Gillespie, A., Carlson, E. J., Epstein, C. J., and Verkman, A. (1999). Defective secretion of saliva in transgenic mice lacking aquaporin-5 water channels. *J. Biol. Chem.* 274, 20071–20074. doi: 10.1074/jbc.274.29.20071

Ma, T., Song, Y., Yang, B., Gillespie, A., Carlson, E. J., Epstein, C. J., et al. (2000). Nephrogenic diabetes insipidus in mice lacking aquaporin-3 water channels. *Proc. Natl. Acad. Sci. U.S.A.* 97, 4386–4391. doi: 10.1073/pnas.080499597

Ma, T., Yang, B., and Verkman, A. (1997a). Cloning of a novel water and urea-permeable aquaporin from mouse expressed strongly in colon, placenta, liver, and heart. *Biochem. Biophys. Res. Commun.* 240, 324–328. doi: 10.1006/bbrc.1997.7664

Ma, T., Yang, B., Gillespie, A., Carlson, E. J., Epstein, C. J., and Verkman, A. (1997b). Generation and phenotype of a transgenic knockout mouse lacking the mercurial-insensitive water channel aquaporin-4. *J. Clin. Invest.* 100:957. doi: 10.1172/JCI231

Ma, T., Yang, B., Gillespie, A., Carlson, E. J., Epstein, C. J., and Verkman, A. S. (1998). Severely impaired urinary concentrating ability in transgenic mice lacking aquaporin-1 water channels. *J. Biol. Chem.* 273, 4296–4299. doi: 10.1074/jbc.273.8.4296

Ma, T., Yang, B., Kuo, W.-L., and Verkman, A. S. (1996). cDNA cloning and gene structure of a novel water channel expressed exclusively in human kidney: evidence for a gene cluster of aquaporins at chromosome locus 12q13. *Genomics* 35, 543–550. doi: 10.1006/geno.1996.0396

Machesky, L. M. (2008). Lamellipodia and filopodia in metastasis and invasion. *FEBS Lett.* 582, 2102–2111. doi: 10.1016/j.febslet.2008.03.039

Madeira, A., Fernández-Veledo, S., Camps, M., Zorzano, A., Moura, T. F., Ceperuelo-Mallafré, V., et al. (2014). Human aquaporin-11 is a water and glycerol channel and localizes in the vicinity of lipid droplets in human adipocytes. *Obesity* 22, 2010–2017. doi: 10.1002/oby.20792

Maeda, N., Hibuse, T., and Funahashi, T. (2009). Role of aquaporin-7 and aquaporin-9 in glycerol metabolism; involvement in obesity. *Handb. Exp. Pharmacol.* 2009, 233–249. doi: 10.1007/978-3-540-79885-9_12

Manley, G. T., Fujimura, M., Ma, T., Noshita, N., Filiz, F., Bollen, A. W., et al. (2000). Aquaporin-4 deletion in mice reduces brain edema after acute water intoxication and ischemic stroke. *Nat. Med.* 6, 159–163. doi: 10.1038/72256

Martin, K. H., Slack, J. K., Boerner, S. A., Martin, C. C., and Parsons, J. T. (2002). Integrin connections map: to infinity and beyond. *Science* 296, 1652–1653. doi: 10.1126/science.296.5573.1652

Martins, A. P., Ciancetta, A., de Almeida, A., Marrone, A., Re, N., Soveral, G., et al. (2013). Aquaporin inhibition by gold (III) compounds: new insights. *ChemMedChem* 8, 1086–1092. doi: 10.1002/cmdc.201300107

Martins, A. P., Marrone, A., Ciancetta, A., Cobo, A. G., Echevarría, M., Moura, T. F., et al. (2012). Targeting aquaporin function: potent inhibition of aquaglyceroporin-3 by a gold-based compound. *PLoS ONE* 7:e37435. doi: 10.1371/journal.pone.0037435

Mattila, P. K., and Lappalainen, P. (2008). Filopodia: molecular architecture and cellular functions. *Nat. Rev. Mol. Cell Biol.* 9, 446–454. doi: 10.1038/nrm2406

McCoy, E. S., Haas, B. R., and Sontheimer, H. (2010). Water permeability through aquaporin-4 is regulated by protein kinase C and becomes rate-limiting for glioma invasion. *Neuroscience* 168, 971–981. doi: 10.1016/j.neuroscience.2009.09.020

McCoy, E., and Sontheimer, H. (2007). Expression and function of water channels (aquaporins) in migrating malignant astrocytes. *Glia* 55, 1034–1043. doi: 10.1002/glia.20524

Mcferrin, M. B., and Sontheimer, H. (2006). A role for ion channels in glioma cell invasion. *Neuron Glia Biol.* 2, 39–49. doi: 10.1017/S1740925X06000044

McLean, G. W., Carragher, N. O., Avizienyte, E., Evans, J., Brunton, V. G., and Frame, M. C. (2005). The role of focal-adhesion kinase in cancer—a new therapeutic opportunity. *Nat. Rev. Cancer* 5:505. doi: 10.1038/nrc1647

Medici, D., Hay, E. D., and Olsen, B. R. (2008). Snail and Slug promote epithelial-mesenchymal transition through β-catenin–T-cell factor-4-dependent expression of transforming growth factor-β3. *Mol. Biol. Cell* 19, 4875–4887. doi: 10.1091/mbc.E08-05-0506

Meng, F., Rui, Y., Xu, L., Wan, C., Jiang, X., and Li, G. (2014). Aqp1 enhances migration of bone marrow mesenchymal stem cells through regulation of FAK and beta-catenin. *Stem Cells Dev.* 23, 66–75. doi: 10.1089/scd.2013.0185

Miettinen, P. J., Ebner, R., Lopez, A. R., and Derynck, R. (1994). TGF-beta induced transdifferentiation of mammary epithelial cells to mesenchymal cells: involvement of type I receptors. *J. Cell Biol.* 127, 2021–2036. doi: 10.1083/jcb.127.6.2021

Migliati, E., Meurice, N., DuBois, P., Fang, J. S., Somasekharan, S., Beckett, E., et al. (2009). Inhibition of aquaporin-1 and aquaporin-4 water permeability by a derivative of the loop diuretic bumetanide acting at an internal pore-occluding binding site. *Mol. Pharmacol.* 76, 105–112. doi: 10.1124/mol.108.053744

Miller, E. W., Dickinson, B. C., and Chang, C. J. (2010). Aquaporin-3 mediates hydrogen peroxide uptake to regulate downstream intracellular signaling. *Proc. Natl. Acad. Sci. U.S.A.* 107, 15681–15686. doi: 10.1073/pnas.1005776107

Miller, K. D., Siegel, R. L., Lin, C. C., Mariotto, A. B., Kramer, J. L., Rowland, J. H., et al. (2016). Cancer treatment and survivorship statistics, 2016. *CA. Cancer J. Clin.* 66, 271–289. doi: 10.3322/caac.21349

Mobasheri, A., and Barrett-Jolley, R. (2014). Aquaporin water channels in the mammary gland: from physiology to pathophysiology and neoplasia. *J. Mamm. Gland Biol. Neoplasia* 19, 91–102. doi: 10.1007/s10911-013-9312-6

Monsuez, J.-J., Charniot, J.-C., Vignat, N., and Artigou, J.-Y. (2010). Cardiac side-effects of cancer chemotherapy. *Int. J. Cardiol.* 144, 3–15. doi: 10.1016/j.ijcard.2010.03.003

Monzani, E., Bazzotti, R., Perego, C., and La Porta, C. A. (2009). AQP1 is not only a water channel: it contributes to cell migration through Lin7/beta-catenin. *PLoS ONE* 4:e6167. doi: 10.1371/journal.pone.0006167

Moon, C., Soria, J.-C., Jang, S. J., Lee, J., Hoque, M., Sibony, M., et al. (2003). Involvement of aquaporins in colorectal carcinogenesis. *Oncogene* 22, 6699–6703. doi: 10.1038/sj.onc.1206762

Mott, J. D., and Werb, Z. (2004). Regulation of matrix biology by matrix metalloproteinases. *Curr. Opin. Cell Biol.* 16, 558–564. doi: 10.1016/j.ceb.2004.07.010

Musa-Aziz, R., Chen, L.-M., Pelletier, M. F., and Boron, W. F. (2009). Relative CO2/NH3 selectivities of AQP1, AQP4, AQP5, AmtB, and RhAG. *Proc. Natl. Acad. Sci. U.S.A.* 106, 5406–5411. doi: 10.1073/pnas.0813231106

Nagase, H., and Woessner, J. F. (1999). Matrix metalloproteinases. *J. Biol. Chem.* 274, 21491–21494. doi: 10.1074/jbc.274.31.21491

Nakhoul, N. L., Davis, B. A., Romero, M. F., and Boron, W. F. (1998). Effect of expressing the water channel aquaporin-1 on the CO_2 permeability of *Xenopus oocytes*. *Am. J. Physiol. Cell Physiol.* 274, C543–C548. doi: 10.1152/ajpcell.1998.274.2.C543

Nakhoul, N. L., Hering-Smith, K. S., Abdulnour-Nakhoul, S. M., and Hamm, L. L. (2001). Transport of NH3/NH 4+ in oocytes expressing aquaporin-1. *Am. J. Physiol. Renal Physiol.* 281, F255–F263. doi: 10.1152/ajprenal.2001.281.2.F255

Neely, J. D., Amiry-Moghaddam, M., Ottersen, O. P., Froehner, S. C., Agre, P., and Adams, M. E. (2001). Syntrophin-dependent expression and localization of Aquaporin-4 water channel protein. *Proc. Natl. Acad. Sci. U.S.A.* 98, 14108–14113. doi: 10.1073/pnas.241508198

Netzel-Arnett, S., Hooper, J. D., Szabo, R., Madison, E. L., Quigley, J. P., Bugge, T. H., et al. (2003). Membrane anchored serine proteases: a rapidly expanding group of cell surface proteolytic enzymes with potential roles in cancer. *Cancer Metastasis Rev.* 22, 237–258. doi: 10.1023/A:1023003616848

Ng, W. H., Hy, J. W., Tan, W. L., Liew, D., Lim, T., Ang, B. T., et al. (2009). Aquaporin-4 expression is increased in edematous meningiomas. *J. Clin. Neurosci.* 16, 441–443. doi: 10.1016/j.jocn.2008.04.028

Nicchia, G. P., Srinivas, M., Li, W., Brosnan, C. F., Frigeri, A., and Spray, D. C. (2005). New possible roles for aquaporin-4 in astrocytes: cell cytoskeleton and functional relationship with connexin43. *FASEB J.* 19, 1674–1676. doi: 10.1096/fj.04-3281fje

Nielsen, S., Chou, C.-L., Marples, D., Christensen, E. I., Kishore, B. K., and Knepper, M. A. (1995). Vasopressin increases water permeability of kidney collecting duct by inducing translocation of aquaporin-CD water channels to plasma membrane. *Proc. Natl. Acad. Sci. U.S.A.* 92, 1013–1017. doi: 10.1073/pnas.92.4.1013

Nielsen, S., Smith, B. L., Christensen, E. I., and Agre, P. (1993). Distribution of the aquaporin CHIP in secretory and resorptive epithelia and capillary endothelia. *Proc. Natl. Acad. Sci. U.S.A.* 90, 7275–7279. doi: 10.1073/pnas.90.15.7275

Niemietz, C. M., and Tyerman, S. D. (2002). New potent inhibitors of aquaporins: silver and gold compounds inhibit aquaporins of plant and human origin. *FEBS Lett.* 531, 443–447. doi: 10.1016/S0014-5793(02)03581-0

Nishida, N., Yano, H., Nishida, T., Kamura, T., and Kojiro, M. (2006). Angiogenesis in cancer. *Vasc. Health Risk Manag.* 2, 213–219. doi: 10.2147/vhrm.2006.2.3.213

Njauw, C.-N., Yuan, H., Zheng, L., Yao, M., and Martins-Green, M. (2008). Origin of periendothelial cells in microvessels derived from human microvascular endothelial cells. *Int. J. Biochem. Cell Biol.* 40, 710–720. doi: 10.1016/j.biocel.2007.10.012

Oshio, K., Watanabe, H., Song, Y., Verkman, A., and Manley, G. T. (2005). Reduced cerebrospinal fluid production and intracranial pressure in mice lacking choroid plexus water channel Aquaporin-1. *FASEB J.* 19, 76–78. doi: 10.1096/fj.04-1711fje

Pagan, R., Sánchez, A., Martin, I., Llobera, M., Fabregat, I., and Vilar,ó S. (1999). Effects of growth and differentiation factors on the epithelial-mesenchymal transition in cultured neonatal rat hepatocytes. *J. Hepatol.* 31, 895–904. doi: 10.1016/S0168-8278(99)80292-X

Palecek, S. P., Huttenlocher, A., Horwitz, A. F., and Lauffenburger, D. A. (1998). Physical and biochemical regulation of integrin release during rear detachment of migrating cells. *J. Cell Sci.* 111, 929–940.

Pan, H., Sun, C. C., Zhou, C. Y., and Huang, H. F. (2008). Expression of aquaporin -1 in normal, hyperplasic, and carcinomatous endometria. *Int. J. Gynecol. Obstet.* 101, 239–244. doi: 10.1016/j.ijgo.2007.12.006

Pan, X. Y., Guo, H., Han, J., Hao, F., An, Y., Xu, Y., et al. (2012). Ginsenoside Rg3 attenuates cell migration via inhibition of aquaporin 1 expression in PC-3M prostate cancer cells. *Eur. J. Pharmacol.* 683, 27–34. doi: 10.1016/j.ejphar.2012.02.040

Papadopoulos, M. C., Saadoun, S., and Verkman, A. S. (2008). Aquaporins and cell migration. *Pflug Arch. Eur. J. Phys.* 456, 693–700. doi: 10.1007/s00424-007-0357-5

Pei, J. V., Kourghi, M., De Ieso, M. L., Campbell, E. M., Dorward, H. S., Hardingham, J. E., et al. (2016). Differential Inhibition of water and ion channel activities of mammalian aquaporin-1 by two structurally related bacopaside compounds derived from the medicinal plant *Bacopa monnieri*. *Mol. Pharmacol.* 90, 496–507. doi: 10.1124/mol.116.105882

Pelagalli, A., Nardelli, A., Fontanella, R., and Zannetti, A. (2016). Inhibition of AQP1 hampers osteosarcoma and hepatocellular carcinoma progression mediated by bone marrow-derived mesenchymal stem cells. *Int. J. Mol. Sci.* 17, 1102. doi: 10.3390/ijms17071102

Pepper, M. S., Tille, J.-C., Nisato, R., and Skobe, M. (2003). Lymphangiogenesis and tumor metastasis. *Cell Tissue Res.* 314, 167–177. doi: 10.1007/s00441-003-0748-7

Pierini, L. M., Lawson, M. A., Eddy, R. J., Hendey, B., and Maxfield, F. R. (2000). Oriented endocytic recycling of α5β1 in motile neutrophils. *Blood* 95, 2471–2480.

Pollard, T. D., and Borisy, G. G. (2003). Cellular motility driven by assembly and disassembly of actin filaments. *Cell* 112, 453–465. doi: 10.1016/S0092-8674(03)00120-X

Preston, G. M., and Agre, P. (1991). Isolation of the cDNA for erythrocyte integral membrane protein of 28 kilodaltons: member of an ancient channel family. *Proc. Natl. Acad. Sci. U.S.A.* 88, 11110–11114. doi: 10.1073/pnas.88.24.11110

Preston, G. M., Carroll, T. P., Guggino, W. B., and Agre, P. (1992). Appearance of water channels in *Xenopus oocytes* expressing red cell CHIP28 protein. *Science* 256, 385–387. doi: 10.1126/science.256.5055.385

Preston, G. M., Jung, J. S., Guggino, W. B., and Agre, P. (1993). The mercury-sensitive residue at cysteine 189 in the CHIP28 water channel. *J. Biol. Chem.* 268, 17–20.

Price, L. S., Leng, J., Schwartz, M. A., and Bokoch, G. M. (1998). Activation of Rac and Cdc42 by integrins mediates cell spreading. *Mol. Biol. Cell* 9, 1863–1871. doi: 10.1091/mbc.9.7.1863

Raina, S., Preston, G. M., Guggino, W. B., and Agre, P. (1995). Molecular cloning and characterization of an aquaporin cDNA from salivary, lacrimal, and respiratory tissues. *J. Biol. Chem.* 270, 1908–1912. doi: 10.1074/jbc.270.4.1908

Rhee, S. G. (2006). H_2O_2, a necessary evil for cell signaling. *Science* 312, 1882–1883. doi: 10.1126/science.1130481

Ridley, A. J., Paterson, H. F., Johnston, C. L., Diekmann, D., and Hall, A. (1992). The small GTP-binding protein rac regulates growth factor-induced membrane ruffling. *Cell* 70, 401–410. doi: 10.1016/0092-8674(92)90164-8

Ridley, A. J., Schwartz, M. A., Burridge, K., Firtel, R. A., Ginsberg, M. H., Borisy, G., et al. (2003). Cell migration: integrating signals from front to back. *Science* 302, 1704–1709. doi: 10.1126/science.1092053

Rivera, E., and Cianfrocca, M. (2015). Overview of neuropathy associated with taxanes for the treatment of metastatic breast cancer. *Cancer Chemother. Pharmacol.* 75, 659–670. doi: 10.1007/s00280-014-2607-5

Rodrigues, C., Mósca, A. F., Martins, A. P., Nobre, T., Prista, C., Antunes, F., et al. (2016). Rat Aquaporin-5 is pH-Gated induced by phosphorylation and is implicated in oxidative stress. *Int. J. Mol. Sci.* 17:2090. doi: 10.3390/ijms17122090

Rojek, A. M., Skowronski, M. T., Füchtbauer, E.-M., Füchtbauer, A. C., Fenton, R. A., Agre, P., et al. (2007). Defective glycerol metabolism in aquaporin 9 (AQP9) knockout mice. *Proc. Natl. Acad. Sci. U.S.A.* 104, 3609–3614. doi: 10.1073/pnas.0610894104

Rojek, A., Füchtbauer, E.-M., Kwon, T.-H., Frøkiaer, J., and Nielsen, S. (2006). Severe urinary concentrating defect in renal collecting duct-selective AQP2 conditional-knockout mice. *Proc. Natl. Acad. Sci. U.S.A.* 103, 6037–6042. doi: 10.1073/pnas.0511324103

Rojek, A., Praetorius, J., Frøkiaer, J., Nielsen, S., and Fenton, R. A. (2008). A current view of the mammalian aquaglyceroporins. *Annu. Rev. Physiol.* 70, 301–327. doi: 10.1146/annurev.physiol.70.113006.100452

Roussos, E. T., Condeelis, J. S., and Patsialou, A. (2011). Chemotaxis in cancer. *Nat. Rev. Cancer* 11:573. doi: 10.1038/nrc3078

Saadoun, S., Papadopoulos, M. C., Hara-Chikuma, M., and Verkman, A. (2005a). Impairment of angiogenesis and cell migration by targeted aquaporin-1 gene disruption. *Nature* 434:786. doi: 10.1038/nature03460

Saadoun, S., Papadopoulos, M. C., Watanabe, H., Yan, D., Manley, G. T., and Verkman, A. (2005b). Involvement of aquaporin-4 in astroglial cell migration and glial scar formation. *J. Cell Sci.* 118, 5691–5698. doi: 10.1242/jcs.02680

Saadoun, S., Papadopoulos, M. C., Davies, D. C., Bell, B., and Krishna, S. (2002a). Increased aquaporin 1 water channel expression inhuman brain tumours. *Br. J. Cancer* 87, 621–623. doi: 10.1038/sj.bjc.6600512

Saadoun, S., Papadopoulos, M. C., Davies, D. C., Krishna, S., and Bell, B. A. (2002b). Aquaporin-4 expression is increased in oedematous human brain tumours. *J. Neurol. Neurosurg. Psychiatr.* 72, 262–265. doi: 10.1136/jnnp.72.2.262

Saparov, S. M., Kozono, D., Rothe, U., Agre, P., and Pohl, P. (2001). Water and ion permeation of aquaporin-1 in planar lipid bilayers. Major differences in structural determinants and stoichiometry. *J. Biol. Chem.* 276, 31515–31520. doi: 10.1074/jbc.M104267200

Saparov, S. M., Liu, K., Agre, P., and Pohl, P. (2007). Fast and selective ammonia transport by aquaporin-8. *J. Biol. Chem.* 282, 5296–5301. doi: 10.1074/jbc.M609343200

Satooka, H., and Hara-Chikuma, M. (2016). Aquaporin-3 controls breast cancer cell migration by regulating hydrogen peroxide transport and its downstream cell signaling. *Mol. Cell. Biol.* 36, 1206–1218. doi: 10.1128/MCB.00971-15

Schaller, M. D., Borgman, C. A., Cobb, B. S., Vines, R. R., Reynolds, A. B., and Parsons, J. T. (1992). pp125FAK a structurally distinctive protein-tyrosine kinase associated with focal adhesions. *Proc. Natl. Acad. Sci. U.S.A.* 89, 5192–5196. doi: 10.1073/pnas.89.11.5192

Schnermann, J., Chou, C.-I., Ma, T., Traynor, T., Knepper, M. A., and Verkman, A. S. (1998). Defective proximal tubular fluid reabsorption in transgenic aquaporin-1 null mice. *Proc. Natl. Acad. Sci. U.S.A.* 95, 9660–9664. doi: 10.1073/pnas.95.16.9660

Schwab, A., Nechyporuk-Zloy, V., Fabian, A., and Stock, C. (2007). Cells move when ions and water flow. *Pflug. Arch. Eur. J. Phys.* 453, 421–432. doi: 10.1007/s00424-006-0138-6

Seeliger, D., Zapater, C., Krenc, D., Haddoub, R., Flitsch, S., Beitz, E., et al. (2012). Discovery of novel human aquaporin-1 blockers. *ACS Chem. Biol.* 8, 249–256. doi: 10.1021/cb300153z

Sekine, S., Okumura, T., Nagata, T., Shibuya, K., Yoshioka, I., Matsui, K., et al. (2016). Expression analysis of aquaporin-1 (Aqp-1) in human biliary tract carcinoma. *J. Cancer Ther.* 7:17. doi: 10.4236/jct.2016.71003

Serna, A., Galán-Cobo, A., Rodrigues, C., Sánchez-Gomar, I., Toledo-Aral, J. J., Moura, T. F., et al. (2014). Functional inhibition of Aquaporin-3 with a gold-based compound induces blockage of cell proliferation. *J. Cell. Physiol.* 229, 1787–1801. doi: 10.1002/jcp.24632

Shen, L., Zhu, Z., Huang, Y., Shu, Y., Sun, M., Xu, H., et al. (2010). Expression profile of multiple aquaporins in human gastric carcinoma and its clinical significance. *Biomed. Pharmacother.* 64, 313–318. doi: 10.1016/j.biopha.2009.12.003

Shi, Y.-H., Chen, R., Talafu, T., Nijiati, R., and Lalai, S. (2012). Significance and expression of aquaporin 1, 3, 8 in cervical carcinoma in Xinjiang Uygur women of China. *Asian Pac. J. Cancer Prev.* 13, 1971–1975. doi: 10.7314/APJCP.2012.13.5.1971

Shi, Y.-H., Rehemu, N., Ma, H., Tuokan, T., Chen, R., and Suzuke, L. (2013). Increased migration and local invasion potential of SiHa cervical cancer cells expressing Aquaporin 8. *Asian Pac. J. Cancer Prev.* 14, 1825–1828. doi: 10.7314/APJCP.2013.14.3.1825

Shi, Y.-H., Tuokan, T., Lin, C., and Chang, H. (2014). Aquaporin 8 involvement in human cervical cancer SiHa migration via the EGFR-Erk1/2 pathway. *Asian Pac. J. Cancer Prev.* 15, 6391–6395. doi: 10.7314/APJCP.2014.15.15.6391

Søgaard, R., and Zeuthen, T. (2008). Test of blockers of AQP1 water permeability by a high-resolution method: no effects of tetraethylammonium ions or acetazolamide. *Pflüg. Arch. Eur. J. Physiol.* 456, 285–292. doi: 10.1007/s00424-007-0392-2

Song, Y., and Verkman, A. (2001). Aquaporin-5 dependent fluid secretion in airway submucosal glands. *J. Biol. Chem.* 276, 41288–41292. doi: 10.1074/jbc.M107257200

Spano, D., Heck, C., De Antonellis, P., Christofori, G., and Zollo, M. (2012). Molecular networks that regulate cancer metastasis. *Semin. Cancer Biol.* 22, 234–249. doi: 10.1016/j.semcancer.2012.03.006

Stroka, K. M., Jiang, H., Chen, S.-H., Tong, Z., Wirtz, D., Sun, S. X., et al. (2014). Water permeation drives tumor cell migration in confined microenvironments. *Cell* 157, 611–623. doi: 10.1016/j.cell.2014.02.052

Sudo, K., Ito, H., Iwamoto, I., Morishita, R., Asano, T., and Nagata, K.-,i (2006). Identification of a cell polarity-related protein, Lin-7B, as a binding partner for a Rho effector, Rhotekin, and their possible interaction in neurons. *Neurosci. Res.* 56, 347–355. doi: 10.1016/j.neures.2006.08.003

Sui, H., Han, B.-G., Lee, J. K., Walian, P., and Jap, B. K. (2001). Structural basis of water-specific transport through the AQP1 water channel. *Nature* 414, 872–878. doi: 10.1038/414872a

Suzuki, R., Okuda, M., Asai, J., Nagashima, G., Itokawa, H., Matsunaga, A., et al. (2006). Astrocytes co-express aquaporin-1,-4, and vascular endothelial growth factor in brain edema tissue associated with brain contusion. *Acta Neurochir. Suppl.* 96, 398–401. doi: 10.1007/3-211-30714-1_82

Swaney, K. F., Huang, C.-H., and Devreotes, P. N. (2010). Eukaryotic chemotaxis: a network of signaling pathways controls motility, directional sensing, and polarity. *Annu. Rev. Biophys.* 39:265. doi: 10.1146/annurev.biophys.093008.131228

Tan, D. S., Agarwal, R., and Kaye, S. B. (2006). Mechanisms of transcoelomic metastasis in ovarian cancer. *Lancet Oncol.* 7, 925–934. doi: 10.1016/S1470-2045(06)70939-1

Tan, G., Sun, S. Q., and Yuan, D. L. (2008). Expression of the water channel protein aquaporin-9 in human astrocytic tumours: correlation with pathological grade. *J. Int. Med. Res.* 36, 777–782. doi: 10.1177/147323000803600420

Tanaka, A., Sakurai, K., Kaneko, K., Ogino, J., Yagui, K., Ishikawa, K., et al. (2011). The role of the hypoxia-inducible factor 1 binding site in the induction of aquaporin-1 mRNA expression by hypoxia. *DNA Cell Biol.* 30, 539–544. doi: 10.1089/dna.2009.1014

Tanimura, Y., Hiroaki, Y., and Fujiyoshi, Y. (2009). Acetazolamide reversibly inhibits water conduction by aquaporin-4. *J. Struct. Biol.* 166, 16–21. doi: 10.1016/j.jsb.2008.11.010

Thannickal, V. J., and Fanburg, B. L. (2000). Reactive oxygen species in cell signaling. *Am. J. Physiol. Lung Cell. Mol. Physiol.* 279, L1005–L1028. doi: 10.1152/ajplung.2000.279.6.L1005

Theriot, J. A., and Mitchison, T. J. (1991). Actin microfilament dynamics in locomoting cells. *Nature* 352, 126–131. doi: 10.1038/352126a0

Thiery, J. P. (2002). Epithelial–mesenchymal transitions in tumour progression. *Nat. Rev. Cancer* 2, 442–454. doi: 10.1038/nrc822

Thiery, J. P. (2003). Epithelial–mesenchymal transitions in development and pathologies. *Curr. Opin. Cell Biol.* 15, 740–746. doi: 10.1016/j.ceb.2003.10.006

Tie, L., Lu, N., Pan, X.-Y., Pan, Y., An, Y., Gao, J.-W., et al. (2012). Hypoxia-induced up-regulation of aquaporin-1 protein in prostate cancer cells in a p38-dependent manner. *Cell. Physiol. Biochem.* 29, 269–280. doi: 10.1159/000337608

Tsukaguchi, H., Shayakul, C., Berger, U. V., Mackenzie, B., Devidas, S., Guggino, W. B., et al. (1998). Molecular characterization of a broad selectivity neutral solute channel. *J. Biol. Chem.* 273, 24737–24743. doi: 10.1074/jbc.273.38.24737

Tsunoda, S. P., Wiesner, B., Lorenz, D., Rosenthal, W., and Pohl, P. (2004). Aquaporin-1, nothing but a water channel. *J. Biol. Chem.* 279, 11364–11367. doi: 10.1074/jbc.M310881200

Vacca, A., Frigeri, A., Ribatti, D., Nicchia, G. P., Nico, B., Ria, R., et al. (2001). Microvessel overexpression of aquaporin 1 parallels bone marrow angiogenesis in patients with active multiple myeloma. *Br. J. Haematol.* 113, 415–421. doi: 10.1046/j.1365-2141.2001.02738.x

van Zijl, F., Krupitza, G., and Mikulits, W. (2011). Initial steps of metastasis: cell invasion and endothelial transmigration. *Mutat.Res.* 728, 23–34. doi: 10.1016/j.mrrev.2011.05.002

Verkman, A. (2005). More than just water channels: unexpected cellular roles of aquaporins. *J. Cell Sci.* 118, 3225–3232. doi: 10.1242/jcs.02519

Verkman, A. S., Anderson, M. O., and Papadopoulos, M. C. (2014). Aquaporins: important but elusive drug targets. *Nat. Rev. Drug Discov.* 13, 259–277. doi: 10.1038/nrd4226

Verkman, A. S., and Mitra, A. K. (2000). Structure and function of aquaporin water channels. *Am. J. Physiol. Renal Physiol.* 278, F13–F28. doi: 10.1152/ajprenal.2000.278.1.F13

Vicent, S., López-Picazo, J. M., Toledo, G., Lozano, M. D., Torre, W., Garcia-Corchón, C., et al. (2004). ERK1/2 is activated in non-small-cell lung cancer and associated with advanced tumours. *Br. J. Cancer* 90:1047. doi: 10.1038/sj.bjc.6601644

Vicente-Manzanares, M., and Horwitz, A. R. (2011). Cell migration: an overview. *Methods Mol. Biol.* 769, 1–24. doi: 10.1007/978-1-61779-207-6_1

Vicente-Manzanares, M., Ma, X., Adelstein, R. S., and Horwitz, A. R. (2009). Non-muscle myosin II takes centre stage in cell adhesion and migration. *Nat. Rev. Mol. Cell Biol.* 10, 778–790. doi: 10.1038/nrm2786

Vičovac, L., and Aplin, J. (1996). Epithelial-mesenchymal transition during trophoblast differentiation. *Cells Tissues Organs* 156, 202–216. doi: 10.1159/000147847

Wang, W., Li, Q., Yang, T., Bai, G., Li, D., Li, Q., et al. (2012). Expression of AQP5 and AQP8 in human colorectal carcinoma and their clinical significance. *World J. Surg. Oncol.* 10:242. doi: 10.1186/1477-7819-10-242

Wang, Y.-L. (1985). Exchange of actin subunits at the leading edge of living fibroblasts: possible role of treadmilling. *J. Cell Biol.* 101, 597–602. doi: 10.1083/jcb.101.2.597

Wasilewski-Masker, K., Seidel, K. D., Leisenring, W., Mertens, A. C., Shnorhavorian, M., Ritenour, C. W., et al. (2014). Male infertility in long-term survivors of pediatric cancer: a report from the childhood cancer survivor study. *J. Cancer Survivorship* 8, 437–447. doi: 10.1007/s11764-014-0354-6

Watanabe, S., Moniaga, C. S., Nielsen, S., and Hara-Chikuma, M. (2016). Aquaporin-9 facilitates membrane transport of hydrogen peroxide in mammalian cells. *Biochem. Biophys. Res. Commun.* 471, 191–197. doi: 10.1016/j.bbrc.2016.01.153

Weaver, A. M. (2006). Invadopodia: specialized cell structures for cancer invasion. *Clin. Exp. Metastasis* 23, 97–105. doi: 10.1007/s10585-006-9014-1

Wei, X., and Dong, J. (2015). Aquaporin 1 promotes the proliferation and migration of lung cancer cell *in vitro*. *Oncol. Rep.* 34, 1440–1448. doi: 10.3892/or.2015.4107

Willemse, P., Burggraaf, J., Hamdy, N., Weijl, N., Vossen, C., Van Wulften, L., et al. (2013). Prevalence of the metabolic syndrome and cardiovascular disease risk in chemotherapy-treated testicular germ cell tumour survivors. *Br. J. Cancer* 109, 60–67. doi: 10.1038/bjc.2013.226

Wolf, K., Wu, Y. I., Liu, Y., Geiger, J., Tam, E., Overall, C., et al. (2007). Multi-step pericellular proteolysis controls the transition from individual to collective cancer cell invasion. *Nat. Cell Biol.* 9, 893–904. doi: 10.1038/ncb1616

Wu, B., Altmann, K., Barzel, I., Krehan, S., and Beitz, E. (2008). A yeast-based phenotypic screen for aquaporin inhibitors. *Pflüg. Arch. Eur. J. Physiol.* 456, 717–720. doi: 10.1007/s00424-007-0383-3

Wyckoff, J. B., Jones, J. G., Condeelis, J. S., and Segall, J. E. (2000). A critical step in metastasis: *in vivo* analysis of intravasation at the primary tumor. *Cancer Res.* 60, 2504–2511.

Xia, H., Ma, Y. F., Yu, C. H., Li, Y. J., Tang, J., Li, J. B., et al. (2014). Aquaporin 3 knockdown suppresses tumour growth and angiogenesis in experimental non-small cell lung cancer. *Exp. Physiol.* 99, 974–984. doi: 10.1113/expphysiol.2014.078527

Xiang, Y., Ma, B., Li, T., Gao, J.-W., Yu, H.-M., and Li, X.-J. (2004). Acetazolamide inhibits aquaporin-1 protein expression and angiogenesis. *Acta Pharmacol. Sin.* 25, 812–816.

Xiang, Y., Ma, B., Li, T., Yu, H.-M., and Li, X.-J. (2002). Acetazolamide suppresses tumor metastasis and related protein expression in mice bearing Lewis lung carcinoma. *Acta Pharmacol. Sin.* 23, 745–751.

Xiong, G., Chen, X., Zhang, Q., Fang, Y., Chen, W., Li, C., et al. (2017). RNA interference influenced the proliferation and invasion of XWLC-05 lung cancer cells through inhibiting aquaporin 3. *Biochem. Biophys. Res. Commun.* 485, 627–634. doi: 10.1016/j.bbrc.2017.02.013

Xu, H., Xu, Y., Zhang, W., Shen, L., Yang, L., and Xu, Z. (2011). Aquaporin-3 positively regulates matrix metalloproteinases via PI3K/AKT signal pathway in human gastric carcinoma SGC7901 cells. *Nat. Rev. Cancer* 30:86. doi: 10.1186/1756-9966-30-86

Xu, J., Lamouille, S., and Derynck, R. (2009). TGF-β-induced epithelial to mesenchymal transition. *Cell Res.* 19, 156–172. doi: 10.1038/cr.2009.5

Yakata, K., Tani, K., and Fujiyoshi, Y. (2011). Water permeability and characterization of aquaporin-11. *J. Struct. Biol.* 174, 315–320. doi: 10.1016/j.jsb.2011.01.003

Yamaguchi, H., Wyckoff, J., and Condeelis, J. (2005). Cell migration in tumors. *Curr. Opin. Cell Biol.* 17, 559–564. doi: 10.1016/j.ceb.2005.08.002

Yamamoto, T., Kuramoto, H., and Kadowaki, M. (2007). Downregulation in aquaporin 4 and aquaporin 8 expression of the colon associated with the induction of allergic diarrhea in a mouse model of food allergy. *Life Sci.* 81, 115–120. doi: 10.1016/j.lfs.2007.04.036

Yang, B., and Verkman, A. (1997). Water and glycerol permeabilities of aquaporins 1–5 and MIP determined quantitatively by expression of epitope-tagged constructs inXenopus oocytes. *J. Biol. Chem.* 272, 16140–16146. doi: 10.1074/jbc.272.26.16140

Yang, B., Fukuda, N., van Hoek, A., Matthay, M. A., Ma, T., and Verkman, A. (2000). Carbon dioxide permeability of aquaporin-1 measured in erythrocytes and lung of aquaporin-1 null mice and in reconstituted proteoliposomes. *J. Biol. Chem.* 275, 2686–2692. doi: 10.1074/jbc.275.4.2686

Yang, B., Kim, J. K., and Verkman, A. (2006). Comparative efficacy of HgCl2 with candidate aquaporin-1 inhibitors DMSO, gold, TEA+ and acetazolamide. *FEBS Lett.* 580, 6679–6684. doi: 10.1016/j.febslet.2006.11.025

Yang, J., Mani, S. A., Donaher, J. L., Ramaswamy, S., Itzykson, R. A., Come, C., et al. (2004). Twist, a master regulator of morphogenesis, plays an essential role in tumor metastasis. *Cell* 117, 927–939. doi: 10.1016/j.cell.2004.06.006

Yasui, M., Hazama, A., Kwon, T.-H., Nielsen, S., Guggino, W. B., and Agre, P. (1999). Rapid gating and anion permeability of an intracellular aquaporin. *Nature* 402, 184–187. doi: 10.1038/46045

Yool, A. J. (2007). Functional domains of aquaporin-1: keys to physiology, and targets for drug discovery. *Curr. Pharm. Des.* 13, 3212–3221. doi: 10.2174/138161207782341349

Yool, A. J., Brokl, O. H., Pannabecker, T. L., Dantzler, W. H., and Stamer, W. D. (2002). Tetraethylammonium block of water flux in Aquaporin-1 channels expressed in kidney thin limbs of Henle's loop and a kidney-derived cell line. *BMC Physiol.* 2:4. doi: 10.1186/1472-6793-2-4

Yool, A. J., Stamer, W. D., and Regan, J. W. (1996). Forskolin stimulation of water and cation permeability in aquaporin-1 water channels. *Science* 273, 1216–1218. doi: 10.1126/science.273.5279.1216

Yu, J., Yool, A. J., Schulten, K., and Tajkhorshid, E. (2006). Mechanism of gating and ion conductivity of a possible tetrameric pore in aquaporin-1. *Structure* 14, 1411–1423. doi: 10.1016/j.str.2006.07.006

Yun, S., Sun, P.-L., Jin, Y., Kim, H., Park, E., Park, S. Y., et al. (2016). Aquaporin 1 is an independent marker of poor prognosis in lung adenocarcinoma. *J. Pathol. Transl. Med.* 50:251. doi: 10.4132/jptm.2016.03.30

Zelenina, M., Bondar, A. A., Zelenin, S., and Aperia, A. (2003). Nickel and extracellular acidification inhibit the water permeability of human aquaporin-3 in lung epithelial cells. *J. Biol. Chem.* 278, 30037–30043. doi: 10.1074/jbc.M302206200

Zelenina, M., Tritto, S., Bondar, A. A., Zelenin, S., and Aperia, A. (2004). Copper inhibits the water and glycerol permeability of aquaporin-3. *J. Biol. Chem.* 279, 51939–51943. doi: 10.1074/jbc.M407645200

Zhang, D., Vetrivel, L., and Verkman, A. (2002). Aquaporin deletion in mice reduces intraocular pressure and aqueous fluid production. *J. Gen. Physiol.* 119:561–569. doi: 10.1085/jgp.20028597

Zhang, H., and Verkman, A. (2008). Evidence against involvement of aquaporin-4 in cell–cell adhesion. *J. Mol. Biol.* 382, 1136–1143. doi: 10.1016/j.jmb.2008.07.089

Zhang, H., and Verkman, A. S. (2010). Aquaporin-1 tunes pain perception by interaction with Nav1. 8 Na+ channels in dorsal root ganglion neurons. *J. Biol. Chem.* 285, 5896–5906. doi: 10.1074/jbc.M109.090233

Zhang, T., Zhao, C., Chen, D., and Zhou, Z. (2012). Overexpression of AQP5 in cervical cancer: correlation with clinicopathological features and prognosis. *Med. Oncol.* 29, 1998–2004. doi: 10.1007/s12032-011-0095-6

Zhang, W.-G, Li, C.-F, Liu, M., Chen, X.-F, Shuai, K., Kong, X., et al. (2016). Aquaporin 9 is down-regulated in hepatocellular carcinoma and its over-expression suppresses hepatoma cell invasion through

inhibiting epithelial-to-mesenchymal transition. *Cancer Lett.* 378, 111–119. doi: 10.1016/j.canlet.2016.05.021

Zhang, Z., Chen, Z., Song, Y., Zhang, P., Hu, J., and Bai, C. (2010). Expression of aquaporin 5 increases proliferation and metastasis potential of lung cancer. *J. Pathol.* 221, 210–220. doi: 10.1002/path.2702

Zhao, X., and Guan, J.-L. (2011). Focal adhesion kinase and its signaling pathways in cell migration and angiogenesis. *Adv. Drug Deliv. Rev.* 63, 610–615. doi: 10.1016/j.addr.2010.11.001

Zou, L.-B., Shi, S., Zhang, R.-J., Wang, T.-T., Tan, Y.-J., Zhang, D., et al. (2013). Aquaporin-1 plays a crucial role in estrogen-induced tubulogenesis of vascular endothelial cells. *J. Clin. Endocrinol. Metab.* 98, E672–E682. doi: 10.1210/jc.2012-4081

Zou, L.-B., Zhang, R.-J., Tan, Y.-J., Ding, G.-L., Shi, S., Zhang, D., et al. (2011). Identification of estrogen response element in theaquaporin-2 gene that mediates estrogen-induced cell migration and invasion in human endometrial carcinoma. *J. Clin. Endocrinol. Metab.* 96, E1399–E1408. doi: 10.1210/jc.2011-0426

Conflict of Interest Statement: The authors declare that the research was conducted in the absence of any commercial or financial relationships that could be construed as a potential conflict of interest.

Bioscience Reports (2018) **38** BSR20180698
https://doi.org/10.1042/BSR20180698

Review Article

An accurate and cost-effective alternative method for measuring cell migration with the circular wound closure assay

Michael L. De Ieso and Jinxin Victor Pei

Department of Physiology, Adelaide Medical School, University of Adelaide, Adelaide, SA 5005, Australia

Correspondence: Jinxin Pei (jinxin.pei@adelaide.edu.au)

Cell migration is important in many physiological and pathological processes. Mechanisms of two-dimensional cell migration have been investigated most commonly by evaluating rates of cell migration into linearly scratched zones on the surfaces of culture plates. Here, we present a detailed description of a simple adaptation for the well-known and popular wound closure assay, using a circular wound instead of a straight line. This method demonstrates improved precision, reproducibility, and sampling objectivity for measurements of wound sizes as compared with classic scratch assays, enabling more accurate calculations of migration rate. The added benefits of the method are simplicity and low cost as compared with commercially available assays for generating circular wounds.

Introduction

Cell migration is a multistep process that is essential for diverse life functions in multicellular and single-celled organisms, and includes both collective and individual cell movements across extracellular spaces or through tissues [1,2]. In normal physiological processes, migration enables morphogenesis, immunity, and tissue repair [2,3]; in pathological processes, migration has been linked to cancer, atherosclerosis, rheumatoid arthritis, multiple sclerosis, and others [4-9]. Understanding the mechanisms of cell migration could facilitate the development of therapeutic interventions for a wide range of diseases.

Existing literature provides a comprehensive comparison of advantages and disadvantages of approaches for measuring two-dimensional (2D) cell migration [10]. A technique commonly used for measuring 2D cell migration is the scratch wound assay. In brief, the 2D scratch wound assay involves creating a linear 'scratch' or wound across a confluent monolayer of cultured cells, and capturing images to measure cell migration rate by the decrease in distance across the open wound as a function of time [11,12]. Though useful, the 2D scratch wound assay has disadvantages (summarized in Table 1), stemming primarily from the fact that the scratch wound is usually longer (but not wider) than the field of view used during analysis. Without live-cell imaging facilities (to capture images in identical locations at repeated intervals), experimenters are faced with the challenge of recapturing the same position on the scratch at multiple time points without subjective error. This is especially difficult for high-throughput assays with multiwell plates, and is likely to result in reduced reproducibility of results. A second disadvantage is that typically scratch wound images are quantitated by visually estimating the positions of the boundaries of the scratch, assuming lines to approximate the walls, and measuring the distances across the gap. Manually taking multiple measurements of the gap distances at various locations is intended to reduce variability by generating an average value of the distance across the scratch [13], but the reliability is handicapped by the fact that the boundary edges are ragged; the selected positions for the boundaries will vary between samples and within samples. Analyses with the classic scratch method must be done blinded to reduce the risk of unintentional bias in the acquisition of data. Improvements on the method

Received: 06 May 2018
Revised: 28 August 2018
Accepted: 10 September 2018

Accepted Manuscript Online: 19 September 2018
Version of Record published: 31 October 2018

Bioscience Reports (2018) **38** BSR20180698
https://doi.org/10.1042/BSR20180698

Table 1 Summary of assays used previously for measuring 2D cell migration, including advantages and disadvantages

Assay	Method	Advantages	Disadvantages	Diagram
Scratch wound assay	(1) Generate confluent monolayer of cells (2) Use pipette tip to scratch a portion of cells away, leaving a 'wound'	• Cost effective • Minimal equipment required	• Difficult to relocate exact wound sites at sequential time points without expensive live-cell imaging facilities, reducing accuracy of results	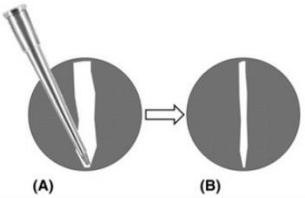
Cell exclusion zone assay with stopper	(1) Insert stopper in well prior to seeding cells (2) Allow cells to grow around the stopper (3) Remove stopper to expose circular wound	• Consistent initial wound size • High throughput • Semi-automatic	• High cost • Technically complex • Unknown effects of stopper-derived components on cell properties	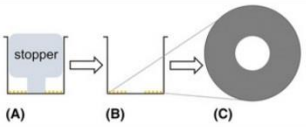
Cell exclusion zone assay with biocompatible gel	(1) Apply gel in the center of each well prior to seeding cells (2) Allow cells to grow around the gel (3) Remove gel to expose circular wound	• Consistent initial wound size	• High cost • Gel needs to be manually removed, which may alter cell or substrate properties • Low throughput (24 wells per assay)	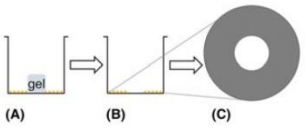

have used image analysis software to find lines of best fit to measure the boundaries or areas of wounds [14,15], but the scratch method is still vulnerable to variability in the image locations selected at each time point. The third consideration is that most studies with the 2D scratch wound assay have not accounted for the potentially confounding effects of cell proliferation on the apparent rate of closure of the wound, a factor that might not be addressed fully by a 'serum-starvation' step prior to commencing the assay [16-18].

The concept for generating a circular wound for measuring 2D cell migration has been previously established [19-21]. The circular wound closure assay (CWCA) permits the analyst to easily relocate the wound at any time point, and it enables accurate analysis by calculating the area or the radius of the circular wound using image analysis software. Current techniques to generate circular wounds, such as exclusion zone assays, [22] involve growing the cells around circular barriers (poly-dimethylsiloxane micropillars, stoppers, or biocompatible gels) of uniform size [21], or using a stabilized, rotating, silicone-tipped drill press to create uniform, circular wounds in an intact confluent monolayer of cells (Table 1) [19]. One advantage to these techniques is that they can generate highly consistent initial wounds; however, they are more complex and costlier than the CWCA described here. The CWCA uses a sterile 10 µl (P10) micropipette tip attached to an aspirator to remove a small circular area of cells (Figure 1). The complete wound can be reliably relocated for manual or automatic imaging at all subsequent time points. Processing images of circular wounds for analysis can be done with the freely available cross-platform Fiji (ImageJ) software [23]. Use of a mitotic inhibitor minimizes confounding effects of proliferation on apparent wound closure rates; this step is optional depending on cell type and assay duration. In summary, with this protocol easily relocatable, clean, sufficiently uniform circular wounds can be generated in diverse cell lines (Figure 2) that are amenable to streamlined computer-assisted data analysis, without costly equipment or reagents. These modifications reduce the cost and simplify the analysis of *in vitro* cell migration assays.

Materials and methodology

Cell lines

Lines used for the present study were: (1) human colorectal adenocarcinoma HT29 (supplied by the American Type Culture Collection (ATCC®), catalog number HTB-38™), and SW480 (ATCC®, catalog number CCL-228™); (2) human glioblastoma cell line U251-MG (supplied by the European Collection of Cell Cultures [ECACC; Salisbury, U.K.], catalog number 09063001 purchased from CellBank Australia [Westmead, NSW, Australia]); (3) mammary adenocarcinoma MDA-MB-231 (ATCC®, catalog number HTB-26™); and (4) human embryonic kidney HEK-293 (ATCC®, catalog number CRL-1573™).

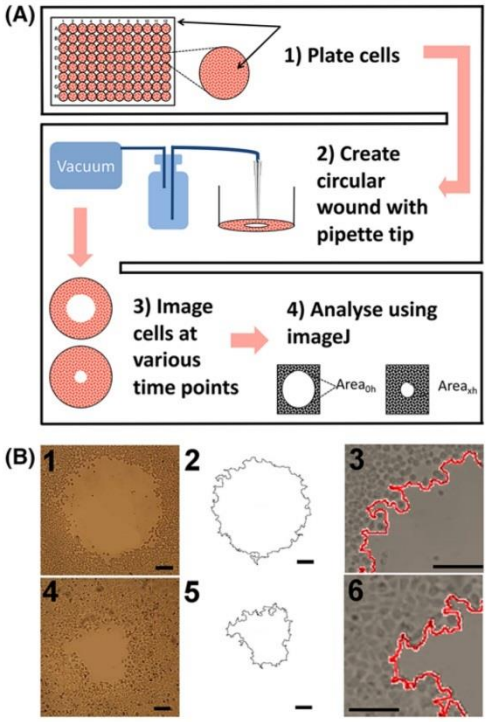

Figure 1. Schematic summary of procedures and examples of results for the CWCA in HT29 cells

(**A**) (1) Seed the cells in a 96-well plates and grow to full confluence. (2) Connect a p10 pipette tip to a vacuum pump and gently press the end of the pipette tip perpendicularly down onto the cell monolayer (without lateral movement) to detach cells from the substratum, creating a circular wound. (3) Image the wound at various time points. (4) Measure cell migration by calculating the percent change in wound area over time, standardized to the initial area at time zero. (**B**) Raw images of the same circular wound at 0 (B1) and 24 h (B4). Outlines of circular wound perimeters at 0 (B2) and 24 (B5) h were generated by ImageJ software. Magnified superimposed views of circular wounds show outlines at 0 (B3) and 24 (B6) h, illustrating the precision of the data capture method. Black bars represent 100 μm.

Reagents

- Cell culture medium and supplements appropriate for cell line
- 5-Fluoro-2'-deoxyuridine (FUDR) (100 ng/ml final solution)
- Lifting solution, 0.25 mM EDTA with 0.25% trypsin (2.5%, Gibco)
- Phosphate buffer saline (PBS, Gibco)

Equipment

- Cell culture incubator at 37°C with 5% CO_2
- Inverted light microscope with camera attachment
- Flat bottom 96-well plates
- Vacuum pump for molecular biology (Welch Laboratory, 2511B-01, 219 mmHg vacuum pressure)

Bioscience Reports (2018) **38** BSR20180698
https://doi.org/10.1042/BSR20180698

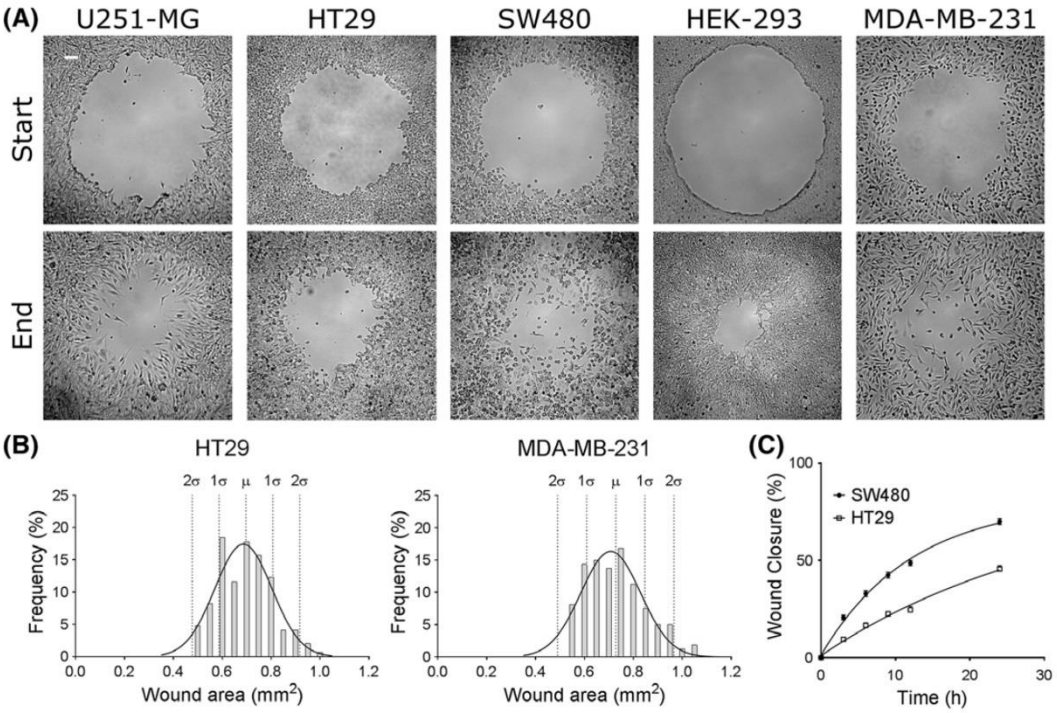

Figure 2. Wounds can be generated consistently for various cell lines using CWCA

(**A**) Start-point represents 0 h and end-point represents various time points depending on the cell line. The end points for cell lines shown are: U251-MG 20 h, HT29 24 h, SW480 24 h, HEK-293 24 h, and MDA-MB-231 20 h. White bar represents 100 μm; the scale is consistent for all images. (**B**) Wounds were generated by two different experimenters (subjects) for two different cell lines (MDA-MB-231 and HT29), using the CWCA technique described here. The initial wound sizes were calculated (in mm^2), and the datasets from each subject were combined for each cell line. The plots depict Gaussian distributions of the resulting initial wound areas. For -MB-231, the mean (μ) wound area is 0.728 mm^2 (S.D. (σ) $\pm$ 0.119 mm^2). *N*-value is 160. For HT29, μ is 0.697 mm^2 (σ $\pm$ 0.110 mm^2). *N*-value is 146. (**C**) Wound closure was recorded as the percent change in wound area with time (3, 6, 9, 12, and 24 h) in HT29 and SW480 cells. SW480 cells show a faster rate of migration than HT29 cells. Non-linear (sigmoidal) regression functions showed the best fit of wound closure as a function of time, yielding a correlation coefficient of $r^2 = 0.95$ for SW480 (n=16), and $r^2 = 0.94$ for HT29 (n=7).

- p10 pipette tips (Labcon, LC1038-290)
- Hemocytometer

Free software

- XnConvert version 1.73 (https://www.xnview.com/en/xnconvert/#downloads)
- Fiji (ImageJ) version 1.51h (http://imagej.nih.gov/ij/)

Procedure

Note: Perform assays under sterile conditions. See Figure 1 for short summary and example of wound and outline appearance.

(1) Passage the cells: When the cells to be used for the assay are approximately 70–80% confluent, detach the cells with trypsin and EDTA cell-lifting solution, and centrifuge cells at 125 ***g*** for 5–7 min. Resuspend cells and perform a cell count using a hemocytometer. Note: The CWCA can be used to generate wounds in diverse cell lines (Figure 2A).

(2) Plate the cells: Prepare an appropriate volume of working cell solution at 5×10^5 cells/ml. Plate the working cell solution at 500 µl/well for 24-well plates or 100 µl/well for 96-well plates. Incubate the plate until cells reach 90% confluency. Note: Incubation time will vary depending on the cell line.

(3) Mitotic inhibitor and serum starvation: When the cells reach 90% confluency, exchange the media with FUDR-containing reduced-serum medium (1–2% serum), and incubate overnight. Use FUDR at a concentration of 100 ng/ml. Note: The use of a mitotic inhibitor is not required although recommended to reduce potential overestimation of apparent migration due to cell proliferation (Supplementary Figure S1). The serum-starvation step is essential.

(4) Create wound using vacuum pump: Attach a p10 pipette tip to the end of vacuum tube (to do this, it may be necessary to first attach a p200 pipette tip to the tubing, and then overlay a p10 pipette tip on the p200 pipette tip). With medium still in the well, position the pipette tip perpendicularly above the center of the well. Gently lower the tip and make brief contact with the base to aspirate off a circular layer of cells and create a circular wound (Figure 1). Figure 2B shows the consistency of initial wound sizes generated using this technique. Note: Gentle perpendicular contact between the pipette tip and the cell monolayer is important for clean and consistent wounds. Practicing the technique in several wells prior to the first experiment is recommended (see Supplementary Figure S2 for examples of good and bad wounds). Flat pipette tips from two different vendors (Labcon, LC1038-290 and Brand Z740066) and vacuum pumps with different pressure settings (219 and 449 mmHg) have been tested in our lab with no distinctive differences in wound quality.

(5) Wash the wound: Aspirate any remaining medium from the edge of the well, and wash with PBS. One wash is usually sufficient, but some cell lines will require an extra washing step to clear any residual cellular debris.

(6) Apply treatments: Remove the PBS/media from wells and replace with culture medium containing the treatments or control samples that are being tested. Prepare treatments and controls in the same FUDR-containing reduced-serum medium as used previously. For example, if certain chemicals are being tested for their effect on cell migration, dissolve these chemicals at the appropriate final concentration in FUDR-containing reduced-serum medium.

(7) Imaging: Using microscopy imaging facilities, capture images of each complete circular wound centered in the field of view. Once all wells have been imaged, return the plate back to the incubator until the next time point (if imaging is being performed manually). If desired, wound closure can be monitored over multiple time points (Figure 2C). The final time point for imaging depends on the cell line, as some cells migrate faster than others. Note: The maximal duration of the experiment should ensure the wounds do not fully close during the treatment period of interest.

(8) XnConvert: This software can be used for batch image processing to crop to regions of interest or to change resolution of pictures.

(9) Process images in ImageJ: Use NIH ImageJ software to calculate the wound area and to generate an outline of the perimeter of the wound area. The following steps illustrate how to analyze the wound area on ImageJ, and also how to use the 'macro' feature to semi-automate the analysis for each image, improving consistency and objectivity of measurements. The same macro settings should be used for all sampled images collected in an experiment.
   (a) Download and open Fiji (ImageJ).
   (b) Select **File> Open** and then select the image file to be analyzed.
   (c) Go to **Analyze> Set Scale** and input the scale information relative to your image.
   (d) To begin recording the macro to be used for all images, select **Plugins> Macro> Record . . .** A 'Record' box will appear, and the macro will now begin to record all following selections.
   (e) Select **Image> Type> 8-bit.** This will convert the image to binary image.
   (f) Select **Process> Find Edges**.
   (g) Select **Process> Sharpen**.

Bioscience Reports (2018) **38** BSR20180698
https://doi.org/10.1042/BSR20180698

(h) Select **Image>Adjust>Threshold.** Be sure the settings are set to 'Default' and 'B&W' and untick the 'Dark background', and 'Stack histogram' boxes.

(i) Move the two bars until the best clarity and contrast is achieved for the image. See image below for how the image should look following adjustment.

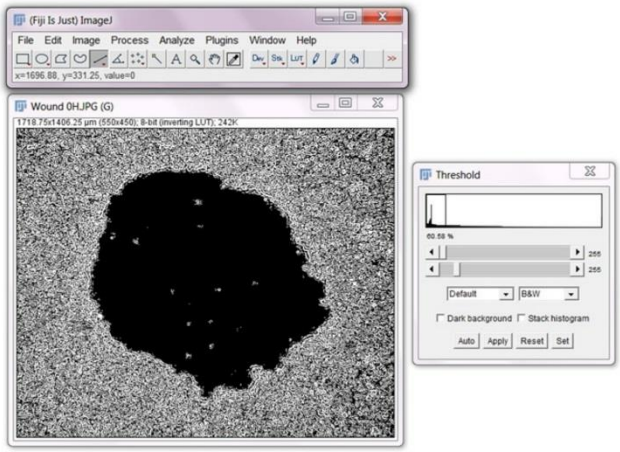

(j) Select **Set** and a 'Set Threshold Level' box should appear. Select **OK**.

(k) Now select **Apply** in 'Threshold' box.

(l) Select **Process>Find Edges.**

(m) Select **Image>Lookup Tables>Invert LUT**. See image below for how the image should look after LUT inversion.

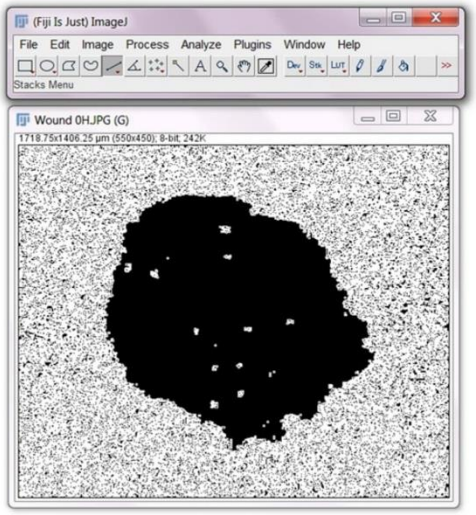

(n) Select **Analyze>Analyze Particles . . .**

(o) In the 'Size (pixel^2)' section, select minimum and maximum pixel areas you would like the program to identify. For example, if there are artifacts ('holes') that are visible in the current image, and you do not want to program to mistake these 'holes' for wounds, it is important to input the range of areas within which wounds are likely to

fall. Try '2000-Infinity' to begin, and adjust accordingly. If the program is detecting 'holes' that are not wounds, increase the first value. If the program is not detecting anything at all, including wounds, decrease the first value.

(p) Set 'Circularity' to '0.00–1.00'.
(q) In the 'Show' section, choose 'Bare Outlines' to generate an outline of the wound.
(r) Be sure 'Summarize' is ticked to generate data of the wound area.
(s) Select **OK**.
(t) A summary box will appear, which will include the area value of the wound to be used for further statistical analysis. An outline of the wound will also appear. See below image for summary and outline following this step.

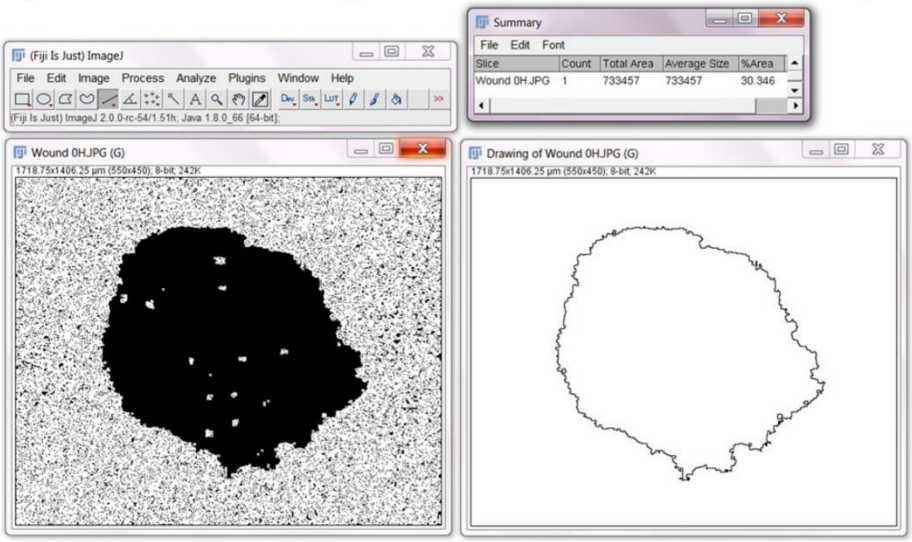

(u) Find the 'Record' box for the macro and select **Create**.
(v) A new box will appear labeled, 'Macro.ijm'. In this box, select **Save As**, and save as a .txt file.
(w) Now go to **Plugins**>**Macros**>**Install . . .**
(x) Find and select the .txt macro file from step (v).
(y) Open a new wound image for analysis.
(z) Select **Plugins**>**Macros**>'**Your Macro**'. Your macro should be located at the bottom of the dropdown box.

(10) Check for initial wound size consistency: Run an ANOVA statistical test to confirm the absence of significant differences between the initial wound areas across all the control and treatment groups in an experiment. This rules out the possibility that differences in wound closure observed between treatment groups were an indirect result of initial wound size.

(11) Analyze wound closure: The wound area measured at time zero (the start of the treatment) serves as a reference point for standardization. Subsequent samples can be evaluated in different ways to estimate the magnitude of cell migration. One method is to calculate the radius of the initial wound minus the radius of the end wound. This method determines distance moved but assumes circularity of the wound shapes. A second method is to calculate the final wound area as a percentage of the initial wound area. This method requires consistency of initial wound sizes, but is more tolerant of non-circular wounds. The percent closure method has been the analysis of choice for published work [24,25]; however, results from both methods show a robust correlation, demonstrating reliability (Figure 3).

Conclusion

This CWCA technique provides a simple and reliable alternative method with distinct advantages over older methods such as the scratch wound assay or cell exclusion zone assays. Accurate data measurements enable straightforward

Bioscience Reports (2018) **38** BSR20180698
https://doi.org/10.1042/BSR20180698

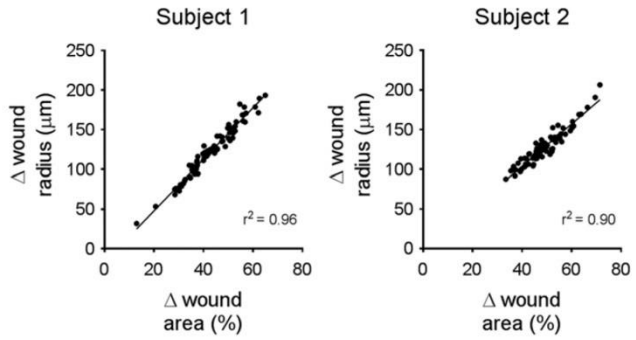

Figure 3. Results obtained from calculations of percent wound closure and wound radius decrease are strongly correlated

Plots generated from the experimental results obtained by two different experimenters (subjects). Each experiment had various treatment groups, with some treatments exhibiting inhibitory effects on cell migration (explaining that wide range of wound closure in both plots). Analysis was done by calculating both the percentage wound closure and the change in wound radius for each wound image. The results from each method were compared and linear regression yielded a correlation coefficient of $r^2 = 0.96$ for subject 1, and $r^2 = 0.9$ for subject 2. *N*-value is 73 for each subject. These results suggest that both techniques of analysis produce data that is strongly correlated.

objective computer-assisted analyses. This simple adaptation of a well-established protocol generates results that are comparable in consistency and quality to expensive commercial options and supports relatively high-throughput screening of novel therapeutic agents that regulate cell migration rates [24,25]. The main limitation of CWCA is that manual wound generation can yield higher variability in initial wound sizes and shapes as compared with cell exclusion zone or silicone-tipped drill-wounding methods; however, this limitation exists for any assays involving the manual generation of wounds. Variability is reduced with practice. Ruling out the potential impact of variability is addressed by running an ANOVA statistical test on initial wound sizes across all treatment groups in a given experiment. Absence of a significant difference rules out non-specific effects of initial wound sizes on measures of closure. Analyzing data by determining wound radius change, as opposed to percentage wound closure, is less sensitive to initial wound size, but more sensitive to the circularity of wound shape; however, both methods are reliable. In summary, this protocol offers a quality advance in methodology that is possible without specialized equipment or costly resources. Cutting edge research on cell migration can be carried out by laboratories, including those located in developing countries where research funding and facilities might be limited.

Acknowledgments

We thank Prof. A. Yool for input into the method design and implementation, and assistance with editing the manuscript. We also thank Saeed Nourmohammadi for providing images of circular wounds and data from his own archives.

Competing interests

The authors declare that there are no competing interests associated with the manuscript.

Author contribution

J.V.P. and M.L.D. invented the technique. J.V.P. and M.L.D. wrote and edited the manuscript.

Funding

This work was supported by a grant from the Australian Research Council [grant number DP160104641].

Abbreviations

CWCA, circular wound closure assay; FUDR, 5-Fluoro-2'-deoxyuridine; 2D, two-dimensional.

References

1 Klausen, M., Aaes-Jørgensen, A., Molin, S. and Tolker-Nielsen, T. (2003) Involvement of bacterial migration in the development of complex multicellular structures in Pseudomonas aeruginosa biofilms. *Mol. Microbiol.* **50**, 61–68, https://doi.org/10.1046/j.1365-2958.2003.03677.x
2 Friedl, P., Hegerfeldt, Y. and Tusch, M. (2004) Collective cell migration in morphogenesis and cancer. *Int. J. Dev. Biol.* **48**, 441–450, https://doi.org/10.1387/ijdb.041821pf
3 Friedl, P. and Weigelin, B. (2008) Interstitial leukocyte migration and immune function. *Nat. Immunol.* **9**, 960–969, https://doi.org/10.1038/ni.f.212
4 Yamaguchi, H., Wyckoff, J. and Condeelis, J. (2005) Cell migration in tumors. *Curr. Opin. Cell Biol.* **17**, 559–564, https://doi.org/10.1016/j.ceb.2005.08.002
5 Ross, R. (1993) The pathogenesis of atherosclerosis: a perspective for the 1990s. *Nature* **362**, 801, https://doi.org/10.1038/362801a0
6 McInnes, I.B., Al-Mughales, J., Field, M., Leung, B.P., Huang, F.-p., Dixon, R. et al. (1996) The role of interleukin–15 in T–cell migration and activation in rheumatoid arthritis. *Nat. Med.* **2**, 175, https://doi.org/10.1038/nm0296-175
7 Leppert, D., Waubant, E., Bürk, M.R., Oksenberg, J.R. and Hauser, S.L. (1996) Interferon β-1b inhibits gelatinase secretion and *in vitro* migration of human T cells: a possible mechanism for treatment efficacy in multiple sclerosis. *Ann. Neurol.* **40**, 846–852, https://doi.org/10.1002/ana.410400606
8 Billuart, P., Bienvenu, T., Ronce, N., Des Portes, V., Vinet, M.C., Zemni, R. et al. (1998) Oligophrenin-1 encodes a rhoGAP protein involved in X-linked mental retardation. *Nature* **392**, 923, https://doi.org/10.1038/31940
9 De Ieso, M.L. and Yool, A.J. (2018) Mechanisms of aquaporin-facilitated cancer invasion and metastasis. *Front. Chem.*, https://doi.org/10.3389/fchem.2018.00135
10 Ascione, F., Vasaturo, A., Caserta, S., D'esposito, V., Formisano, P. and Guido, S. (2016) Comparison between fibroblast wound healing and cell random migration assays *in vitro*. *Exp. Cell Res.* **347**, 123–132, https://doi.org/10.1016/j.yexcr.2016.07.015
11 Liang, C.-C., Park, A.Y. and Guan, J.-L. (2007) *In vitro* scratch assay: a convenient and inexpensive method for analysis of cell migration *in vitro*. *Nat. Protoc.* **2**, 329, https://doi.org/10.1038/nprot.2007.30
12 Justus, C.R., Leffler, N., Ruiz-Echevarria, M. and Yang, L.V. (2014) *In vitro* cell migration and invasion assays. *J. Vis. Exp.* **88**, e51046–e51046, https://doi.org/10.3791/51046
13 Dorward, H.S., Du, A., Bruhn, M.A., Wrin, J., Pei, J.V., Evdokiou, A. et al. (2016) Pharmacological blockade of aquaporin-1 water channel by AqB013 restricts migration and invasiveness of colon cancer cells and prevents endothelial tube formation *in vitro*. *J. Exp. Clin. Cancer Res.* **35**, 36, https://doi.org/10.1186/s13046-016-0310-6
14 Pan, X.Y., Guo, H., Han, J., Hao, F., An, Y., Xu, Y. et al. (2012) Ginsenoside Rg3 attenuates cell migration via inhibition of aquaporin 1 expression in PC-3M prostate cancer cells. *Eur. J. Pharmacol.* **683**, 27–34, https://doi.org/10.1016/j.ejphar.2012.02.040
15 Meng, F., Rui, Y., Xu, L., Wan, C., Jiang, X. and Li, G. (2014) Aqp1 enhances migration of bone marrow mesenchymal stem cells through regulation of FAK and β-catenin. *Stem Cells Dev.* **23**, 66–75, https://doi.org/10.1089/scd.2013.0185
16 Saxena, N.K., Sharma, D., Ding, X., Lin, S., Marra, F., Merlin, D. et al. (2007) Concomitant activation of the JAK/STAT, PI3K/AKT, and ERK signaling is involved in leptin-mediated promotion of invasion and migration of hepatocellular carcinoma cells. *Cancer Res.* **67**, 2497–2507, https://doi.org/10.1158/0008-5472.CAN-06-3075
17 Hu, J. and Verkman, A.S. (2006) Increased migration and metastatic potential of tumor cells expressing aquaporin water channels. *FASEB J.* **20**, 1892–1894, https://doi.org/10.1096/fj.06-5930fje
18 Jiang, Y. (2009) Aquaporin-1 activity of plasma membrane affects HT20 colon cancer cell migration. *IUBMB Life* **61**, 1001–1009, https://doi.org/10.1002/iub.243
19 Kam, Y., Guess, C., Estrada, L., Weidow, B. and Quaranta, V. (2008) A novel circular invasion assay mimics *in vivo* invasive behavior of cancer cell lines and distinguishes single-cell motility *in vitro*. *BMC Cancer* **8**, 198, https://doi.org/10.1186/1471-2407-8-198
20 Daniel, T.O., Liu, H., Morrow, J.D., Crews, B.C. and Marnett, L.J. (1999) Thromboxane A2 is a mediator of cyclooxygenase-2-dependent endothelial migration and angiogenesis. *Cancer Res.* **59**, 4574–4577
21 Li, D.S., Zimmermann, J. and Levine, H. (2016) Modeling closure of circular wounds through coordinated collective motion. *Phys. Biol.* **13**, 016006, https://doi.org/10.1088/1478-3975/13/1/016006
22 Hulkower, K.I. and Herber, R.L. (2011) Cell migration and invasion assays as tools for drug discovery. *Pharmaceutics* **3**, 107–124, https://doi.org/10.3390/pharmaceutics3010107
23 Schindelin, J., Arganda-Carreras, I., Frise, E., Kaynig, V., Longair, M., Pietzsch, T. et al. (2012) Fiji: an open-source platform for biological-image analysis. *Nat. Methods* **9**, 676, https://doi.org/10.1038/nmeth.2019
24 Kourghi, M., Pei, J.V., De Ieso, M.L., Flynn, G. and Yool, A.J. (2015) Bumetanide derivatives AqB007 and AqB011 selectively block the aquaporin-1 ion channel conductance and slow cancer cell migration. *Mol. Pharmacol.* **89**, 133–140, https://doi.org/10.1124/mol.115.101618
25 Pei, J.V., Kourghi, M., De Ieso, M.L., Campbell, E.M., Dorward, H.S., Hardingham, J.E. et al. (2016) Differential inhibition of water and ion channel activities of mammalian aquaporin-1 by two structurally related bacopaside compounds derived from the medicinal plant bacopa monnieri. *Mol. Pharmacol.* **90**, 496–507, https://doi.org/10.1124/mol.116.105882

Appendix II: Co-author Publications as PDFs Arising from This Thesis

Supplemental material to this article can be found at:
http://molpharm.aspetjournals.org/content/suppl/2016/07/29/mol.116.105882.DC1

1521-0111/90/4/496–507$25.00
MOLECULAR PHARMACOLOGY

http://dx.doi.org/10.1124/mol.116.105882
Mol Pharmacol 90:496–507, October 2016

MOLECULAR PHARMACOLOGY

Differential Inhibition of Water and Ion Channel Activities of Mammalian Aquaporin-1 by Two Structurally Related Bacopaside Compounds Derived from the Medicinal Plant *Bacopa monnieri*[S]

Jinxin V. Pei, Mohamad Kourghi, Michael L. De Ieso, Ewan M. Campbell, Hilary S. Dorward, Jennifer E. Hardingham, and Andrea J. Yool

School of Medicine (J.V.P., M.K., M.L.D.I., J.E.H., A.J.Y.), and Institute for Photonics and Advanced Sensing (J.V.P., A.J.Y.), University of Adelaide, Adelaide, Australia; School of Biological Sciences, University of Aberdeen, Aberdeen, Scotland, United Kingdom (E.M.C.); Molecular Oncology Laboratory, Basil Hetzel Institute, Queen Elizabeth Hospital, Woodville, Australia (H.S.D., J.E.H.)

Received July 3, 2016; accepted July 26, 2016

ABSTRACT

Aquaporin-1 (AQP1) is a major intrinsic protein that facilitates flux of water and other small solutes across cell membranes. In addition to its function as a water channel in maintaining fluid homeostasis, AQP1 also acts as a nonselective cation channel gated by cGMP, a property shown previously to facilitate rapid cell migration in a AQP1-expressing colon cancer cell line. Here we report two new modulators of AQP1 channels, bacopaside I and bacopaside II, isolated from the medicinal plant *Bacopa monnieri*. Screening was conducted in the *Xenopus* oocyte expression system, using quantitative swelling and two-electrode voltage clamp techniques. Results showed bacopaside I blocked both the water (IC_{50} 117 μM) and ion channel activities of AQP1 but did not alter AQP4 activity, whereas bacopaside II selectively blocked the AQP1 water channel (IC_{50} 18 μM) without impairing the ionic conductance. These results fit with predictions from in silico molecular modeling. Both bacopasides were tested in migration assays using HT29 and SW480 colon cancer cell lines, with high and low levels of AQP1 expression, respectively. Bacopaside I (IC_{50} 48 μM) and bacopaside II (IC_{50} 14 μM) impaired migration of HT29 cells but had minimal effect on SW480 cell migration. Our results are the first to identify differential AQP1 modulators isolated from a medicinal plant. Bacopasides could serve as novel lead compounds for pharmaceutic development of selective aquaporin modulators.

Introduction

Aquaporin (AQP) water channels are in the family of major intrinsic proteins found from bacteria to humans (Agre et al., 1993; Reizer et al., 1993; Calamita et al., 1995) and are targets for the discovery of selective pharmacologic modulators. Classes of aquaporins transport water and small uncharged molecules such as glycerol and urea through individual pores located in each subunit (Fu et al., 2000; Tajkhorshid et al., 2002).

An expanding role for aquaporins as multifunctional channels is being recognized (Yool and Campbell, 2012). In addition to facilitating water flux through intrasubunit pores, AQP1 also functions as a nonselective monovalent cation channel using the central pore at the 4-fold axis of symmetry (Yool and Weinstein, 2002; Yu et al., 2006; Campbell et al., 2012). The ion channel conductance is activated by interaction of cGMP in the intracellular loop D domain, and modulated by the carboxyl terminal domain (Anthony et al., 2000; Saparov et al., 2001; Boassa and Yool, 2003; Zhang et al., 2007). Cyclic GMP appears to trigger opening of cytoplasmic hydrophobic barriers in the central pore, allowing hydration and cation permeation (Yu et al., 2006). Inhibition of the AQP1 ion channel has been shown to slow cell migration rates in a colon cancer cell line that expresses high levels of AQP1 (Kourghi et al., 2016).

Defining pharmacologic modulators of aquaporins has been an area of keen interest (Papadopoulos and Verkman, 2008; Devuyst and Yool, 2010; Seeliger et al., 2013). Early work identified blockers such as mercury (Preston et al., 1993), silver and gold (Niemietz and Tyerman, 2002), acetazolamide (Gao et al., 2006), and tetraethylammonium ion (Brooks et al., 2000; Yool et al., 2002; Detmers et al., 2006), but these remained limited in usefulness because of toxicity, lack of specificity, or variable efficacy across experimental systems (Yang et al., 2006; Yool, 2007).

More recently, small molecule pharmacologic agents with therapeutic potential have been identified. Complexes of

This work was supported by funding from the University of Adelaide Institute for Photonics and Advanced Sensing 2015 Pilot Grant program, and Australian Research Council Discovery Project grant DP160104641.
dx.doi.org/10.1124/mol.116.105882.
[S] This article has supplemental material available at molpharm.aspetjournals.org.

ABBREVIATIONS: AQP, aquaporin; AqBxxx, numbered series of aquaporin modulators derived from bumetanide; AqFxxx, numbered series of aquaporin modulators derived from furosemide; FBS, fetal bovine serum; FUDR, 5-fluoro-2′-deoxyuridine; meWB, methanol extract of whole *Bacopa*; NCBI, National Center for Biotechnology Information; qRT-PCR, quantitative reverse-transcription polymerase chain reaction.

gold-based compounds have promise for the selective block of specific classes of aquaporins; functionalized bipyrene and terpyridines coordinating Au(III) were shown to block aquaglyceroporin AQP3 with little effect on AQP1 (Martins et al., 2013). Intracellular arylsulfonamide modulators of AQP1 include the bumetanide derivative, AqB013, which blocks AQP1 and AQP4 water permeability (Migliati et al., 2009); AqB011, which blocks the AQP1 cation channel (Kourghi et al., 2016); and the furosemide derivative AqF026, which potentiates water channel activity of AQP1 (Yool et al., 2013). Other arylsulfonamide agents have been proposed as blockers of AQP4 (Huber et al., 2007, 2009). Growing evidence has demonstrated that specific arylsulfonamides act as AQP modulators in vitro and in vivo (Pei et al., 2016).

Diverse small molecules acting at the extracellular side present a valuable array of novel inhibitors of AQP1 (Seeliger et al., 2013), indicating that other compounds in addition to coordinated metal ligands and arylsulfonamides are of interest for the development of AQP modulators. Lack of effect for a broad panel of AQP modulators tested in one study might reflect problems with synthesis or solubilization of the agents or could indicate that the type of bioassay used influences apparent drug efficacy (Esteva-Font et al., 2016).

Our study has broadened the panel of AQP modulatory agents by evaluating natural medicinal plants as sources of active compounds. Quantitative swelling assays of mammalian AQP1 and AQP4 channels in the *Xenopus* expression system, used for screening extracts from a variety of traditional medicinal herbs, have identified *Bacopa monnieri* as one of several promising sources. Work here tested the hypothesis that chemical constituents of *B. monnieri* could be identified and characterized as pharmacologic agents that modulate mammalian AQP1 by interacting at domains associated with pore functions.

Data here show that bacopaside I blocks both the water and ion channel activities of AQP1 but does not alter AQP4 activity, and bacopaside II selectively blocks the AQP1 water channel without impairing the ionic conductance. These results fit well with in silico docking for predicted energies of interaction at a pore-occluding intracellular site. Bacopasides I and II showed the same order of efficacy in blocking migration of AQP1-expressing HT29 colon cancer cells, with minimal effects on SW480 cells that express AQP1 at low levels. Our results are the first to identify AQP1 channels as one of the candidate targets of action of the Ayurvedic medicinal plant water hyssop, and to define new lead compounds for the development of AQP modulators.

Materials and Methods

Bacopa Methanol Extraction and Fractionation. *Bacopa monnieri* stems and leaves were obtained with permission from the Botanic Gardens of Adelaide (Adelaide, South Australia). Chopped *Bacopa* plant material (100 g) was dried, then refluxed in 500 ml of methanol for 2 hours at room temperature. The suspension was filtered using Whatman No. 1 paper to obtain a methanol extract of whole *Bacopa* (meWB). Half the meWB extract was aliquoted into microfuge tubes, dried under vacuum (SpeedVac; Thermo Fisher Scientific, Waltham, MA) into a solid brown paste, and reconstituted in saline for oocyte swelling assays. The other half of the meWB was fractionated using small-scale reverse phase C18 silica column (Alltech Prevail C18; Grace, Deerfield, IL). The mobile phases used for fractionation were a series of six water–methanol mixtures with H_2O:CH_3OH ratios ranging from 5:0 to 0:5. The fractions were dried in under vacuum and reconstituted in saline for oocyte swelling assays.

Fractions containing AQP1 blocking activity were analyzed with mass spectrometry by Flinders Analytical (Flinders University, South Australia). Bacopaside I was identified by precise molecular weight as a major component in the active fractions, and bacopasides I and II were purchased from a commercial source (Chromadex, Irvine CA), solubilized in methanol to yield 100× stock solutions, and stored at -20°C. Experimental solutions were prepared by mixing the bacopaside stocks (1 part in 100) with isotonic saline or culture medium to yield final concentrations of 10 to 200 μM. Vehicle control salines were made using the same volume of methanol alone in isotonic saline or culture medium.

Oocyte Preparation and cRNA Injection. Unfertilized oocytes were isolated from *Xenopus laevis* frogs in accord with the university animal ethics committee-approved protocols, defolliculated by treatment with collagenase (type 1A, 2 mg/ml; Sigma-Aldrich, St. Louis, MO) and trypsin inhibitor (0.67 mg/ml; Sigma-Aldrich) in OR-2 saline (82 mM NaCl, 2.5 mM KCl, 1 mM $MgCl_2$, and 5 mM HEPES; pH 7.6) at 16°C for 1.5 hours, washed in OR-2 saline, and then incubated in isotonic oocyte saline [96 mM NaCl, 2 mM KCl, 0.6 mM $CaCl_2$, 5 mM $MgCl_2$, and 5 mM HEPES supplemented with 10% horse serum (Sigma-Aldrich), 100 U/ml penicillin, 100 μg/ml streptomycin, and 50 μg/ml tetracycline, pH 7.6] at 16°C. Oocytes were injected with 1–4 ng of AQP1, AQP4, or AQP1 R159A+R160A cRNA in 50 nl of sterile water and incubated for 2 to 3 days at 16–18°C to allow protein expression. The oocytes not injected with cRNA served as non-AQP-expressing control cells.

Human AQP1 [National Center for Biotechnology Information (NCBI) GenBank: BC022486.1] and rat AQP4 (AF144082.1) cDNAs from P. Agre (Johns Hopkins University, Baltimore, MD) were subcloned into a modified *Xenopus* β-globin expression plasmid. The double mutant construct human AQP1 R159A+R160A cDNA was generated by site-direct mutation (QuikChange; Stratagene, La Jolla, CA) and sequenced to confirm no errors were introduced (Yu et al., 2006). The cDNAs were linearized with BamHI and transcribed using T3 polymerase (T3 mMessage mMachine; Ambion, Austin, TX). The cRNAs were resuspended in sterile water and stored at −80°C.

Quantitative Oocyte Swelling Assays. Immediately before the swelling assays, the control and AQP-expressing oocytes were preincubated in isotonic saline (serum and antibiotic free) with or without meWB or bacopaside compounds or with methanol vehicle at 16–18°C, for incubation periods as indicated. Osmotic water permeability was determined as the linear rate of change in volume as a function of time, immediately after introduction into 50% hypotonic saline (isotonic saline diluted with equal volume of water).

Oocytes were imaged using a computer controlled charge-coupled-device grayscale camera (Cohu, San Diego, CA) mounted on a dissecting microscope (Olympus SZ-PT; Olympus, Macquarie Park, Australia). Images were taken at 0.5 frames per second for 60 seconds; cross-sectional areas were quantified using ImageJ software (Research Services Branch, National Institutes of Health, Bethesda, MD). Swelling rates were calculated as the slopes of linear regression fits of volume as a function of time in hypotonic saline. Data were analyzed and compiled for multiple batches of oocytes for statistical analyses and to generate dose–response curves, which were fit by sigmoidal nonlinear variable-slope dose–response regression functions using Prism (GraphPad Software, San Diego, CA).

Molecular Docking. In silico modeling was performed with methods reported previously elsewhere (Yool et al., 2013). The protein crystal structures for human AQP1 (PDB ID 1FQY) and human AQP4 (PDB ID 3GDB) were obtained from the protein data bank (NCBI Structure). Bacopaside I and II structures were obtained from PubChem (NCBI) and converted into a software-compatible 3D structures in .pdb format using the Online SMILES Translator and Structure File Generator (National Cancer Institute, U.S. National Institutes of Health, Bethesda, MD). Ligand and receptor coordinates were prepared for docking using Autodock (version 4.2; Scripps

Research Institute, La Jolla, CA). Autodock Vina (Trott and Olson, 2010) was used to run the flexible ligand docking simulations with two docking grids covering both intracellular and extracellular faces of the monomeric pores. The three-dimensional docking result files and docking energy values were exported from Autodock, and the results were viewed using PyMOL software (version 1.8; Schrödinger, Cambridge, MA). Data for AQP1 and AQP4 docking results in .pdb format are provided as supplemental data files.

Electrophysiology. For two-electrode voltage clamp, capillary glass electrodes (1–3 MΩ) were filled with 1 M KCl. Recordings were done in a standard isotonic Na^+ bath saline containing 100 mM NaCl, 2 mM KCl, 4.5 mM $MgCl_2$, and 5 mM HEPES, pH 7.3. We applied cGMP extracellularly at a final concentration of 10–20 μM using the membrane-permeable cGMP analog [Rp]-8-[para-chlorophenylthio]-cGMP (Sigma Chemical, Castle Hill, Australia). Ionic conductance was monitored for at least 20 minutes after cGMP addition to allow development of maximal plateau responses. Conductance was determined by linear fit of the current amplitude as a function of voltage, with a step protocol from +60 to −110mV and holding potential of −40 mV.

After the first activation by cGMP, oocytes were incubated in isotonic saline with or without bacopaside I or bacopaside II for 2 hours to allow recovery. After incubation, a second application of cGMP was used to test for reactivation, to determine whether any block of the ionic conductance was evident. Using the same protocol, AQP1-expressing oocytes were demonstrated previously to show cGMP-dependent activation, complete recovery during a 2-hour incubation in saline alone, and full reactivation of the ionic conductance response to a second application of cGMP, whereas non-AQP1-expressing control oocytes showed a low ionic conductance and no significant response to drug treatments throughout the same protocol (Kourghi et al., 2016). Recordings were made with a GeneClamp amplifier and pClamp 9.0 software (Molecular Devices, Sunnyvale, CA).

Cancer Cell Culture and Migration Assays. HT29 and SW480 colon cancer cell lines (from American Type Culture Collection [ATCC], Manassas, VA) were cultured in complete medium composed of Dulbecco's modified Eagle's medium supplemented with 1× glutaMAX (Life Technologies, Mulgrave, Australia), penicillin and streptomycin (100 U/ml each), and 10% fetal bovine serum. Cultures were maintained in 5% CO_2 at 37°C. Cells were seeded in a flat-bottom 96-well plates at 1.25×10^6 cells/ml to produce a confluent monolayer.

For 12 to 18 hours before wounding, cells were serum-starved in 2% fetal bovine serum (FBS), in the presence of 400 nM of the mitotic inhibitor 5-fluoro-2′-deoxyuridine (FUDR) (Parsels et al., 2004). For wounding, a sterile p10 pipette tip was attached to the end of a vacuum tube, and a circular wound was created by brief perpendicular contact of the tip with base of the well. Each well was then washed 3 times with phosphate-buffered saline to remove detached cell debris. Cultures were maintained during the wound closure assay in 2% FBS medium with FUDR.

Wound images were imaged at 10× magnification with a Canon EOS 6D camera (Canon, Macquarie Park, Australia) mounted on an Olympus inverted microscope (Olympus Corp., Waltham, MA). Image dimensions and pixel density were standardized across each image series using XnConvert software (XnSoft, Reims, France). Linear outlines and areas of the wound were generated using ImageJ software (National Institutes of Health). Wound closure data as a function of time were calculated as a percentage of the initial wound areas for the same wells.

Quantitative Reverse-Transcription Polymerase Chain Reaction. Cells at 70%–80% confluence were harvested, and the RNA was extracted using the PureLink RNA Mini kit (Life Technologies, Carlsbad, CA). RNA was quantified using the NanoDrop 2000 spectrophotometer (Thermo Scientific) and the integrity (RIN score) assessed using the 2100 Bioanalyzer (Agilent Technologies, Santa Clara, CA). The RNA (500 ng) was reverse transcribed using the iScript cDNA synthesis kit (Bio-Rad Laboratories, Hercules, CA). Quantitative reverse-transcription polymerase chain reaction (qRT-PCR) of AQP1 and the reference gene phosphomannose mutase 1 (PMM1) was performed using multiplex Taqman expression assays (Life Technologies) and SsoFast probes supermix (Bio-Rad Laboratories) in triplicate in the Rotorgene 6000 (Qiagen).

Western Blot Analysis. Cultured cells were lysed with RIPA buffer containing 1% β-mercaptoethanol, 1% HALT protease inhibitor 100× solution, 150 U Benzonase (all from Sigma-Aldrich) on ice for 10 minutes, homogenized by passing through a 21-gauge syringe and centrifuged 14,000*g* for 15 minutes at 4°C to pellet the cell debris. Protein was quantified (EZQ Assay; Life Technologies). Each sample (50 μg) was resolved by SDS-PAGE on a 12% Mini-PROTEAN TGX Stain-Free Gels (Bio-Rad Laboratories) and transferred to polyvinylidene fluoride membranes using the Trans-Blot Turbo Transfer Pack and System (Bio-Rad Laboratories). Membranes were blocked with Tris-buffered saline with Tween 20 containing 5% skim milk for 1 hour and incubated overnight at 4°C with anti-AQP1 (H-55) (1/500; Santa Cruz). After three washes in Tris-buffered saline with Tween 20, membranes were incubated with goat anti-rabbit IgG horseradish peroxidase secondary antibody (1/2000) and Strep-Tactin-HRP Conjugate (1/10,000) (both Bio-Rad Laboratories) at room temperature for 1 hour, and washed.

Chemiluminescence using Clarity Western ECL Blotting Substrate (Bio-Rad Laboratories) was used for detection and blots imaged using the ChemiDoc Touch Imaging System (Bio-Rad Laboratories). Image Laboratory Software was used to validate the Western blotting data via total protein normalization (Bio-Rad Laboratories).

Immunocytochemistry. HT29 and SW480 cells grown on coverslips to 50% confluence were fixed with 4% paraformaldehyde and permeabilized with 0.5% Triton X-100. Image-iT FX Signal Enhancer (Life Technologies) was used as per manufacturer's instructions. AQP1 was labeled with a 1/400 dilution of rabbit polyclonal anti-human AQP1 (Abcam, Cambridge, United Kingdom) and visualized with a secondary antibody at 1/200 dilution (goat anti rabbit IgG H&L Alexa Fluor 568; Life Technologies). Cells were counterstained with NucBlue Fixed Cell Ready Probes Reagent (Life Technologies). Coverslips were mounted in ProLong Gold antifade reagent (Life Technologies) and imaged with a Zeiss LSM 700 microscope (Carl Zeiss, Jena, Germany).

Live Cell Imaging. Cells were seeded on an eight-well uncoated Ibidi μ-Slide (Ibidi, Munich, Germany) at a density of 1.0×10^6 cells/ml. For 12 to 18 hours before wounding, cells were serum-starved in medium with 2% FBS in the presence of FUDR (400 nM). Five circular wounds were created in each well using techniques described earlier for the migration assays. The slide was mounted on a Nikon Ti E Live Cell Microscope (Nikon, Tokyo, Japan) in an enclosed chamber kept at 37°C with 5% CO_2. Images were taken at 5-minute intervals for 24 hours, using Nikon NIS-Elements software. AVI files were exported from NIS-Elements and converted into TIFF files using ImageJ (U.S. National Institutes of Health). Converted files were analyzed using Fiji software (Schindelin et al., 2012) with the Manual Tracking plug-in.

Cytotoxicity Assay. HT29 cell viability was quantified using the AlamarBlue assay (Molecular Probes, Eugene, OR). The cells were plated at 10^4 cells/well in 96-well plates, and the fluorescence signal levels were measured with a FLUOstar Optima microplate reader (BMG Labtech, Ortenberg, Germany) after 24 hours of incubation with concentrations of bacopaside I from 0 to 100 μM or bacopaside II from 0 to 30 μM, to obtain quantitative measures of cell viability. Mercuric chloride (100 μM) was used as a positive control for cytotoxicity.

Results

Extracted Compounds from *Bacopa monnieri* Inhibited AQP1 Water Channel Activity. Methanol-extracted whole *Bacopa* (meWB) reconstituted in isotonic saline ("water hyssop extract") inhibited the water permeability of AQP1-expressing oocytes (Fig. 1A). After 2 hours preincubation in 1 mg/ml meWB, the swelling rates of

AQP1-expressing oocytes were significantly reduced ($P < 0.001$) as compared with untreated AQP1-expressing oocytes. Fractionated samples of meWB reconstituted at 0.1 mg/ml each were tested for biologic activity using oocyte swelling assays (Fig. 1B) after 2 hours of preincubation. AQP1-mediated swelling was significantly decreased by fractions 3 and 4; other fractions had no effect.

Combined fractions 3 and 4 were analyzed by mass spectrometry and revealed the presence of a major compound identified by precise molecular weight as bacopaside I. Commercially purchased bacopasides I and II were found to block osmotic water permeability in AQP1-expressing oocytes (Fig. 1C) and showed a dose-dependent effect (Fig. 1D). The inhibition of AQP1-mediated osmotic water fluxes showed IC_{50} values of approximately 18 μM for bacopaside II, and approximately 117 μM for bacopaside I. The chemical structures are shown in Fig. 1E.

Inhibition by Bacopasides I and II Was Time-Dependent and Reversible. AQP4-expressing oocytes showed no block of water channel activity after 2 hours of preincubation in isotonic saline containing bacopaside I at 178 μM (Fig. 2A). The blocking effect of bacopaside was specific for AQP1. The inhibitory effect of bacopasides I and II on AQP1 water channel activity took time to develop, with near maximum block achieved by approximately 2 hours (Fig. 2B). The magnitude of inhibition of AQP water flux increased as a function of the duration of preincubation in 178 μM bacopaside I or 35 μM bacopaside II. For bacopaside I, half-maximal block was reached after approximately 50 minutes, and maximum block after 120 minutes of preincubation. For bacopaside II, half-maximal block was reached after approximately 30 minutes, and maximum block after 80 minutes of preincubation. Longer times provided no appreciable further enhancement of the magnitude of inhibition. A comparably slow time-dependent onset of block has been noted previously for other AQP1 ligands such as AqB013, AqB011, and AqF026, which are thought to bind at the intracellular side of the channel (Migliati et al., 2009; Yool et al., 2013; Kourghi et al., 2016) and require time to travel across the plasma membrane to the cytoplasmic side.

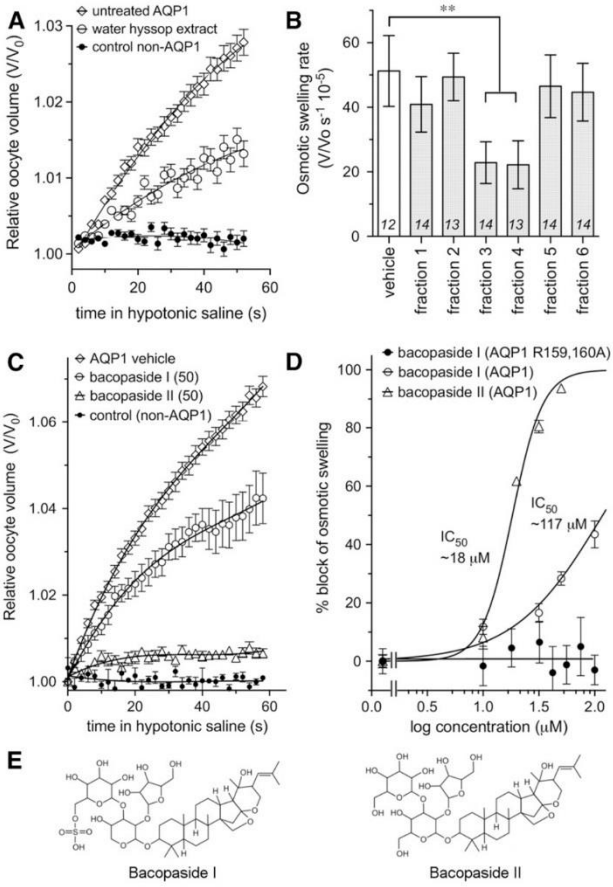

Fig. 1. Block of osmotic water permeability in AQP1-expressing oocytes by water hyssop (*Bacopa monnieri*) extract, and constituent compounds bacopaside I and bacopaside II. (A) Mean swelling responses of AQP1-expressing oocytes in 50% hypotonic saline, standardized to the initial volume V_0, were blocked by 2 hours of preincubation in reconstituted extract of water hyssop (at 1 mg/ml). Control non-AQP1 oocytes showed little change in volume. Data are mean values for all oocytes assessed from a single batch of oocytes; error bars are S.E.M.; n values are 6 per treatment group. (B) Column elution of methanol-extracted *Bacopa* identified two active fractions which caused block of AQP1 osmotic water permeability at 0.1 mg/ml each (which were further analyzed by mass spectroscopy to identify candidate compounds). Data are mean ± S.E.M.; n values in italics are above the x-axis. (C) Candidate compounds bacopaside I and bacopaside II at 50 μM differentially blocked osmotic water permeability in AQP1-expressing oocytes, causing a decrease in the rate of swelling as compared with untreated AQP1-expressing oocytes. Data are mean ± S.E.M.; n values are 8 (AQP1 vehicle), 5 (bacopaside I), 7 (bacopaside II), and 8 (non-AQP1 control). (D) Dose-dependent block of AQP1-mediated osmotic swelling by bacopasides I and II, with estimated IC_{50} values of 117 μM and 18 μM, respectively. No sensitivity to bacopaside I was seen for the AQP1 R159,160A double mutant at doses up to 100 μM. (E) Chemical structures of bacopasides I and II.

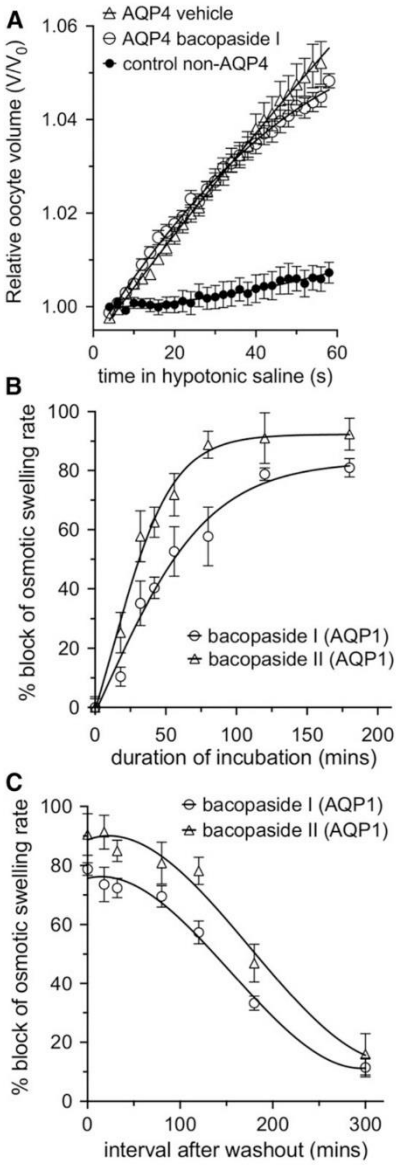

Fig. 2. Subtype selectivity and temporal properties of block onset and recovery with bacopasides I and II in AQP-expressing oocytes. (A) Mean swelling responses of AQP4-expressing oocytes in 50% hypotonic saline were not affected after 2 hours of preincubation in 178 μM bacopaside I. Data are mean ± S.E.M.; n values are 8 (AQP4 alone), 8 (AQP4 with bacopaside I), and 6 (non-AQP4 control). (B) Time-dependent establishment of block of AQP1-mediated osmotic water permeability required preincubation of oocytes in 178 μM bacopaside I or 35 μM bacopaside II, with approximately 2 hours needed to achieve maximal inhibition. The n values are 12 to 14 oocytes per time point; each oocyte was used for a single measurement. (C) Time-dependent recovery from block in AQP1-expressing oocytes preincubated 2 hours in 178 μM bacopaside I or 35 μM bacopaside II, and assessed at different intervals after transfer back into standard isotonic saline at time 0 (washout). The n values are 10 to 13 oocytes per time point; each oocyte was used for a single measurement.

The blocking effects of bacopasides I and II on AQP1 water channel activity were reversible (Fig. 2C). AQP1-expressing oocytes were preincubated 2 hours with 178 μM bacopaside I or 35 μM bacopaside II, followed by washout of the drug with isotonic saline. The osmotic water permeability showed approximately 25% recovery by 120 minutes after the washout of bacopaside I, and half-maximal recovery by 160 minutes. For bacopaside II, water permeability showed 25% recovery by 150 minutes after washout of the blocker, and half-maximal recovery by 200 minutes.

Ion Channel Conductance of AQP1 Was Inhibited by Bacopaside I but Not by Bacopaside II. Two-electrode voltage clamp recordings from AQP1-expressing oocytes demonstrated the cGMP-dependent activation of the ionic conductance (Fig. 3A) as described previously elsewhere (Anthony et al., 2000), which was reversible by 2 hours of incubation in saline without membrane-permeable cGMP (Kourghi et al., 2016). Reactivation of the ionic response by a second dose of cGMP was partly blocked in AQP1-expressing oocytes after 2-hour incubation in 50 μM bacopaside I, and strongly blocked at 100 μM bacopaside I (Fig. 3B). In contrast, the reactivation of the ion conductance was unimpaired after incubation with 10 μM or 20 μM bacopaside II.

Identification of Candidate Intracellular Binding Sites. Protein crystal structures of AQP1 and AQP4, and three-dimensional structural renditions of bacopaside I and bacopaside II were prepared and run on interaction simulations using Autodock Vina software to identify predicted binding sites. An array of candidate docking sites for bacopasides I and II on AQP1 and AQP4 channels were considered with in silico computational docking analyses. Of a total of eight possible positions evaluated for bacopaside I, the dominant energetically favored configurations for intracellular binding yielded values of −9.2 kcal/mol for AQP1 (Data Supplement 1), and −8.0 Kcal/mol for AQP4 (Data Supplement 2). Similarly out of all possible positions evaluated, the energetically favored configurations for bacopaside II yielded values of −9.3 kcal/mol for AQP1 (Data Supplement 3), and −7.8 kcal/mol for AQP4 (Data Supplement 4).

In the poses reflecting the most favored docking positions, the intracellular face of the water pore was effectively occluded by bacopasides I and II in AQP1, but not in AQP4 channels (Fig. 4, A–D). For AQP1, the bacopasides appeared to nest well into the internal vestibule of the intrasubunit water pore. For AQP4 the optimal interaction was seen for bacopaside sitting in a groove between transmembrane domains 4 and 5, a position where subunits interface near the central pore that might not be accessible in the assembled tetrameric channel.

Closer inspection of specific amino acid residues in the predicted AQP1 docking site (using Chimera visualization software) suggested that the poly-arginine motif in the loop D domain could enable hydrogen bond formation with the sulfonyl moiety on the glucopyranosyl sugar of bacopaside I (Fig. 4E) at residues corresponding to R159 and R160 in human AQP1. These arginines are part of a highly conserved amino acid pattern seen in AQP1 channels from diverse species, and they are required for cGMP gating of the AQP1 ionic conductance (Yu et al., 2006). The site-directed double

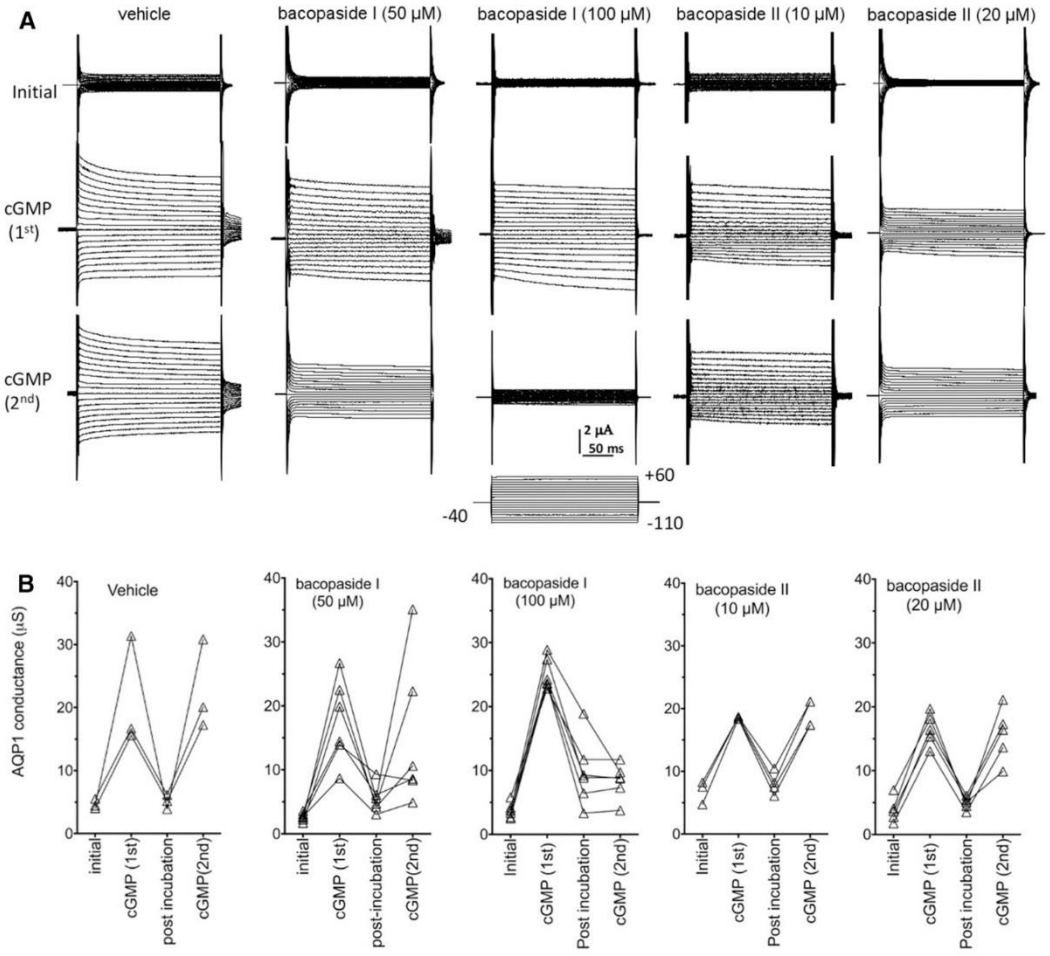

Fig. 3. Block of the cGMP-dependent ionic conductance of AQP1-expressing oocytes by bacopaside I, but not bacopaside II. (A) Representative sets of traces recorded by two-electrode voltage clamp of AQP1-expressing oocytes showing the initial conductance; the response induced by the first application of membrane-permeable cGMP; the recovery of the response to near initial levels after 2 hours of incubation in isotonic saline containing bacopaside I (50 or 100 μM) or bacopaside II (10 or 20 μM); and the final response to a second application of cGMP. (B) Trend plots showing the amplitude of the ionic currents, before and after the first activation by GMP, the recovery after incubation, and the response reactivated by a second cGMP application. Consistent recovery was seen after 10 or 20 μM bacopaside II, but not after incubation with 50 or 100 μM bacopaside I indicating establishment of ion channel block. The n values are as shown; each line represents a series of recordings from one oocyte.

mutation of arginines R159 and R160 to alanines did not prevent normal expression of AQP1-mediated osmotic water permeability, indicating that the AQP1 mutant constructs were expressed and targeted to the oocyte plasma membrane as described previously elsewhere (Yu et al., 2006); however, the efficacy of bacopaside I in inhibiting osmotic water permeability was abolished in the mutant construct at doses up to 100 μM (Fig. 1D, supporting the suggested role of the loop D arginine residues in stabilizing the docking of the bacopaside I ligand.

Bacopaside II Was More Effective Than Bacopaside I in Blocking Migration of AQP1-Expressing Colon Cancer Cells. HT29 cells have a higher endogenous level of AQP1 expression as compared with SW480 cells, as demonstrated by qRT-PCR (Fig. 5A), western blot (Fig. 5B), and immunocytochemistry (Fig. 5C) analyses.

Wound closure assays showed robust migration of HT29 cells in medium with vehicle (Fig. 6A), resulting in little open area remaining at 24 hours. In contrast, treatment with bacopaside II (Fig. 6B) substantially reduced the amount of wound closure. A dose-dependent block of cell migration measured by wound closure (Fig. 6C) was observed for both bacopaside I and bacopaside II on HT29 cells. The calculated IC_{50} value for bacopaside I was approximately 48 μM and for bacopaside II was 14 μM in HT29 cells. There was a small

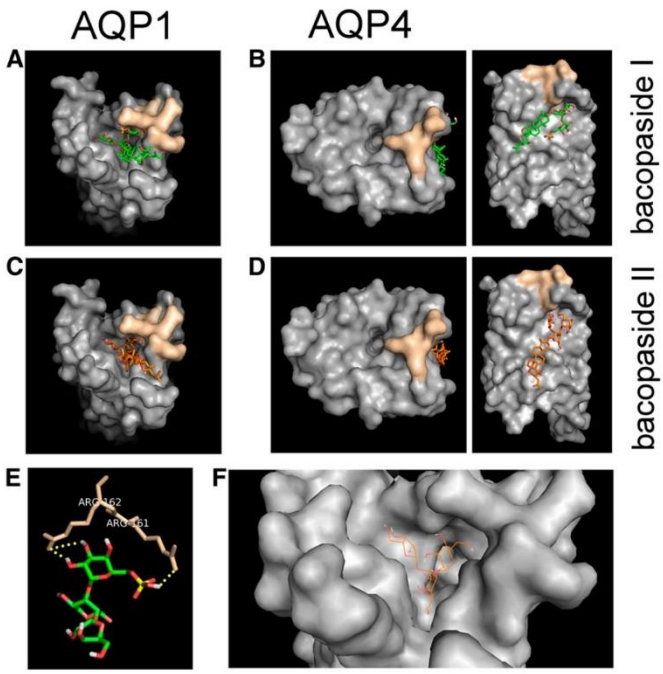

Fig. 4. In silico docking models illustrating predictions for the most favorable sites of interaction of bacopaside I and bacopaside II on AQP1 and AQP4 subunit proteins. AQP subunit models were assembled from crystal structural data for human AQP1 (PDB ID 1FQY) and human AQP4 (PDB ID 3GDB); see *Materials and Methods* for details. Subunit views are from the cytoplasmic side, with the water pore in the center. The intracellular loop D domain, adjacent to the channel tetrameric axis of symmetry, is highlighted in dark gold. (A) Bacopaside I is predicted by in silico docking to occlude the cytoplasmic side of the intrasubunit water pore in AQP1. (B) Favorable interactions at the AQP4 water pore are not evident for bacopaside I; the best fit is seen near membrane-spanning domains distant from the pore (inset). (C) Bacopaside II is predicted to have the most favorable energy of interaction at a position occluding the cytoplasmic side of the AQP1 water pore. (D) Predicted binding of bacopaside II with AQP4 is distant from the water pore (inset), in a position similar to that seen for bacopaside I. (E) Enlarged view of the predicted interaction of the sugar-linked sulfur group of bacopaside I with the conserved loop D arginine residues in AQP1. (F) Enlarged view of the predicted binding of the trisaccharide moiety of bacopaside II deep into the cytoplasmic vestibule of the AQP1 water pore.

reduction of migration observed for SW480 cells treated with bacopasides I and II (Fig. 6C), which was consistent with the relatively low expression of AQP1 channels in this cell line.

Time-Lapse Imaging Demonstrated Bacopasides I and II Differentially Decreased the Rate of Migration of AQP1-Expressing HT29 Colon Cancer Cells. Cultured HT29 cancer cells showed differences in rates of migration into the open wound areas in the vehicle, bacopaside I and bacopaside II treatment conditions (Fig. 7, A–C). Time-lapse images showed the rates of cell migration were significantly impeded in 50 μM bacopaside I and in 15 μM bacopaside II (Fig. 7, B and C) as compared with vehicle-treated HT29 cells (Fig. 7A). No appreciable difference in cell viability was observed in any of the treatment groups during the 24-hour time course of the experiment.

In the vehicle-treated group, trajectory plots of individual cells sampled at 50-minute intervals over 24 hours (Fig. 7D) showed generally directional movements of HT29 cells into the open wound spaces. In bacopaside I treatment group, the HT29 cells lacked directional migration and moved short distances between successive frames. In the bacopaside II treated group, the impairment of movement was evident but less severe. The collective trend of trajectories of the vehicle-treated group appeared to be linear and extended, whereas that in the bacopaside I treated group was recursive and compressed; the bacopaside II group showed an intermediate level of restriction of movement.

The net displacement (distance traveled) per time interval was greater in the vehicle-treated group than in the bacopasides I and II treatment groups. Frequency histograms, summarizing all events observed, were compiled as the binned values of distances traveled per 50-minute interval (Fig. 7E). These histograms showed that more cells traveled longer distances per time interval in the vehicle-treated group than in the bacopaside-treated groups. Distributions moved were well fit by Gaussian functions; the decreased mean distances moved in the bacopaside treatments were seen as left shifts in the peaks of the frequency histograms. Compiled data in a summary histogram (Fig. 7F) confirmed the significant decrease in mean total distance traveled by cells during the 24 hours of tracking in bacopaside I or II as compared with vehicle-treated cells. Analysis of cytotoxicity by AlamarBlue assay showed that bacopaside I had no significant effect on cell viability at 50 or 75 μM, and bacopaside II had no effect on viability at 15 or 20 μM (Table 1). Concentrations of bacopasides that significantly blocked AQP1 water channel activity and HT29 cell migration were not appreciably cytotoxic.

Discussion

Our results have demonstrated that two structurally similar compounds, bacopaside I and bacopaside II, derived from a medicinal herb, act differentially as pharmacologic inhibitors of mammalian aquaporin channels. In silico modeling predicted that bacopasides I and II have favorable energies of interaction at the intracellular vestibule of AQP1, occluding the intrasubunit water pore. Modeling results were consistent with the observed effects of these agents as AQP1 inhibitors.

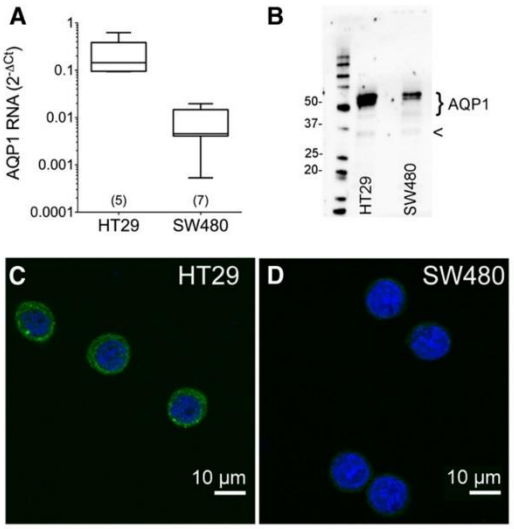

Fig. 5. HT29 cells have higher level of AQP1 expression than SW480 cells. (A) The AQP1 RNA level was higher in HT29 cells as compared with SW480 cells as assessed using qRT-PCR. (B) The AQP1 protein level was higher in HT29 than SW480 cells as demonstrated by Western blot, with monomeric subunit band seen near the predicted size of 28 kD with higher molecular mass glycosylated bands. (C) The AQP1 immunopositive signal (green) associated with the cell membrane was stronger in HT29 than in SW480 cells. Cell nuclei were counterstained (blue). See *Materials and Methods* for details.

The predicted energies of interaction for docking on AQP1 were higher for bacopaside II than bacopaside I, fitting the observed order of efficacy in blocking AQP1-mediated swelling of oocytes and the same order of efficacy in blocking migration of AQP1-expressing HT29 colon cancer cells, with minimal effects on SW480 cells that express little AQP1. The docking of bacopasides I and II to occlude the water pore appeared principally to involve the trisaccharide rings, which projected down into the AQP1 intrasubunit pore.

Future work exploring polysaccharides and related osmolytes as endogenous modulators of AQP channels could be of interest. The lack of a favorable docking interaction of bacopaside with the AQP4 water pore was consistent with the insensitivity of AQP-4 expressing oocytes to bacopaside I in osmotic swelling assays. Based on the docking model, candidate residues that could contribute to the proposed binding of bacopaside sugar rings in the hAQP1 intracellular water pore appear to include amino acids serine 71 in the loop B region, and tyrosine 97 in the adjacent membrane spanning domains, but remain to be defined.

Inhibition of AQP1 water channel activity by bacopasides I and II showed a slow onset that was consistent with prerequisite transit of the agent across the membrane to access the intracellular side. The latency period (approximately 2 hours) was comparable to that described for other aquaporin modulators AqB013 and AqF026, also thought to act at the cytoplasmic side (Migliati et al., 2009; Yool et al., 2013).

Accumulating evidence suggests pharmacologic agents can be defined with subtype selectivity for AQP classes. Prior work showed external application of AqF026 potentiated water permeability in AQP1 (EC_{50} 3.3 μM), but a 15-fold higher concentration was required to potentiate AQP4 (Yool et al., 2013). Metal complexes acted as blockers of glycerol permeability in AQP3 (at an external site predicted to involve cysteine [C40] and arginine [R218] residues), with comparatively small effects on AQP1 water permeability (Martins et al., 2013). Results here for bacopaside I showed block of osmotic water permeability for AQP1 but not AQP4 channels. This difference in bacopaside sensitivity between related aquaporins suggests that the inhibitory effects seen for AQP1 are exerted directly on the heterologously expressed channel and are not due to side effects on endogenous oocyte channels or transporters.

The reversibility of the block indicated that functional properties and expression of the channels in plasma membrane were not impaired. Data here cannot rule out actions of bacopasides on other molecules not yet assessed; however, the

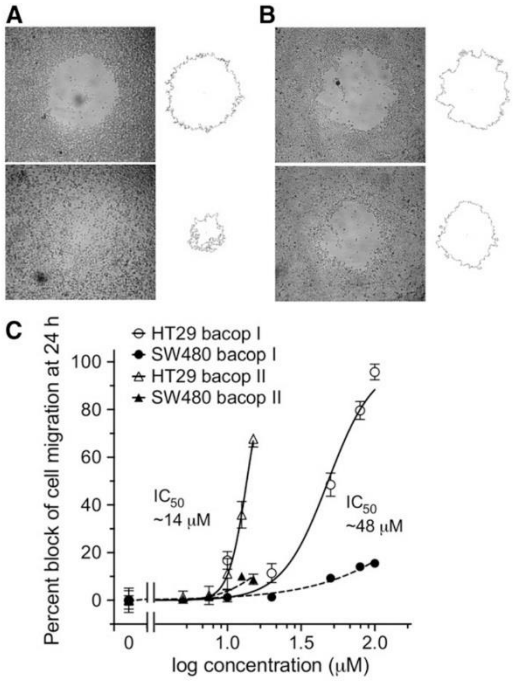

Fig. 6. Dose-dependent inhibition of migration by bacopasides I and II in AQP1-expressing HT29 cells, but not in SW480 cells with low AQP1 expression. Cell migration in the presence of a mitotic inhibitor was assessed by rates of closure of circular wounds, created by aspiration with a pipette tip in confluent cultures (see *Materials and Methods* for details). (A, B) Cell migration was assessed in vehicle (A) or with 15 μM bacopaside II (B) added immediately after wounding. Images are shown for confluent HT29 cultures after initial wounding at time 0 (upper panels) and at 24 hours (lower panels). (C) Dose-dependent block of HT29 cell migration was seen with bacopasides I and II, with IC_{50} values estimated at 48 and 14 μM, respectively. Partial block of SW480 migration at the highest doses tested did not exceed 20%. Doses beyond the ranges shown were not considered valid due to the onset of cytotoxicity.

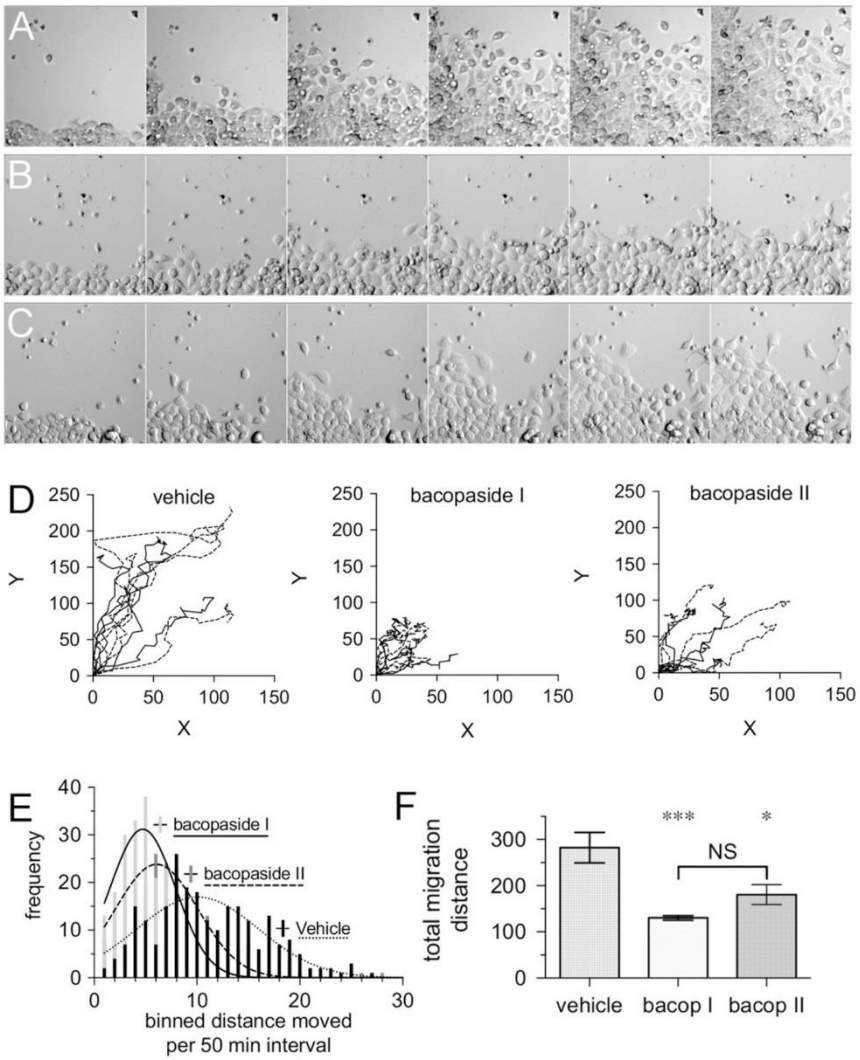

Fig. 7. Live-cell imaging of the inhibitory effects of bacopasides I and II on migration of HT29 cells. Single cells at the boundaries of circular wounds were tracked with time-lapse images taken at 25-minute intervals for 10 hours at 37°C. (A–C) Panels of six images each from time-lapse series are shown at 50-minute intervals: (A) HT29 cells with vehicle treatment. (B) HT29 cells treated with 50 μM bacopaside I. (C) HT29 cells treated with 15 μM bacopaside II. (D) Trajectory plots of 10 individual cells per treatment group, monitored by cell nucleus position as a function of time. Data were converted to absolute values and referenced to the starting position at time 0; X and Y values are in pixels (7.45 pixels per mm). Trajectory plots illustrate the total movement of 10 individual cells per treatment over a duration of 600 minutes, with vehicle, bacopaside I or with bacopaside II. (E) Frequency histograms of the distances moved by individual cells per 50-minute interval over 600 minutes of imaging, for 10 cells per treatment group. Histograms were fit with Gaussian distribution functions (R^2 values > 0.94); best-fit values for the mean distances moved per cell per 50-minute interval were 10.1 $\pm$ 0.5 for untreated, 4.7 $\pm$ 0.2 for bacopaside I treated, and 7.8 $\pm$ 0.2 for bacopaside II treated (mean $\pm$ S.E.M.). (F) Summary histogram showing the mean total distance traveled by cells in 600 minutes, showing significant inhibition of cell motility by both bacopaside I and II as compared with vehicle-treated cells (analysis of variance test $P < 0.05$; post hoc Bonferroni $^*P < 0.05$; $^{***}P < 0.001$). Data are mean $\pm$ S.E.M.; n values are 10 cells per treatment group.

lack of effect of bacopaside on migration in SW480 cells with low AQP1 expression suggests the mechanism of action is reasonably selective, and does not appreciably impact diverse signaling and transport processes needed for basic maintenance and non-AQP1 dependent motility. Cytotoxicity assays showed the viability of AQP1-expressing HT29 cancer cells was not affected by bacopasides I and II at doses that significantly blocked ion flux and cell migration.

TABLE 1
Analysis of cytotoxicity in HT29 colon cancer cells at 24 hours of treatment, using an AlumarBlue fluorescence assay

Concentration (μM)	Mean Normalized Cell Viability (%)[a]	*n* value	*P* value
bacopaside I			
0	108 ± 4.8	17	N.S.
0 (vehicle)	100 ± 3.1	17	—
50	97 ± 2.1	8	N.S.
75	79 ± 4.2	8	N.S.
100	59 ± 3.2	8	[b]
bacopaside II			
0	113 ± 6.2	16	N.S.
0 (vehicle)	100 ± 5.7	16	—
15	104 ± 18	8	N.S.
20	123 ± 17	8	N.S.
30	47 ± 5.7	8	[b]
$HgCl_2$			
100	16.1 ± 4.6	6	[b]

[a]Mean ± S.E.M. The percentage of viability was standardized as a percentage of the vehicle-treated mean value, measured as changes in AlumarBlue fluorescence signal intensity. See *Materials and Methods* for details.
[b]Statistically significant differences ($P < 0.05$), compared with vehicle-treated, were analyzed by analysis of variance with post hoc Dunnett's multiple comparison test (GraphPad Prism). N.S. is not statistically significant.

Bacopasides I and II are triterpene glycosides, composed of a hydrophobic pentacyclic terpene backbone (estimated logP value approximately 9; enabling membrane permeability), and three linked polar sugar groups (arabinofuranosyl—glucopyranosyl—arabinopyranose in bacopaside I; and arabinofuranosyl—sulfonyl-glucopyranosyl—glucopyranose in bacopaside II) that appear from in silico modeling to lodge via H-bonds into the water pore entrance of AQP1, with the exception of the sulfonyl group which appears to require an interface with positively charged residues (arginines in the adjacent AQP1 loop D domain). Mutation of the key loop D arginines to alanines appeared to cause destabilization of the overall binding of the bacopaside I compound on AQP1, seen as a decreased efficacy of water pore block and increased IC_{50} value in the R159A+R160A mutant.

The ability of modulators to block the central pore ionic conductance is an important consideration in processes such as rapid cell migration which appear to require the AQP1 cation channel activity (Kourghi et al., 2016). Interaction of the sulfonyl group with loop D arginines was consistent with the observed block of the cGMP-activated ionic conductance by bacopaside I, not II. Bacopaside II lacked an effect on the ionic conductance, and showed similar IC_{50} values for the block of AQP1 water channel activity in oocytes, and the block of cell migration in HT29 cells. In contrast, bacopaside I showed a lower IC_{50} value for inhibiting HT29 cancer cell migration (~48 μM) than for inhibiting the AQP1 osmotic water flux in oocytes (~117 μM), suggesting that simultaneous block of both water and ion channel activities of AQP1 might be more effective in blocking cell migration. This is consistent with the observed migration trajectories, which were more compressed in bacopaside I-treated group than in the bacopaside II-treated group.

Although the overall amino acid sequence similarity between AQP1 and AQP4 channels is high (>40% identity and 60% homology), AQP4-mediated osmotic swelling was not sensitive to block by bacopaside I. The docking model suggested the bulky terpene might sterically hinder docking near the AQP4 water pore. As well, the loop D domain of AQP4 lacks the key arginines 159 and 160, suggested here to be important for the sulfonyl group coordination, showing instead serine and lysine in the equivalent positions, which might be less effective as putative coordination sites.

The identification of bacopasides as novel AQP modulators expands the database of pharmacophore properties of AQP ligands. Bacopasides I and II themselves might not be ideal as drug candidates, exceeding limits of Lipinski's Rule of Five for molecular weight, hydrophobicity, and numbers of hydrogen bond donors and acceptors—although natural products often show biologic activity as exceptions to the rule (Ganesan, 2008). Bacopasides administered in vivo are likely to act as metabolic derivatives as well as intact compounds. More work is needed to define in vivo metabolites of bacopasides and characterize their effects on aquaporins. Nonetheless, bacopasides could serve as lead compounds for the design of small-molecule blockers of aquaporins.

Our results suggest the trisaccharide moiety is a key component. An intriguing idea would be to design compact membrane-permeable trisaccharides for blocking water flux; addition of key sulfonyl or other groups could inhibit parallel AQP functions. Endogenous polysaccharide osmolytes in cells might function as natural modulators of aquaporin channels, a concept that has not to our knowledge been considered previously.

Bacopa monnieri extract (also known as brahmi) has been used in Ayurvedic remedies since ancient times to improve memory and treat anxiety and depression (Russo and Borrelli, 2005). Brahmi has been suggested to have beneficial effects on psychologic state, cognitive performance, and memory in human subjects and animal models; neuroprotective effects after ischemic brain injury; and anti-inflammatory actions in processes linked to neurodegenerative disorders (Singh and Dhawan, 1982; Sairam et al., 2002; Rehni et al., 2007; Zhou et al., 2007; Saraf et al., 2010; Aguiar and Borowski, 2013; Downey et al., 2013; Liu et al., 2013; Kongkeaw et al., 2014; Williams et al., 2014). A meta-analysis of human clinical studies (generally with *B. monnieri* administered 250–450 mg/day for up to several months) improved mental response time and attention, and had potential benefits on memory (Kongkeaw et al., 2014). No serious adverse events were noted; minor side effects included diarrhea and dry mouth.

Beneficial outcomes ascribed to brahmi could in part involve block of AQP1 channels. AQP1 is expressed abundantly in brain choroid plexus where cerebral spinal fluid is produced (Boassa and Yool, 2005; Johansson et al., 2005) and in proximal kidney to facilitate water reabsorption (Nielsen and Agre, 1995). AQP1 is found in peripheral vasculature endothelia, red blood cells, and other cell types (Nielsen et al., 1993). Block of AQP1 could contribute to the anti-inflammatory benefits of brahmi treatment. Macrophages express AQP1 channels, which are required for interleukin-1β release and neutrophilic inflammation responses (Rabolli et al., 2014). An alcoholic extract of *B. monnieri* decreased tumor necrosis factor-α production in mouse macrophages preincubated for 1 hour, with an IC_{50} near 1 mg/ml (Williams et al., 2014).

Pharmacologic inhibitors of AQP1 channels could be useful for intervention in many conditions, including slowing metastasis in AQP1-positive cancer subtypes. In a subset of aggressive cancers, AQP1 expression is up-regulated (Saadoun et al., 2002; Moon et al., 2003; Yool et al., 2010; El Hindy et al., 2013). AQP1 channels located at lamellipodial edges have been implicated in enhancing migration and

metastasis (Hu and Verkman, 2006; McCoy and Sontheimer, 2007). Block of the AQP1 ion channel impairs migration in AQP1-expressing HT29 colon cancer cells (Kourghi et al., 2016).

A comprehensive portfolio of selective aquaporin modulators is needed for clinical and basic research. Further exploration of AQP modulators in traditional herbal medicines is merited (Pei et al., 2016). New ligand modulators of aquaporin channel activity could be present in the armamentarium of traditional herbal medicines, but they remain to be discovered.

Acknowledgments

The authors thank John Sandham and the Botanic Gardens of Adelaide for identified samples of the water hyssop *Bacopa monnieri*, and Dr. Agatha Labrinidis and the Adelaide Microscopy core facility for access to equipment, support, and training in live cell imaging.

Authorship Contributions

Participated in research design: Pei, Campbell, Hardingham, Yool.
Conducted experiments: Pei, Kourghi, De Ieso, Campbell, Doward.
Performed data analysis: Pei, Kourghi, De Ieso, Yool.
Wrote or contributed to the writing of the manuscript: Pei, Kourghi, De Ieso, Yool.

References

Agre P, Preston GM, Smith BL, Jung JS, Raina S, Moon C, Guggino WB, and Nielsen S (1993) Aquaporin CHIP: the archetypal molecular water channel. *Am J Physiol* **265**:F463–F476.
Aguiar S and Borowski T (2013) Neuropharmacological review of the nootropic herb Bacopa monnieri. *Rejuvenation Res* **16**:313–326.
Anthony TL, Brooks HL, Boassa D, Leonov S, Yanochko GM, Regan JW, and Yool AJ (2000) Cloned human aquaporin-1 is a cyclic GMP-gated ion channel. *Mol Pharmacol* **57**:576–588.
Boassa D and Yool AJ (2003) Single amino acids in the carboxyl terminal domain of aquaporin-1 contribute to cGMP-dependent ion channel activation. *BMC Physiol* **3**:12.
Boassa D and Yool AJ (2005) Physiological roles of aquaporins in the choroid plexus. *Curr Top Dev Biol* **67**:181–206.
Brooks HL, Regan JW, and Yool AJ (2000) Inhibition of aquaporin-1 water permeability by tetraethylammonium: involvement of the loop E pore region. *Mol Pharmacol* **57**:1021–1026.
Calamita G, Bishai WR, Preston GM, Guggino WB, and Agre P (1995) Molecular cloning and characterization of AqpZ, a water channel from Escherichia coli. *J Biol Chem* **270**:29063–29066.
Campbell EM, Birdsell DN, and Yool AJ (2012) The activity of human aquaporin 1 as a cGMP-gated cation channel is regulated by tyrosine phosphorylation in the carboxyl-terminal domain. *Mol Pharmacol* **81**:97–105.
Detmers FJ, de Groot BL, Müller EM, Hinton A, Konings IB, Sze M, Flitsch SL, Grubmüller H, and Deen PM (2006) Quaternary ammonium compounds as water channel blockers. Specificity, potency, and site of action. *J Biol Chem* **281**: 14207–14214.
Devuyst O and Yool AJ (2010) Aquaporin-1: new developments and perspectives for peritoneal dialysis. *Perit Dial Int* **30**:135–141.
Downey LA, Kean J, Nemeh F, Lau A, Poll A, Gregory R, Murray M, Rourke J, Patak B, Pase MP, et al. (2013) An acute, double-blind, placebo-controlled crossover study of 320 mg and 640 mg doses of a special extract of *Bacopa monnieri* (CDRI 08) on sustained cognitive performance. *Phytother Res* **27**:1407–1413.
El Hindy N, Bankfalvi A, Herring A, Adamzik M, Lambertz N, Zhu Y, Siffert W, Sure U, and Sandalcioglu IE (2013) Correlation of aquaporin-1 water channel protein expression with tumor angiogenesis in human astrocytoma. *Anticancer Res* **33**: 609–613.
Esteva-Font C, Jin BJ, Lee S, Phuan PW, Anderson MO, and Verkman AS (2016) Experimental evaluation of proposed small-molecule inhibitors of water channel aquaporin-1. *Mol Pharmacol* **89**:686–693.
Fu D, Libson A, Miercke LJ, Weitzman C, Nollert P, Krucinski J, and Stroud RM (2000) Structure of a glycerol-conducting channel and the basis for its selectivity. *Science* **290**:481–486.
Ganesan A (2008) The impact of natural products upon modern drug discovery. *Curr Opin Chem Biol* **12**:306–317.
Gao J, Wang X, Chang Y, Zhang J, Song Q, Yu H, and Li X (2006) Acetazolamide inhibits osmotic water permeability by interaction with aquaporin-1. *Anal Biochem* **350**:165–170.
Hu J and Verkman AS (2006) Increased migration and metastatic potential of tumor cells expressing aquaporin water channels. *FASEB J* **20**:1892–1894.
Huber VJ, Tsujita M, Kwee IL, and Nakada T (2009) Inhibition of aquaporin 4 by antiepileptic drugs. *Bioorg Med Chem* **17**:418–424.
Huber VJ, Tsujita M, Yamazaki M, Sakimura K, and Nakada T (2007) Identification of arylsulfonamides as aquaporin 4 inhibitors. *Bioorg Med Chem Lett* **17**: 1270–1273.
Johansson PA, Dziegielewska KM, Ek CJ, Habgood MD, Møllgård K, Potter A, Schuliga M, and Saunders NR (2005) Aquaporin-1 in the choroid plexuses of developing mammalian brain. *Cell Tissue Res* **322**:353–364.
Kongkeaw C, Dilokthornsakul P, Thanarangsarit P, Limpeanchob N, and Norman Scholfield C (2014) Meta-analysis of randomized controlled trials on cognitive effects of *Bacopa monnieri* extract. *J Ethnopharmacol* **151**:528–535.
Kourghi M, Pei JV, De Ieso ML, Flynn G, and Yool AJ (2016) Bumetanide derivatives AqB007 and AqB011 selectively block the aquaporin-1 ion channel conductance and slow cancer cell migration. *Mol Pharmacol* **89**:133–140.
Liu X, Yue R, Zhang J, Shan L, Wang R, and Zhang W (2013) Neuroprotective effects of bacopaside I in ischemic brain injury. *Restor Neurol Neurosci* **31**:109–123.
Martins AP, Ciancetta A, de Almeida A, Marrone A, Re N, Soveral G, and Casini A (2013) Aquaporin inhibition by gold(III) compounds: new insights. *ChemMedChem* **8**:1086–1092.
McCoy E and Sontheimer H (2007) Expression and function of water channels (aquaporins) in migrating malignant astrocytes. *Glia* **55**:1034–1043.
Migliati E, Meurice N, DuBois P, Fang JS, Somasekharan S, Beckett E, Flynn G, and Yool AJ (2009) Inhibition of aquaporin-1 and aquaporin-4 water permeability by a derivative of the loop diuretic bumetanide acting at an internal pore-occluding binding site. *Mol Pharmacol* **76**:105–112.
Moon C, Soria JC, Jang SJ, Lee J, Obaidul Hoque M, Sibony M, Trink B, Chang YS, Sidransky D, and Mao L (2003) Involvement of aquaporins in colorectal carcinogenesis. *Oncogene* **22**:6699–6703.
Nielsen S and Agre P (1995) The aquaporin family of water channels in kidney. *Kidney Int* **48**:1057–1068.
Nielsen S, Smith BL, Christensen EI, and Agre P (1993) Distribution of the aquaporin CHIP in secretory and resorptive epithelia and capillary endothelia. *Proc Natl Acad Sci USA* **90**:7275–7279.
Niemietz CM and Tyerman SD (2002) New potent inhibitors of aquaporins: silver and gold compounds inhibit aquaporins of plant and human origin. *FEBS Lett* **531**:443–447.
Papadopoulos MC and Verkman AS (2008) Potential utility of aquaporin modulators for therapy of brain disorders. *Prog Brain Res* **170**:589–601.
Parsels LA, Parsels JD, Tai DC, Coughlin DJ, and Maybaum J (2004) 5-fluoro-2′-deoxyuridine-induced cdc25A accumulation correlates with premature mitotic entry and clonogenic death in human colon cancer cells. *Cancer Res* **64**: 6588–6594.
Pei JV, Burton JL, Kourghi M, De Ieso ML, and Yool AJ (2016) Drug discovery and therapeutic targets for pharmacological modulators of aquaporin channels, in *Aquaporins in Health and Disease: New Molecular Targets For Drug Discovery* (Soveral G, Casinin A, and Nielsen S, eds) pp 275–297, CRC Press, Oxfordshire, United Kingdom.
Preston GM, Jung JS, Guggino WB, and Agre P (1993) The mercury-sensitive residue at cysteine 189 in the CHIP28 water channel. *J Biol Chem* **268**:17–20.
Rabolli V, Wallemme L, Lo Re S, Uwambayinema F, Palmai-Pallag M, Thomassen L, Tyteca D, Octave JN, Marbaix E, Lison D, et al. (2014) Critical role of aquaporins in interleukin 1β (IL-1β)-induced inflammation. *J Biol Chem* **289**: 13937–13947.
Rehni AK, Pantlya HS, Shri R, and Singh M (2007) Effect of chlorophyll and aqueous extracts of *Bacopa monniera* and *Valeriana wallichii* on ischaemia and reperfusion-induced cerebral injury in mice. *Indian J Exp Biol* **45**:764–769.
Reizer J, Reizer A, and Saier MH, Jr (1993) The MIP family of integral membrane channel proteins: sequence comparisons, evolutionary relationships, reconstructed pathway of evolution, and proposed functional differentiation of the two repeated halves of the proteins. *Crit Rev Biochem Mol Biol* **28**:235–257.
Russo A and Borrelli F (2005) *Bacopa monniera*, a reputed nootropic plant: an overview. *Phytomedicine* **12**:305–317.
Saadoun S, Papadopoulos MC, Davies DC, Bell BA, and Krishna S (2002) Increased aquaporin 1 water channel expression in human brain tumours. *Br J Cancer* **87**: 621–623.
Sairam K, Dorababu M, Goel RK, and Bhattacharya SK (2002) Antidepressant activity of standardized extract of *Bacopa monniera* in experimental models of depression in rats. *Phytomedicine* **9**:207–211.
Saparov SM, Kozono D, Rothe U, Agre P, and Pohl P (2001) Water and ion permeation of aquaporin-1 in planar lipid bilayers. Major differences in structural determinants and stoichiometry. *J Biol Chem* **276**:31515–31520.
Saraf MK, Prabhakar S, and Anand A (2010) Neuroprotective effect of *Bacopa monniera* on ischemia induced brain injury. *Pharmacol Biochem Behav* **97**: 192–197.
Schindelin J, Arganda-Carreras I, Frise E, Kaynig V, Longair M, Pietzsch T, Preibisch S, Rueden C, Saalfeld S, Schmid B, et al. (2012) Fiji: an open-source platform for biological-image analysis. *Nat Methods* **9**:676–682.
Seeliger D, Zapater C, Krenc D, Haddoub R, Flitsch S, Beitz E, Cerdà J, and de Groot BL (2013) Discovery of novel human aquaporin-1 blockers. *ACS Chem Biol* **8**: 249–256.
Singh HK and Dhawan BN (1982) Effect of *Bacopa monniera* Linn. (brahmi) extract on avoidance responses in rat. *J Ethnopharmacol* **5**:205–214.
Tajkhorshid E, Nollert P, Jensen MO, Miercke LJ, O'Connell J, Stroud RM, and Schulten K (2002) Control of the selectivity of the aquaporin water channel family by global orientational tuning. *Science* **296**:525–530.
Trott O and Olson AJ (2010) AutoDock Vina: improving the speed and accuracy of docking with a new scoring function, efficient optimization, and multithreading. *J Comput Chem* **31**:455–461.
Williams R, Münch G, Gyengesi E, and Bennett L (2014) *Bacopa monnieri* (L.) exerts anti-inflammatory effects on cells of the innate immune system in vitro. *Food Funct* **5**:517–520.
Yang B, Kim JK, and Verkman AS (2006) Comparative efficacy of $HgCl_2$ with candidate aquaporin-1 inhibitors DMSO, gold, TEA+ and acetazolamide. *FEBS Lett* **580**:6679–6684.
Yool AJ (2007) Functional domains of aquaporin-1: keys to physiology, and targets for drug discovery. *Curr Pharm Des* **13**:3212–3221.
Yool AJ, Brokl OH, Pannabecker TL, Dantzler WH, and Stamer WD (2002) Tetraethylammonium block of water flux in aquaporin-1 channels expressed in kidney thin limbs of Henle's loop and a kidney-derived cell line. *BMC Physiol* **2**:4.

Yool AJ, Brown EA, and Flynn GA (2010) Roles for novel pharmacological blockers of aquaporins in the treatment of brain oedema and cancer. *Clin Exp Pharmacol Physiol* **37**:403–409.
Yool AJ and Campbell EM (2012) Structure, function and translational relevance of aquaporin dual water and ion channels. *Mol Aspects Med* **33**:553–561.
Yool AJ, Morelle J, Cnops Y, Verbavatz JM, Campbell EM, Beckett EA, Booker GW, Flynn G, and Devuyst O (2013) AqF026 is a pharmacologic agonist of the water channel aquaporin-1. *J Am Soc Nephrol* **24**:1045–1052.
Yool AJ and Weinstein AM (2002) New roles for old holes: ion channel function in aquaporin-1. *News Physiol Sci* **17**:68–72.
Yu J, Yool AJ, Schulten K, and Tajkhorshid E (2006) Mechanism of gating and ion conductivity of a possible tetrameric pore in aquaporin-1. *Structure* **14**:1411–1423.
Zhang W, Zitron E, Hömme M, Kihm L, Morath C, Scherer D, Hegge S, Thomas D, Schmitt CP, Zeier M, et al. (2007) Aquaporin-1 channel function is positively regulated by protein kinase C. *J Biol Chem* **282**:20933–20940.
Zhou Y, Shen YH, Zhang C, Su J, Liu RH, and Zhang WD (2007) Triterpene saponins from *Bacopa monnieri* and their antidepressant effects in two mice models. *J Nat Prod* **70**:652–655.

Address correspondence to: Dr. Andrea J. Yool, Medical School South level 4, Frome Road, Adelaide SA 5005 Australia. E-mail: andrea.yool@adelaide.edu.au

Supplemental material to this article can be found at:
http://molpharm.aspetjournals.org/content/suppl/2015/10/14/mol.115.101618.DC1

1521-0111/89/1/133–140$25.00
MOLECULAR PHARMACOLOGY

http://dx.doi.org/10.1124/mol.115.101618
Mol Pharmacol 89:133–140, January 2016

Bumetanide Derivatives AqB007 and AqB011 Selectively Block the Aquaporin-1 Ion Channel Conductance and Slow Cancer Cell Migration[S]

Mohamad Kourghi,[1] Jinxin V. Pei,[1] Michael L. De Ieso, Gary Flynn, and Andrea J. Yool

School of Medicine (M.K., J.V.P., M.L.D.I., A.J.Y.) and Institute for Photonics and Advanced Sensing (J.V.P., A.J.Y.), University of Adelaide, Adelaide, South Australia, Australia; and Spacefill Enterprises LLC, Oro Valley, Arizona (G.F.)

Received September 3, 2015; accepted October 13, 2015

ABSTRACT

Aquaporins (AQPs) in the major intrinsic family of proteins mediate fluxes of water and other small solutes across cell membranes. AQP1 is a water channel, and under permissive conditions, a nonselective cation channel gated by cGMP. In addition to mediating fluid transport, AQP1 expression facilitates rapid cell migration in cell types including colon cancers and glioblastoma. Work here defines new pharmacological derivatives of bumetanide that selectively inhibit the ion channel, but not the water channel, activity of AQP1. Human AQP1 was analyzed in the *Xenopus laevis* oocyte expression system by two-electrode voltage clamp and optical osmotic swelling assays. The aquaporin ligand bumetanide derivative AqB011 was the most potent blocker of the AQP1 ion conductance (IC_{50} of 14 μM), with no effect on water channel activity (at up to 200 μM). The order of potency for inhibition of the ionic conductance was AqB011 > AqB007 >> AqB006 ≥ AqB001. Migration of human colon cancer (HT29) cells was assessed with a wound-closure assay in the presence of a mitotic inhibitor. AqB011 and AqB007 significantly reduced migration rates of AQP1-positive HT29 cells without affecting viability. The order of potency for AQP1 ion channel block matched the order for inhibition of cell migration, as well as in silico modeling of the predicted order of energetically favored binding. Docking models suggest that AqB011 and AqB007 interact with the intracellular loop D domain, a region involved in AQP channel gating. Inhibition of AQP1 ionic conductance could be a useful adjunct therapeutic approach for reducing metastasis in cancers that upregulate AQP1 expression.

Introduction

Osmotic water transport across biologic membranes is facilitated by membrane proteins known as aquaporins (AQPs), which are found in all kingdoms of life (Reizer et al., 1993; Park and Saier, 1996; Campbell et al., 2008). To date, at least 15 mammalian subfamilies have been identified: AQP0–AQP14 (Ishibashi, 2009; Finn et al., 2014). Aquaporin is organized as a tetramer of subunits, each comprising six transmembrane domains and five loops (A–E) and carrying a monomeric pore that allows the movement of water or other small solutes (Jung et al., 1994; Fu et al., 2000; Sui et al., 2001).

There is increasing recognition that certain classes of aggressive cancers depend on upregulation of AQP1 for fast migration and metastasis (Monzani et al., 2007). Although the precise mechanism for AQP1-enhanced motility remains unknown, both ion and water channels are essential in the cellular migration process (Schwab et al., 2007). AQP1 expression has been linked to metastasis and invasiveness of colon cancer cells (Jiang, 2009; Yoshida et al., 2013). In mammary and melanoma cancer cells, AQP1 facilitates tumor cell migration in vitro and metastasis in vivo (Hu and Verkman, 2006). Increased levels of AQP1 expression in astrocytoma correlate with the clinical grade, serving as a diagnostic indicator of poor prognoses (El Hindy et al., 2013). AQP1-facilitated cell migration in glioma cannot be substituted by AQP4, indicating more than a simple water channel function is involved in the migration-enhancing mechanism (McCoy and Sontheimer, 2007).

A subset of aquaporins have been shown to have ion channel function, including AQP0, AQP1, AQP6, plant nodulin, and *Drosophila* big brain (Yool and Campbell, 2012). In AQP1, multiple lines of evidence have shown the cGMP-dependent monovalent cation channel is located in the central pore at the 4-fold axis of symmetry and is pharmacologically distinct from the monomeric water pores (Anthony et al., 2000; Saparov et al., 2001; Boassa and Yool, 2003; Yu et al., 2006; Zhang et al., 2007). The AQP1 ion channel has a unitary conductance of 150 picosiemens in physiologic saline, slow activation and deactivation kinetics, and is permeable to Na^+, K^+, and Cs^+, but not divalent cations (Yool et al., 1996; Anthony et al., 2000). Loop D has been shown previously to be involved in cGMP-dependent gating of AQP1 ion channels (Yu et al.,

This work was supported in part by the National Institutes of Health [Grant R01 GM059986] and a 2015 pilot grant from the Institute for Photonics and Advanced Sensing, University of Adelaide.
[1]M.K. and J.V.P. are co-first authors.
dx.doi.org/10.1124/mol.115.101618.
[S] This article has supplemental material available at molpharm.aspetjournals.org.

ABBREVIATIONS: AqB, aquaporin ligand bumetanide derivative (in numbered series); AQP1, aquaporin-1; DMSO, dimethylsulfoxide; EtOAC, ethyl acetate; MW, molecular weight.

2006). The low proportion of AQP1 water channels that are available to be gated as ion channels in reconstituted bilayers and heterologous expression systems has prompted uncertainty regarding the physiologic relevance of the dual water and ion channel function in AQP1 (Saparov et al., 2001; Tsunoda et al., 2004). Further work has indicated that the availability of AQP1 ion channels to be activated by cGMP depends in part on tyrosine phosphorylation at the carboxyl terminal domain (Campbell et al., 2012).

Our characterization here of selective nontoxic pharmacological blockers of the AQP1 ion channel opens the first opportunity to define the functional roles of the AQP1 ion conductance. Prior to 2009, available AQP1 blockers were limited by low potency, lack of specificity, or toxicity. Mercury potently blocks AQP1 water permeability by covalent modification of a cysteine residue in loop E (Preston et al., 1993), but is highly toxic. The tetrethylammonium ion blocks the AQP1 water pore, although not in all cell types (Brooks et al., 2000; Detmers et al., 2006; Sogaard and Zeuthen, 2008), and the cadmium ion blocks the AQP1 ion channel (Boassa et al., 2006), but both lack selectivity for aquaporins. Effective compounds discovered recently include the arylsulfonamides AqB013, which blocks AQP1 and AQP4 water channel permeability (Migliati et al., 2009), and AqF026, which strongly potentiates AQP1 water channel activity (Yool et al., 2013). Other arylsulfonamides have been proposed as blockers of AQP4 channels (Huber et al., 2009). A distinct class of agents acting on the external side of the membrane to block human AQP1 water flux has been identified as a source of candidate lead compounds for drug development (Seeliger et al., 2013).

Work here characterizes a novel set of aquaporin ligand bumetanide derivative (AqB) compounds that differentially block the AQP1 ion channel without affecting water permeability. The most potent of these, AqB011, is a promising tool for dissecting the role of the AQP1 ion channel while sparing osmotic water permeability. Understanding the functional roles and regulation of AQP1 is essential for determining the full range of physiologic roles it might serve and its possible value as a therapeutic target in cancer metastasis.

Materials and Methods

Oocyte Preparation and Injection. The use of animals in this study has been carried out in accordance with the Guide for the Care and Use of Laboratory Animals, licensed under the South Australian Animal Welfare Act 1985, with protocols approved by the University of Adelaide Animal Ethics Committee. Unfertilized oocytes were harvested from anesthetized *Xenopus laevis* frogs and defoliculated by incubation in type 1A collagenase (2 mg/ml) with a trypsin inhibitor (0.3 mg/ml) in OR-2 saline (82 mM NaCl, 2.5 mM KCl, 1 mM $MgCl_2$, and 5 mM HEPES; pH 7.3) at 16–18°C for 2 to 3 hours. Human aquaporin-1 cDNA was provided by Professor P. Agre (Preston et al., 1992; GenBank accession number NM_198098). AQP1 subcloned into a *X. laevis* β-globin plasmid was linearized with BamHI and transcribed in vitro (T3 mMessage mMachine; Ambion Inc., Austin, TX), and cRNA was resuspended in sterile water. Prepared oocytes were injected with 50 nl of water (non–AQP1-expressing control oocytes) or 50 nl of water containing 1 ng of AQP1 cRNA and incubated for 2 or more days at 16°C in ND96 saline (96 mM NaCl, 2 mM KCl, 1 mM $MgCl_2$, 1.8 mM $CaCl_2$, and 5 mM HEPES, pH 7.3) to allow protein expression. Successful expression was confirmed by osmotic swelling assays. Batches of AQP1-expressing oocytes that lacked robust cGMP-activated conductance responses were further incubated overnight in ND96 saline with the tyrosine phosphatase inhibitor bisperoxovanadium (100 μM; Santa Cruz Biotechnology, Dallas, TX) per published methods (Campbell et al., 2012). Chemicals were purchased from Sigma-Aldrich (St. Louis, MO) unless otherwise specified.

AqB Compounds: Synthesis and Preparation. The AqB compounds (custom-designed bumetanide derivatives) were synthesized by Dr. G. Flynn (Spacefill Enterprises LLC, Oro Valley, AZ) as described in U.S. patent 8,835,491-B2. To make AqB001, bumetanide was mixed with diazomethane (CH_2N_2) generated by reaction with Diazald to create bumetanide methyl ester [molecular weight (MW) 344.8; ClogP 2.10], which was dissolved in hot $CHCl_3$, diluted with hexanes and allowed to cool to provide the purified methyl ester as white flakes, whose mass and NMR spectra were consistent with the desired product. Reaction of bumetanide with 1.2 equivalents of 1,1′-carbonyldiimidazole in ethyl acetate (EtOAC) under argon with heating afforded an intermediate imidazolide, which upon cooling, formed a white solid that could be isolated by filtration and stored under argon for later use. Alternatively, the imidazolide solution could be reacted in situ with two equivalents of an amine to form the corresponding amides. In a typical reaction, the reaction mixture would be partitioned between water and EtOAC, the organic layer would be washed with brine, the solution would be filtered and concentrated, and the residue would be crystallized to form EtOAc/hexanes. AqB-006 (MW 413.9; ClogP 1.04) was prepared using morpholine as the amine; AqB007 (MW 470.0; ClogP 0.79) resulted from 2-(4-methylpiperazine-1-yl) ethylamine; and AqB011 (MW 434.9; ClogP 1.80) was prepared using 2-(morpholine-1-yl)ethylamine. The structures of all the compounds were confirmed by high-resolution mass spectrometry and NMR analysis. Chemicals were purchased from Sigma-Aldrich unless otherwise specified.

Powdered compounds were dissolved in dimethylsulfoxide (DMSO) to create 1000× stock solutions for each desired final dosage. An equal dilution of DMSO (0.1%) alone in saline was used as the vehicle control.

Quantitative Swelling Assay. For double-swelling assays, each oocyte served as its own control. Swelling rates were assayed first without drug treatment (S1), and then oocytes incubated for 2 hours in isotonic saline with or without the AqB compounds were reassessed in a second swelling assay (S2). Swelling rates in 50% hypotonic saline (isotonic Na saline diluted with an equal volume of water) were quantified by relative increases in the oocyte cross-sectional area imaged by videomicroscopy (charge-coupled device camera; Cohu, San Diego, CA) at 0.5 frames per second for 30 seconds using National Institutes of Health ImageJ software (Bethesda, MD). Rates were measured as the slopes of the linear regression fits of relative volume as a function of time using Prism (GraphPad Software Inc., San Diego, CA).

Electrophysiology. For the two-electrode voltage clamp, capillary glass electrodes (1–3 MΩ) were filled with 1 M KCl. Recordings were done in standard Na^+ bath saline containing 100 mM NaCl, 2 mM KCl, 4.5 mM $MgCl_2$, and 5 mM HEPES, pH 7.3. cGMP was applied extracellularly at a final concentration of 10–20 μM using the membrane-permeable cGMP analog (Rp)-8-(*para*-chlorophenylthio)-cGMP. Ionic conductance was monitored for at least 20 minutes after cGMP addition to allow development of maximal plateau responses. Conductance was determined by voltage step protocols from +60 to −110 mV from a holding potential of −40 mV. Recordings were made with a GeneClamp amplifier and pClamp 9.0 software (Molecular Devices, Sunnyvale, CA).

Circular Wound Closure Assay. The cancer cell lines used in this study were HT29 human colorectal adenocarcinoma cells (Chen et al., 1987) purchased from American Type Culture Collection (HTB-38; Manassas, VA), which strongly express endogenous AQP1, and SW480 human colorectal adenocarcinoma cells (CCL-228; from American Type Culture Collection), which express AQP5 but show little AQP1 expression. mRNA levels were evaluated by quantitative polymerase chain reaction and protein levels by western blot (H. Dorward et al., submitted manuscript). Confluent cultures of

HT29 and SW480 cells were used in migration assays to measure the effects of AqB treatments on rates of wound closure. Cells were plated in flat-bottom 96-well plates at 1.25×10^5 cells/well in Dulbecco's modified Eagle's medium with 10% fetal bovine serum and incubated at 37°C and 5% CO_2 for 12–18 hours to allow monolayer formation. Circular wounds were created by aspirating a central circle of cells with a p10 pipette. Wells were washed 2 to 3 times with phosphate-buffered saline to remove cell debris. Culture media (Dulbecco's modified Eagle's medium with 2% bovine calf serum) containing either vehicle or drug treatments in the presence of a mitotic inhibitor 5-fluoro-2′-deoxyuridine (100 ng/ml) were administered into the wells. Cultures were imaged at 0 and 24 hours and analyzed using ImageJ software to calculate the percent wound closure by the change in area:

$$[(\text{Area}_0 - \text{Area}_{24})/\text{Area}_0] \times 100$$

Cytotoxicity Assay. Cell viability was quantified using the alamarBlue cell viability assay (Molecular Probes, Eugene, OR). Cells were plated at 10^4 cells/well in 96-well plates, and fluorescence signal levels were measured with a FLUOstar Optima microplate reader (BMG Labtech, Victoria, Australia) after 24-hour incubation, with concentrations of AqB011 ranging from 1 to 80 μM, to obtain quantitative measures of cell viability. Mercuric chloride (20 μM) was used as a positive control for cytotoxicity.

Molecular Modeling. In silico modeling was conducted with methods reported previously (Yool et al., 2013). The crystal structure of human AQP1 was obtained from the Protein Data Bank (PDB) (identity 1FQY). The tetrameric model (Supplemental Material) was generated in Pymol (Version 1.7.4; Schrödinger, LLC; Mannheim, Germany) using coordinates provided in the pdb file. Renderings of the AqB ligands were generated in Chemdraw (Version 13.0; PerkinElmer, MA) and then converted into the pdb format using the online SMILES translation tool (National Cancer Institute, U.S. Department Health and Human Services, Washington, DC). Both AQP1 and ligand coordinates were prepared for docking using MGLtools (Version 1.5.4; Scripps Institute, San Diego, CA). The docking was carried using Autodock Vina (Trott and Olson, 2010), with a docking grid covering the intracellular face of tetrameric pore.

Data Compilation and Statistics. The results compiled from replicate experiments are presented as box plots. The boxes represent 50% of the data, the error bars indicate the full range, and the horizontal bars are the median values. The n values are in italics above the x-axis. Statistical differences were analyzed with one-way analysis of variance and post hoc Bonferroni tests and reported as $^{**}P < 0.0001$, $^{*}P < 0.05$, and N.S. ($P > 0.05$).

Results

AQP1 Ion Channel Inhibition by Novel Bumetanide Derivatives. A set of four related compounds with structural modifications at the carboxylic acid moiety of bumetanide was tested for effects on the cGMP-activated ionic conductance in AQP1-expressing oocytes. Two-electrode voltage clamp recordings of AQP1-expressing oocytes (Fig. 1) illustrate the inhibition of the ionic conductance by extracellular application of AqB007 (200 μM) and AqB011 (20 μM), but no appreciable block of the AQP1 ion channel with 200 μM AqB001 or AqB006. Initial recordings before cGMP application and responses to the first application of cGMP recordings showed typical cGMP-dependent activation, as described previously (Anthony et al., 2000). Oocytes were then transferred into saline with the indicated agents for 2 hours, during which time the ionic conductances uniformly recovered to initial levels (Fig. 2). In response to the second application of cGMP, oocytes treated with vehicle (DMSO), AqB001, or AqB006 showed increases in conductance that were comparable to the first response. However, the cGMP-activated conductance responses were inhibited after treatment with AqB007 or AqB011.

Trend plots (Fig. 2A) show that the ionic conductance in AQP1-expressing oocytes was initially low and activated by the first bath application of membrane-permeable cGMP. The ionic conductance then recovered to the basal level during 2-hour incubation without cGMP and was tested for reactivation by a second application of cGMP after treatment with vehicle or AqB compounds. Recordings for oocytes incubated in saline without DMSO during the recovery period were comparable to

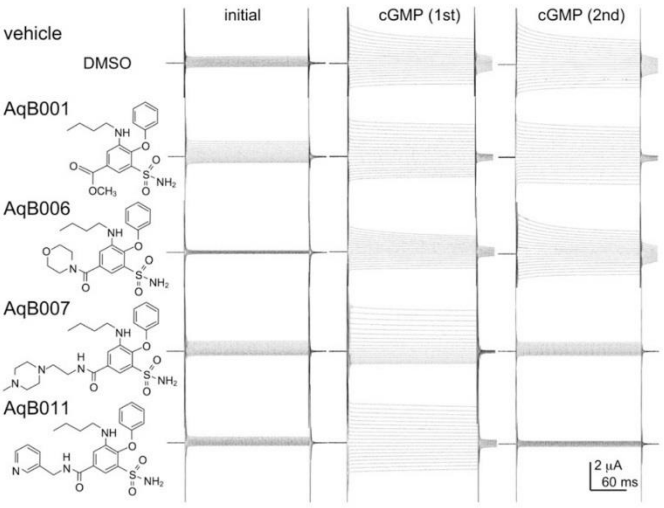

Fig. 1. Chemical structures of selected bumetanide derivatives and electrophysiology traces showing representative effects of AqB001, AqB006, AqB007, and AqB011 on the ionic conductance responses activated by bath application of CPT-cGMP before and after 2-hour incubation in saline with and without the AqB compounds. See *Materials and Methods* for details.

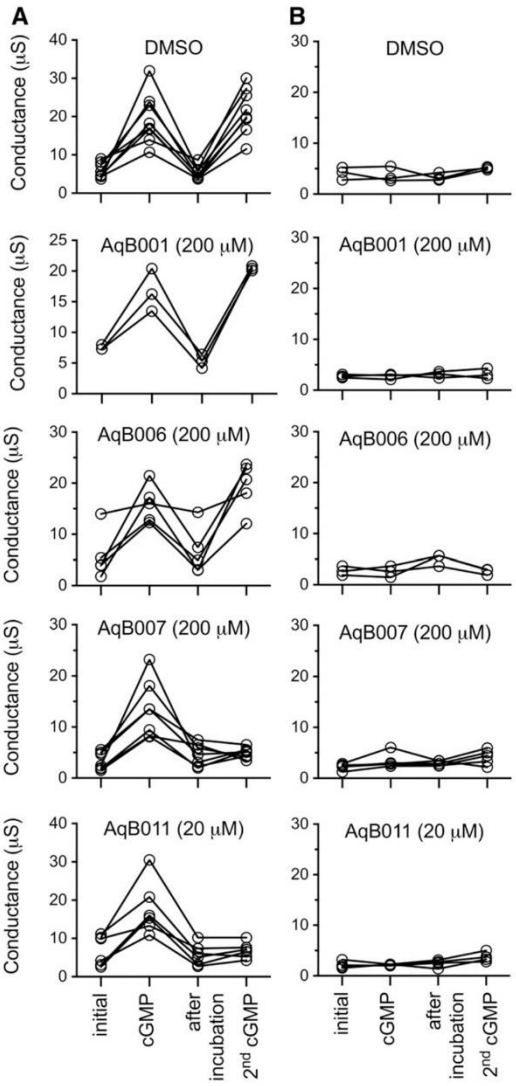

Fig. 2. Trend plots showing the ionic conductance responses for individual oocytes measured prior to cGMP (initial), after the first cGMP application, after 2-hour incubation in saline without cGMP containing DMSO (vehicle) or AqB agents, and after the second application of cGMP. Reversible cGMP-dependent activation of an ionic conductance in AQP1-expressing oocytes (A) was not seen in non-AQP1 control oocytes (B). Inhibition was seen after treatment with AqB007 and AqB011, but not with vehicle, AqB001, or AqB006.

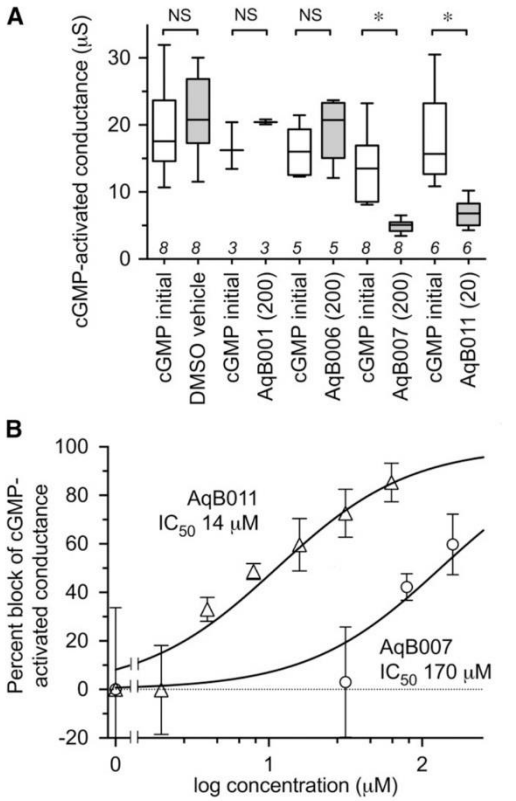

Fig. 3. Dose-dependent block of the AQP1 ionic conductance. (A) Compiled box plot data showing a statistically significant block of the cGMP-activated ionic conductance in AQP1-expressing oocytes by AqB007 and AqB011, but not with vehicle, AqB001, or AqB006. See *Materials and Methods* for details. (B) Dose-response curves showing percent block of the activated ionic conductance in AQP1-expressing oocytes and estimated IC_{50} values. *n* values for dose-response data (in order of increasing concentration) for AqB007 and AqB011 were 8, 4, 2, 8 and 8, 2, 2, 3, 6, 4, 3, respectively.

those for the DMSO-treated group (not shown). Non–AQP1-expressing control oocytes showed no ionic conductance response to cGMP and no effect of the vehicle or drug treatments (Fig. 2B).

Compiled data for the cGMP-activated ionic conductance values in AQP1-expressing oocytes are shown in the box plot (Fig. 3A) and indicate the levels of block by 200 μM AqB007 and 20 μM AqB011 were statistically significant as compared with initial responses to cGMP prior to treatment. Dose-response relationships (Fig. 3B) yielded estimated IC_{50} values of 14 μM for AqB011 and 170 μM for AqB007.

AqB Ion Channel Blockers Have No Effect on Osmotic Water Permeability. Data for oocyte volumes that were standardized as a percentage of the initial volume at time zero illustrate the mean swelling responses over 60 seconds after introduction of the oocytes into 50% hypotonic saline (Fig. 4A). AQP1-expressing oocytes showed consistent osmotic swelling, which was unaffected by treatment with vehicle (DMSO 0.1%) or AqB compounds at 200 μM each. Non–AQP1-expressing control oocytes showed little osmotic water permeability.

To analyze the possible effects of the AqB compounds on water channel activity, a double-swelling assay was used (Fig. 4B).

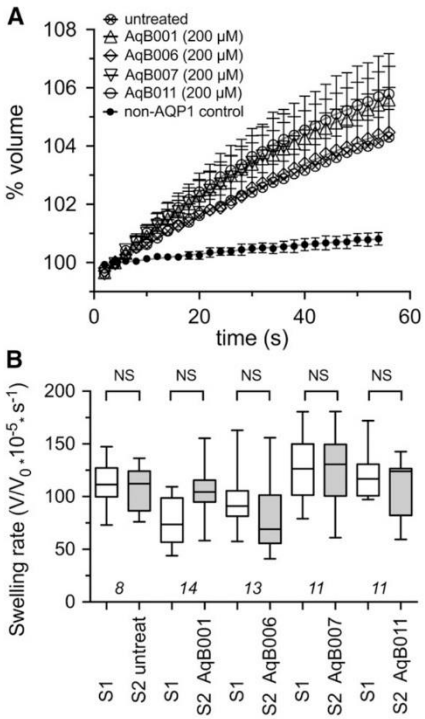

Fig. 4. Lack of effect of AqB compounds on AQP1 osmotic water permeability measured by optical swelling assays. (A) Mean oocyte volume, standardized as a percentage of the initial volume for each oocyte, as a function of time after introduction into 50% hypotonic saline, with and without 2-hour pretreatment with AqB compounds at 200 μM or vehicle (0.1% DMSO). (B) Compiled box plot data showing the absence of any statistically significant differences between the first and second swelling rates measured before (S1) and after (S2) 2-hour incubations in saline alone or saline with 200 μM AqB compounds as indicated. See *Materials and Methods* for details.

After the first swelling (S1) in hypotonic saline, oocytes were incubated in isotonic saline with or without the AqB compounds (200 μM) for 2 hours before assessing the second swelling response (S2). There were no significant differences between the first and second swelling rates in any of the treatment groups, confirming that the AqB ion channel agents did not affect AQP1 osmotic water permeability.

Molecular Modeling of Candidate Intracellular Binding Sites. Putative binding sites on the AQP1 ion pore for AqB011 and AqB007 in the intracellular loop D domain can be suggested based on structural modeling and docking analyses (Fig. 5). In silico modeling suggested the sites for the most favorable energies of interaction for AqB007 and AqB011 were located at the intracellular face of the central pore (Fig. 5A). Interestingly, the model predicted hydrogen bonding between the uniquely elongated moieties of the two effective AqB ligands and the initial pairs of arginine residues in the highly conserved loop D motifs from two adjacent subunits (Fig. 5B). The same arginines (R159 and R160 in human AQP1) have been shown to be involved in

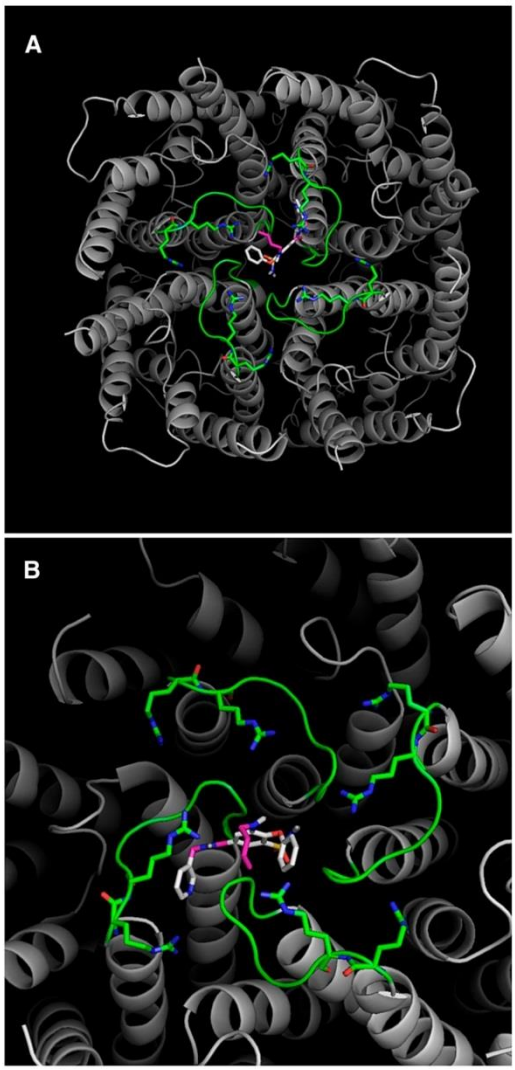

Fig. 5. In silico modeling of the energetically favored binding site for AqB011 in the center of the tetrameric channel of AQP1 (gray) at the intracellular side and bracketed by the gating loop D domains (green). The putative binding site suggests an interaction with two of the loop D domains from adjacent subunits. (A) is the full view of the tetramer, and (B) is a closer view slightly rotated to show proximity of the ligand to the conserved arginine residues in loop D.

AQP1 ion channel gating, but not water channel activity, in prior work (Yu et al., 2006). The more compact AqB006 docked weakly at a different position in the central vestibule (not shown). Although in silico modeling does not define actual binding sites, it provides a testable hypothesis for future work and offers intriguing support for the role of loop D in modulating AQP1 ion channel gating. The most

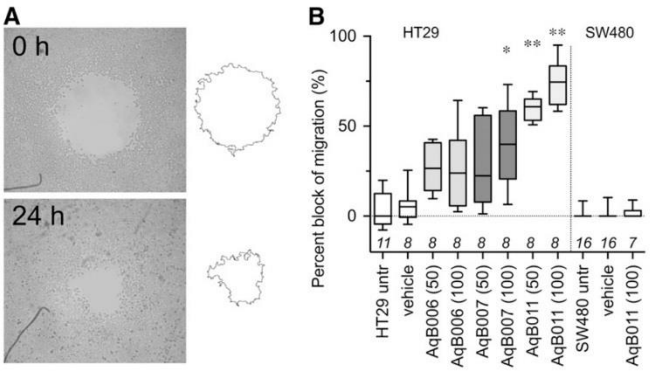

Fig. 6. Block of cell migration in AQP1-expressing HT29, but not SW480, cells treated with AqB011. (A) Illustrative diagram of the circular wound healing method showing substantial closure of the wounded area in normal culture medium by 24 hours. (B) Compiled box plot data from wound closure assays showing the dose-dependent inhibitory effects of AqB007 and AqB011 compared with DMSO and AqB006 on wound closure at 24 hours in HT29 cell cultures. Migration of SW480 cells was not altered by AqB011.

favorable energy of interaction was calculated for AqB011 (at −9.2 kcal/mol). The next most favorable energy of interaction for AqB compounds with the AQP1 channel was for AqB007 (at −7.0 kcal/mol), followed by AqB006 (at −6.0 kcal/mol). This order of interaction strength for the AqB series matched their order of efficacy for inhibition of the AQP1 ion channel conductance (Fig. 3).

Inhibition of AQP1 Ion Channel Activity Slows Cancer Cell Migration. The effects of AqB006, AqB007, and AqB011 were tested in migration assays of human HT29 colon cancer cells (Fig. 6), which natively express AQP1. Net migration rates were calculated from the percent closure of a circular wound area at 24 hours (Fig. 6A). The results showed that cancer cell migration was not impaired by AqB006, but was significantly impaired by AqB007 at 100 μM and AqB011 at 50 and 100 μM, as compared with vehicle-treated control HT29 cells (Fig. 6B). AqB011 was more effective than AqB007 in blocking migration, which is consistent with the relative efficacies of the agents as blockers of the ion channel conductance. In contrast, AqB011 at 100 μM had no effect on the migration rate of SW480 colon cancer cells (Fig. 6B), which express AQP5, but not AQP1, suggesting that the inhibitory effect of AqB011 appears to be selective for AQP1.

AqB Compounds Show Low Cytotoxicity. There was no significant difference in the viability of vehicle-treated and untreated cells and no effect of treatment with AqB011 for HT29 cells (Table 1). Cell viability was assessed with alamarBlue assays. The persistence of the fluorescent signal at 24 hours confirmed there was no appreciable cytotoxic effect of AqB011 treatment on HT29 cells at concentrations of up to 80 μM. Mercuric chloride as a positive control caused significant cell death, which was measured as a decrease in fluorescence. AqB011 at doses used to block the AQP1 ionic conductance and cancer cell migration did not impact cell viability.

Discussion

The aim of this study was to search for selective small-molecule pharmacological agents that are capable of blocking the cGMP-activated cationic conductance in AQP1. Discovery of pharmacological modulators for AQP1 channels has been an important goal in the aquaporin field. AQP1 antagonist and agonist agents are expected to be useful for defining the complex roles of aquaporins in fundamental biologic processes as well as characterizing AQP1 modulators as potential clinical agents in various conditions, such as cancer metastasis (Yool et al., 2010). AQP1 expression is upregulated in subtypes of aggressive cancer cells, in which it facilitates cancer migration. The results here show that selective blockers of the AQP1 ion channel slow the migration of human colon cancer cells in culture. Pharmacological inhibition of AQP1 is predicted to have a protective effect in reducing metastasis in cancer, but remains to be demonstrated in vivo.

Using bumetanide as a starting scaffold, we created an array of novel synthetic derivatives. Based on pilot data indicating a small inhibitory effect of AqB050 on the AQP1 ion channel at high doses (unpublished data), we investigated a series of structurally related derivatives, AqB006, AqB007, and AqB011, as well as a simple methylated version of bumetanide, AqB001, to test for possible inhibitors of the AQP1 ionic conductance. Our findings demonstrated that AqB007 and AqB011 are effective inhibitors of the central ion pore of AQP1, with estimated IC_{50} values of 170 and 14 μM, respectively. Both AqB007 and AqB011 showed dose-dependent inhibition of the central ion pore, whereas the intrasubunit water pores were unaffected, enabling the first dissection of physiologic roles of the distinct channel functions. Measuring fluorescence signal intensity with the alamarBlue

TABLE 1
HT29 cell levels of cytotoxicity after 24-hour incubation in culture medium with vehicle, AqB011, or $HgCl_2$

Agent (AqB011)	Mean Normalized Cell Viability ± S.E.M.[a]	*n* Value	Statistical Significance
μM	%		
0 (untreated)	100.0 ± 0.70	8	—
0 (0.1% DMSO)	103.9 ± 0.91	8	N.S.
1	104.0 ± 1.06	4	N.S.
5	102.3 ± 2.26	4	N.S.
10	110.6 ± 2.12	4	N.S.
20	114.0 ± 0.84	4	N.S.
40	111.8 ± 1.33	4	N.S.
80	102.4 ± 2.95	4	N.S.
$HgCl_2$ (100 μM)	16.2 ± 0.20	3	**

[a]Percent viability was standardized as a percentage of the untreated mean value measured as changes in alamarBlue fluorescence signal intensity. See *Materials and Methods* for details.

cell viability assay showed that AqB011 was not cytotoxic at doses that produced maximal ion channel inhibition.

The inhibition by AqB011 of AQP1 ionic conductance was consistent with molecular docking studies, suggesting the site of interaction is at the intracellular face of the central pore. The results revealed that AqB011 is the most energetically favored compound, followed by AqB007. The predicted interaction site of AqB011 and AqB007 with AQP1 is at the loop D domain. Differences in the structures and efficacies of AqB006, AqB007, and AqB011 indicate that the structure-activity relationship of ion channel inhibition is sensitive to specific chemical modifications at the carboxylic acid position of bumetanide. The length and structure of the modification appears to be critical and based on in silico modeling to be the region that interacts with the AQP1 channel gating loop D domain. The absence of cytotoxic effects of AqB011 at doses sufficient to block the AQP1 ion channel activity indicates that the inhibition of migration is not indirectly due to cell death. The observation that AqB011 inhibited migration in AQP1-expressing HT29 colon cancer cells, but had no effect on the migration of AQP-5–expressing SW480 colon cancer cells, provides support for the idea that AqB011 is selective for AQP1. The inhibition of migration seen with AqB011 is unlikely to result from off-target effects on general metabolic function, cytoskeletal organization, actin polymerization, or signaling pathways involved in cell motility since SW480 cell migration remained unaffected by the presence of AqB011.

AQP1 is present in barrier epithelia involved in fluid movement in the body, including the proximal tubule and choroid plexus (Agre et al., 1993). It is also expressed in peripheral microvasculature, dorsal root ganglion cells, eye ciliary epithelium and trabecular meshwork, heart ventricles, and other regions, in which a direct role for osmotic water flux is less evident (Yool, 2007). Additional roles suggested for AQP1 include angiogenesis (Nicchia et al., 2013), signal transduction (Oshio et al., 2006), increased mechanical compliance to changes in pressure (Baetz et al., 2009), axonal regeneration of spinal nerves (Zhang and Verkman, 2015), recovery from injury (Hara-Chikuma and Verkman, 2006), and exocytosis (Arnaoutova et al., 2008). Relative contributions of the ion and water channel functions in these diverse processes remain to be defined.

A possible role for the AQP1 ionic conductance (potentially in combination with water fluxes) in the control of cell volume associated with migration was supported by the results of the wound closure assays with AQP1-expressing HT29 cells. Cell migration was significantly impaired by AqB011 and AqB007, but not by AqB006. The greatest efficacy of migration block was seen with administration of AqB011. The comparable orders of efficacy for the block of AQP1 ion channels in the oocyte expression system and for the block of cell migration in HT29 cultures support the idea that the AqB011 effect on migration is mediated by direct block of the AQP1 ion channels. These data provide evidence that the ion channel activity of AQP1 has physiologic relevance. Further work is needed to evaluate the effects of blocking both water and ion channel activities of AQP1 together in migrating cells.

AqB011 is a new research tool for probing the physiologic role of the AQP1 ion channel function in biologic systems. This compound holds future promise as a possible adjunct clinical intervention in cancer metastasis. Exciting opportunities are likely to emerge from continuing discovery of pharmacological modulators for aquaporins for new treatments in cancers and other diseases.

Authorship Contributions

Participated in research design: Kourghi, Pei, De Ieso, Yool.
Conducted experiments: Kourghi, Pei, De Ieso.
Contributed new reagents or analytic tools: Flynn.
Performed data analysis: Kourghi, Pei, De Ieso, Yool.
Wrote or contributed to the writing of the manuscript: Kourghi, Pei, Flynn, Yool.

References

Agre P, Preston GM, Smith BL, Jung JS, Raina S, Moon C, Guggino WB, and Nielsen S (1993) Aquaporin CHIP: the archetypal molecular water channel. *Am J Physiol* **265**:F463–F476.

Anthony TL, Brooks HL, Boassa D, Leonov S, Yanochko GM, Regan JW, and Yool AJ (2000) Cloned human aquaporin-1 is a cyclic GMP-gated ion channel. *Mol Pharmacol* **57**:576–588.

Arnaoutova I, Cawley NX, Patel N, Kim T, Rathod T, and Loh YP (2008) Aquaporin 1 is important for maintaining secretory granule biogenesis in endocrine cells. *Mol Endocrinol* **22**:1924–1934.

Baetz NW, Hoffman EA, Yool AJ, and Stamer WD (2009) Role of aquaporin-1 in trabecular meshwork cell homeostasis during mechanical strain. *Exp Eye Res* **89**: 95–100.

Boassa D, Stamer WD, and Yool AJ (2006) Ion channel function of aquaporin-1 natively expressed in choroid plexus. *J Neurosci* **26**:7811–7819.

Boassa D and Yool AJ (2003) Single amino acids in the carboxyl terminal domain of aquaporin-1 contribute to cGMP-dependent ion channel activation. *BMC Physiol* **3**: 12.

Brooks HL, Regan JW, and Yool AJ (2000) Inhibition of aquaporin-1 water permeability by tetraethylammonium: involvement of the loop E pore region. *Mol Pharmacol* **57**:1021–1026.

Campbell EM, Ball A, Hoppler S, and Bowman AS (2008) Invertebrate aquaporins: a review. *J Comp Physiol B* **178**:935–955.

Campbell EM, Birdsell DN, and Yool AJ (2012) The activity of human aquaporin 1 as a cGMP-gated cation channel is regulated by tyrosine phosphorylation in the carboxyl-terminal domain. *Mol Pharmacol* **81**:97–105.

Chen TR, Drabkowski D, Hay RJ, Macy M, and Peterson W, Jr (1987) WiDr is a derivative of another colon adenocarcinoma cell line, HT-29. *Cancer Genet Cytogenet* **27**:125–134.

Detmers FJ, de Groot BL, Müller EM, Hinton A, Konings IB, Sze M, Flitsch SL, Grubmüller H, and Deen PM (2006) Quaternary ammonium compounds as water channel blockers. Specificity, potency, and site of action. *J Biol Chem* **281**: 14207–14214.

El Hindy N, Bankfalvi A, Herring A, Adamzik M, Lambertz N, Zhu Y, Siffert W, Sure U, and Sandalcioglu IE (2013) Correlation of aquaporin-1 water channel protein expression with tumor angiogenesis in human astrocytoma. *Anticancer Res* **33**: 609–613.

Finn RN, Chauvigné F, Hlidberg JB, Cutler CP, and Cerdà J (2014) The lineage-specific evolution of aquaporin gene clusters facilitated tetrapod terrestrial adaptation. *PLoS One* **9**:e113686.

Fu D, Libson A, Miercke LJ, Weitzman C, Nollert P, Krucinski J, and Stroud RM (2000) Structure of a glycerol-conducting channel and the basis for its selectivity. *Science* **290**:481–486.

Hara-Chikuma M and Verkman AS (2006) Aquaporin-1 facilitates epithelial cell migration in kidney proximal tubule. *J Am Soc Nephrol* **17**:39–45.

Hu J and Verkman AS (2006) Increased migration and metastatic potential of tumor cells expressing aquaporin water channels. *FASEB J* **20**:1892–1894.

Huber VJ, Tsujita M, and Nakada T (2009) Identification of aquaporin 4 inhibitors using in vitro and in silico methods. *Bioorg Med Chem* **17**:411–417.

Ishibashi K (2009) New members of mammalian aquaporins: AQP10-AQP12. *Handb Exp Pharmacol* 251–262.

Jiang Y (2009) Aquaporin-1 activity of plasma membrane affects HT20 colon cancer cell migration. *IUBMB Life* **61**:1001–1009.

Jung JS, Bhat RV, Preston GM, Guggino WB, Baraban JM, and Agre P (1994) Molecular characterization of an aquaporin cDNA from brain: candidate osmoreceptor and regulator of water balance. *Proc Natl Acad Sci USA* **91**:13052–13056.

McCoy E and Sontheimer H (2007) Expression and function of water channels (aquaporins) in migrating malignant astrocytes. *Glia* **55**:1034–1043.

Migliati E, Meurice N, DuBois P, Fang JS, Somasekharan S, Beckett E, Flynn G, and Yool AJ (2009) Inhibition of aquaporin-1 and aquaporin-4 water permeability by a derivative of the loop diuretic bumetanide acting at an internal pore-occluding binding site. *Mol Pharmacol* **76**:105–112.

Monzani E, Shtil AA, and La Porta CA (2007) The water channels, new druggable targets to combat cancer cell survival, invasiveness and metastasis. *Curr Drug Targets* **8**:1132–1137.

Nicchia GP, Stigliano C, Sparaneo A, Rossi A, Frigeri A, and Svelto M (2013) Inhibition of aquaporin-1 dependent angiogenesis impairs tumour growth in a mouse model of melanoma. *J Mol Med (Berl)* **91**:613–623.

Oshio K, Watanabe H, Yan D, Verkman AS, and Manley GT (2006) Impaired pain sensation in mice lacking aquaporin-1 water channels. *Biochem Biophys Res Commun* **341**:1022–1028.

Park JH and Saier MH, Jr (1996) Phylogenetic characterization of the MIP family of transmembrane channel proteins. *J Membr Biol* **153**:171–180.

Preston GM, Carroll TP, Guggino WB, and Agre P (1992) Appearance of water channels in Xenopus oocytes expressing red cell CHIP28 protein. *Science* **256**:385–387.
Preston GM, Jung JS, Guggino WB, and Agre P (1993) The mercury-sensitive residue at cysteine 189 in the CHIP28 water channel. *J Biol Chem* **268**:17–20.
Reizer J, Reizer A, and Saier MH, Jr (1993) The MIP family of integral membrane channel proteins: sequence comparisons, evolutionary relationships, reconstructed pathway of evolution, and proposed functional differentiation of the two repeated halves of the proteins. *Crit Rev Biochem Mol Biol* **28**:235–257.
Saparov SM, Kozono D, Rothe U, Agre P, and Pohl P (2001) Water and ion permeation of aquaporin-1 in planar lipid bilayers. Major differences in structural determinants and stoichiometry. *J Biol Chem* **276**:31515–31520.
Schwab A, Nechyporuk-Zloy V, Fabian A, and Stock C (2007) Cells move when ions and water flow. *Pflugers Arch* **453**:421–432.
Seeliger D, Zapater C, Krenc D, Haddoub R, Flitsch S, Beitz E, Cerdà J, and de Groot BL (2013) Discovery of novel human aquaporin-1 blockers. *ACS Chem Biol* **8**: 249–256.
Søgaard R and Zeuthen T (2008) Test of blockers of AQP1 water permeability by a high-resolution method: no effects of tetraethylammonium ions or acetazolamide. *Pflugers Arch* **456**:285–292.
Sui H, Han B-G, Lee JK, Walian P, and Jap BK (2001) Structural basis of water-specific transport through the AQP1 water channel. *Nature* **414**:872–878.
Trott O and Olson AJ (2010) AutoDock Vina: improving the speed and accuracy of docking with a new scoring function, efficient optimization, and multithreading. *J Comput Chem* **31**:455–461.
Tsunoda SP, Wiesner B, Lorenz D, Rosenthal W, and Pohl P (2004) Aquaporin-1, nothing but a water channel. *J Biol Chem* **279**:11364–11367.
Yool AJ (2007) Functional domains of aquaporin-1: keys to physiology, and targets for drug discovery. *Curr Pharm Des* **13**:3212–3221.
Yool AJ, Brown EA, and Flynn GA (2010) Roles for novel pharmacological blockers of aquaporins in the treatment of brain oedema and cancer. *Clin Exp Pharmacol Physiol* **37**:403–409.
Yool AJ and Campbell EM (2012) Structure, function and translational relevance of aquaporin dual water and ion channels. *Mol Aspects Med* **33**:553–561.
Yool AJ, Morelle J, Cnops Y, Verbavatz JM, Campbell EM, Beckett EA, Booker GW, Flynn G, and Devuyst O (2013) AqF026 is a pharmacologic agonist of the water channel aquaporin-1. *J Am Soc Nephrol* **24**:1045–1052.
Yool AJ, Stamer WD, and Regan JW (1996) Forskolin stimulation of water and cation permeability in aquaporin 1 water channels. *Science* **273**:1216–1218.
Yoshida T, Hojo S, Sekine S, Sawada S, Okumura T, Nagata T, Shimada Y, and Tsukada K (2013) Expression of aquaporin-1 is a poor prognostic factor for stage II and III colon cancer. *Mol Clin Oncol* **1**:953–958.
Yu J, Yool AJ, Schulten K, and Tajkhorshid E (2006) Mechanism of gating and ion conductivity of a possible tetrameric pore in aquaporin-1. *Structure* **14**: 1411–1423.
Zhang H and Verkman AS (2015) Aquaporin-1 water permeability as a novel determinant of axonal regeneration in dorsal root ganglion neurons. *Exp Neurol* **265**:152–159.
Zhang W, Zitron E, Hömme M, Kihm L, Morath C, Scherer D, Hegge S, Thomas D, Schmitt CP, and Zeier M et al. (2007) Aquaporin-1 channel function is positively regulated by protein kinase C. *J Biol Chem* **282**:20933–20940.

Address correspondence to: Professor Andrea Yool, Medical School South, Level 4, Frome Rd., University of Adelaide, Adelaide SA 5005 Australia. E-mail: andrea.yool@adelaide.edu.au

Received: 25 September 2017 | Revised: 6 November 2017 | Accepted: 16 November 2017

DOI: 10.1111/1440-1681.12900

SYMPOSIUM PAPER

WILEY CEPP Clinical and Experimental Pharmacology and Physiology

Fundamental structural and functional properties of Aquaporin ion channels found across the kingdoms of life

Mohamad Kourghi | Jinxin V. Pei | Michael L. De Ieso | Saeed Nourmohammadi | Pak Hin Chow | Andrea J. Yool

Adelaide Medical School, University of Adelaide, Adelaide, SA, Australia

Correspondence
Mohamad Kourghi and Andrea Yool, Medical School South, University of Adelaide, Adelaide, SA, Australia.
Emails: mohamad.kourghi@adelaide.edu.au and andrea.yool@adelaide.edu.au

Funding information
Australian Research Council, Grant/Award Number: DP160104641

Summary

Aquaporin (AQP) channels in the major intrinsic protein (MIP) family are known to facilitate transmembrane water fluxes in prokaryotes and eukaryotes. Some classes of AQPs also conduct ions, glycerol, urea, CO_2, nitric oxide, and other small solutes. Ion channel activity has been demonstrated for mammalian AQPs 0, 1, 6, Drosophila Big Brain (BIB), soybean nodulin 26, and rockcress AtPIP2;1. More classes are likely to be discovered. Newly identified blockers are providing essential tools for establishing physiological roles of some of the AQP dual water and ion channels. For example, the arylsulfonamide AqB011 which selectively blocks the central ion pore of mammalian AQP1 has been shown to impair migration of HT29 colon cancer cells. Traditional herbal medicines are sources of selective AQP1 inhibitors that also slow cancer cell migration. The finding that plant AtPIP2;1 expressed in root epidermal cells mediates an ion conductance regulated by calcium and protons provided insight into molecular mechanisms of environmental stress responses. Expression of lens MIP (AQP0) is essential for maintaining the structure, integrity and transparency of the lens, and Drosophila BIB contributes to neurogenic signalling pathways to control the developmental fate of fly neuroblast cells; however, the ion channel roles remain to be defined for MIP and BIB. A broader portfolio of pharmacological agents is needed to investigate diverse AQP ion channel functions in situ. Understanding the dual water and ion channel roles of AQPs could inform the development of novel agents for rational interventions in diverse challenges from agriculture to human health.

KEYWORDS

Aquaporin, arylsufonamide, cation channel, divalent cation, fluid homeostasis, major intrinsic protein, metastasis, traditional herbal medicine, volume regulation, water channel

1 | INTRODUCTION

Aquaporins (AQPs) are involved in many functions, including maintaining osmotic water homeostasis, cellular structure, and volume regulation; enabling fluid flow across barrier tissues; supporting metabolic demands, cellular migration, and more. Maintaining water homeostasis is vital to every living organism. AQPs allow the transport of water molecules through intrasubunit pores down osmotic or hydrostatic pressure gradients,[1] and are found across diverse species in prokaryotes and eukaryotes.[2,3] Fifteen aquaporin genes have been identified in mammals (AQP0- AQP14).[3,4] Plants express many different MIP channels. Hundreds of AQP loci detected from genomic analyses of higher plants are divided into five subfamilies.[5,6]

Presented at the *Transporters and channels as drug targets in cancer* Symposium at the joint AuPS and ASB meeting, Adelaide, 2016. The papers in these proceedings were peer reviewed under the supervision of the AuPS Editor, and are being published with the permission of the AuPS.

AQPs organize as tetrameric pores in cell membranes (Figure 1). Each subunit consists of six membrane spanning helices and five loops (A to E); the amino and carboxyl terminal domains reside on the cytosolic side.[7] Loops B and E, on the intracellular and extracellular sides respectively, fold inward to span the membrane as short helices, each with a conserved asparagine-proline-alanine (NPA) signature motif.[7] The classification of mammalian AQPs 3, 7, 9 and 10 as aquaglyceroporins reflects their ability to allow permeation of small uncharged molecules such as glycerol in addition to water.[4]

As illustrated in Figure 2, aquaporins −0, −1, and −6, *Drosophila* Big Brain, plant AtPIP2;1 and Nodulin-26 have been shown to have ion channel activity.[8-13] In AQP1 and AtPIP2;1 channels, the central pore of the tetramer has been proposed as the pathway for cation conductance.[9,14,15] Intrasubunit pores are thought to be pathways for ion transport in BIB, AQP0 and AQP6 channels.[16-18] Evidence for intrasubunit ion pores in BIB comes from mutational studies in which the change of a conserved glutamic acid at position 71 to aspargine (E71N) in BIB diminished the ionic conductance, whereas the equivalent mutation in AQP1 E17N did not prevent ion channel activity, but blocked AQP1 water channel function.[18] In AQP6, the key residues that affect ion channel properties are located in loop B, a domain typically associated with the intrasubunit pore.[16,17]

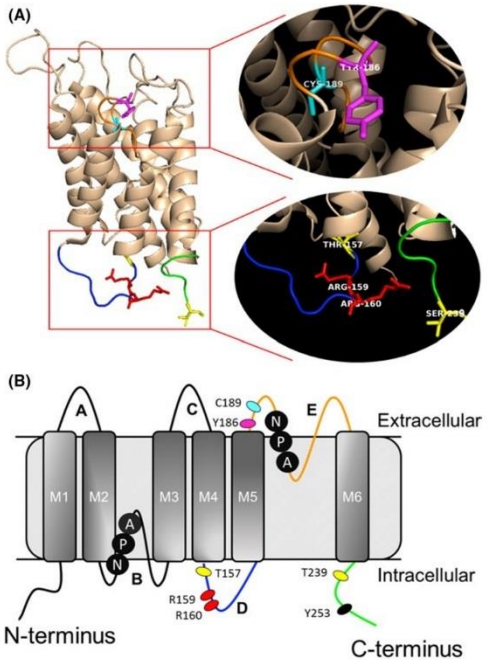

FIGURE 1 Structural organization of the Aquaporin-1 channel subunit.(a) Crystal structure of the human AQP1 monomer. Highlighted in blue is the loop D domain, in red are the double arginine residues at positions 159 and 160 (R159 + R160) located in the loop D domain. The double arginine site is proposed to be involved in binding of the agonist cGMP and antagonists AqB011 and bacopaside I.[15,38,109] Cysteine at position 189 (cyan) is the mercury binding site.[88] Tyrosine 186 (magenta) influences the binding of tetraethylammonium as a water pore blocker.[110] Threonines 157 and 239 (yellow) are thought to be PKC regulatory sites.[36] The amino terminal domain is highlighted in green. (b) Membrane topology diagram of AQP1 showing membrane spanning helices, connected by 5 loops (extracellular A, C and E; intracellular B and D). The Asn-Pro-Ala (NPA) signature motifs are located on loops B and E. Key regulatory sites (as summarized in [a]) are highlighted, and include tyrosine Y253 (black) which when phosphorylated enhances activation of AQP1 ion channel currents[32]

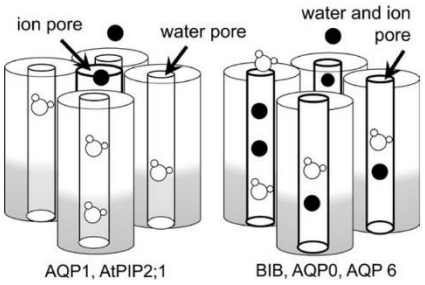

FIGURE 2 Models illustrating the two proposed schemes for ion and water channel permeation through AQP1, AtPIP2;1, BIB, AQP0 and AQP6 channels. For AQP1 and AtPIP2;1 channels (left), ions are thought to move through the central pore of the tetramer,[9,14,15] and the major water transport is through individual monomeric pores.[7,111] For BIB, AQP 0 and AQP6 (right), ion and water permeation is proposed to occur through the individual intrasubunit pores, not the central pore.[16-18] Big Brain channels have not been found to have appreciable water permeability under conditions tested[108]

2 | FUNCTIONAL ROLES OF MAMMALIAN AQP1 ION CHANNELS

The concept of ion channel activity in an aquaporin has been most comprehensively studied in mammalian AQP1 in terms of structure-function relationships, pharmacology, and physiological relevance. The number of AQPs designated as aquaporin ion channels is likely continue to increase as the originally disputed concept[19] gains acceptance and lines of evidence accumulate.[20] Ongoing research is addressing the roles of AQP1 and other ion channels in key health challenges such as cancer metastasis and brain oedema.

2.1 | Ion conductances needed for cancer cell migration

Malignant transformation in cancers is marked by increased proliferation, aberrant apoptosis, angiogenesis, migration and invasion, all processes that are influenced by ion channels.[21-25] Other work has

added aquaporin water and glycerol channels to the list of channels that contribute to cancer cell migration and metastasis.[26-30]

The AQP1 ion channel, gated by cyclic GMP,[31-33] mediates non-selective monovalent cation currents (eg, Na^+, K^+, and Cs^+), but is not appreciably permeant to divalent cations or protons.[31,34] Tetrameric organization of subunits around a central pore is a theme noted for many types of ion channels.[14,35] Evidence from molecular dynamic modelling and site-directed mutagenesis have converged on the idea that in AQP1 the ion permeation pathway is the central pore at the 4-fold axis of symmetry.[15,32] The gating of the AQP1 ion channel depends on cyclic GMP[31] which is thought to interact with an arginine-rich region of loop D, opening the central pore to allow hydration and permeation of water and cations.[15] The responsiveness of AQP1 ionic conductance to cGMP is modulated by tyrosine phosphorylation at position 253 in carboxyl terminal domain of human AQP1,[32] and protein-kinase-C mediated phosphorylation at threonine residues 157 and 239.[36] AQP1 ionic current activation is less efficient when two key residues aspartate (D237) and lysine (K243) in the carboxyl terminal domain are mutated,[37] further indicating the C-terminal domain influences the efficacy of cGMP-mediated activation. Site-directed mutagenesis of a conserved pair of arginine residues in loop D decreases the efficacy of inhibition by the AQP1 ion channel blocker AqB011 (Kourghi et al., 2017), confirming an earlier proposal that the compound interacts at the loop D gating region.[38] AQP1-expressing HT29 colon cancer cells treated with AqB011 show impaired cell migration at doses that match the dose-dependent block of the ion channel conductance, recorded from cloned human AQP1 channels expressed in Xenopus oocytes.[38] AQP1 expression also is associated with tumour angiogenesis; AQP1 knockdown or inhibition correlates with reduced growth.[39]

Various classes of channels and transporters have been identified as key components in cell migration. The Na^+/H^+ exchanger (NHE1) influences cell migration, proliferation and volume regulation.[40-42] Inhibition of NHE1 leads to decreased motility of tumour cells.[43,44] K^+ and Ca^{2+} channels influence cell migration by regulating cell volume and membrane potential.[45] Blocking SK3 K^+ channels reduces cancer cell migration and metastatic potential.[46] The epithelial sodium channel (ENaC) and acid sensitive ionic channel (ASIC) also are linked to cell migration and invasiveness.[47,48] Reduced levels of ASIC1 and ENaC expression inhibit the migration of glioblastoma cells.[49] Piezo ion channels, sensitive to membrane tension, function to transduce mechanical stimuli in diverse species, and serve roles that include cell migration, sensory perception and homeostatic regulation, with links to cardiovascular disease and cancer.[50-52]

Multiple Ca^{2+} signalling pathways influence cancer cell migration and proliferation.[25,53,54] Transient receptor potential (TRP) channels enable the localized entry of Ca^{2+} in lamellipodial leading edges; *TRPM7* knockdown abolished Ca^{2+} flickers in fibroblasts and impaired chemotactic steering of cell migration.[55] Stores-operated Ca^{2+} entry augments intracellular Ca^{2+} via a calcium release-activated calcium channel (Orai1) and a stromal interaction molecule 1 $(STIM1)^+$;[56] block of the Ca^{2+} entry pathway by SKF96365 and 2-APB (2-aminoethyl diphenylborinate) decreased cancer cell migration and proliferation in clear cell renal cell carcinoma.[57]

Relative contributions of the diverse classes of channels and transporters to cancer cell migration are expected to depend on tumour cell type, patterns of gene expression, interacting proteins, environmental conditions, and levels of activation of intracellular signalling pathways. AQP1 interacts with signalling pathways including MAP kinase, protein kinase C, Wnt, PI3 kinase, and TGF-β,[36,58-60] and is modulated by protein-protein interactions with carbonic anhydrase[61] and others. AQP1 in bone marrow mesenchymal stem cells promotes migration through focal-adhesion kinase and PI3K/Akt signalling pathways.[62] Knockdown of AQP1 in human endothelial and melanoma cell lines disrupts actin cytoskeletal organization, reduces levels of interacting proteins such as Lin-7, and impairs cell migration,[60] outcomes expected to compromise metastasis and angiogenesis.

AQP1 is one of many ion channels that merits exploration as a therapeutic target to control migration and metastasis during the progression of certain types of cancers. Inhibition of AQP1 ion channels would be expected to have clinical potential selectively for the subset of cancer types in which upregulation of AQP1 serves a key role in metastasis and angiogenesis.[63]

2.2 | Ion and water flux in cerebrospinal fluid (CSF) production

A principal role of choroid plexus is secretion of cerebrospinal fluid (CSF). CSF fills the brain ventricles and spinal canal, providing physical support and a specialized environment for transport of nutrients, peptides, and hormones throughout the CNS.[64,65] The choroid plexus, lining the ventricles in the brain, is a layer of cuboidal epithelial cells that interfaces between the blood capillary system and ventricular space.[66,67] The mechanism of CSF secretion involves bulk ion movement from the blood to the ventricle across the choroid plexus through transcellular transporters.[68] In choroid plexus, transporters and ion pumps are differentially located on apical and basal membranes to create an apico-basolateral polarity. AQP1 is highly expressed in choroid plexus, specifically on the apical side.[69,70] The major function of AQP1 in choroid plexus is thought to be facilitation of water movement from the basolateral to the apical side of the barrier, following the gradient created by active transport of sodium ions through pumps and exchangers.[71-73]

A role for the cation channel function of AQP1 in modulating CSF flow rate in choroid plexus was proposed in 2006,[33] but selective pharmacological agents for AQP1 were not available at the time to confirm the findings. The AQP1 ion conductance in primary cultures of choroid plexus was activated by cGMP, and the rate of CSF production was stimulated by application of atrial natriuretic peptide (ANP) which binds to an endogenous guanylate cyclase receptor, producing cGMP.[74] When AQP1 ion channels were blocked with a non-selective antagonist Cd^{2+}, CSF production was slowed, as measured in a transwell primary culture model.[33] Further work is needed to evaluate whether the AQP1 ion channel function regulates CSF secretion in vivo.

AQP1 ion channels could also contribute to functional roles in other tissues, in processes such as angiogenesis,[75] fluid transport in renal proximal tubule,[14] red blood cell adaptation to stressors, cancer metastasis, glaucoma, brain oedema, and more.

3 | DIVERSE PROPERTIES OF ION CHANNEL AQUAPORINS

3.1 | Mammalian aquaporin 0

Mammalian aquaporin 0 (AQP0), also known as lens MIP or MIP26, is the major protein component of isolated lens junctions.[76,77] AQP0 has been shown to function as a water channel when expressed exogenously in Xenopus oocytes[78,79] and endogenously in membrane vesicles generated from freshly isolated preparations of mouse, frog and rabbit lens fibres.[80-82] The primary function of AQP0 in the lens may be more than membrane water permeability alone, and could involve cell-cell adhesion of lens fibres or regulation of gap junction channels. AQP0 has the lowest water permeability of mammalian AQPs 1 to 5, with single channel water permeability about 1/40th that of AQP1.[78] AQP0 is required for maintaining the transparency of the ocular lens;[83] humans and mice lacking AQP0 develop congenital cataracts.[84]

When reconstituted in bilayers, AQP0 shows ion channel activity[10,77,85,86] characterized by large single channel conductance, a slight anionic selectivity, and symmetrical voltage dependence.[77] Bovine AQP0 is voltage- and pH-sensitive, and generally closed at neutral pH.[77] AQP0 channel openings have two main conductance states with amplitudes of 380 and 160 pS in 100 mmol/L KCl. The water channel activity of AQP0 is dependent upon pH and calcium,[87] suggesting that regulatory mechanisms modulate both the water flux and the ion conductance properties of AQP0. Minimizing extracellular space in the lens by enabling fluid flow into lens fibres could reduce light scattering, and thus assist in maintaining optimal transparency.[86] Maintaining optimal lens transparency could utilise both the water and ion channel functions of AQP0.

3.2 | Mammalian aquaporin 6

Aquaporin-6 (AQP6) is an anion channel and water channel that is atypically activated rather than blocked by mercuric chloride ($HgCl_2$),[13] unlike AQP1[88] and other AQPs. AQP6 assembles as a tetramer, possessing monomeric pores for water and anions, with a permeability series of NO_3>I>>Br>Cl>>F.[16,17] Interestingly, when expressed in *Xenopus laevis* oocytes, AQP6 channels show low water permeability; however, exposure to $HgCl_2$ at concentrations up to 300 μmol/L stimulates AQP6 water permeability more than five-fold, and the ion conductance more than six-fold.[13,17] Two cysteine residues (C155 and C190) are important for the $HgCl_2$ gating of AQP6. The AQP6 water channel activity and anion conductance are reversibly potentiated by low pH, suggesting a mechanism of activation with some potential physiological relevance.[17]

AQP6 is present in intercalated cells of the renal collecting duct in mammals.[89,90] In α-intercalated cells, AQP6 was found to be colocalized with H^+/ATPases in intracellular vesicles but not in plasma membrane,[17] and was suggested to contribute to urinary acid secretion and acid/base regulation.[91] Significant upregulation of AQP6 expression was observed in rats exposed to chronic alkalosis or water loading, but not chronic acidosis.[92] Expression of AQP6 in rat gastrointestinal epithelium, near tight junctions and secretory granule membranes in rat parotid acinar cells, and in some ovarian cancers[93-95] has suggested other possible roles in tissues involving acid-base regulation, although the physiological significance of AQP6 in these systems is not yet fully elucidated.

AQP6 has been proposed to contribute a protective role in some types of viral pathologies based on data showing AQP6 expression levels were inversely correlated with susceptibility to viral infection in host cell lines. Molinas and colleagues introduced GFP-tagged AQP6 into mouse fibroblast cells that were infected with Hazara virus, as a model for Crimean–Congo haemorrhagic fever. Overexpression of AQP6 reduced the infectivity of Hazara virus; conversely, cells that were infected with Hazara virus showed altered cell morphology and a reduced level of AQP6 expression at both protein and mRNA levels.[96] Understanding the mechanism linking the AQP6 channel to pathological outcomes could open new opportunities for modifying cellular vulnerability to pathologies caused by certain vectors such as Hazara virus.

3.3 | Arabidopsis thaliana PIP2;1

The plant aquaporin AtPIP2;1 is a plasma membrane protein highly expressed in *Arabidopsis* roots and stomata, and is involved in maintaining plant water homeostasis.[97] Water transport studies conducted on proteoliposomes showed that the osmotic water permeability of AtPIP2;1 channels was impaired by divalent cations, with the highest inhibitory efficacies shown by Ca^{2+}, Cd^{2+} and Mn^{2+} Protons also blocked the water flux, with half-maximal inhibition at pH 7.15.[98] Calcium plays an important role in signal transduction in plants, particularly under stress conditions.[99]

AtPIP2;1 channels expressed in *X. laevis* oocytes carry cation currents that are sensitive to block by divalent cations and pH,[9] confirming this channel is another example of the expanding list of dual water and ion channel aquaporins. AtPIP2;1 ion currents are blocked by extracellular Ca^{2+} and Cd^{2+}.[9] The biphasic dose-response curve plotted for the ionic conductance amplitude as a function of EGTA-buffered free Ca^{2+} level had a component with an IC_{50} value of 0.32 mmol/L which corresponds with values reported for Ca^{2+} block of non-selective cation channels in Arabidopsis root protoplasts. Low external pH inhibited the ionic conductance (IC_{50} pH 6.8). These data suggest that the AtPIP2;1 might carry the cationic conductance described in roots and guard cells that is known to be important for plant responses to environmental conditions, but was not previously defined at the molecular level. The ionic current in AtPIP2;1-expressing oocytes cannot be explained as an indirect result of native oocyte channels activating in response to swelling, since the co-expression of another related channel (AtPIP1;2) with AtPIP2;1 did increase water permeability but did not confer an ionic conductance response in the same conditions.

Furthermore, the mutation of glycine at position 103 to tryptophan (G103W) in AtPIP2;1 impaired both ion and water channel activity, demonstrating the cation permeation is intrinsic to the AtPIP2;1 channel.[9] Based on patterns of expression, AtPIP2;1 ion channels might explain the coupled ion and water transport known to facilitate rapid volume responses for guard cell closing,[100,101] and hypo-osmotic turgor in plants in the absence of water potential differences.[102]

Water permeability through membranes expressing AtPIP2;1 channels is regulated via phosphorylation.[100,103] Precedent for the regulation of aquaporin ion channels by phosphorylation has been established for mammalian AQP1, in which the phosphorylation of tyrosine 253 in the carboxyl terminal domain of AQP1 has been shown to govern the responsiveness of the ion channel to cGMP.[32] The probability of AQP1 being available to be gated as an ion channel is enhanced when the tyrosine phosphorylated state of the channel is favored via treatment with a tyrosine phosphatase inhibitor, bisperoxo-(1,10-phenanthroline)-oxovanadate-(V).[32] Similar intracellular cascades involving cyclic nucleotide signalling in roots and phosphorylation of plant AQP channels[104,105] could be explored as mechanisms for controlling dual water and ion transport through AtPIP2;1.

3.4 | Drosophila big brain

The transmembrane protein Big Brain (BIB), encoded by a Drosophila neurogenic gene, is a member of the aquaporin channel family.[106] During neurogenesis in the early development of Drosophila, a loss-of-function mutation of the Big Brain gene (*bib*) causes the overproduction of neuroblasts.[107] In parallel with other neurogenic genes *Notch* and *Delta*, BIB is involved in the process of lateral inhibition, and its absence leads to a pathological phenotype involving overproduction of neuroblasts.[106,107]

When expressed in *Xenopus* oocytes, BIB functions as a monovalent cation channel activated by membrane pricking or pharmacological modulation of tyrosine kinase signalling pathways, but is not a water channel.[11] The BIB ion channel is inhibited by insulin-like receptor activation of a tyrosine kinase pathway; and conversely is activated by a tyrosine kinase inhibitor, lavendustin A.[11] Tyrosine phosphorylation at predicted consensus sites in the carboxyl terminal domain was validated by western blot.[11] The BIB ion channel showed voltage-sensitive block by divalent cations such as Ca^{2+} and Ba^{2+}, suggesting the divalent binding site is within the electrical field. A glutamate residue in the first transmembrane domain Glu,[64] a position that is highly conserved in the MIP family, was defined as essential for divalent cation binding in BIB.[108] A possible role for the predicted depolarising effect of BIB activation, as one of the components of lateral inhibitory signalling remains to be tested in developing Drosophila in vivo.

4 | FUTURE DIRECTIONS

Acquiring a broad perspective on the functional roles and regulatory controls for aquaporin dual water and ion channels will be critical for understanding the spectrum of potentially important physiological roles that these channels might serve, as well as their potential value as targets in an impressively diverse array of applications. Aquaporin modulators have promise for future therapeutic interventions in clinical disorders including cancer metastasis, renal failure, and brain pathophysiology, as well as in enhancing agricultural productivity in challenging environments, managing vectors of transmitted diseases, and much more.

The development of selective blockers has been a long awaited milestone, and is now allowing the characterization of aquaporin functions in living cells. Block by AqB011 of the AQP1 ionic conductance demonstrated that the cation channel activity is a key component for HT29 cancer cell migration Figure 3.[38] The continuing evaluation of traditional medicinal plants as sources of blockers of AQP1 has produced agents that selectively inhibit water permeability (such as bacopaside II), or that block both the water and ion channel pores (such as bacopaside I); these also are promising tools for controlling migration

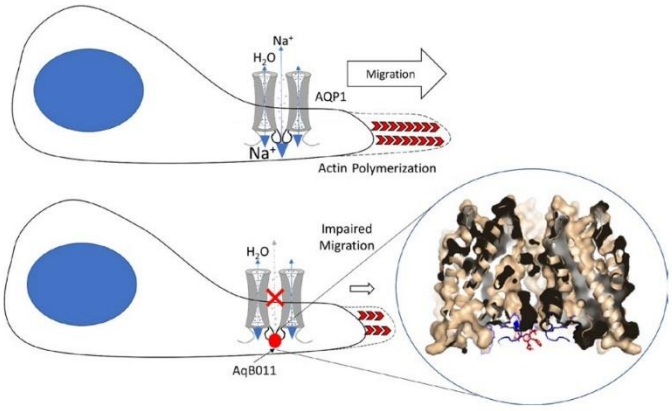

FIGURE 3 AqB011 is a specific blocker of AQP1 ion channel and impairs cancer cell migration in HT29 cancer cells.[38] AqB011 is predicted to interact with the loop D gating domain of the channel. Inset: View of the putative binding site for AqB011 in the tetrameric AQP1 channel, predicted from in silico docking. The ligand is thought to interact with two conserved arginine residues (hAQP1 R159 and R160) in the loop D gating domain, a site needed for cGMP-mediated activation of the ionic conductance

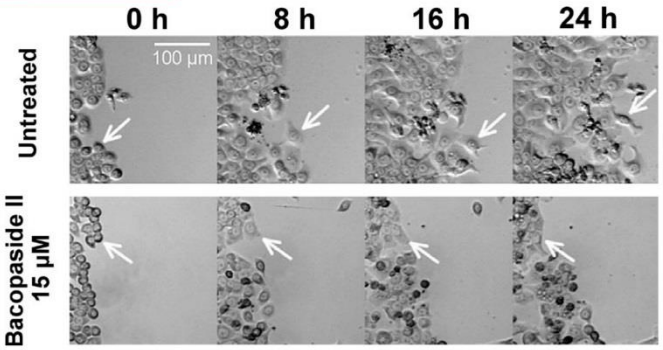

FIGURE 4 Temporal sequence from a live cell-imaging assay of wound closure, illustrating the robust inhibition of cell motility caused by treatment of HT29 colon cancer cells with the AQP1 water pore blocker bacopaside II (15 µmol/L). Circular wounds were created in confluent non-proliferating monolayers of HT29 cancer cells. Single cells at the edge of the wounds were tracked in time lapse images over 24 h periods, with and without bacopaside II. For clarity, only images at 8 h intervals are shown. White arrows identify a single cell in each treatment at 0 h, followed through subsequent frames

```
BIB       NLQAAISHSAALAAWERFGVEFILTFLVVLCYFVSTDPMKKFMGN-----SAASIGCAYS
hAQP1     NSLGRNDLADGVNSGQGLGIEIIGTLQLVLCVLATTDRRRRDLGG----SAPLAIGLSVA
AtPIP2;7  LGGGANTVADGYSKGTALGAEIIGTFVLVYTVFSATDPKRSARDSHIPVLAPLPIGFAVF
AtPIP2;1  YGGGANSLADGYSTGTGLAAEIIGTFVLVYTVFSATDPKRSARDSHVPVLAPLPIGFAVF
AtPIP2;2  YGGGANSLADGYNTGTGLAAEIIGTFVLVYTVFSATDPKRNARDSHVPVLAPLPIGFAVF
             .             :  *:* *: :.   : : *  :    .         ** :
```

FIGURE 5 Amino acid sequence alignment of loop D regions for BIB, hAQP1, AtPIP2;1 AtPIP2;2 and AtPIP2;7. After a conserved aspartate (D) residue, these selected channels show at least two positively charged amino acids (K lysine, or R arginine) in proximity. AQP1 lacks the adjacent proline (P), and instead has four arginines in series. The first two arginines (R159 and R160 in hAQP1) are implicated in ion channel gating and block by AqB011. Pharmacology for BIB, AtPIP2;1 AtPIP2;2 and AtPIP2;7 channels remains to be defined

in the subset of cancers that rely on AQP1 expression.[109] Bacopaside II isolated from the traditional medicinal herb Bacopa monnieri blocks the migration of cancer cells measured in live-cell-imaging assays (Figure 4) without toxicity at effective doses.[109]

Dual water and ion channel AQPs are being recognized as important for modulation of transmembrane fluid gradients, volume regulation, signal transduction, and adaptations to environmental factors for many different types of organisms. The analysis of similarities in amino acid sequence in key domains such as the loop D gating region (Figure 5) suggests that blocking agents such as AqB011 might be selective for specific classes; for example, the plant channel AtPIP2;1 does not carry the poly-arginine sequence of hAQP1 and is not blocked by AqB011.[112] An exciting future might harness AQP blockers as novel agents for slowing cancer metastasis, to be incorporated as adjunct treatments during primary surgical, chemo, or radiotherapy procedures. However, the translational value of new AQP pharmacological agents for limiting cancer metastasis awaits validation from in vivo studies and clinical trials. Work in progress suggests that selective inhibitors of AQP1 ion channels might also be useful in protecting red blood cells from pathological changes in cell morphology in some disease conditions (personal communication). Uncovering the multifunctional roles of aquaporins offers new pathways for basic research discovery and translational advances, and compels a renewed appreciation of the diversity and complexity of aquaporins in essential processes of physiology and pathology across all forms of life.

ORCID

Andrea J. Yool http://orcid.org/0000-0003-1283-585X

REFERENCES

1. Agre P, King LS, Yasui M, et al. Aquaporin water channels–from atomic structure to clinical medicine. *J Physiol*. 2002;542:3-16.
2. Gomes D, Agasse A, Thiebaud P, Delrot S, Geros H, Chaumont F. Aquaporins are multifunctional water and solute transporters highly divergent in living organisms. *Biochim Biophys Acta*. 2009;1788:1213-1228.
3. Finn RN, Chauvigne F, Hlidberg JB, Cutler CP, Cerda J. The lineage-specific evolution of aquaporin gene clusters facilitated tetrapod terrestrial adaptation. *PLoS One*. 2014;9:e113686.
4. Ishibashi K. New members of mammalian aquaporins: AQP10-AQP12. *Handb Exp Pharmacol*. 2009;190:251-262.
5. Zhang DY, Ali Z, Wang CB, et al. Genome-wide sequence characterization and expression analysis of major intrinsic proteins in soybean (Glycine max L.). *PLoS One*. 2013;8:e56312.
6. Shivaraj SM, Deshmukh RK, Rai R, Belanger R, Agrawal PK, Dash PK. Genome-wide identification, characterization, and expression

profile of aquaporin gene family in flax (Linum usitatissimum). *Sci Rep*. 2017;7:46137.
7. Jung JS, Preston GM, Smith BL, Guggino WB, Agre P. Molecular-structure of the water channel through aquaporin chip - the hourglass model. *J Biol Chem*. 1994;269:14648-14654.
8. Anthony TL, Brooks HL, Boassa D, et al. Cloned human aquaporin-1 is a cyclic GMP-gated ion channel. *Mol Pharmacol*. 2000;57:576-588.
9. Byrt CS, Zhao M, Kourghi M, et al. Non-selective cation channel activity of aquaporin AtPIP2;1 regulated by Ca2+ and pH. *Plant, Cell Environ*. 2016;40:802-815.
10. Modesto E, Barcellos L, Campos-de-Carvalho AC. MIP 28 forms channels in planar lipid bilayers. *Braz J Med Biol Res*. 1990;23:1029-1032.
11. Yanochko GM, Yool AJ. Regulated cationic channel function in *Xenopus* oocytes expressing *Drosophila* big brain. *J Neurosci*. 2002;22:2530-2540.
12. Weaver CD, Shomer NH, Louis CF, Roberts DM. Nodulin 26, a nodule-specific symbiosome membrane protein from soybean, is an ion channel. *J Biol Chem*. 1994;269:17858-17862.
13. Hazama A, Kozono D, Guggino WB, Agre P, Yasui M. Ion permeation of AQP6 water channel protein. Single channel recordings after Hg^{2+} activation. *J Biol Chem*. 2002;277:29224-29230.
14. Yool AJ, Weinstein AM. New roles for old holes: ion channel function in aquaporin-1. *News Physiol Sci*. 2002;17:68-72.
15. Yu J, Yool AJ, Schulten K, Tajkhorshid E. Mechanism of gating and ion conductivity of a possible tetrameric pore in aquaporin-1. *Structure*. 2006;14:1411-1423.
16. Ikeda M, Beitz E, Kozono D, Guggino WB, Agre P, Yasui M. Characterization of aquaporin-6 as a nitrate channel in mammalian cells. Requirement of pore-lining residue threonine 63. *J Biol Chem*. 2002;277:39873-39879.
17. Yasui M, Hazama A, Kwon TH, Nielsen S, Guggino WB, Agre P. Rapid gating and anion permeability of an intracellular aquaporin. *Nature*. 1999;402:184-187.
18. Yool AJ. Dominant-negative suppression of big brain ion channel activity by mutation of a conserved glutamate in the first transmembrane domain. *Gene Expr*. 2007;13:329-337.
19. Agre P, Lee MD, Devidas S, Guggino WB. Aquaporins and ion conductance. *Science*. 1997;275:1490; author reply 2.
20. Yool AJ, Campbell EM. Structure, function and translational relevance of aquaporin dual water and ion channels. *Mol Aspects Med*. 2012;33:443-561.
21. Wang H, Zhang Y, Cao L, et al. HERG K^+ channel, a regulator of tumor cell apoptosis and proliferation. *Cancer Res*. 2002;62:4843-4848.
22. Stringer BK, Cooper AG, Shepard SB. Overexpression of the G-protein inwardly rectifying potassium channel 1 (GIRK1) in primary breast carcinomas correlates with axillary lymph node metastasis. *Cancer Res*. 2001;61:582-588.
23. Ge R, Tai Y, Sun Y, et al. Critical role of TRPC6 channels in VEGF-mediated angiogenesis. *Cancer Lett*. 2009;283:43-51.
24. Flourakis M, Lehen'kyi V, Beck B, et al. Orai1 contributes to the establishment of an apoptosis-resistant phenotype in prostate cancer cells. *Cell Death Dis*. 2010;1:e75.
25. Prevarskaya N, Skryma R, Shuba Y. Calcium in tumour metastasis: new roles for known actors. *Nature Rev Cancer*. 2011;11:609-618.
26. McCoy ES, Haas BR, Sontheimer H. Water permeability through aquaporin-4 is regulated by protein kinase C and becomes rate-limiting for glioma invasion. *Neuroscience*. 2010;168:971-981.
27. McCoy E, Sontheimer H. Expression and function of water channels (aquaporins) in migrating malignant astrocytes. *Glia*. 2007;55:1034-1043.
28. Hu J, Verkman AS. Increased migration and metastatic potential of tumor cells expressing aquaporin water channels. *FASEB J*. 2006;20:1892-1894.
29. Kang BW, Kim JG, Lee SJ, et al. Expression of aquaporin-1, aquaporin-3, and aquaporin-5 correlates with nodal metastasis in colon cancer. *Oncology*. 2015;88:369-376.
30. Li A, Lu D, Zhang Y, et al. Critical role of aquaporin-3 in epidermal growth factor-induced migration of colorectal carcinoma cells and its clinical significance. *Oncol Rep*. 2013;29:535-540.
31. Anthony TL, Brooks HL, Boassa D, et al. Cloned human aquaporin-1 is a cyclic GMP-gated ion channel. *Molec Pharmacol*. 2000;57:576-588.
32. Campbell EM, Birdsell DN, Yool AJ. The activity of human aquaporin 1 as a cGMP-gated cation channel is regulated by tyrosine phosphorylation in the carboxyl-terminal domain. *Molec Pharmacol*. 2012;81:97-105.
33. Boassa D, Stamer WD, Yool AJ. Ion channel function of aquaporin-1 natively expressed in choroid plexus. *J Neurosci*. 2006;26:7811-7819.
34. Yool AJ, Stamer WD, Regan JW. Forskolin stimulation of water and cation permeability in aquaporin 1 water channels. *Science*. 1996;273:1216-1218.
35. Jan LY, Jan YN. Structural elements involved in specific K^+ channel functions. *Ann Rev Physiol*. 1992;54:537-555.
36. Zhang W, Zitron E, Homme M, et al. Aquaporin-1 channel function is positively regulated by protein kinase C. *J Biol Chem*. 2007;282:20933-20940.
37. Boassa D, Yool AJ. Single amino acids in the carboxyl terminal domain of aquaporin-1 contribute to cGMP-dependent ion channel activation. *BMC Physiol*. 2003;3:12.
38. Kourghi M, Pei JV, De Ieso ML, Flynn G, Yool AJ. Bumetanide derivatives AqB007 and AqB011 selectively block the aquaporin-1 ion channel conductance and slow cancer cell migration. *Mol Pharmacol*. 2016;89:133-140.
39. Nicchia GP, Stigliano C, Sparaneo A, Rossi A, Frigeri A, Svelto M. Inhibition of aquaporin-1 dependent angiogenesis impairs tumour growth in a mouse model of melanoma. *J Mol Med (Berl)*. 2013;91:613-623.
40. Grinstein S, Rotin D, Mason MJ. Na^+/H^+ exchange and growth factor-induced cytosolic pH changes. Role in cellular proliferation. *Biochim Biophys Acta*. 1989;988:73-97.
41. Lang F, Busch GL, Ritter M, et al. Functional significance of cell volume regulatory mechanisms. *Physiol Rev*. 1998;78:247-306.
42. Shi Y, Yuan H, Kim D, et al. Stimulation of Na^+/H^+ exchanger isoform 1 promotes microglial migration. *PLoS One*. 2013;8:e74201.
43. Stock C, Ludwig F, Schwab A. Is the multifunctional Na^+/H^+ exchanger isoform 1 a potential therapeutic target in cancer? *Curr Med Chem*. 2012;19:647-660.
44. Stock C, Schwab A. Protons make tumor cells move like clockwork. *Pflügers Archiv*. 2009;458:981-992.
45. Schwab A, Hanley P, Fabian A, Stock C. Potassium channels keep mobile cells on the go. *Physiology*. 2008;23:212-220.
46. Girault A, Haelters J-P, Potier-Cartereau M, et al. New alkyl-lipid blockers of SK3 channels reduce cancer cell migration and occurrence of metastasis. *Curr Cancer Drug Targets*. 2011;11:1111-1125.
47. Del Mónaco SM, Marino GI, Assef YA, Damiano AE, Kotsias BA. Cell migration in BeWo cells and the role of epithelial sodium channels. *J Membrane Biol*. 2009;232:1-13.
48. Wang S, He G, Yang Y, et al. Reduced expression of ENaC in placental tissues of patients with severe preeclampsia is related to compromised trophoblastic cell migration and invasion during pregnancy. *PLoS One*. 2013;8:e72153.
49. Kapoor N, Bartoszewski R, Qadri YJ, et al. Knockdown of ASIC1 and epithelial sodium channel subunits inhibits glioblastoma whole cell current and cell migration. *J Biol Chem*. 2009;284:24526-24541.
50. Bagriantsev SN, Gracheva EO, Gallagher PG. Piezo proteins: regulators of mechanosensation and other cellular processes. *J Biol Chem*. 2014;289:31673-31681.

51. Syeda R, Florendo MN, Cox CD, et al. Piezo1 channels are inherently mechanosensitive. *Cell Rep*. 2016;17:1739-1746.
52. Pappu P, Madduru D, Chandrasekharan M, Modhukur V, Nallapeta S, Suravajhala P. Next generation sequencing analysis of lung cancer datasets: a functional genomics perspective. *Indian J Cancer*. 2016;53:1-7.
53. Monteith GR, Davis FM, Roberts-Thomson SJ. Calcium channels and pumps in cancer: changes and consequences. *J Biol Chem*. 2012;287:31666-31673.
54. Roderick HL, Cook SJ. Ca^{2+} signalling checkpoints in cancer: remodelling Ca^{2+} for cancer cell proliferation and survival. *Nat Rev Cancer*. 2008;8:361-375.
55. Wei C, Wang X, Chen M, Ouyang K, Song L-S, Cheng H. Calcium flickers steer cell migration. *Nature*. 2009;457:901-905.
56. Barritt GJ, Litjens TL, Castro J, Aromataris E, Rychkov GY. Store-operated Ca2 + channels and microdomains of Ca2 + in liver cells. *Clin Exp Pharmacol Physiol*. 2009;36:77-83.
57. Kim J-H, Lkhagvadorj S, Lee M-R, et al. Orai1 and STIM1 are critical for cell migration and proliferation of clear cell renal cell carcinoma. *Biochem Biophys Res Comm*. 2014;448:76-82.
58. Han Z, Patil RV. Protein kinase A-dependent phosphorylation of aquaporin-1. *Biochem Biophys Res Comm*. 2000;273:328-332.
59. Umenishi F, Schrier RW. Hypertonicity-induced aquaporin-1 (AQP1) expression is mediated by the activation of MAPK pathways and hypertonicity-responsive element in the AQP1 gene. *J Biol Chem*. 2003;278:15765-15770.
60. Monzani E, Bazzotti R, Perego C, La Porta CA. AQP1 is not only a water channel: it contributes to cell migration through Lin7/beta-catenin. *PLoS One*. 2009;4:e6167.
61. Vilas G, Krishnan D, Loganathan SK, et al. Increased water flux induced by an aquaporin-1/carbonic anhydrase II interaction. *Mol Biol Cell*. 2015;26:1106-1118.
62. Meng F, Rui Y, Xu L, Wan C, Jiang X, Li G. Aqp1 enhances migration of bone marrow mesenchymal stem cells through regulation of FAK and β-catenin. *Stem Cells Devel*. 2013;23:66-75.
63. Yool AJ, Brown EA, Flynn GA. Roles for novel pharmacological blockers of aquaporins in the treatment of brain oedema and cancer. *Clin Exp Pharmacol Physiol*. 2009;37:403-409.
64. Speake T, Brown PD. Ion channels in epithelial cells of the choroid plexus isolated from the lateral ventricle of rat brain. *Brain Res*. 2004;1005:60-66.
65. Wright EM, Saito Y. The choroid plexus as a route from blood to brain. *Ann N Y Acad Sci*. 1986;481:214-220.
66. Johansson PA, Dziegielewska KM, Ek CJ, et al. Aquaporin-1 in the choroid plexuses of developing mammalian brain. *Cell Tissue Res*. 2005;322:353-364.
67. Redzic ZB, Preston JE, Duncan JA, Chodobski A, Szmydynger-Chodobska J. The choroid plexus-cerebrospinal fluid system: from development to aging. *Curr Top Dev Biol*. 2005;71:1-52.
68. Segal MB, Pollay M. The secretion of cerebrospinal fluid. *Exp Eye Res*. 1977;25(Suppl):127-148.
69. Nielsen S, Smith BL, Christensen EI, Agre P. Distribution of the aquaporin CHIP in secretory and resorptive epithelia and capillary endothelia. *Proc Natl Acad Sci U S A*. 1993;90:7275-7279.
70. Agre P, Preston GM, Smith BL, et al. Aquaporin CHIP: the archetypal molecular water channel. *Am J Physiol*. 1993;265:F463-F476.
71. Miyajima M, Arai H. Evaluation of the production and absorption of cerebrospinal fluid. *Neurol Med Chir (Tokyo)*. 2015;55:647-656.
72. Masuzawa T, Ohta T, Kawamura M, Nakahara N, Sato F. Immunohistochemical localization of Na^+, K^+-ATPase in the choroid plexus. *Brain Res*. 1984;302:357-362.
73. Boassa D, Yool AJ. Physiological roles of aquaporins in the choroid plexus. *Curr Top Dev Biol*. 2005;67:181-206.
74. Tsutsumi K, Niwa M, Kawano T, Ibaragi M, Ozaki M, Mori K. Atrial natriuretic polypeptides elevate the level of cyclic GMP in the rat choroid plexus. *Neurosci Lett*. 1987;79:174-178.
75. Saadoun S, Papadopoulos MC, Hara-Chikuma M, Verkman AS. Impairment of angiogenesis and cell migration by targeted aquaporin-1 gene disruption. *Nature*. 2005;434:786-792.
76. Bloemendal H, Hockwin O. Lens protein. *Crit Rev Biochem*. 1982;12:1-38.
77. Zampighi GA, Hall JE, Kreman M. Purified lens junctional protein forms channels in planar lipid films. *Proc Natl Acad Sci U S A*. 1985;82:8468-8472.
78. Chandy G, Zampighi GA, Kreman M, Hall JE. Comparison of the water transporting properties of MIP and AQP1. *J Membr Biol*. 1997;159:29-39.
79. Kushmerick C, Rice S, Baldo G, Haspel H, Mathias R. Ion, water and neutral solute transport in Xenopus oocytes expressing frog lens MIP. *Experim Eye Res*. 1995;61:351-362.
80. Varadaraj K, Kumari S, Shiels A, Mathias RT. Regulation of aquaporin water permeability in the lens. *Investig Ophthal Vis Sci*. 2005;46:1393-1402.
81. Varadaraj K, Kumari SS, Mathias RT. Functional expression of aquaporins in embryonic, postnatal, and adult mouse lenses. *Devel Dyn*. 2007;236:1319-1328.
82. Varadaraj K, Kushmerick C, Baldo G, Bassnett S, Shiels A, Mathias R. The role of MIP in lens fiber cell membrane transport. *J Membrane Biol*. 1999;170:191-203.
83. Chepelinsky AB. Structural function of MIP/aquaporin 0 in the eye lens; genetic defects lead to congenital inherited cataracts. *Handb Exp Pharmacol*. 2009;190:265-297.
84. Berry V, Francis P, Kaushal S, Moore A, Bhattacharya S. Missense mutations in MIP underlie autosomal dominant 'polymorphic' and lamellar cataracts linked to 12q. *Nat Genet*. 2000;25:15-17.
85. Shen L, Shrager P, Girsch SJ, Donaldson PJ, Peracchia C. Channel reconstitution in liposomes and planar bilayers with HPLC-purified MIP26 of bovine lens. *J Membrane Biol*. 1991;124:21-32.
86. Ehring GR, Zampighi G, Horwitz J, Bok D, Hall JE. Properties of channels reconstituted from the major intrinsic protein of lens fiber membranes. *J Gen Physiol*. 1990;96:631-664.
87. Németh-Cahalan KL, Hall JE. pH and calcium regulate the water permeability of aquaporin 0. *J Biol Chem*. 2000;275:6777-6782.
88. Preston GM, Jung JS, Guggino WB, Agre P. The mercury-sensitive residue at cysteine 189 in the CHIP28 water channel. *J Biol Chem*. 1993;268:17-20.
89. Kwon T-H, Hager H, Nejsum LN, Andersen M-LE, Frøkiaer J, Nielsen S. Physiology and pathophysiology of renal aquaporins. *Sem Nephrology* 2001;268:231-238.
90. Yasui M, Kwon T-H, Knepper MA, Nielsen S, Agre P. Aquaporin-6: An intracellular vesicle water channel protein in renal epithelia. *Proc Natl Acad Sci*. 1999;96:5808-5813.
91. Carbrey JM, Agre P. Discovery of the aquaporins and development of the field. In: Beitz E, ed. *Aquaporins 190*. Berlin, Heidelberg, Germany: Springer; 2009:3-28.
92. Promeneur D, Kwon T-H, Yasui M, et al. Regulation of AQP6 mRNA and protein expression in rats in response to altered acid-base or water balance. *Am J Physiol Renal Physiol*. 2000;279:F1014-F1026.
93. Matsuki-Fukushima M, Hashimoto S, Shimono M, Satoh K, Fujita-Yoshigaki J, Sugiya H. Presence and localization of aquaporin-6 in rat parotid acinar cells. *Cell Tiss Res*. 2008;332:73-80.
94. Laforenza U, Gastaldi G, Polimeni M, et al. Aquaporin-6 is expressed along the rat gastrointestinal tract and upregulated by feeding in the small intestine. *BMC Physiol*. 2009;9:18.
95. Ma J, Zhou C, Yang J, Ding X, Zhu Y, Chen X. Expression of AQP6 and AQP8 in epithelial ovarian tumor. *J Molec Histol*. 2016;47:129-134.
96. Molinas A, Mirazimi A, Holm A, Loitto VM, Magnusson KE, Vikstrom E. Protective role of host aquaporin 6 against Hazara virus, a model for Crimean-Congo hemorrhagic fever virus infection. *FEMS Microbiol Lett*. 2016;363. doi: 10.1093/femsle/fnw058

97. Alexandersson E, Fraysse L, Sjovall-Larsen S, et al. Whole gene family expression and drought stress regulation of aquaporins. *Plant Mol Biol*. 2005;59:469-484.
98. Verdoucq L, Grondin A, Maurel C. Structure-function analysis of plant aquaporin AtPIP2;1 gating by divalent cations and protons. *Biochem J*. 2008;415:409-416.
99. Sanders D, Pelloux J, Brownlee C, Harper JF. Calcium at the crossroads of signaling. *Plant Cell*. 2002;14:S401-S417.
100. Grondin A, Rodrigues O, Verdoucq L, Merlot S, Leonhardt N, Maurel C. Aquaporins contribute to ABA-triggered stomatal closure through OST1-mediated phosphorylation. *Plant Cell*. 2015;27:1945-1954.
101. MacRobbie EA. Control of volume and turgor in stomatal guard cells. *J Membr Biol*. 2006;210:131-142.
102. Wegner LH. Root pressure and beyond: energetically uphill water transport into xylem vessels? *J Exp Bot*. 2014;65:381-393.
103. Prado K, Boursiac Y, Tournaire-Roux C, et al. Regulation of Arabidopsis leaf hydraulics involves light-dependent phosphorylation of aquaporins in veins. *Plant Cell*. 2013;25:1029-1039.
104. Isner JC, Nuhse T, Maathuis FJ. The cyclic nucleotide cGMP is involved in plant hormone signalling and alters phosphorylation of Arabidopsis thaliana root proteins. *J Exp Bot*. 2012;63:3199-3205.
105. Maurel C, Kado RT, Guern J, Chrispeels MJ. Phosphorylation regulates the water channel activity of the seed-specific aquaporin alpha-TIP. *EMBO J*. 1995;14:3028-3035.
106. Rao Y, Bodmer R, Jan LY, Jan YN. The big brain gene of *Drosophila* functions to control the number of neuronal precursors in the peripheral nervous system. *Development*. 1992;116:31-40.
107. Lehmann R, Jimenez F, Dietrich U, Campos-Ortega JA. On the phenotype and development of mutants of early neurogenesis in *Drosophila melanogaster*. *Wilehm Roux Arch Dev Biol*. 1983;192:62-74.
108. Yanochko GM, Yool AJ. Block by extracellular divalent cations of *Drosophila* big brain channels expressed in Xenopus oocytes. *Biophys J* . 2004;86:1470-1478.
109. Pei JV, Kourghi M, De Ieso ML, et al. Differential inhibition of water and ion channel activities of mammalian aquaporin-1 by two structurally related bacopaside compounds derived from the medicinal plant *Bacopa monnieri*. *Mol Pharmacol*. 2016;90:496-507.
110. Brooks HL, Regan JW, Yool AJ. Inhibition of aquaporin-1 water permeability by tetraethylammonium: involvement of the loop E pore region. *Mol Pharmacol*. 2000;57:1021-1026.
111. Preston GM, Jung JS, Guggino WB, Agre P. Membrane topology of aquaporin CHIP. Analysis of functional epitope-scanning mutants by vectorial proteolysis. *J Biol Chem*. 1994;269:1668-1673.
112. Kourghi M, Nourmohammadi S, Pei JV, et al. Divalent cations regulate the ion conductance properties of diverse classes of aquaporins. *Intl J Molec Sci*. 2017;18:2323. doi: 10.3390/ijms1811232

How to cite this article: Kourghi M, Pei JV, De Ieso ML, Nourmohammadi S, Chow PH, Yool AJ. Fundamental structural and functional properties of Aquaporin ion channels found across the kingdoms of life. *Clin Exp Pharmacol Physiol*. 2018;00:1–9. https://doi.org/10.1111/1440-1681.12900